SPINAL CIRCUITRY UNDERLYING CROSSED REFLEX

By

Olivier D. Laflamme

Submitted in partial fulfilment of the requirements
for the degree of Doctor of Philosophy

at

Dalhousie University
Halifax, Nova Scotia
August 2022

Dalhousie University is located in Mi'kma'ki, the
ancestral and unceded territory of the Mi'kmaq.
We are all Treaty people.

À la mémoire de ceux qui nous ont quittés trop tôt

Gilles Laflamme

(1957-2021)

Robin Beaulieu

(1990-2022)

Étiennette Laflamme

(1930-2022)

TABLE OF CONTENTS

LIST OF FIGURES

ABSTRACT

Sensory information is used to generate various behaviour including protective and corrective reflexes. Following perturbation in one leg, motor activity can be elicited in the contralateral side of the body known as a crossed reflex. It has been shown that neuronal pathways underlying crossed reflexes involve commissural interneurons with cell bodies located in the Rexed Lamina VIII as described in cats. The existence of analogous crossed reflexes has been shown in rodents. However, we have no insights into the organization of these crossed reflex pathways and their function in awake animals. Utilizing the mouse model, my Ph.D. work has focused on: 1) Understanding how sensory information (cutaneous and/or proprioceptive) is transferred to the contralateral spinal cord, and which muscles are being targeted by these pathways, and 2) investigating the spinal circuitry underlying crossed reflex. First, I reveal that in WT mice, crossed reflexes include an excitatory and inhibitory component which are modulated during locomotion depending on the activity of the muscle prior to the stimulation. Furthermore, the origin of the crossed reflex stimulation results in mostly similar outputs with slight differences. Notably, the existence of a long latency crossed reflex responses when the common peroneal nerve is stimulated, but not when the tibial or sural nerves are stimulated. To study the role of commissural interneurons, involve in the transmission of sensory afferent information, I used genetically engineered mice with manipulated (killed or silenced) V0 and V3 commissural interneurons respectively. Crossed reflexes between $V0^{kill}$ and WT mice were mostly similar with a stronger inhibitory component observed in $V0^{kill}$ mice. Meanwhile, $V3^{off}$ mice exhibit a non-significant decrease in the excitatory response and significant disruption in the inhibitory crossed reflex responses. As V3 interneurons represent a mostly excitatory interneuronal population, I investigated the role of a deep dorsal horn interneuron (dPVs) in crossed reflex. In dPV^{ablat} mice, crossed inhibitory reflex occurrence remained similar to control, suggesting that dPVs interneurons are not involved in inhibitory crossed reflex pathways. Taken together, my thesis provides the first framework to draw a spinal circuitry for the transmission of sensory afferent information in the spinal cord.

LIST OF ABBREVIATIONS USED

˚C	Degree Celsius
~	Approximately
%	Percent
1.2xT	1.2 times threshold
5xT	5 times threshold
µa	Microampere
µm	Micrometer
ACSF	Artificial cerebrospinal fluid
c-Fos	Cellular Fos Proto-oncogene
CIN	Commissural interneurons
CPG	Central pattern generator
Cp. n.	Common peroneal nerve
Cp. n. stim.	Common peroneal nerve stimulation
Cre	Cause recombinase
Curr.	Current
dI#	Dorsal Interneuron class #
Dbx1	Developing Brain Homeobox 1
dILA/B	Dorsal Interneuron late A/B
DMRT3	Doublesex and Mab-3 Related Transcription Factor 3
dPV	parvalbumin-expressing glycinergic interneurons in the mDDH
DRG	Dorsal root ganglia
DTx	Diphtheria Toxin
EMG	Electromyography
EPSP	Excitatory Postsynaptic Potentials
FRA	Flexor reflex afferent
Gs_l	Left Gastrocnemius
Gs_r	Right Gastrocnemius
GTO	Golgi tendon organ
h	Hours
Hz	Hertz
IHC	Immunohistochemistry
IN	Interneuron
INi	Local inhibitory interneuron
Ip_r	Right Iliopsoas
IPSP	Inhibitory Postsynaptic Potentials
I.T	Intrathecal injection
kg	Kilogram
L#	Lumbar segment #
Lbx1	Ladybird Homeobox 1
LTMR	Low threshold mechanoreceptor
m/s	Meter/second
mDDH	medial deep dorsal horn
mg	Milligram
MLR	Mesencephalic locomotor region

MN	Motor neuron
ms	millisecond
mV	millivolts
Nkx2.2	NK2 Homeobox 2
oEPSCs	Optogenetically-evoked excitatory postsynaptic currents
oIPSC	Optogenetically-evoked inhibitory postsynaptic currents
P#	Postnatal day #
Pax 7	Paired box protein 7
PBS	Phosphate Buffered Saline
PFA	Paraformaldehyde
Pitx2	Paired like Homeodomain 2
PV	Parvalbumin
RORβ	Retinoid-related orphan receptor beta
saph. N.	Saphenous nerve
sAP	Spontaneous action potential
SD	Standard deviation
Sens.	Sensory neurons
Sim1	Single-minded homolog 1
St_r	Right Semitendinosus
sur. n	Sural nerve
sur. n. stim.	Sural nerve stimulation
T	Threshold
TA_l	Left Tibialis Anterior
TA_r	Right Tibialis Anterior
TF	Tonic Firing
TF_{Ac}	Tonic Firing accommodating
TF_{Na}	Tonic Firing-non-accommodating
tib. n.	Tibial nerve
tib. n. stim.	Tibial nerve stimulation
V#	Ventral interneuron class #
V0c	Cholinergic V0
V0d	V0 dorsal
V0g	V0 glutamatergic
$V0^{kill}$	Hoxb8 ::cre; Dbx1 ::DTA
V0v	V0 ventral
V3d	Dorsal V3
$V3^{off}$	Sim1 ::cre; vGlut2flox/flox
V3v	Ventral V3
V3vl	Ventrolateral V3
V3vm	Ventromedial V3
Vglut2	Vesicular glutamate transporter 2
VL_r	Right Vastus lateralis
WT	Wild-type
Wt1	Wilms Tumor 1

ACKNOWLEDGEMENTS

Foremost, I would like to thank my supervisor, Dr. Turgay Akay. Thank you for supporting me as we went through the last six years together. Thank you for letting me pursue science, building a wonderful lab that I could be a part of, and teaching me many things inside the lab. Thank you for taking me on and letting me explore the world of science under you.

I would like to thank all members of the Akay lab, past and present. Thank you for making the lab a supportive environment and a joy to participate in. First, I would like to thank Brenda Ross for all her help with the animal colonies. My work would not have been possible without her tireless support. I would like to thank Dr. William Mayer and Lauren Landoni for accepting me into the lab and teaching me the technique used to complete this thesis. I would like to further acknowledge Tyler Wells and Reynaldo Popoli for being wonderful colleagues and friends over the last several years. Thank you for giving me your money during our poker night. I would also like to thank the work of Marwan Ibrahim and Rachel Banks, two formidable undergraduate students that I had the pleasure to mentor during my Ph.D. for their help over the year analyzing and acquiring data. I would like to thank my committee members, Dr. Ying Zhang, and Dr. Victor Rafuse. Thank you for helping me over the years. Thank you, Dr. Simon Danner, Dr. Sergey Markin, Dr. Victoria Abraira, and Nofar Ozeri-Engelhard for our collaborative projects and discussions.

I would like to thank my parents Louise Dagnault and Yves Laflamme for installing in me an undying desire to learn and explore. Thank you for showing me love and being good role models for how to live a fulfilling life.

I would like to thank the friends that I have made along the way. My friends helped me get through every aspect of this degree. I would like to particularly give a warm thank you to Dr. Julia Harrison, Dr. Shannon Hall, and Kaitlyn Keller for welcoming me to Halifax and being dear friends for the last six years. I can always count on you to babysit Reggie and be there when I need help. I would like to thank all member of the Halifax convoy soccer club, playing soccer with you have always been fun. Lastly, thank you, Maral, for putting up with me for the last five years and always making me laugh. Nobody could ask for a better partner. I would like to acknowledge Robin Beaulieu, Gilles Laflamme, and Étiennette Laflamme, we will miss you, may you rest in peace.

CHAPTER 1. INTRODUCTION

1.1 LOCOMOTION

Locomotion is the primary motor function that allows one to interact with their environment. In limbed terrestrial animals, walking is the most common form of locomotion, though other forms of locomotion include swimming and climbing. In mammals, locomotion is mostly in a quadrupedal setting where the left and right limbs, as well as the forelimbs and hindlimbs, are coordinated to generate motor movement. In all cases, it is characterized by the coordination of the movement of the left and right legs to propel the body while ensuring postural stability. This movement is then modulated by a myriad of different external and internal inputs to adapt and offer a smooth interaction between the body and the immediate environment.

1.2 CROSSED REFLEX

Coordinated leg movements during locomotion are generated by the patterned activation of multiple motor neuron pools that drive the orchestrated contraction of multiple leg muscles, both within and between legs. More than a century ago, Sherrington (1910) described reflex movements evoked in another limb following the flexion reflex. In cats, he noticed that the reflex movement of the contralateral limb was almost invariably an extension of the hip, knee, and ankle (Sherrington, 1910). In the description of the crossed extensor pathways, Sherrington laid the table for all reflex pathways that convey sensory information to the contralateral side, henceforth called crossed reflex pathways.

In the decades following Sherrington's description, other researchers reported on the crossed reflex in cats. Using horseradish peroxidase tracer, commissural interneurons implicated in the transmission of the crossed reflex were discovered in the Rexed lamina VIII of the spinal cord (Harrison et al. 1986). These neurons project through the ventral commissure to the contralateral side and synapse with motoneurons and with interneurons in the lamina VI-VIII (Bannatyne et al. 2003; 2006; Matsuyama et al. 2004a; 2004b; 2006). These crossed reflex responses were shown to be elicited by the stimulation of proprioceptive sensory afferents (groups I and II), cutaneous afferents, and flexor reflex

afferents (FRAs: high-threshold afferents from joints, muscles, and skin involved in ipsilateral limb flexion and contralateral limb extension) (Jankowska and Noga, 1990). In anesthetized cats, EPSPs and IPSPs were shown during intracellular recordings of motoneurons and commissural interneurons (Harrison et al. 1986; Jankowska and Noga, 1990; Arya et al. 1991; Aggelopoulos et al. 1995; Aggelopoulos and Edgley, 1995), suggesting that crossed excitatory and inhibitory pathways exist in the spinal cord. Commissural interneurons involved in these pathways include mostly excitatory glutamatergic and a small subset of inhibitory glycinergic interneurons that may synapse with contralateral motoneurons directly. They may also influence the activity of motoneurons indirectly by acting through interneurons on the contralateral side (Bannatyne et al. 2003). Interestingly, intracellular recording of commissural interneurons revealed that they can be separated into two major non-overlapping subpopulations based on their functional role, in which both subpopulations can induce crossed excitatory and crossed inhibitory responses (Jankowska et al. 2005).

During locomotion, crossed flexor and extensor responses were observed in cats following stimulation of proprioceptive and cutaneous afferents (Duysen, 1977; Duysen et al. 1980; Duysens and Loeb, 1980; Frigon and Rossignol, 2008; Hurteau et al. 2017) Subsequent studies demonstrated that contralateral excitatory responses during locomotion were almost always preceded by a short period of inhibition (Frigon and Rossignol, 2008), suggesting that crossed excitatory and crossed inhibitory responses are also present during locomotion. Furthermore, stimulation of the tibial, sural, or superficial peroneal nerve influences the timing and duration of the hip flexor and ankle extensor activity during specific phases of the step cycle (Duysens, 1977; Rossignol and Frigon, 2008). Additionally, crossed flexor responses observed during stimulation of proprioceptive and cutaneous afferents during locomotion are replaced by a crossed extensor response when the stimuli occur at the end of the contralateral stance phase (Duysens et al. 1980), suggesting that crossed reflexes are modulated in a phase-dependent manner.

Crossed reflex has also been observed in humans. When the sural or tibial nerve (at the level of the ankle) is stimulated, suppression of the activity of the contralateral gastrocnemius medialis is elicited in synchrony with a facilitation of the contralateral

soleus muscle activity during walking (Duysen et al. 1991). Subsequent studies observed short-latency crossed inhibitory responses in the human soleus muscle induced by the activation of group I and group II sensory afferents (Stubbs and Mrachacz-Kersting, 2009; Stubbs et al. 2011; 2012; Gervasio et al. 2015; 2017; Mrachacz-Kerting et al. 2017). As with other species, crossed reflexes in humans are believed to be important for dynamic stability during walking (Gervasio et al. 2015). In humans, the spinal circuitry involved in crossed reflexes was studied using a paired stimulation paradigm, which suggested that ipsilateral and contralateral afferents converge on common inhibitory interneurons and/or directly onto motoneurons. (Harrison and Zytnicki, 1984; Jankowska et al. 2009; Stubbs and Mrachacz-Kersting, 2009; Mrachacz-Kersting et al. 2017).

Overall, experiments performed in cats and humans have shown that the activation of sensory afferents can trigger contralateral motor neuron responses. These responses can be excitatory or inhibitory depending on the external and internal conditions. Sensory input also seems to converge, be it on specific interneurons or directly onto motoneurons, which could increase the flexibility of the nervous system. However, the spinal circuitry underlying crossed reflex remains unknown because of the inability to manipulate and investigate the role of specific interneurons inside the spinal cord.

1.3 SPINAL CIRCUITRY

From experiments in mice, it was discovered that neuronal subtypes of the spinal cord become distinct depending on their position along the dorsoventral axis of the developing neural tube (Jessell, 2000). So far, 12 embryonic progenitor cell domains have been identified (pdI1-pdI6, pdIL, p0-p3, pMN), which are distinguished by the combination of transcription factors that they express (Alaynick et al. 2011; Lu et al. 2015). During locomotion, the four ventral populations (V0-V3), as well as the dorsal interneurons dI6, are considered to be important members of the spinal CPG circuits and play distinctive roles during locomotion (Goulding, 2009; Arber, 2012; Kiehn, 2016; Gosgnach et al. 2017; Deska-Gauthier and Zhang, 2019). From that group, three of the progenitor domains give rise to commissural interneurons shown to be relevant for left-right coordination.

1.3.1 dI6 interneuron

dI6 interneurons originate from progenitor cells located dorsally in the developing neural tube. By postnatal stages of development, these interneurons settle more ventrally into lamina VII/VIII (Gross et al. 2002; Andersson et al. 2012; Griener et al. 2017). As with the other dorsal interneuron populations, dI6 interneurons express the transcription factor Lbx1 (Gross et al. 2002). They can also be divided into three subpopulations based on their expression of the transcription factors Wt1 and DMRT3: those that express Wt1, those that express DMRT3, and those that express both Wt1 and DMRT3. dI6 interneurons are mainly inhibitory (Andersson et al. 2012) and predominantly commissural, although they form monosynaptic and disynaptic contacts with both contralateral and ipsilateral motoneurons (Griener et al. 2017).

Whole-cell patch-clamp recordings of dI6 interneurons in isolated mouse spinal cords have indicated that most of these cells are rhythmically active during fictive locomotion (Dyck et al. 2012; Haque et al. 2018). Previous work has indicated those rhythmically active neurons that maintain oscillatory activity during non-resetting deletions are likely to be involved in rhythm generation, while those that fall silent are involved in pattern formation (Zhong et al. 2012). An analysis of their activity during non-resetting deletion was performed to understand the role of dI6 interneurons during locomotion. dI6 interneurons were found to be implicated in the rhythm generator and pattern formation layers of the locomotor spinal circuits, as shown by their intrinsic electrophysiological properties (Griener et al. 2017). Furthermore, functional and genetic ablation of either Wt1 (Haque et al. 2018) or DMRT3 (Andersson et al. 2012) interneurons in isolated neonatal spinal cords generate irregular fictive locomotor output with non-coherent left-right alternation. However, thus far, only DMRT3 dI6 interneuron functional output has been investigated in vivo. DMRT3 mutated horses display difficulty transitioning from trotting to galloping with increasing locomotor speed. Instead, these horses express a pace gate defined by synchronized movement of the legs on one side of the body at a higher speed (Andersson et al. 2012). Overall, the dI6 interneurons' functional role in locomotion remains unclear. However, their synaptic connectivity and role in fictive locomotion suggest that dI6 interneurons are important during locomotion and limb coordination.

1.3.2 V0 interneuron

V0 interneurons are mostly commissural and originate from the P0 domain, expressing the transcription factor Dbx1 (Pierani et al. 2001). V0 interneurons are composed of several subpopulations, two of the largest being the ventral excitatory subpopulation (V0v) expressing Evx1, and the dorsal inhibitory subpopulation (V0d) expressing Pax7 (Lanuza et al. 2004; Pierani et al. 2001; Talpalar et al. 2013). V0 interneurons constitute a substantial proportion of the commissural interneurons (CINs) in the ventral spinal cord that form direct connections with contralateral MN pools (Lanuza et al. 2004). Deletion of the V0v and V0d interneurons abolishes left-right alternation at all speeds, resulting in a hopping gait in mice (Bellardita and Kiehn, 2015). When the V0v interneurons are selectively abolished, mutant mice have normal left-right alternation at low locomotor speeds. However, at high locomotor speeds, the mice are incapable of trotting, the hindlimbs become synchronous, and the mice display a hopping gait (Talpalar et al. 2013; Bellardita and Kiehn, 2015). These results suggest that the V0v helps drive left-right alternation during high-speed but not during low-speed locomotion. Meanwhile, the role of V0d remains more elusive as mutant mice lacking V0d interneurons die shortly after birth. Nevertheless, embryonic in vitro spinal cord preparations have shown that, when the V0d are absent, left-right alternation is lost at low locomotor frequencies but not at higher locomotor frequencies during drug-evoked fictive locomotion (Talpalar et al. 2013). These results suggest that V0v and V0d subpopulations are functionally distinct circuits that are recruited at different locomotor speeds.

A smaller subset of the V0 population was identified near the central canal which expresses the Pitx2 transcription factor. These interneurons have either cholinergic (V0c) or glutamatergic (V0g) neurotransmission projecting either ipsilaterally or bilaterally to motoneurons (Zagoraiou et al. 2009). Although not much is known about the V0g, V0c interneurons are important for regulating the strength of MN output. V0c interneurons form large synapses, called C-boutons, onto MNs, serving as a neuromodulator of the locomotor system. The recruitment of V0c interneurons increases MNs' input-output gain through increased action potential firing frequencies (Miles et al. 2007). During swimming, mice lacking V0c interneurons are unable to increase MN output in the ankle extensor muscle (Zagoraiou et al. 2009).

1.3.3 V3 interneuron

V3 interneurons are a mostly excitatory glutamatergic population derived from the P3 progenitor domain expressing the Nkx2.2 gene and Sim1 transcription factor (Briscoe et al. 1999; Zhang et al. 2008). Most of the V3 interneurons project contralaterally (85%), but a small subset synapse with ipsilateral motoneurons (15%) (Zhang et al. 2008; Blacklaw et al. 2015). In isolated mouse spinal cords, when the synaptic transmission of the V3 interneurons was blocked and fictive locomotion was induced, a significantly uncoordinated and variable left-right and flexor-extensor ventral root bursting were observed. Furthermore, genetic deletion of the V3 interneurons in vivo also leads to an unstable and unbalanced gait when the animals walk; however, left-right alternation is preserved when V3 interneurons are silenced (Zhang et al. 2008). Furthermore, the maximal locomotor speed is reduced in V3-silenced mice, and these mice have an unstable trot because of the lack of synchronization between their diagonal limbs. These mice also display high step-to-step variability in left-right coordination close to their maximum locomotor speed, which is associated with a distortion of the interlimb coordination. In particular, these mice lack properly synchronized limb coupling, which is necessary for trot, gallop, and bound gaits that are normally used at higher frequencies (Zhang et al. 2022). These results suggest that the V3 interneurons are important for coordination and balance between distinct limbs' flexor-extensor spinal circuits.

As for most interneuron populations, the V3 interneurons are heterogeneous, as determined by their location, intrinsic membrane properties, axon projection profile, and morphology (Borowaska et al. 2013; 2015; Blacklaws et al. 2015). Although not much is known about the specific role of each subpopulation, the ventral V3 (V3v) and the dorsal V3 (V3d) subpopulations are physiologically distinct at birth, whose electrophysiological properties undergo a significant maturation process during the first three weeks after birth in mice (Borowska et al. 2015).

Using single-cell patch-clamp recording in combination with holographic glutamate uncaging, allowing for the mapping of local cell-cell V3 connectivity in the spinal cord, Chopek et al. (2018) revealed that the majority of V3v interneurons form commissural ascending and descending propriospinal projections. Some of the V3v

interneurons also exhibit ipsilateral or bifurcating projections. Furthermore, smaller, medial, and contralaterally projecting V3v interneurons also synapse ipsilaterally with larger lateral V3v interneurons, which in turn innervate adjacent motoneuron networks. Ipsilateral motoneurons also form excitatory glutamatergic synapses back onto both lateral V3v and medial V3v interneurons (Chopek et al. 2018). These results suggest that commissural V3 interneurons form positive feedback microcircuits with local ipsilateral motoneurons and that these microcircuits have a potential role in controlling the activity of the motor output. The precise role of this V3-motoneuron microcircuit, however, remains unknown.

Meanwhile, V3d interneurons form exclusively ascending commissural projections (Blacklaws et al. 2015; Zhang et al. 2022). They project to the contralateral cervical region and engage in diagonal limb synchronization, which is necessary for trotting. Indeed, V3d interneuron recruitment increases as locomotor speed increases (Zhang et al. 2022). Overall, these findings suggest that the V3 interneurons participate in local left-right alternation and diagonal coupling during locomotion, which is necessary for the emergence of locomotor gaits such as trot, bound, and gallop at higher speeds.

Taken together, interlimb coordination has been extensively studied during locomotion and a general idea of the role of different interneurons in the locomotor pattern has been discovered. However, under natural conditions, locomotion is an interactive process between centrally generated motor activities and afferent input from sensory receptors of the body that are activated by movement. Spinal sensorimotor networks integrate sensory afferent information into ongoing locomotion, thus adapting the locomotor pattern and ensuring that locomotion is coordinated with the requirements of the environment. So far, the role of these commissural interneurons in the integration of sensory afferents remains unknown.

1.4 SOMATOSENSORY SYSTEM

Somatosensation collectively refers to the bodily senses of nociception (pain), thermosensation (temperature), pruriception (itch), mechanosensation (cutaneous/touch), and proprioception (limb and body position). During locomotion, the absence of sensory

feedback from proprioception and cutaneous afferents leads to incoordination and maladaptive movement (Bouyer and Rossignol, 2003a; 2003b; Rossignol et al. 2006; Akay et al. 2014; Santuz et al. 2019; Mayer and Akay, 2021). However, locomotion can still occur after most of the sensory afferents are removed via dorsal rhizotomy. Sensory inputs are, therefore, not necessary to produce locomotor movements (Giulinani and Smith, 1987; Goldberger, 1977; 1983; Grillner and Zanger, 1984; Wetzel et al. 1976). Furthermore, in vitro experiments have shown that the spinal cord alone is sufficient to generate locomotor-like activity (Smith and Feldman, 1987; Kudo and Yamada, 1987). Yet, when sensory feedback is removed, the CPG and supraspinal pathways are not able to produce robust locomotion in the presence of external perturbations (Santuz et al. 2019; Akay, 2020; Grillner and El Manira, 2020).

1.4.1 Proprioception

Proprioception is important for monitoring the contraction state of muscles. Proprioceptive afferents mainly originate from the muscle spindles and Golgi tendons organs (GTOs) located in muscles that measure the stretch and tension applied to the muscle, respectively. GTOs are located in the muscle tendons and measure changes in muscle tension. GTOs relay this information to the spinal cord via group Ib afferent fibers (Houk and Henneman, 1967). On the other hand, muscle spindles are proprioceptive sensory organs consisting of sensory and motor endings embedded among the muscle fibers (Ruffini, 1898). Each muscle spindle transmits sensory afferents via group Ia and group II fibers. Group Ia fibers transmit sensory information regarding the change in the muscle spindle length, while group II fibers transmit information related to the tonic stretch of the spindles (Hulliger, 1984). Muscle spindles also receive input from gamma motoneurons, which ensure that the muscle spindles are at functional lengths and that the muscle spindles are sensitive throughout the muscle contraction (Ellaway et al. 2002; Taylor et al. 2006).

Muscle afferent feedback modulates the duration and amplitude of muscle activity during the different subphases of the step cycle (Rossignol et al. 2006). Experiments in mice have shown that removing proprioceptive afferents disrupts the locomotor pattern (Akay et al. 2014; Takeoka and Arber, 2019), or their ability to adjust to external

perturbation (Santuz et al. 2019) while mice born without muscle spindles present signs of gait ataxia (Tourtellotte and Milbrandt, 1998; Akay et al. 2014). During locomotion, proprioceptive sensory information is necessary to regulate the temporal parameters of rhythmic movements at individual joints as well as regulate cross-joint muscle coordination. Group Ia/II sensory afferents originating from the muscle spindle regulate alternating flexor muscle activity while GTOs determine the pattern of extensor muscle firing (Akay et al. 2014). When group Ib afferents are either removed or inactivated by putting the animal in the water, the temporal motor recruitment and motor pattern organization are disturbed (Akay et al. 2014; Santuz et al. 2019). Subsequent studies demonstrated that ankle extensor muscle spindle feedback is involved in regulating muscle activity strength and speed-dependent amplitude modulation (Mayer et al. 2018). Dynamic stability is also impaired during walking in the absence of muscle spindle feedback due to improper muscle activity recruitment throughout the step cycle (Santuz et al. 2019). Similarly, mice display significant degradation of their locomotor pattern, especially in their ability to adjust to different speeds when selective ablation of muscle spindle and GTOs occurs after birth (Takeoka and Arber, 2019).

Proprioceptive afferents are also responsible for determining the hindlimb paw position in relation to the ipsilateral forelimb position. Indeed, when a perturbation elicits a stumbling corrective reaction of the hindlimb, the position of the forelimb and hindlimb paws shifts more posteriorly relative to the body (Mayer and Akay, 2021), indicating that proprioceptive input from one leg is important for modulating the motor activity of other limbs (Mayer and Akay, 2021) suggesting that proprioceptive input from one leg is important to modulate the motor activity of other limbs. To summarize, these findings suggest that locomotor deficits induced by the removal of proprioceptive feedback are also proportionally correlated with the level of ablation (i.e., if only muscle spindles are ablated or if both spindles and GTOs are ablated). Henceforth, constant proprioceptive feedback from the muscle spindle and GTOs are required to maintain a robust locomotor pattern.

1.4.2 Cutaneous afferents

Cutaneous sensory afferents come from a variety of sensory receptors located in the skin that convey information about vibration, stretch, and touch. This information is

relayed from the skin through low threshold mechanoreceptor (LTMR) primary sensory afferents of varying sizes and conduction velocities (Abraira and Ginty, 2013; Lai et al. 2016). During locomotion, cutaneous afferents provide information regarding the pressure of the foot, step progression, and level of weight-bearing on a step-by-step basis (Rossignol et al. 2006). The absence of cutaneous input does not prevent the expression of the locomotor rhythm (Sherrington, 1910; Endberg, 1964; Forssberg et al. 1977; Prochazka et al. 1978; Duysen and Stein, 1978; Wand et al. 1980; Bouyer and Rossignol, 2003a). However, subtle adaptations such as a faster swing phase, increased foot lift, and increases in double support (i.e., both limbs on the ground) can be seen in cats following cutaneous ablation. Furthermore, recently denervated cats were unable to walk on a horizontal ladder. Eventually, the denervated cats developed adaptative strategies that had them grasp the rungs to perform the task instead of placing their paw pads on the rung (Bouyer and Rossignol, 2003a). Interestingly, denervated and spinalized cats were unable to correctly place their feet on the plantar surface or bear weight during spinal locomotion. In contrast, a non-denervated spinalized cat was able to regain correct plantar foot placement and steadily walk on a treadmill (Bouyer and Rossignol, 2003b). These findings suggest that animals can maintain locomotor rhythm without cutaneous inputs. This ability is most likely induced by compensatory mechanisms from other sensory afferents and supraspinal structures that substitute for the missing cutaneous information. Since cutaneous inputs participate in the control of the paw placement during locomotion in spinalized animals, then they likely play a role in the adaptation of locomotion and the recovery of locomotor activity after spinal cord injury.

1.5 RATIONALE AND AIMS

The study of dynamic sensorimotor interactions during locomotion is of interest not only to determine how various reflex responses may give rise to coherent corrections of locomotion to perturbations, but it may also reveal basic mechanisms of sensorimotor integration during movement. It is more than likely that the dynamic regulation of responses to unexpected perturbations also applies to the regulation of the normal step cycle by the same afferents during unperturbed walking. Studying reflexes during rhythmic processes thus permits the understanding of many of the processes occurring in the

background that are revealed only if unexpected events occur. These processes may be important in pathological conditions in which they may be absent or reduced. Thus, it might well be that after neurotrauma or neurological diseases, the ability to correct planned movements is also impaired, as well as the movements themselves (Zehr et al. 1998).

Locomotion is one of the most essential behaviours that allow animals to move. In legged animals, locomotion is characterized by the coordinated movement of legs on both sides of the body. This involves a complex interaction between supraspinal command, spinal locomotor circuitry, and inputs from somatosensory afferents. Over the years, significant progress has been made in decoding the organization and function of spinal locomotor circuitry. Using novel molecular genetic tools, we can investigate interneuron populations and their roles in distinct behaviours. Commissural interneurons coordinate and control interlimb coordination, yet our understanding of their interaction with somatosensory feedback during locomotion is incomplete. Contralateral reflex responses involve commissural interneurons which modulate motor activity. However, the relationship between the commissural pathways involved in the crossed reflex, and those involved in locomotion is unknown. Therefore, the use of genetically manipulated mice could advance our understanding of the networks that control the transmission of sensory afferents to the contralateral leg.

Analogous crossed reflexes have been observed in rodents such as the mouse (Jiang et al., 1999; Nakanishi & Whelan, 2012), rat (Valero-Cabré et al. 2004), and hamster (Bagust and Kerkut, 1987). Using in vitro spinal cord preparations of these animals, ipsilateral motor neuron responses were evoked after contralateral sensory afferents were activated in the presence of strychnine, a glycine receptor antagonist. This, however, was only to a limited degree (Bagust and Kerkut, 1987; Jiang et al. 1999). More recently, crossed reflexes have been recorded in vivo in decerebrate and immobilized adult mice, which were initiated by a moderately strong toe pinch (Nakanishi and Whelan, 2012). Clearly, sensory afferents on one side of the body can induce motor activity on the contralateral side. However, the crossed reflex was not the primary focus of these experiments Henceforth, the spinal circuitry underlying crossed reflexes is thus unknown.

The first aim of my Ph.D. thesis is to understand how the mouse crossed reflex compares to other animal models previously described, and to understand the underlying somatosensory circuitry that modulates the crossed reflex. To do this, I used a combination of electrophysiological and behavioural recordings to provide a detailed description of crossed reflexes in mice. The second aim of my thesis is to understand the relationship between the commissural pathways involved in locomotion and those involved in the crossed reflex.

In chapter 2, I describe the motor output following stimulation of proprioceptive and cutaneous afferents at rest and during locomotion. To do this, I recorded motor output in one leg while I stimulated nerves with proprioceptive and cutaneous afferents in the contralateral leg in vivo. It demonstrates that crossed reflex involves a short-latency inhibitory followed by an excitatory pathway in flexor and extensor muscles.

In chapter 3, I investigate how, in the crossed reflex, the origin of the sensory input impacts the motor output. To do this, we stimulated the common peroneal nerve, innervating the ankle flexor muscles and the skin covering the anterolateral aspect in mice in vivo and compared it to the tibial nerve. It demonstrates that crossed reflexes regardless of the stimulated nerves are mostly similar with slight differences, mainly in the existence of long-latency crossed reflex responses when the common peroneal nerve is stimulated.

In chapter 4, I investigate the involvement of two commissural interneurons important for left-right coordination during locomotion (V0 and V3 commissural interneurons) and assess their role in the transmission of sensory afferents. It demonstrates that V3 but not V0 commissural interneurons are involved in the transmission of sensory afferents. As V3 interneurons are mainly excitatory, this suggests that local inhibitory interneurons are also involved in the inhibitory crossed reflex pathways.

In chapter 5, I investigate the role of dorsal interneurons (dPVs) in the crossed inhibitory pathways described in the previous chapters. It demonstrates that although dPVs tend to show signs of crossed reflex inhibition in mice, these results are not significant. Subsequent analysis revealed that dPVs interneurons were, however, important for mediating local inhibitory pathways.

In chapter 6, I summarize, discuss, and conclude the major findings reached in our work. Taken together, my work highlights the spinal circuitry involved in the crossed reflex and sheds new light on the somatosensory component of locomotion.

1.6 FIGURES

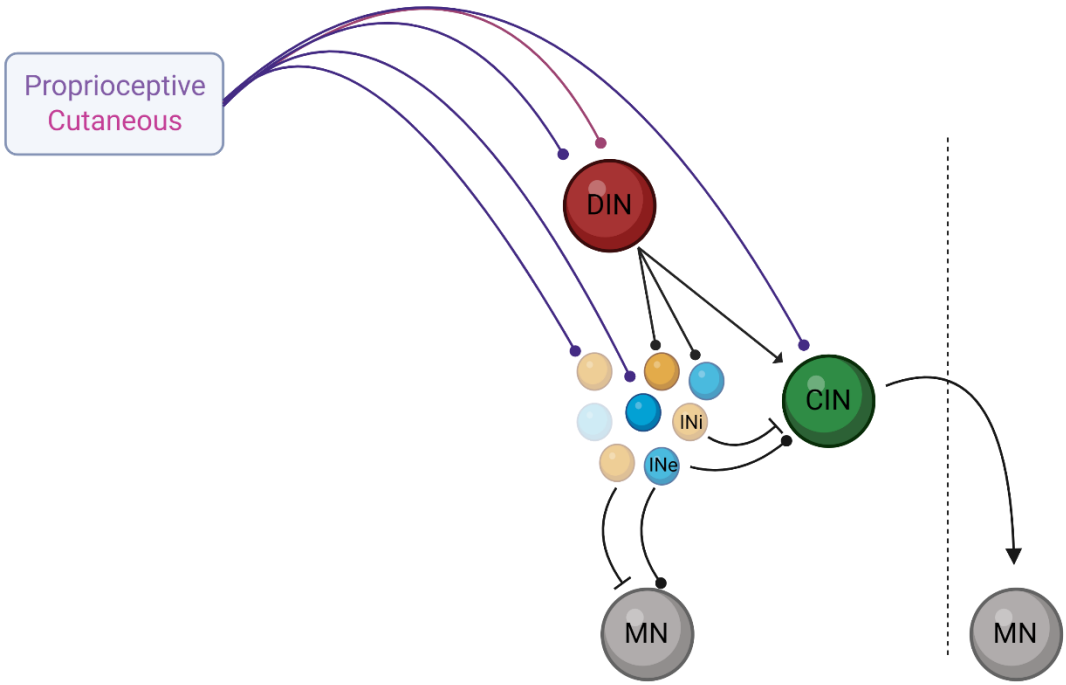

Figure 1.1. Simplified diagram of the hypothetical connections underlying crossed reflex pathway. The diagram shows ventrally located commissural interneurones (CIN) which connect to motoneurones (MN). These are activated by proprioceptive afferents both monosynaptically and polysynaptically, the latter via dorsal horn neurons (DIN) or excitatory (INe) or inhibitory (INi) premotor interneurons. Many dorsal horn neurons have monosynaptic input from cutaneous afferents, which provides the link in the pathway. Adapted from Edgley and Aggelopoulos, 2006 and Jankowska, 2010.

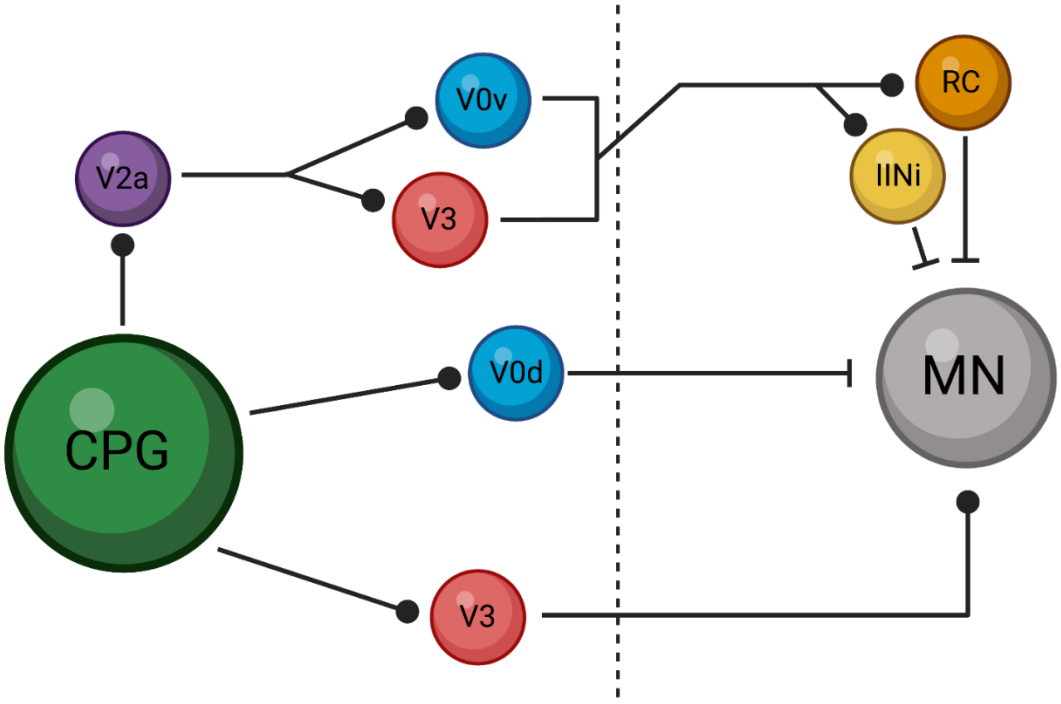

Figure 1.2. Organization of left-right coordinating CPG circuits. The core of the left-right system in rodents is composed of commissural interneurons (CINs) acting directly via inhibitory CINs, or indirectly, via excitatory CINs on contralateral motor neurons (MN). This system is involved in left-right alternation. Left-right coordination is also obtained via a single excitatory system acting directly on motor neurons. To obtain left-right coordination during locomotion, these crossed connections should also connect to the rhythm-generating core (indicated with dotted lines) on the other side of the cord and/or corresponding commissural interneurons. The dotted line indicates the midline. Abbreviations: IINi: ipsilaterally projecting inhibitory interneuron. RC: Renshaw Cell. MN: motor neuron, CPG Central Pattern Generator. Adapted from Kiehn 2011.

1.7 REFERENCES

Abraira VE, Ginty DD. The sensory neurons of touch. **Neuron** 79:618–639, 2013

Aggelopoulos NC, Burton MJ, Clarke RW, Edgley SA. Characterization of a descending system that enables crossed group II inhibitory reflex pathways in the cat spinal cord. **J Neurosci** 16:723–729, 1996.

Aggelopoulos NC, Edgley SA. Segmental localisation of the relays mediating crossed inhibition of hindlimb motoneurones from group II afferents in the anaesthetized cat spinal cord. **Neurosci Lett** 185:60–64, 1995.

Akay T. Sensory Feedback Control of Locomotor Pattern Generation in Cats and Mice. **Neuroscience** 450:161–167, 2020. https://doi.org/10.1016/j.neuroscience.2020.05.008.

Akay T, Tourtellotte WG, Arber S, Jessell TM. Degradation of mouse locomotor pattern in the absence of proprioceptive sensory feedback. **Proc Natl Acad Sci U S A** 111:16877–16882, 2014.

Alaynick WA, Jessell TM, Pfaff SL SnapShot : Spinal Cord Development. **Cell** 146:178-178.e1, 2011.

Andersson LS, Larhammar M, Memic F, Wootz H, Schwochow D, Rubin C-J, Patra K, Arnason T, Wellbring L, Hjälm G, Imsland F, Petersen JL, McCue ME, Mickelson JR, Cothran G, Ahituv N, Roepstorff L, Mikko S, Vallstedt A, Lindgren G, Andersson L, Kullander K. Mutations in DMRT3 affect locomotion in horses and spinal circuit function in mice. **Nature** 488: 642–6, 2012.

Arber S. Motor Circuits in Action: Specification, Connectivity, and Function. **Neuron** 74: 975–989, 2012.

Arya T, Bajwa S, Edgley SA. Crossed reflex actions from group II muscle afferents in the lumbar spinal cord of the anaesthetized cat. **J physiology** 444: 117–131, 1991.

Bagust J, Kerkut GA. Crossed reflex activity in an entire, isolated, spinal cord preparation taken from juvenile rodents. **Brain Res** 411: 397–399, 1987.

Bannatyne BA. Differential Projections of Excitatory and Inhibitory Dorsal Horn Interneurons Relaying Information from Group II Muscle Afferents in the Cat Spinal Cord. **J Neurosci** 26: 2871–2880, 2006.

Bannatyne BA, Edgley SA, Hammar I, Jankowska E, Maxwell DJ. Networks of inhibitory and excitatory commissural interneurons mediating crossed reticulospinal actions. **Eur J Neurosci** 18: 2273–2284, 2003.

Bellardita C, Kiehn O. Phenotypic Characterization of Speed-Associated Gait Changes in Mice Reveals Modular Organization of Locomotor Networks. **Curr Biol** 25: 1426–1436, 2015.

Blacklaws J, Deska-Gauthier D, Jones CT, Petracca YL, Liu M, Zhang H, Fawcett JP, Glover JC, Lanuza GM, Zhang Y. Sim1 is required for the migration and axonal projections of V3 interneurons in the developing mouse spinal cord. **Dev Neurobiol** 75: 1003–1017, 2015.

Borowska J, Jones CT, Deska-Gauthier D, Zhang Y. V3 interneuron subpopulations in the mouse spinal cord undergo distinctive postnatal maturation processes. **Neuroscience** 295: 221–228, 2015.

Borowska J, Jones CT, Zhang H, Blacklaws J, Goulding M, Zhang Y. Functional subpopulations of V3 interneurons in the mature mouse spinal cord. **J Neurosci** 33: 18553–65, 2013.

Bouyer L, Rossignol S. Contribution of cutaneous inputs from the hindpaw to the control of locomotion in rats. **Behav Brain Res** 176: 193–201, 2003.

Chopek JW, Nascimento F, Beato M, Brownstone RM, Chopek JW, Nascimento F, Beato M, Brownstone RM, Zhang Y. Sub-populations of Spinal V3 Interneurons Form Focal Modules of Layered Pre-motor Microcircuits Article Sub-populations of Spinal V3 Interneurons Form Focal Modules of Layered Pre-motor Microcircuits. **CellReports** 25: 146-156.e3, 2018.

Deska-gauthier D, Zhang Y. The functional diversity of spinal interneurons and locomotor control. **Curr. Opin. Psychol.** (2019). doi: 10.1016/j.cophys.2019.01.005.

Duysens J. Reflex control of locomotion as revealed by stimulation of cutaneous afferents in spontaneously walking premammillary cats. **J Neurophysiol** 40: 737–751, 1977.

Duysens J, Loeb GE. Modulation of ipsi- and contralateral reflex responses in unrestrained walking cats. **J Neurophysiol** 44: 1024–1037, 1980.

Duysens J, Loeb GE, Weston BJ. Crossed flexor reflex responses and their reversal in freely walking cats. **Brain Res** 197: 538–42, 1980.

Duysens J, Stein RB. Reflexes induced by nerve stimulation in walking cats with implanted cuff electrodes. **Exp Brain Res** 32: 213–224, 1978.

Duysens J, Tax AAM, van der Doelen B, Trippel M, Dietz V. Selective activation of human soleus or gastrocnemius in reflex responses during walking and running. **Exp Brain Res** 87: 193–204, 1991.

Dyck J, Lanuza GM, Gosgnach S. Functional characterization of dI6 interneurons in the neonatal mouse spinal cord. **J Neurosci** 107: 3256–3266, 2012.

Ellaway P, Taylor A, Durbaba R, Rawlinson S. Role of the Fusimotor System in Locomotion. In: *Sensorimotor Control of Movement and Posture*, edited by Gandevia SC, Proske U, Stuart DG. Springer US, p. 335–342.

Engberg I. Reflexes to Foot Muscles in the Cat. **Acta Physiol. Scand. Suppl**.1964 http://www.ncbi.nlm.nih.gov/pubmed/14188019.

Forssberg H, Grillner S, Rossignol S. Phasic gain control of reflexes from the dorsum of the paw during spinal locomotion. **Brain Res** 132: 121–139, 1977.

Frigon A, Rossignol S. Short-latency crossed inhibitory responses in extensor muscles during locomotion in the cat. **J Neurophysiol** 99: 989–998, 2008.

Gervasio S, Kersting UG, Farina D, Mrachacz-Kersting N. The effect of crossed reflex responses on dynamic stability during locomotion. **J Neurophysiol** 114: 1034–1040, 2015.

Gervasio S, Voigt M, Kersting UG, Farina D, Sinkjaer T, Mrachacz-Kersting N. Sensory feedback in interlimb coordination: Contralateral afferent contribution to the short-latency crossed response during human walking. **PLoS One** 12: 1–24, 2017.

Giuliani CA, Smith JL. Stepping behaviors in chronic spinal cats with one hindlimb deafferented. **J Neurosci** 7: 2537–2546, 1987.

Goldberger ME. Locomotor recovery after unilateral hindlimb deafferentation in cats. **Brain Res** 123: 59–74, 1977.

Gosgnach S, Bikoff JB, Kimberly X, Dougherty J, Manira A El, Lanuza GM, Zhang Y. Delineating the Diversity of Spinal Interneurons in Locomotor Circuits. **J Neurosci** 37: 10835–10841, 2017.

Goulding M. Circuits controlling vertebrate locomotion: moving in a new direction. **Nat Rev Neurosci** 10: 507–518, 2009.

Griener A, Zhang W, Kao H, Haque F, Gosgnach S. Anatomical and electrophysiological characterization of a population of dI6 interneurons in the neonatal mouse spinal cord. **Neuroscience** 362: 47–59, 2017.

Grillner S, El Manira A. Current principles of motor control, with special reference to vertebrate locomotion. **Physiol Rev** 100: 271–320, 2020.

Grillner S, Zangger P. The effect of dorsal root transection on the efferent motor pattern in the cat's hindlimb during locomotion. **Acta Physiol Scand** 120: 393–405, 1984.

Gross MK, Dottori M, Goulding M. Lbx1 specifies somatosensory association interneurons in the dorsal spinal cord. **Neuron** 34: 535–549, 2002.

Haque F, Rancic XV, Zhang W, Clugston XR, Ballanyi XK, Gosgnach XS. WT1 - Expressing Interneurons Regulate Left – Right Alternation during Mammalian Locomotor Activity. **J Neurosci** 38: 5666–5676, 2018.

Harrison PJ, Jankowska E, Zythicki D. Lamina VIII interneurones interposed in crossed reflex pathways in the cat. **J physiology**: 90–91, 1986.

Harrison PJ, Zytnicki D. Crossed actions of group I muscle afferents in the cat. **J Physiol** 356: 263–273, 1984.

Houk J, Henneman E. Responses of Golgi tendon organs to active contractions of the soleus muscle of the cat. **J Neurophysiol** 30: 466–481, 1967.

Hulliger M. The mammalian muscle spindle and its central control. **Rev Physiol Biochem Pharmacol** 101: 1–110, 1984.

Hurteau M-F, Thibaudier Y, Dambreville C, Chraibi A, Desrochers E, Telonio A, Frigon A. Nonlinear Modulation of Cutaneous Reflexes with Increasing Speed of Locomotion in Spinal Cats. **J Neurosci** 37: 3896–3912, 2017.

J. Briscoe, L. Sussel, P. Serup, D. Hartigan-O'Connor, T. M. Jessell, J. L. R. Rubenstein, J. Ericson*. Homeobox gene Nkx2.2 and specification of neuronal identity by graded Sonic hedgehog signalling. **Nature** 398: 622–627, 1999.

Jankowska E, Bannatyne BA, Stecina K, Hammar I, Cabaj A, Maxwell DJ. Commissural interneurons with input from group I and II muscle afferents in feline lumbar segments: Neurotransmitters, projections and target cells. **J Physiol** 587: 401–418, 2009.

Jankowska E, Edgley S a, Krutki P, Hammar I. Functional differentiation and organization of feline midlumbar commissural interneurones. **J Physiol** 565: 645–658, 2005.

Jankowska E, Noga BRR. Contralaterally projecting lamina VIII interneurones in middle lumbar segments in the cat. **Brain Res** 535: 327–330, 1990.

Jessell TM. Neuronal specification in the spinal cord: inductive signals and transcriptional codes. **Nat Rev Genet** 1: 20–29, 2000.

Jiang Z, Carlin KP, Brownstone RM. An in vitro functionally mature mouse spinal cord preparation for the study of spinal motor networks. **Brain Res** 816: 493–499, 1999.

Kiehn O. Decoding the organization of spinal circuits that control locomotion. **Nat Rev Neurosci** 17: 224–238, 2016.

Kudo N, Yamada T. N-Methyl-d,l-aspartate-induced locomotor activity in a spinal cord-hindlimb muscles preparation of the newborn rat studied in vitro. **Neurosci Lett** 75: 43–48, 1987.

Lai HC, Seal RP, Johnson JE. Making sense out of spinal cord somatosensory development. **Development** 143: 3434–3448, 2016.

Lanuza GM, Gosgnach S, Pierani A, Jessell TM, Goulding M. Genetic identification of spinal interneurons that coordinate left-right locomotor activity necessary for walking movements. **Neuron** 42: 375–386, 2004.

Lu DC, Niu T, Alaynick WA. Molecular and cellular development of spinal cord locomotor circuitry. **Front Mol Neurosci** 8: 25, 2015.

Matsuyama K, Kobayashi S, Aoki M. Projection patterns of lamina VIII commissural neurons in the lumbar spinal cord of the adult cat: An anterograde neural tracing study. **Neuroscience** 140: 203–218, 2006.

Matsuyama K, Mori F, Nakajima K, Drew T, Aoki M, Mori S. Locomotor role of the corticoreticular-reticulospinal-spinal interneuronal system. **Prog Brain Res** 143: 239–249, 2004a.

Matsuyama K, Nakajima K, Mori F, Aoki M, Mori S. Lumbar commissural interneurons with reticulospinal inputs in the cat: Morphology and discharge patterns during fictive locomotion. **J Comp Neurol** 474: 546–561, 2004b.

Mayer WP, Akay T. Stumbling corrective reaction elicited by mechanical and electrical stimulation of the saphenous nerve in walking mice. **J Exp Biol** 221, 2018.

Mayer WP, Akay T. The role of muscle spindle feedback in the guidance of hindlimb movement by the ipsilateral forelimb during locomotion in mice. **eNeuro** 8: 1–13, 2021.

Miles GB, Hartley R, Todd AJ, Brownstone RM. Spinal cholinergic interneurons regulate the excitability of motoneurons during locomotion. **Proc Natl Acad Sci U S A** 104: 2448–2453, 2007.

Mrachacz-Kersting N, Geertsen SS, Stevenson AJT, Nielsen JB. Convergence of ipsi- and contralateral muscle afferents on common interneurons mediating reciprocal inhibition of ankle plantarflexors in humans. **Exp Brain Res** 235: 1555–1564, 2017.

Nakanishi ST, Whelan PJ. A decerebrate adult mouse model for examining the sensorimotor control of locomotion. **J Neurophysiol** 107: 500–515, 2012.

Pierani A, Moran-Rivard L, Sunshine MJ, Littman DR, Goulding M, Jessell TM. Control of interneuron fate in the developing spinal cord by the progenitor homeodomain protein Dbx1. **Neuron** 29: 367–384, 2001.

Prochazka A, Sontag KH, Wand P. Motor reactions to perturbations of gait: proprioceptive and somesthetic involvement. **Neurosci Lett** 7: 35–39, 1978.

Rossignol S, Dubuc R, Gossard J-P, Dubuc J. Dynamic Sensorimotor Interactions in Locomotion. **Physiol Rev** 86: 89–154, 2006.

Ruffini A, Histology L, Uni- R. the Minute Anatomy of the Neuro- Their Physiological Significance. **J Physiol** 23: 190-208.3, 1898.

Santuz A, Akay T, Mayer WP, Wells TL, Schroll A, Arampatzis A. Modular organization of murine locomotor pattern in the presence and absence of sensory feedback from muscle spindles. **J Physiol** 597: 3147–3165, 2019.

Sherrington CS. Flexion-reflex of the limb crossed extension-reflex, and reflex stepping and standing. **J Physiol** 40: 28–121, 1910.

Smith JC, Feldman JL. In vitro brainstem-spinal cord preparations for study of motor systems for mammalian respiration and locomotion. **J Neurosci Methods** 21: 321–333, 1987.

Stubbs PW, Mrachacz-Kersting N. Short-latency crossed inhibitory responses in the human soleus muscle. **J Neurophysiol** 102: 3596–3605, 2009.

Stubbs PW, Nielsen JF, Sinkjaer T, Mrachacz-Kersting N. Phase Modulation of the Short-Latency Crossed Spinal Response in the Human Soleus Muscle. **J Neurophysiol** 105: 503–511, 2011.

Stubbs PW, Nielsen JF, Sinkjær T, Mrachacz-Kersting N. Short-latency crossed spinal responses are impaired differently in sub-acute and chronic stroke patients. **Clin Neurophysiol** 123: 541–549, 2012.

Takeoka A, Arber S. Functional Local Proprioceptive Feedback Circuits Initiate and Maintain Locomotor Recovery after Spinal Cord Injury. **Cell Rep** 27: 71-85.e3, 2019.

Talpalar AE, Bouvier J, Borgius L, Fortin G, Pierani A, Kiehn O. Dual-mode operation of neuronal networks involved in left-right alternation. **Nature** 500: 85–8, 2013.

Taylor A, Durbaba R, Ellaway PH, Rawlinson S. Static and dynamic γ-motor output to ankle flexor muscles during locomotion in the decerebrate cat. **J Physiol** 571: 711–723, 2006.

Tourtellotte WG, Milbrandt J. Sensory ataxia and muscle spindle agenesis in mice lacking the transcription factor Egr3. **Nat Genet** 20: 87–91, 1998.

Valero-Cabré A, Forés J, Navarro X. Reorganization of Reflex Responses Mediated by Different Afferent Sensory Fibers After Spinal Cord Transection. **J Neurophysiol** 91: 2838–2848, 2004.

Wand P, Pompeiano O, Fayein NA. Impulse decoding process in extensor motoneurons of different size during the vibration reflex. **Arch Ital Biol** 118: 205–242, 1980.

Wetzel MC, Atwater AE, Wait J V., Stuart DG. Kinematics of locomotion by cats with a single hindlimb deafferented. **J Neurophysiol** 39: 667–678, 1976.

Zagoraiou L, Akay T, Martin JF, Brownstone RM, Jessell TM, Miles GB. A Cluster of Cholinergic Premotor Interneurons Modulates Mouse Locomotor Activity. **Neuron** 64: 645–662, 2009.

Zhang H, Shevtsova NA, Deska-Gauthier D, Mackay C, Dougherty KJ, Danner SM, Zhang Y, Rybak IA. The role of V3 neurons in speed-dependent interlimb coordination during locomotion in mice. **Elife** 11: 1–34, 2022.

Zhang Y, Narayan S, Geiman E, Lanuza GM, Velasquez T, Shanks B, Akay T, Dyck J, Pearson K, Gosgnach S, Fan CM, Goulding M. V3 Spinal Neurons Establish a Robust and Balanced Locomotor Rhythm during Walking. **Neuron** 60: 84–96, 2008.

Zhong G, Shevtsova NA, Rybak IA, Harris-Warrick RM. Neuronal activity in the isolated mouse spinal cord during spontaneous deletions in fictive locomotion: insights into locomotor central pattern generator organization. **J Physiol** 590: 4735–4759, 2012.

Chapter 2. Excitatory and inhibitory crossed reflex pathways in mice

Contribution statement

The work presented in this chapter was published in the Journal of Neurophysiology.

Laflamme OD, Akay T. Excitatory and inhibitory crossed reflex pathways in mice. **J Neurophysiol** 120: 2897–2907, 2018. doi:10.1152/jn.00450.2018.

I would like to thank Brenda Ross for her technical assistance with the mouse colony.

2.1 ABSTRACT

Sensory information from one leg has been known to elicit reflex responses in the contralateral leg, known as "crossed reflexes," and these have been extensively investigated in cats and humans. Furthermore, experiments with mice have shown commissural pathways in detail by using in vitro and in vivo physiological approaches combined with genetics. However, the relationship between these commissural pathways discovered in mice and crossed reflex pathways described in cats and humans is not known. In this study, we analyzed the crossed reflex in mice by using in vivo electromyographic recording techniques combined with peripheral nerve stimulation protocols to provide a detailed description of the crossed reflex pathways. We show that excitatory crossed reflexes are mediated by both proprioceptive and cutaneous afferent activation. In addition, we provide evidence for a short-latency inhibitory crossed reflex pathway likely mediated by cutaneous feedback. Furthermore, the short-latency crossed inhibition is downregulated in the knee extensor muscle and the ankle flexor muscle during locomotion. In conclusion, this article provides an analysis of excitatory and inhibitory crossed reflex pathways during resting and locomoting mice in vivo. The data presented in this article pave the way for future research aimed at understanding crossed reflexes using genetics in mice.

2.2 INTRODUCTION

Coordinated leg movement during locomotion is generated by the patterned activation of multiple motor neuron pools (locomotor pattern) that drives the orchestrated contraction of multiple leg muscles both within and between legs. The locomotor pattern of an individual leg is driven by a network of interconnected sets of premotor interneurons in the spinal cord (central pattern generator, CPG) and the sensory feedback, mediated by cutaneous and proprioceptive inputs, from the periphery (McCrea, 2001; Pearson, 2004; Rossignol et al. 2006). Sensory feedback refines the spatiotemporal features of motor output during locomotion (McCrea, 2001; Akay et al. 2014; Böhm and Wyart, 2016), and the removal of sensory feedback severely impairs locomotion (Akay et al. 2014). These data suggest that certain aspects of the locomotor pattern can be generated by the CPG, but

sensory feedback is necessary for a functional locomotor pattern because it occurs during intact locomotion.

Reflex pathways that convey sensory information from one leg to the contralateral leg (crossed reflex pathways) were first described more than a century ago (Sherrington, 1910). By using the cat as an animal model, it has been established that commissural interneurons (CINs), whose cell bodies are located in lamina VIII of the spinal cord, synapse with the spinal circuitry on the contralateral side (Jankowska, 2008; Jankowska and Edgley, 2010). These CINs are thought to be important in left-right coordination during locomotion (Matsuyama et al. 2004a; 2004b) and have been shown to transmit sensory information to contralateral motor neurons (Sherrington, 1910; Arya et al. 1991; Aggelopoulos and Edgley, 1995; Edgley et al. 2003; Jankowska et al. 2005). Proprioceptive sensory afferents (group I and II) and cutaneous afferents mediate crossed reflex responses in flexor and extensor muscles in anesthetized and awake cats during locomotion (Perl, 1957; Duysens and Loeb, 1980; Gauthier and Rossignol, 1981; Arya et al. 1991; Aggelopoulos et al. 1996; Edgley and Aggelopoulos, 2006; Hurteau et al. 2018).

Mice have become important for the investigation of neuronal mechanisms involved in locomotion because of the potential for genetic manipulation of their neural circuits underlying locomotion (Jessell, 2000; Goulding, 2009; Garcia-Campmany et al. 2010). Specifically, it has been shown that the commissural pathways involve genetically distinct classes of CINs that are important in left-right coordination during locomotion (Lanuza et al. 2004; Zhang et al. 2008; Talpalar et al. 2013). As in the CINs identified in cats, the cell bodies of some of these CINs in mice are also located in lamina VIII of the spinal cord (Lanuza et al. 2004; Zhang et al. 2008; Lu et al. 2015). Yet, because of the technical limitations of measuring crossed reflexes in mice in vivo, the role of these CINs in mice in crossed reflexes is not known. Crossed reflexes have been shown in rodents with the use of in vitro spinal cord preparations, where sensory afferents were activated on one side of the spinal cord and motor neuron responses were observed on the contralateral side, but only to a limited degree (Bagust and Kerkut, 1987; Jiang et al. 1999). More recently, crossed reflexes have been recorded in vivo in decerebrate and immobilized adult mice, initiated by a moderately strong toe pinch (Nakanishi and Whelan, 2012), demonstrating

that activation of sensory afferents on one side of the body can induce motor activity on the contralateral side. Insights into the structure of the spinal circuitry underlying crossed reflexes are still obscure. Mutant mice with genetically modified spinal circuitry could resolve this obscurity. This article provides the first detailed description of crossed reflex responses in fully awake mice during resting and walking on a treadmill.

To describe the crossed reflex in awake adult mice, we recorded the electromyogram (EMG) activity from up to five hindlimb muscles while we stimulated peripheral nerves in the contralateral hind leg to activate sensory afferent fibers. We show that crossed reflex actions include flexor and extensor muscle activation mediated by both proprioceptive and cutaneous afferents. Furthermore, our data suggest that inhibitory as well as excitatory crossed reflex pathways can be measured using the techniques presented. Finally, we provide evidence that the inhibitory crossed reflex pathway is subject to modulation when the animal walks. These experiments lay the groundwork in the mouse model to identify specific CIN pathways involved in crossed reflexes and the role of these crossed reflex pathways during motor behaviour.

2.3 METHODS

Experiments were conducted on 2- to 4-mo-old wild-type (WT) C57BL/6 mice of both sexes. None of the mice were trained on the treadmill before the experiments. All studies were performed according to the guidelines of the Canadian Council on Animal Care and approved by the local councils on animal care at Dalhousie University.

2.3.1 Construction of the electrodes.

The electrodes were made using multistranded, Teflon-coated annealed stainless steel wire (catalog no. 793200; A-M Systems). The construction of the EMG electrode and nerve cuff was previously described in detail (Pearson et al. 2005; Akay et al. 2006; Akay, 2014). One or two nerve cuff electrodes and six EMG recording electrodes were attached to the headpiece pin connector (female, part no. SAM1153-12; DigiKey Electronics, Thief River Falls, MN) and covered with epoxy (5 Minute epoxy gel; Devcon).

2.3.2 Electrode implantation surgeries.

All surgeries were performed in aseptic conditions on a warm water-circulated heating pad maintained at 42°C. Each mouse underwent an electrode implantation surgery as previously described (Akay, 2014). Briefly, the animals were anesthetized with isoflurane (5% for inductions, 2% for maintenance of anesthesia), ophthalmic eye ointment was applied to the eyes, and their skin was sterilized with a three-part skin scrub using hibitane, alcohol, and povidone-iodine. Before each surgery, buprenorphine (0.03 mg/kg) and ketoprofen (5 mg/kg) were injected subcutaneously as analgesics while the animals were still under anesthesia. Additional buprenorphine injections were performed at 12-h intervals for 48 h.

A set of six bipolar EMG electrodes and one or two nerve stimulation cuffs were implanted in all experimental mice (Pearson et al. 2005; Akay et al. 2006) as follows: small incisions were made on the shaved areas (neck and both hind legs), and each bipolar EMG electrode and the nerve cuff electrodes were led under the skin from the neck incision to the leg incisions, and the headpiece connector was stitched to the skin around the neck incision. The EMG recording electrodes were implanted into the right (ipsilateral) hip flexor (iliopsoas, Ip_r), knee flexor (semitendinosus, St_r) and extensor (vastus lateralis, VL_r), and ankle flexor (tibialis anterior, TA_r) and extensor (gastrocnemius, Gs_r), as well as the left ankle extensor (gastrocnemius, Gs_l). Nerve stimulation electrodes were chronically implanted in the left leg to activate contralateral proprioceptive and cutaneous feedback (tibial nerve) or predominantly cutaneous afferents (sural nerve), as well as in the right leg to activate ipsilateral cutaneous afferents (sural nerve). Anesthesia was discontinued, and mice were placed in a heated cage for 3 days before being returned to a regular mouse rack. Food mash and hydrogel were provided for the first 3 days after the surgery. Any handling of the mouse was avoided until the animal was fully recovered, and the first recording session started at least 10 days after the electrode implantation surgery.

In total, 19 WT mice received electrode implantation surgeries. In nine mice, a cuff electrode was implanted on the tibial nerve, and in another nine mice, the cuff electrode was implanted on the sural nerve of the left hind leg. In five mice of each group, an

additional cuff electrode was implanted on the sural nerve of the right leg. In one mouse, cuff electrodes were implanted on both the tibial and the sural nerve of the left hind leg.

2.3.3 Crossed reflex recording sessions.

After animals fully recovered (~10 days) from electrode implantation surgeries, crossed reflexes were recorded as follows: under brief anesthesia with isoflurane, a wire to connect the headpiece connector with the amplifier, and the stimulation insulation units (ISO-FLEX; A.M.P.I., Jerusalem, Israel or DS4; Digitimer, Welwyn Garden City, UK) was attached to the mouse. Anesthesia was discontinued, and the mouse was placed on a mouse treadmill (model 802; custom-built in the workshop of the Zoological Institute, University of Cologne, Germany). The electrodes were connected to an amplifier (model 102; custom-built in the workshop of the Zoological Institute, University of Cologne, Germany) and a stimulus isolation unit. After the animal fully recovered from anesthesia (at least 5 min), the minimal (threshold) current that was necessary to elicit a local reflex response was determined to ensure afferent activation. This was done by injecting single impulses lasting 0.2 ms into the tibial nerve (average ± SD threshold current: 113 ± 49 µA; range: 65–200 µA; see *insets* in Fig. 2.1*B*) or double impulses lasting 0.2 ms with 2-ms intervals into the sural nerve (average ± SD threshold current: 518 ± 375 µA; range: 170–1250 µA; *insets* in Fig. 1*C*). Following the determination of threshold currents, the crossed reflex experiments were performed by injecting five current impulses lasting 0.2 ms at 500 Hz into the tibial or the sural nerve, set at either 1.2 times the threshold current (1.2× threshold) or five times the threshold current (5× threshold). The 1.2× threshold stimulation likely activates primary proprioceptive afferents (group Ia and Ib), whereas 5× threshold stimulation activates group Ia, Ib, and the group II proprioceptive afferents, as well as low-threshold cutaneous afferents (group II), as previously described in mice (Steffens et al. 2012; Schomburg et al. 2013).

EMG signals from the five muscles of the right leg and the gastrocnemius muscle of the left leg were simultaneously recorded (sampling rate: 9.803 kHz) while the sural nerve or the tibial nerve of the left leg was electrically stimulated with five brief impulses (impulse duration: 0.2 ms, frequency: 500 Hz) using the ISO-FLEX (A.M.P.I.) and DS4 (Digitimer) stimulation insulation units. In some experiments, the right sural nerve was

also stimulated in combination with contralateral tibial or sural nerve stimulation. Recordings of the crossed reflex were performed while the mice were resting on the treadmill or moving at a constant speed of 0.2 m/s. The EMG signals were amplified (gain 100), bandpass filtered from 400 Hz to 20 kHz, and stored on the computer using the Power1410 interface and Spike2 software (Cambridge Electronic Design, Cambridge, UK). The filter settings were determined empirically to limit noise in freely behaving animals.

2.3.4 Statistical analysis.

All graphical representations of data were made using GraphPad Prism 5 and processed using Illustrator CS5 (Adobe). All data are means ± SD. One-to-one statistical comparisons of the data were done with the t-test or Mann-Whitney test using GraphPad Prism 5. Comparisons involving multiple averages were performed with an ANOVA test for nonparametric data sets (Kruskal-Wallis test). All statistical tests were two-tailed, and differences were considered statistically significant when the P-value was <0.05.

2.4 RESULTS

2.4.1 Crossed reflex motor activity in flexor and extensor muscles.

First, we investigated the role of proprioceptive and cutaneous afferents in crossed reflexes in the mouse. We used in vivo electrophysiological techniques (Akay, 2014) on WT mice in which we stimulated the tibial (proprioceptive and cutaneous) and sural (cutaneous only) nerves of the left leg while simultaneously recording flexor and extensor muscles of the right leg (Fig. 2.1*A*). Low-current stimulation (1.2× threshold) of the left tibial nerve predominantly activated group Ia (from muscle spindles) and Ib (from Golgi tendon organs) proprioceptive afferents (Jack, 1978) and evoked motor responses in either flexor or extensor muscles of the right leg (Fig. 2.1*Bi*). High-current stimulation (5× threshold) of the left tibial nerve activated proprioceptive and cutaneous afferents and evoked stronger motor responses simultaneously in the right flexor and extensor muscles (Fig. 2.1*Bii*). Similarly, activation of cutaneous afferents by sural nerve stimulation induced simultaneous flexor and extensor muscle activity. Low-amplitude motor responses could be recorded at low-current sural nerve stimulation (1.2× threshold; Fig. 2.1*Ci*).

Similar to tibial nerve stimulation, an increase of the current intensity to the 5× threshold (high-current stimulation) evoked higher amplitude motor responses simultaneously in all investigated flexor and extensor muscles (Fig. 2.1*Cii*). Stimulation of either the tibial nerve or the sural nerve elicited crossed reflex responses in all recorded muscles and was more consistent when stimulation strength was set to 5× threshold. In neither of the stimulations was increased activity of the mice or vocalizing observed, suggesting pain receptors were not activated (Bui et al. 2013).

We further investigated the crossed reflex responses by analyzing the rectified EMG signals and averaging them over multiple trials (Fig. 2.2, *A* and *B*). The average EMG traces from all the trials performed at one current stimulation allowed us to determine if proprioceptive and cutaneous sensory afferents could evoke reliable motor activity in flexors and extensors of different joints in the contralateral leg. Our results show that crossed reflex responses in every recorded muscle could be elicited regardless of low- or high-current stimulation (Fig. 2.2). High-current stimulation (Fig. 2.2, *Aii* and *Bii*) evoked higher amplitude crossed reflex responses than low-current stimulation (Fig. 2.2, *Ai* and *Bi*).

In summary, our results show that stimulation of proprioceptive (low-current tibial nerve stimulation) and cutaneous (sural nerve stimulation) afferents evoke excitatory crossed reflex motor responses across the hindlimb flexor and extensor muscles in mice in vivo.

2.4.2 Temporal characteristics of muscle activation pattern during crossed reflex.

We next aimed to describe the overall activation pattern of the different groups of muscles in response to stimulation of the contralateral sensory afferents. The muscle activation patterns in response to contralateral tibial nerve and sural nerve stimulations are illustrated as heat diagrams in Fig. 2.3, *A* and *B*, respectively. At low- and high-current stimulation, replicable motor responses were evoked in the flexor and extensor muscles, confirming the result shown above (Fig. 2.2). We also detected a 10-ms activity gap between nerve stimulation offset and first signs of muscle activation following both the tibial and the sural nerve stimulation. This gap was visible as a darker phase in the color-

coded map, before the activation of the motor responses, lasting for ~10 ms after the stimulation. These data suggest that reliable and stereotyped crossed reflex responses can be elicited by stimulating the tibial nerve or sural nerves.

We further analysed the delays of on- and offsets of EMG activities from all recorded muscles from the onset of the contralateral nerve stimulation (Fig. 2.4). Under low-current tibial nerve stimulation, even though not statistically different, the onset of the Ip_r activity occurred on average first, followed by the distal flexor muscles (St_r and TA_r) and, finally, the extensor muscles (VL_r and Gs_r; Fig. 2.4*Ai*). However, during high-current tibial nerve stimulation, all muscle activity onsets were nearly synchronized. Comparing the latencies onset of different muscles during low- and high-current stimulation revealed that the latencies onset of the Ip_r and TA_r muscle activity, but not the extensor muscle activities, increased under high-current stimulation (Fig. 2.4*B*). This suggests two possibilities: at high-current tibial nerve stimulation, either the excitatory crossed reflex is delayed relative to low-current stimulation, or cutaneous afferents have a crossed inhibitory influence mediated by cutaneous afferents.

When we stimulated the sural nerve, the activation of the recorded muscles was more synchronous even at low-current stimulation, with some subtle differences (Fig. 2.4*C*). When we compared the onsets of EMG activities of low- and high-current left sural nerve stimulation, there was no statistical significance (Fig. 2.4*D*). These data suggest that high-current tibial nerve stimulation and low- or high-current sural nerve stimulation, activating more cutaneous afferent fibers, tend to activate all recorded muscles simultaneously. Our results regarding muscle activity onset synchronization raised two possibilities: either the excitatory crossed reflex could be delayed, or there is an inhibitory crossed reflex pathway mediated by cutaneous afferent fibers.

2.4.3 Short-latency inhibition in crossed and local reflexes.

We next sought to differentiate between the two possibilities described above. We used a paired stimulation protocol where peripheral nerves in both legs were stimulated with different delays. Either the tibial nerve or sural nerve was implanted in the left leg to evoke crossed reflex motor responses transduced by proprioceptive or cutaneous afferents,

respectively. Furthermore, in addition to the five EMG recording electrodes implanted in the five muscles of the right leg, we implanted an additional nerve stimulation electrode on the right sural nerve to evoke local cutaneous reflexes (Figs. 2.5 and 2.6). We predicted that if there is an inhibitory crossed reflex pathway, we should detect decreased activity with a constant delay after contralateral nerve stimulation regardless of the presence of EMG activity initiated by local reflexes.

First, we stimulated the left tibial nerve with high current simultaneously with the right sural nerve at varying delays (Fig. 2.5*A*). Figure 2.5, *B* and *C*, show the average EMG responses from the recorded flexor and extensor muscles, respectively, in response to crossed and local reflexes with varying delays between these two stimulations. Immediately after stimulation of the left tibial nerve (Fig. 2.5, *B* and *C*), we could detect a period of decreased EMG activity regardless of the presence of the local reflex response initiated by right sural nerve stimulation. This response could be detected consistently in all recorded flexor (Fig. 2.5*B*) and extensor (Fig. 2.5*C*) muscles. This finding suggested that, apart from the excitatory crossed reflex pathway indicated by muscle activation, an early inhibitory crossed reflex pathway is also present in mice in vivo.

Similar results were obtained when we stimulated the left sural nerve to initiate the crossed reflex response (Fig. 2.6*A*). Stimulation of the left sural nerve with high current also initiated a period of decreased EMG activity regardless of the delay between the right sural nerve stimulation and the left sural nerve stimulation (Fig. 2.6, *B* and *C*). The decreased EMG activity was present in all recorded flexor (Fig. 2.6*B*) and extensor (Fig. 2.6*C*) muscle recordings. These observations suggest that high-current activation of afferent fibers initiates crossed reflex inhibitory responses that are likely induced by cutaneous afferent activation.

In summary, our results show that sensory information is transmitted to the contralateral motor neurons through inhibitory as well as excitatory pathways following tibial or sural nerve stimulation. Furthermore, this inhibitory pathway affects the activity of all recorded muscles of the contralateral leg, as does the excitatory pathway.

2.4.4 Crossed reflex responses during locomotion.

Do crossed reflex responses occur the same way when the animal is moving compared with when the animal is resting, as described above? To address this question, we performed contralateral tibial or sural nerve stimulation during locomotion on a treadmill and recorded the EMG activity from the contralateral muscles (Fig. 2.7). Our data revealed that the crossed reflex response during locomotion depended on the timing of the nerve stimulation relative to the activity of the muscle before the stimulation, that is, whether the stimulation occurred when the muscle was active before the stimulation or inactive before the stimulation (Fig. 2.7). Therefore, we separated the data into two groups: *1*) the muscle was inactive when the contralateral nerve was stimulated (red traces in Figs. 2.7*A*, 2.7*B*, 2.8*A*, and 2.8*B*); and *2*) the muscle was active at the time the stimulation of the contralateral nerve occurred (black traces in Figs. 2.7*A*, 2.7*B*, 2.8*A*, and 2.8*B*). When the VL_r and TA_r muscles were inactive before nerve stimulation, we consistently detected the same 10-ms delay that we had detected while the mice were at rest. However, when the contralateral nerve stimulation occurred while the VL_r and TA_r muscles were active, the 10-ms silent period was absent (Figs. 2.7 and 2.8). In contrast, the 10-ms delay was always present in the Ip_r, St_r, and Gs_r activity profile, regardless of whether the muscle was already active before nerve stimulation (Figs. 2.7 and 2.8). These data indicate that the inhibitory crossed reflex pathway is downregulated during locomotion selectively for VL_r and TA_r muscles depending on the activity before the contralateral nerve stimulation.

2.5 DISCUSSION

In this article, we present a detailed analysis of the crossed reflex responses in awake mice in vivo at resting and during locomotion. Regardless of whether we stimulated peripheral nerves to activate proprioceptive or cutaneous afferents, activation of all muscles on the contralateral side was observed (Figs. 2.1–2.4). This indicates a widespread excitatory crossed reflex pathway to all motor neuron pools innervating the recorded muscles in this study. A more detailed investigation of the muscle responses indicates the presence of a short-latency inhibitory crossed reflex pathway (Figs. 2.3 and 2.4). To provide evidence for the inhibitory crossed reflex pathway, we demonstrated crossed reflex action in the presence of muscle activation, caused by local reflex activation through

ipsilateral nerve stimulation (Figs. 2.5 and 2.6). Finally, we have shown that the inhibitory crossed reflex pathway controlling the activity of the knee extensor (VL) and ankle flexor (TA) is downregulated during locomotion, whereas it is not changed for other recorded muscles (Figs. 2.7 and 2.8). This study represents the first comprehensive analysis of crossed reflexes in mice in vivo. We show the existence of a common crossed inhibitory pathway in mice that is modulated selectively for the VL and TA muscles during locomotion.

2.5.1 Non-nociceptive sensory afferent activation initiates crossed reflex responses.

In this article, we provide evidence that proprioceptive as well as cutaneous afferent stimulation initiates crossed reflex responses. Our results demonstrate that low-current tibial nerve stimulation, which mainly activates proprioceptive afferents, evokes crossed reflex responses in all recorded muscles. High-current electrical stimulation of the tibial nerve, which recruits additional cutaneous afferents, also causes activation of all contralateral muscles, but in a more synchronized manner. Furthermore, the sural nerve carries predominantly cutaneous afferents innervating the skin on the posterior site of the leg. In rodents, the sural nerve also carries a small amount of motor and proprioceptive afferent fibers to and from the flexor digiti minimi muscle in the foot (Peyronnard and Charron, 1982; Steffens et al. 2012). The reflex response observed in this study through sural nerve stimulation is most likely due to cutaneous afferent activation, but the contribution of efferent and proprioceptive afferent activation to and from the flexor digiti minimi muscle cannot be excluded. Motor fiber activation is unlikely to be a contributor because the delays considered in this study are too short for motor fibers to elicit toe muscle contractions that would elicit feedback in the EMG activity pattern. The contribution of proprioceptive afferent activation from the flexor digiti minimi muscle is a possibility that we cannot entirely exclude.

The highest current used in this study to activate afferent fiber was five times the threshold current to initiate a local reflex response. This was well below the current needed to activate nociceptive afferents, determined by vocalization (Bui et al. 2013), which typically occurs around 8–10 times the threshold current. Therefore, our results provided evidence that cutaneous afferents that initiated crossed reflex responses were non-

nociceptive cutaneous afferents. These results suggest that proprioceptive, as well as non-nociceptive cutaneous afferent, initiates crossed reflex responses. Overall, these results are in accordance with the results of previous research on cats and humans that muscle afferents (Arya et al. 1991; Aggelopoulos and Edgley, 1995; Stubbs and Mrachacz-Kersting, 2009; Jankowska and Edgley, 2010; Stubbs et al. 2011; Gervasio et al. 2017), as well as cutaneous afferents (Perl, 1957; Gauthier and Rossignol, 1981; Edgley and Aggelopoulos, 2006; Stubbs and Mrachacz-Kersting, 2009), mediate crossed reflex responses.

2.5.2 Inhibitory crossed reflex responses initiated by cutaneous afferent activation.

Two observations provide evidence for an inhibitory crossed reflex action initiated by non-nociceptive cutaneous afferent activation. First, stimulation of the tibial nerve, although not statistically significant, initiated a muscle activation sequence starting with the most proximal flexor muscle (Ip_r), followed by the distal flexors (St_r and TA_r) and, finally, the two extensor muscles (VL_r and Gs_r) on the contralateral side. The onsets of the VL_r and Gs_r occurred ~10 ms after the stimulation offset (hatched area in Fig. 2.4*Ai*). When the stimulation strength was increased to additionally recruit cutaneous afferents, the muscle activation sequence was changed to simultaneous activation at ~10 ms after stimulation offset (hatched area in Fig. 2.4*Aii*). Stimulation of the sural nerve, regardless of stimulation strength, elicited an activation pattern resembling high-current tibial nerve stimulation. This finding suggests the possibility that cutaneous afferent activation induces an inhibitory crossed reflex pathway with inhibition of muscle activity lasting ~10 ms. Synchronization of muscle activity onsets with cutaneous afferent activation suggested the existence of an inhibitory crossed reflex pathway as previously described in cats (Arya et al. 1991; Aggelopoulos et al. 1996; Edgley and Aggelopoulos, 2006).

The second observation supporting a crossed inhibitory pathway initiated by cutaneous afferents came from the experiments where the local reflex was suppressed by the crossed reflex. Ipsilateral cutaneous afferent stimulation was paired with contralateral afferent stimulation at different delays, which allowed us to detect a short-latency inhibition for ~10 ms (hatched areas in Figs. 2.5 and 2.6) initiated by contralateral cutaneous afferent stimulation. Our data do not provide evidence for a direct inhibitory

influence that involves inhibitory synaptic input to the motor neurons. One alternative possibility is that the decreased EMG activity reflects motor neurons entering a refractory period following short-latency excitation, which is measured as reduced activity. Indeed, the Ip activity shown in Fig. 2.5*B* indicates increased activity before activity reduction within the 10-ms period. However, this short-latency activation was absent in the TA, VL, and Gs, which does not support the idea of refractory period involvement, but our current data do not allow a definite exclusion of this possibility. Nevertheless, our data support previous findings of inhibitory crossed reflex pathways initiated by cutaneous afferents in cats (Edgley and Aggelopoulos, 2006) and humans (Gervasio et al. 2017). Together, the two observations provide a strong indication that non-nociceptive cutaneous afferent activation initiates inhibitory crossed reflexes that last for ~10 ms.

2.5.3 Crossed reflex during locomotion.

Our data suggest that the crossed inhibitory reflex is downregulated when the animal walks selectively for the knee extensor (VL) and ankle flexor (TA) muscles. We recorded the muscle activity response to contralateral afferent activation while the animals were moving on a treadmill at a constant speed of 0.2 m/s. Stimulation of the contralateral nerves initiated muscle responses that closely resembled the responses in resting mice, except for the VL_r and the TA_r muscles, which depended on whether these muscles were active before nerve stimulation. That is, when VL_r (mainly active during the stance phase) and TA_r (mainly active during the swing phase) were inactive before the nerve stimulation, their responses were almost identical to those during resting. In contrast, when these muscles were active, we did not observe the silent 10-ms latency period, indicating reduced strength of crossed inhibition relative to crossed excitation. Previous experiments in cats also observed downregulated inhibitory crossed reflexes selectively for the VL_r muscle during locomotion (Frigon and Rossignol, 2008). The authors assumed that the absence of crossed inhibitory influence in the VL_r was due to the more rostral location of the motor neuron pool in the spinal cord compared with the other muscle. However, we have shown that the inhibitory crossed reflex influence is not only downregulated in the VL_r (motor neuron cell bodies located between lumbar spinal segments 1–3) but also in the TA_r, whose motor neuron pool is located more caudally (lumbar spinal segments 3–4) (McHanwell and

Biscoe, 1981). The relative location of the motor neuron pool innervating the Ip in the mouse has not been demonstrated, but its location in the cat is even more rostral than the one innervating VL (Vanderhorst and Holstege, 1997). Our results demonstrate that the inhibition of the Ip muscle is not modulated during locomotion as it is for the VL and TA. Therefore, our data do not support the view that the absence of the state-dependent modulation of the inhibitory crossed reflex response is due to motor neuron pool location.

Crossed reflex responses during locomotion can switch from activation of extensor muscles to activation of flexor muscles depending on the phase of the step cycle (Duysens et al. 1980; Gervasio et al. 2013), which contributes to the dynamic stability during locomotion (Gervasio et al. 2015). Separating the contralateral afferent stimulation into phases in which Ip_r was active (approximating swing phase) and phases in which Ip_r was not active (approximating stance phase) did not reveal any conclusive phase dependency in our experiments (data not shown). However, clear and consistent differences in muscle response in VL_r and TA_r were observed when the separation was made based on muscle activity. We observed that the inhibitory crossed reflex pathway was selectively downregulated for the VL_r and TA_r muscles when the muscles were active before stimulation. The short-latency inhibition was replaced by a very short-latency excitation during locomotion. The discrepancy between our results with the previous findings from cat experiments (Duysens et al. 1980; Gauthier and Rossignol, 1981; Frigon and Rossignol, 2008; Hurteau et al. 2017) may indicate differences in mechanisms across species. That is, whereas the nervous system of the cat takes the stance or swing phase as a reference for reflex reversal, mice might prefer individual muscle activity. In addition, differences in these mechanisms might relate to the much smaller size and the much higher stepping frequency of mice relative to cats. Nevertheless, this is a speculation, and further investigation is required for a more definite conclusion.

In this article, we provide a detailed description of the motor output in one leg when sensory afferents in the contralateral leg are stimulated in mice in vivo. Our results demonstrate that crossed reflexes are mediated by cutaneous and proprioceptive afferents and can be evoked in vivo in freely moving mice. Furthermore, crossed reflex pathways involve a short-latency inhibitory component in flexor and extensor muscles that can be

modulated to evoke appropriate motor responses according to the behavioural context of the contralateral leg. This short-latency inhibitory response is followed by an excitatory motor response in flexor and extensor muscles. These results will serve as the groundwork for our efforts to identify the involvement of genetically distinct classes of commissural interneurons (Lanuza et al. 2004; Zhang et al. 2008; Talpalar et al. 2013) involved in crossed reflexes. These insights will be important for understanding how sensory pathways transfer sensory information to the contralateral side of the spinal cord, and how sensory information modulates left-right coordination during locomotion.

2.6 FIGURES

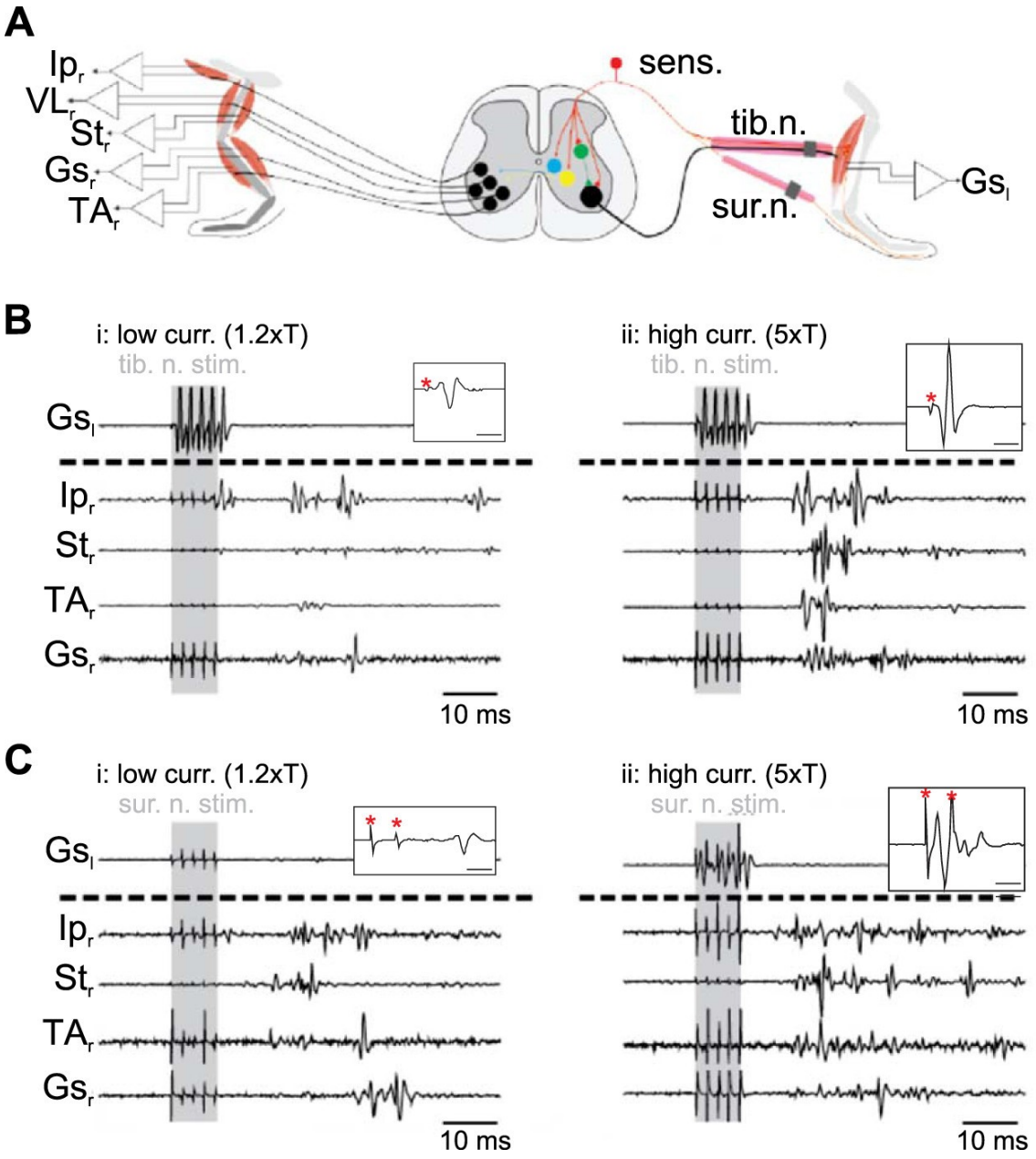
A
Ip_r
VL_r
St_r
Gs_r
TA_r
sens.
tib.n.
sur.n.
Gs_l
B
i: low curr. (1.2xT)
tib. n. stim.
ii: high curr. (5xT)
tib. n. stim.
Gs_l
Ip_r
St_r
TA_r
Gs_r
10 ms
10 ms
C
i: low curr. (1.2xT)
sur. n. stim.
ii: high curr. (5xT)
sur. n. stim.
Gs_l
Ip_r
St_r
TA_r
Gs_r
10 ms
10 ms

Figure 2.1. Schematic of experimental design used to investigate crossed reflex in vivo. *A*: experimental design used to investigate crossed reflex in vivo. *B* and *C*: examples of electromyographic recording at low (low curr. 1.2×T; *i*)- and high (high curr. 5×T; *ii*)-current stimulation from one mouse after stimulation of tibial nerve (tib. n. stim.; *B*) or sural nerve (sur. n. stim.; *C*). Shaded areas indicate stimulation. *Insets* in *B* and *C* show examples of the left gastrocnemius (Gs_l) response to stimulation of the left tibial nerve with a single impulse (*B*) or the left sural nerve with double impulses (*C*). Time bars in *insets* indicate 2 ms, and red asterisks indicate stimulus artifact. Ip_r, right iliopsoas; VL_r, right vastus lateralis; St_r, right semitendinosus; Gs_r, right gastrocnemius; TA_r, right tibialis anterior.

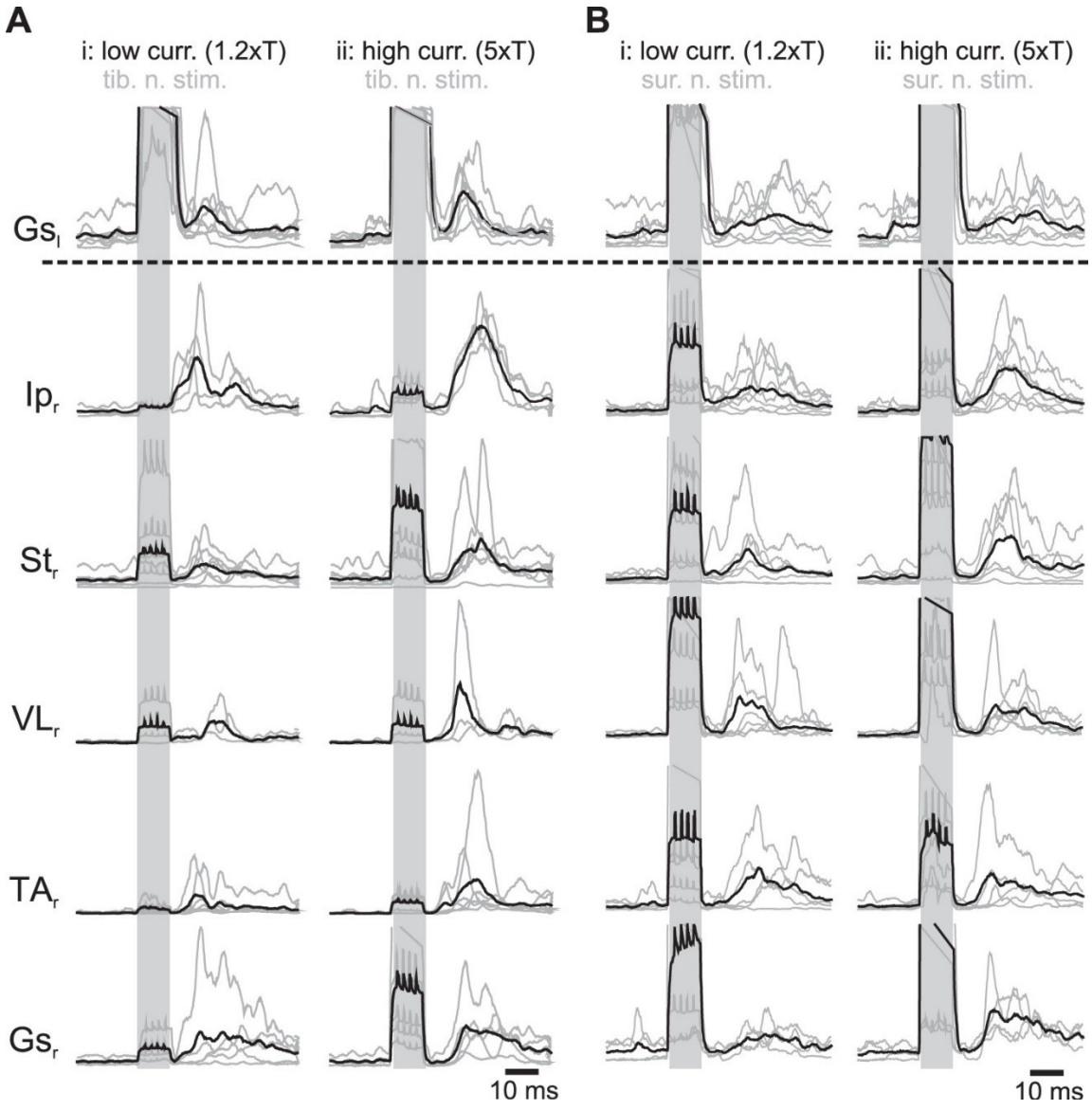

Figure 2.2. Average crossed reflex motor responses. *A* and *B*: average crossed reflex responses from different muscles after low (low curr. 1.2×T; *i*)- and high (high curr. 5×T; *ii*)-current stimulation of tibial nerve from 7 animals (tib. n. stim.; *A*) or sural nerve stimulation from 8 animals (sur. n. stim.; *B*). Gray lines are averages of 20–40 stimulations in each animal. The black line corresponds to the average across all animals. Shaded areas indicate stimulation. Gs_l, left gastrocnemius; Ip_r, right iliopsoas; St_r, right semitendinosus; VL_r, right vastus lateralis; TA_r, right tibialis anterior; Gs_r, right gastrocnemius.

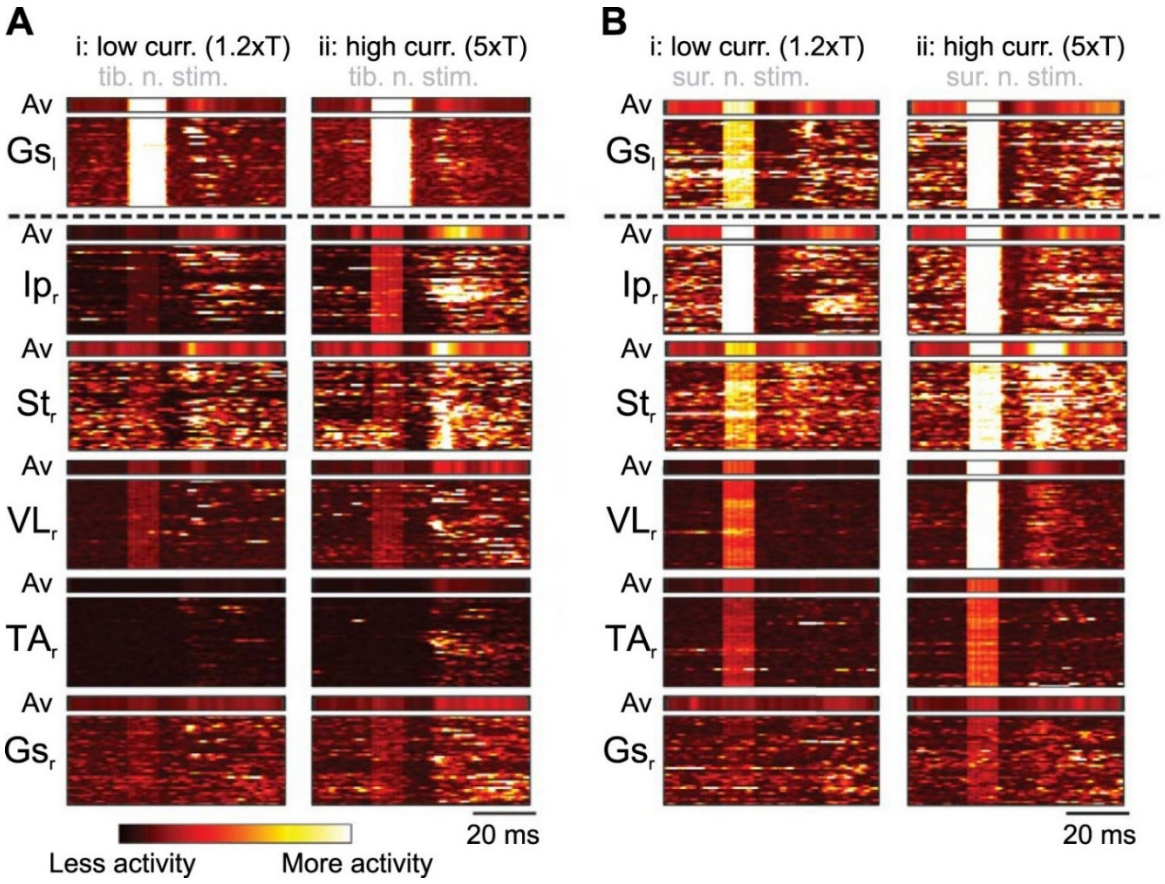

Figure 2.3. Muscle responses in ipsilateral and contralateral muscles are consistent across individual trials. *A* and *B*: heat diagram shows the muscle activity during low (low curr. 1.2×T; *i*)- and high (high curr. 5×T; *ii*)-current stimulation of the contralateral tibial nerve (tib. n. stim.; *A*) and the sural nerve (sur. n. stim.; *B*) from 1 representative animal for each nerve stimulation experiment. Muscle responses to each of 40 nerve stimulations from 1 experiment are staggered on the vertical axis as a function of time. Brighter colors indicate higher muscle activity. Concentrated brighter areas indicate consistent muscle activity to nerve stimulation, whereas dark areas indicate no activity. The average muscle activity of all trials (Av) is shown above each diagram. Gs_l, left gastrocnemius; Ip_r, right iliopsoas; St_r, right semitendinosus; VL_r, right vastus lateralis; TA_r, right tibialis anterior; Gs_r, right gastrocnemius.

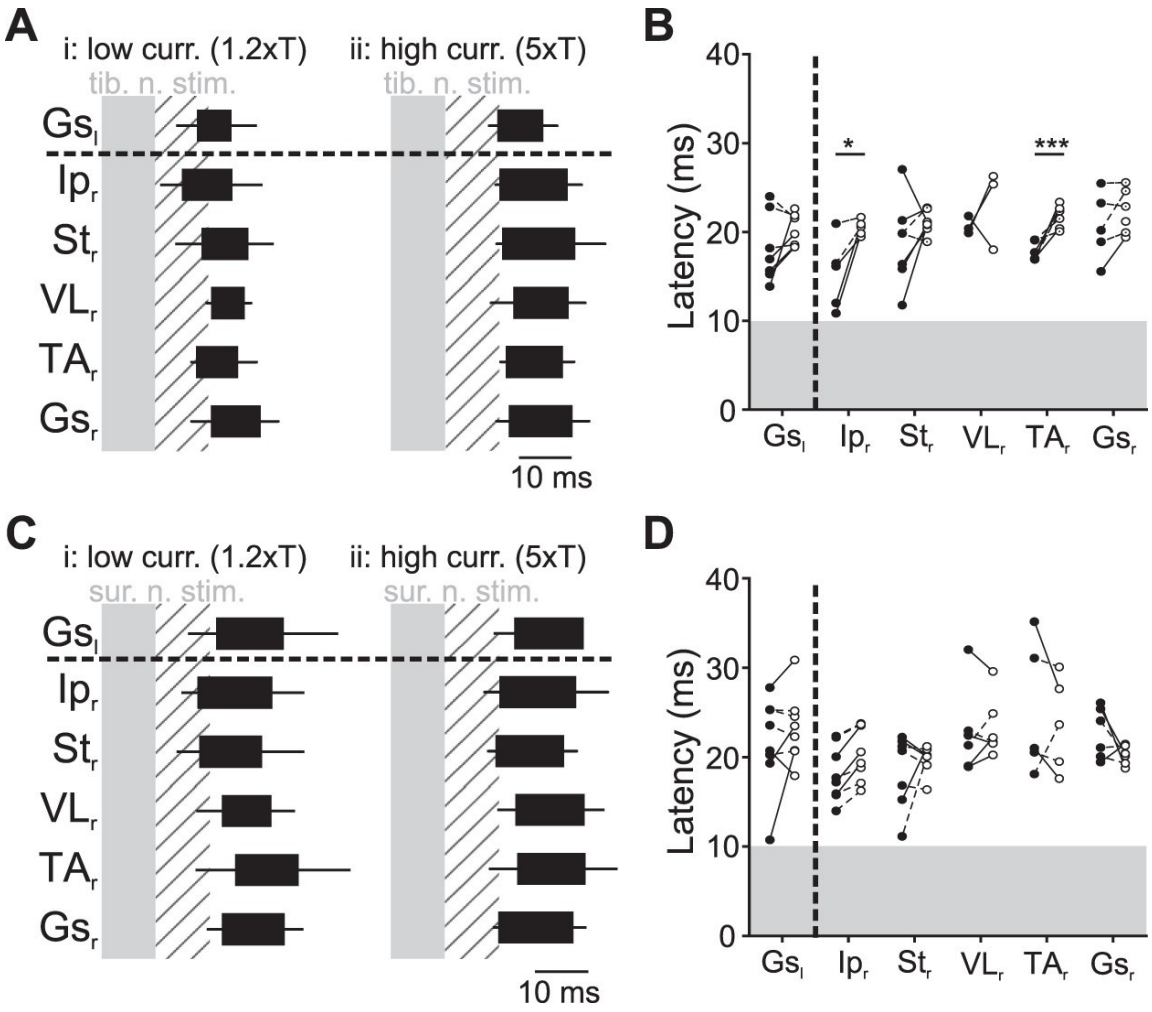
A
i: low curr. (1.2xT)
ii: high curr. (5xT)
tib. n. stim.
tib. n. stim.
Gs$_l$
Ip$_r$
St$_r$
VL$_r$
TA$_r$
Gs$_r$
10 ms
B
Latency (ms)
40
30
20
10
0
*
***
Gs$_l$
Ip$_r$
St$_r$
VL$_r$
TA$_r$
Gs$_r$
C
i: low curr. (1.2xT)
ii: high curr. (5xT)
sur. n. stim.
sur. n. stim.
Gs$_l$
Ip$_r$
St$_r$
VL$_r$
TA$_r$
Gs$_r$
10 ms
D
Latency (ms)
40
30
20
10
0
Gs$_l$
Ip$_r$
St$_r$
VL$_r$
TA$_r$
Gs$_r$

Figure 2.4. Crossed reflex muscle activation pattern. *A*: pattern of muscle activation at low (low curr. 1.2×T; *i*)- and high (high curr. 5×T; *ii*)-current stimulation following tibial nerve stimulation (tib. n. stim.) summarizing data from 7 experiments. *B*: average latency of the different muscles at low (●)- and high (○)-current stimulation following tibial nerve stimulation in individual animals. Latencies were measured from the start of the stimulation to the first visually detectable action potentials in the electromyographic recordings. Statistical significance between individual averages is indicated by a solid line, whereas dashed lines indicate no statistical difference. *$P < 0.05$; ***$P < 0.001$. *C*: pattern of muscle activation at low- and high-current stimulation following sural nerve stimulation (sur. n. stim.) summarizing data from 8 experiments. *D*: pattern of muscle activation at low- and high-current stimulation following sural nerve stimulation. Shaded areas represent the stimulation. Hatched areas represent a 10-ms period after the stimulation. Gs_l, left gastrocnemius; Ip_r, right iliopsoas; St_r, right semitendinosus; VL_r, right vastus lateralis; TA_r, right tibialis anterior; Gs_r, right gastrocnemius.

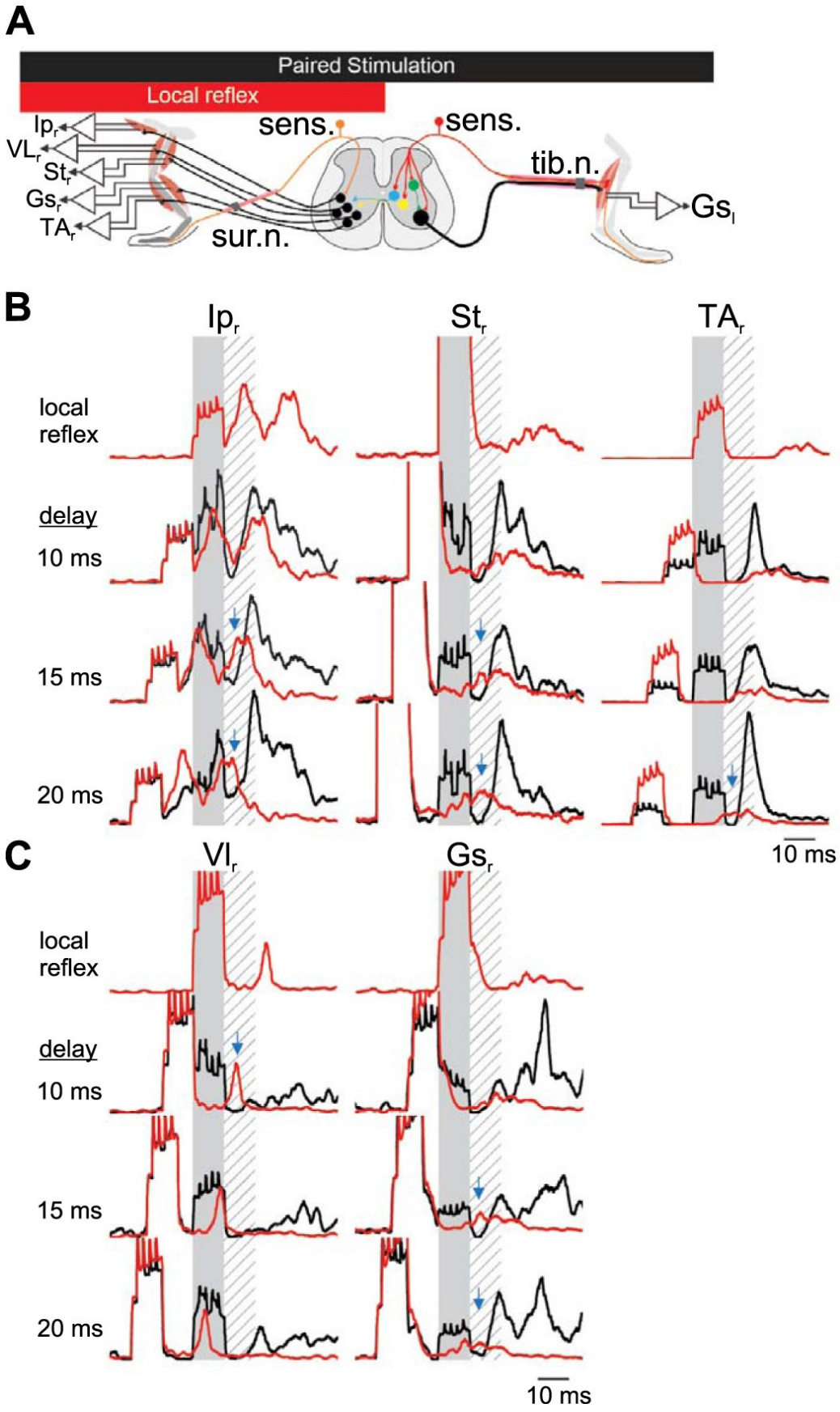
A
Paired Stimulation
Local reflex
Ip$_r$
VL$_r$
St$_r$
Gs$_r$
TA$_r$
sens.
sens.
tib.n.
Gs$_l$
sur.n.
B
Ip$_r$
St$_r$
TA$_r$
local reflex
delay
10 ms
15 ms
20 ms
10 ms
C
Vl$_r$
Gs$_r$
local reflex
delay
10 ms
15 ms
20 ms
10 ms

Figure 2.5. Short-latency inhibition in crossed reflex initiated by tibial nerve stimulation. *A*: schematic representation of the paired stimulation of both legs at different delays to provide evidence of an inhibitory period if there is a suppression of the motor responses from one leg following the stimulation of the other leg. Data are from 40 stimulations from 1 animal, representative of 4 experiments. *B* and *C*: examples of electromyographic (EMG) recording in the contralateral flexor muscles (*B*) or the extensor muscles (*C*) after stimulation of the contralateral tibial nerve. Shaded areas represent stimulation of the contralateral tibial nerve to evoke a crossed reflex. Hatched areas represent the silent period detected previously. Red traces represent the average EMG response to local reflex activation initiated by ipsilateral sural nerve stimulation. Black lines indicate the EMG response when the ipsilateral sural nerve is stimulated with the contralateral tibial nerve with a delay indicated at the *left* of each set of recordings. Blue arrows represent the suppression of the local cutaneous reflex by contralateral sensory stimulation. Gs_l, left gastrocnemius; Ip_r, right iliopsoas; St_r, right semitendinosus; VL_r, right vastus lateralis; TA_r, right tibialis anterior; Gs_r, right gastrocnemius; sens., sensory stimulation; tib. n., tibial nerve; sur. n., sural nerve.

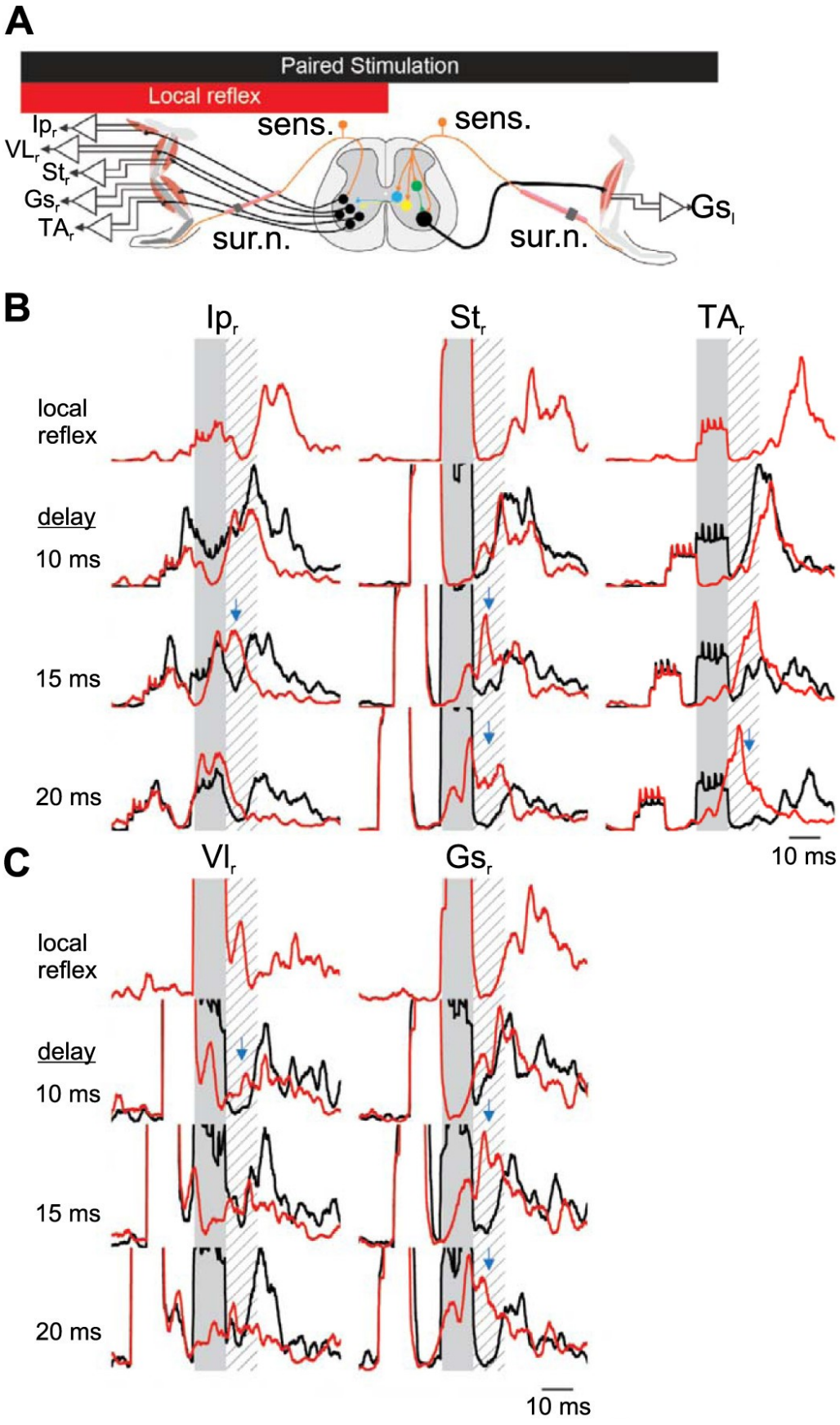
A
Paired Stimulation
Local reflex
Ip$_r$
VL$_r$
St$_r$
Gs$_r$
TA$_r$
sens.
sens.
sur.n.
sur.n.
Gs$_l$
B
Ip$_r$
St$_r$
TA$_r$
local reflex
delay
10 ms
15 ms
20 ms
10 ms
C
Vl$_r$
Gs$_r$
local reflex
delay
10 ms
15 ms
20 ms
10 ms

Figure 2.6. Short-latency inhibition in crossed reflex initiated by sural nerve stimulation. *A*: schematic representation of the paired stimulation of both legs at different delays to provide evidence of an inhibitory period if there is a suppression of the motor responses from one leg following the stimulation of the other leg. Averages are calculated using 40 stimulations from 1 animal, representative of 4 experiments. *B* and *C*: examples of electromyographic (EMG) recordings in the contralateral flexor muscles (*B*) or the extensor muscles (*C*) after stimulation of the contralateral sural nerve. Shaded areas represent stimulation of the contralateral tibial nerve to evoke a crossed reflex. Hatched areas represent the silent period detected previously. Red traces represent the average EMG response to local reflex activation initiated by ipsilateral sural nerve stimulation. Black lines indicate the EMG response when the ipsilateral sural nerve is stimulated with the contralateral sural nerve with a delay indicated at the *left* of each set of recordings. Blue arrows represent the suppression of local cutaneous reflex by contralateral sensory stimulation. Gs_l, left gastrocnemius; Ip_r, right iliopsoas; St_r, right semitendinosus; VL_r, right vastus lateralis; TA_r, right tibialis anterior; Gs_r, right gastrocnemius; sens., sensory stimulation; sur. n., sural nerve.

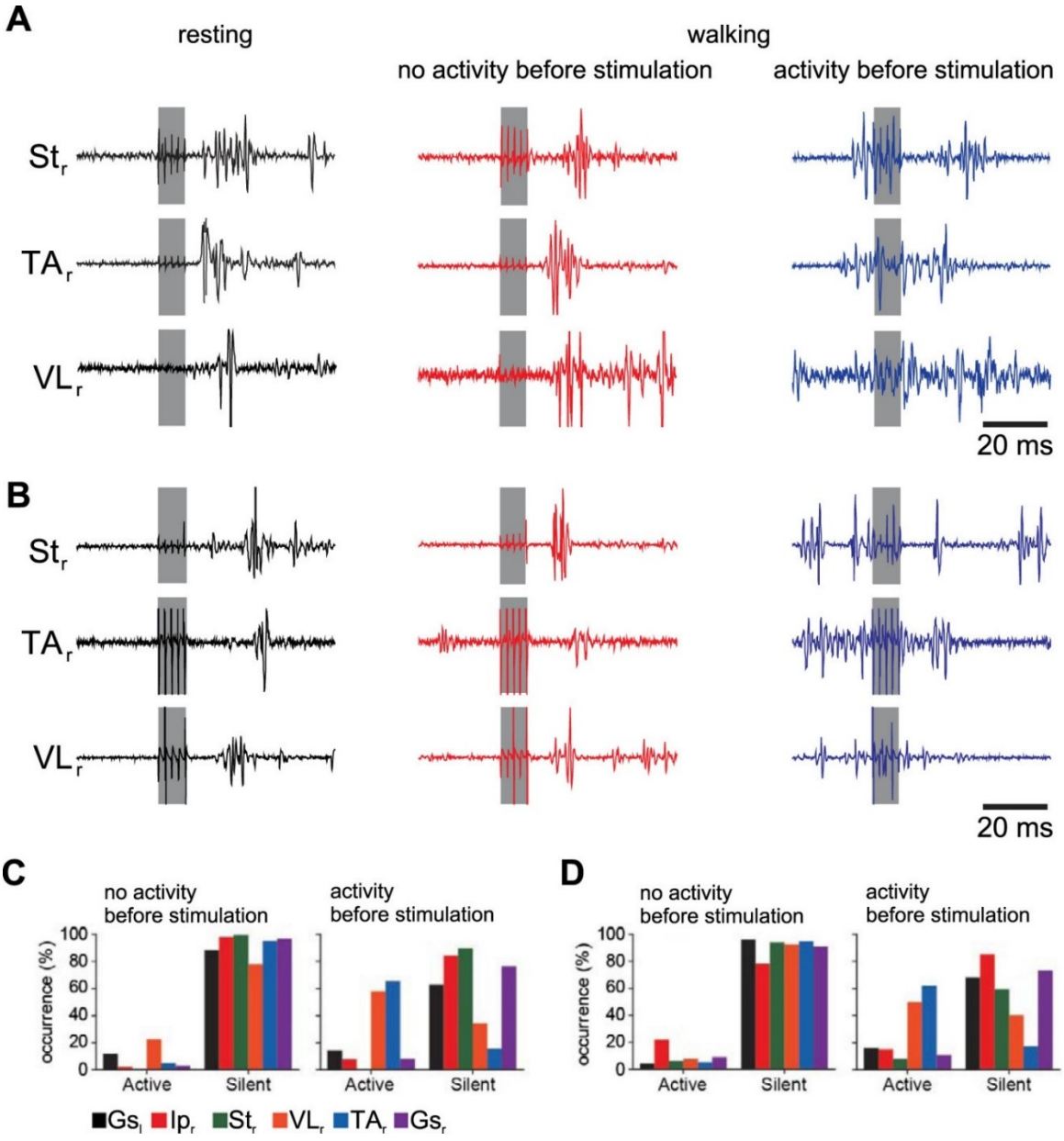
A
resting
walking
no activity before stimulation
activity before stimulation
St$_r$
TA$_r$
VL$_r$
20 ms
B
St$_r$
TA$_r$
VL$_r$
20 ms
C
no activity before stimulation
activity before stimulation
occurrence (%)
100
80
60
40
20
0
Active
Silent
Active
Silent
Gs$_l$ Ip$_r$ St$_r$ VL$_r$ TA$_r$ Gs$_r$
D
no activity before stimulation
activity before stimulation
occurrence (%)
100
80
60
40
20
0
Active
Silent
Active
Silent

Figure 2.7. Crossed reflex response in right vastus lateralis (VL_r) and right tibialis anterior (TA_r) depends on muscle activity status before nerve stimulation during walking. *A* and *B*: electromyographic recording of the contralateral semitendinosus and the contralateral tibialis anterior in resting (black traces) and the two different states during walking: when the muscle was not active (red traces) or active (blue traces) before the tibial nerve (*A*) or the sural nerve (*B*) stimulation. *C* and *D*: relative counts (percentages) of muscle responses, as active or silent within the first 10 ms after stimulation of the tibial nerve in 7 experiments (*C*) or the sural nerve in 5 experiments (*D*). Gs_l, left gastrocnemius; Ip_r, right iliopsoas; St_r, right semitendinosus; Gs_r, right gastrocnemius.

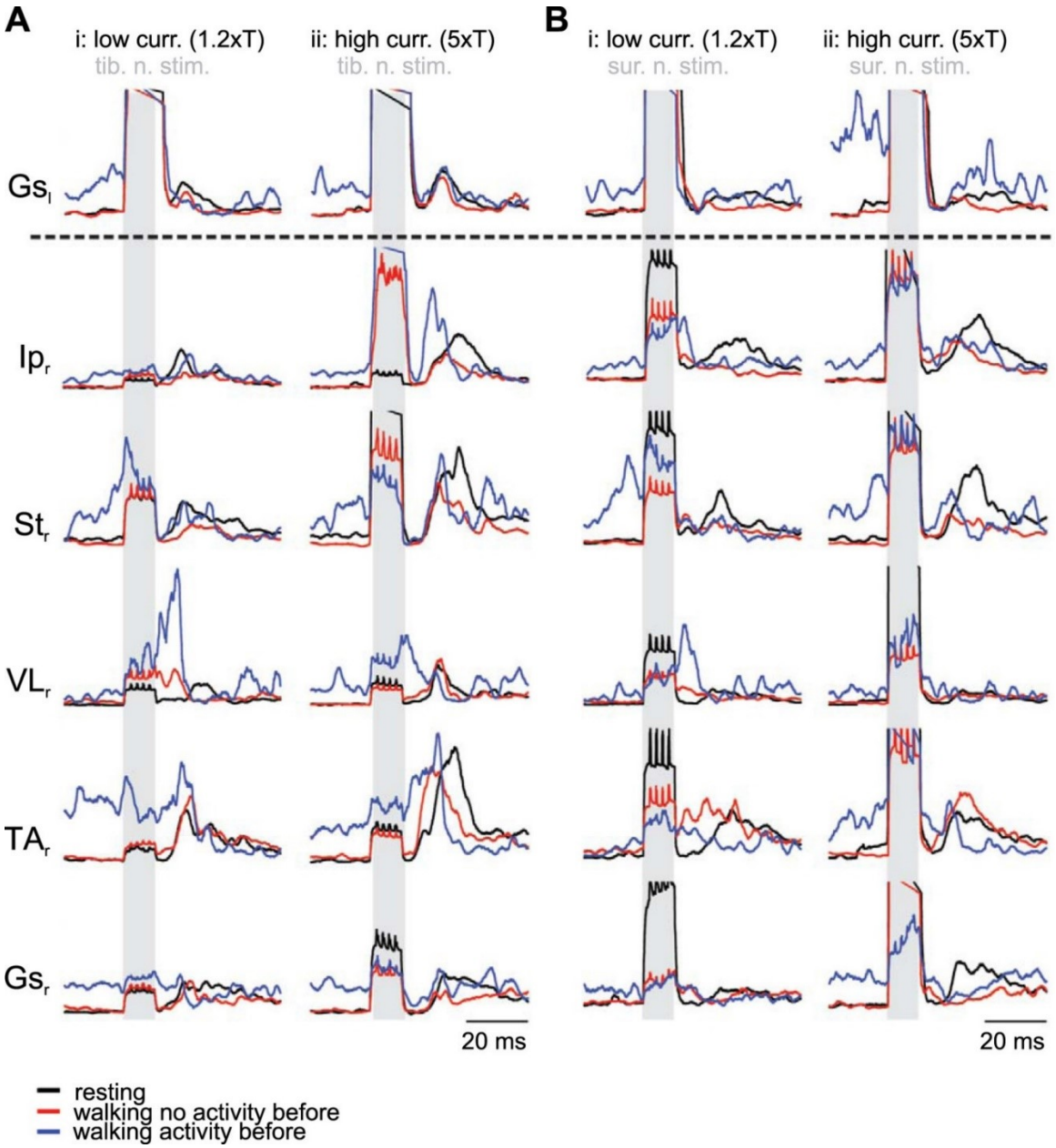
A
i: low curr. (1.2xT)
tib. n. stim.
ii: high curr. (5xT)
tib. n. stim.
B
i: low curr. (1.2xT)
sur. n. stim.
ii: high curr. (5xT)
sur. n. stim.
Gs$_l$
Ip$_r$
St$_r$
VL$_r$
TA$_r$
Gs$_r$
20 ms
20 ms
resting
walking no activity before
walking activity before

Figure 2.8. Muscle responses in crossed reflex during walking. *A* and *B*: electromyographic recording in the contralateral muscles comparing the motor activity while the animal is resting (black traces) or walking when the muscle was not active (red traces) or active (blue traces) before tibial nerve (*A*) or sural nerve (*B*) stimulation. Traces are pooled averages from 7 mice for the tibial nerve stimulation and 5 mice for the sural nerve stimulation. Shaded background indicates nerve stimulation. Gs_l, left gastrocnemius; Ip_r, right iliopsoas; St_r, right semitendinosus; VL_r, right vastus lateralis; TA_r, right tibialis anterior; Gs_r, right gastrocnemius.

2.7 REFERENCES

Aggelopoulos NC, Burton MJ, Clarke RW, Edgley SA. Characterization of a descending system that enables crossed group II inhibitory reflex pathways in the cat spinal cord. **J Neurosci** 16: 723–729, 1996. doi:10.1523/JNEUROSCI.16-02-00723.1996.

Aggelopoulos NC, Edgley SA. Segmental localisation of the relays mediating crossed inhibition of hindlimb motoneurones from group II afferents in the anaesthetized cat spinal cord. **Neurosci Lett** 185: 60–64, 1995. doi:10.1016/0304-3940(94)11225-8.

Akay T. Long-term measurement of muscle denervation and locomotor behavior in individual wild-type and ALS model mice. **J Neurophysiol** 111: 694–703, 2014. doi:10.1152/jn.00507.2013.

Akay T, Acharya HJ, Fouad K, Pearson KG. Behavioral and electromyographic characterization of mice lacking EphA4 receptors. **J Neurophysiol** 96: 642–651, 2006. doi:10.1152/jn.00174.2006.

Akay T, Tourtellotte WG, Arber S, Jessell TM. Degradation of mouse locomotor pattern in the absence of proprioceptive sensory feedback. **Proc Natl Acad Sci USA** 111: 16877–16882, 2014. doi:10.1073/pnas.1419045111.

Arya T, Bajwa S, Edgley SA. Crossed reflex actions from group II muscle afferents in the lumbar spinal cord of the anaesthetized cat. **J Physiol** 444: 117–131, 1991. doi:10.1113/jphysiol.1991.sp018869.

Bagust J, Kerkut GA. Crossed reflex activity in an entire, isolated, spinal cord preparation taken from juvenile rodents. **Brain Res** 411: 397–399, 1987. doi:10.1016/0006-8993(87)91094-8.

Böhm UL, Wyart C. Spinal sensory circuits in motion. **Curr Opin Neurobiol** 41: 38–43, 2016. doi:10.1016/j.conb.2016.07.007.

Bui TV, Akay T, Loubani O, Hnasko TS, Jessell TM, Brownstone RM. Circuits for grasping: spinal dI3 interneurons mediate cutaneous control of motor behavior. **Neuron** 78: 191–204, 2013. doi:10.1016/j.neuron.2013.02.007.

Duysens J, Loeb GE. Modulation of ipsi- and contralateral reflex responses in unrestrained walking cats. **J Neurophysiol** 44: 1024–1037, 1980. doi:10.1152/jn.1980.44.5.1024.

Duysens J, Loeb GE, Weston BJ. Crossed flexor reflex responses and their reversal in freely walking cats. **Brain Res** 197: 538–542, 1980. doi:10.1016/0006-8993(80)91143-9.

Edgley SA, Aggelopoulos NC. Short latency crossed inhibitory reflex actions evoked from cutaneous afferents. **Exp Brain Res** 171: 541–550, 2006. doi:10.1007/s00221-005-0302-9.

Edgley SA, Jankowska E, Krutki P, Hammar I. Both dorsal horn and lamina VIII interneurones contribute to crossed reflexes from feline group II muscle afferents. **J Physiol** 552: 961–974, 2003. doi:10.1113/jphysiol.2003.048009.

Frigon A, Rossignol S. Short-latency crossed inhibitory responses in extensor muscles during locomotion in the cat. **J Neurophysiol** 99: 989–998, 2008. doi:10.1152/jn.01274.2007.

Garcia-Campmany L, Stam FJ, Goulding M. From circuits to behaviour: motor networks in vertebrates. **Curr Opin Neurobiol** 20: 116–125, 2010. doi:10.1016/j.conb.2010.01.002.

Gauthier L, Rossignol S. Contralateral hindlimb responses to cutaneous stimulation during locomotion in high decerebrate cats. **Brain Res** 207: 303–320, 1981. doi:10.1016/0006-8993(81)90366-8.

Gervasio S, Farina D, Sinkjær T, Mrachacz-Kersting N. Crossed reflex reversal during human locomotion. **J Neurophysiol** 109: 2335–2344, 2013. doi:10.1152/jn.01086.2012.

Gervasio S, Kersting UG, Farina D, Mrachacz-Kersting N. The effect of crossed reflex responses on dynamic stability during locomotion. **J Neurophysiol** 114: 1034–1040, 2015. doi:10.1152/jn.00178.2015.

Gervasio S, Voigt M, Kersting UG, Farina D, Sinkjær T, Mrachacz-Kersting N. Sensory feedback in interlimb coordination: contralateral afferent contribution to the short-latency crossed response during human walking. **PLoS One** 12: e0168557, 2017. doi:10.1371/journal.pone.0168557.

Goulding M. Circuits controlling vertebrate locomotion: moving in a new direction. **Nat Rev Neurosci** 10: 507–518, 2009. doi:10.1038/nrn2608.

Hurteau MF, Thibaudier Y, Dambreville C, Chraibi A, Desrochers E, Telonio A, Frigon A. Nonlinear modulation of cutaneous reflexes with increasing speed of locomotion in spinal cats. **J Neurosci** 37: 3896–3912, 2017. doi:10.1523/JNEUROSCI.3042-16.2017.

Hurteau MF, Thibaudier Y, Dambreville C, Danner SM, Rybak IA, Frigon A. Intralimb and interlimb cutaneous reflexes during locomotion in the intact cat. **J Neurosci** 38: 4104–4122, 2018. doi:10.1523/JNEUROSCI.3288-17.2018.

Jack JJ. Some methods for selective activation of muscle afferent fibres. In: **Studies in Neurophysiology: Presented to A. K. McIntyre**, edited by Porter R. London: Cambridge University Press, 1978, p. 155–176.

Jankowska E. Spinal interneuronal networks in the cat: elementary components. **Brain Res Brain Res Rev** 57: 46–55, 2008. doi:10.1016/j.brainresrev.2007.06.022.

Jankowska E, Edgley SA. Functional subdivision of feline spinal interneurons in reflex pathways from group Ib and II muscle afferents; an update. **Eur J Neurosci** 32: 881–893, 2010. doi:10.1111/j.1460-9568.2010.07354.x.

Jankowska E, Edgley SA, Krutki P, Hammar I. Functional differentiation and organization of feline midlumbar commissural interneurones. **J Physiol** 565: 645–658, 2005. doi:10.1113/jphysiol.2005.083014.

Jessell TM. Neuronal specification in the spinal cord: inductive signals and transcriptional codes. **Nat Rev Genet** 1: 20–29, 2000. doi:10.1038/35049541.

Jiang Z, Carlin KP, Brownstone RM. An in vitro functionally mature mouse spinal cord preparation for the study of spinal motor networks. **Brain Res** 816: 493–499, 1999. doi:10.1016/S0006-8993(98)01199-8.

Lanuza GM, Gosgnach S, Pierani A, Jessell TM, Goulding M. Genetic identification of spinal interneurons that coordinate left-right locomotor activity necessary for walking movements. **Neuron** 42: 375–386, 2004. doi:10.1016/S0896-6273(04)00249-1.

Lu DC, Niu T, Alaynick WA. Molecular and cellular development of spinal cord locomotor circuitry. **Front Mol Neurosci** 8: 25, 2015. doi:10.3389/fnmol.2015.00025.

Matsuyama K, Mori F, Nakajima K, Drew T, Aoki M, Mori S. Locomotor role of the corticoreticular-reticulospinal-spinal interneuronal system. **Prog Brain Res** 143: 239–249, 2004a. doi:10.1016/S0079-6123(03)43024-0.

Matsuyama K, Nakajima K, Mori F, Aoki M, Mori S. Lumbar commissural interneurons with reticulospinal inputs in the cat: morphology and discharge patterns during fictive locomotion. **J Comp Neurol** 474: 546–561, 2004b. doi:10.1002/cne.20131.

McCrea DA. Spinal circuitry of sensorimotor control of locomotion. **J Physiol** 533: 41–50, 2001. doi:10.1111/j.1469-7793.2001.0041b.x.

McHanwell S, Biscoe TJ. The localization of motoneurons supplying the hindlimb muscles of the mouse. **Philos Trans R Soc Lond B Biol Sci** 293: 477–508, 1981. doi:10.1098/rstb.1981.0082.

Nakanishi ST, Whelan PJ. A decerebrate adult mouse model for examining the sensorimotor control of locomotion. **J Neurophysiol** 107: 500–515, 2012. doi:10.1152/jn.00699.2011.

Pearson KG. Generating the walking gait: role of sensory feedback. **Prog Brain Res** 143: 123–129, 2004. doi:10.1016/S0079-6123(03)43012-4.

Pearson KG, Acharya H, Fouad K. A new electrode configuration for recording electromyographic activity in behaving mice. **J Neurosci Methods** 148: 36–42, 2005. doi:10.1016/j.jneumeth.2005.04.006.

Perl ER. Crossed reflexes of cutaneous origin. **Am J Physiol** 188: 609–615, 1957. doi:10.1152/ajplegacy.1957.188.3.609.

Peyronnard JM, Charron L. Motor and sensory neurons of the rat sural nerve: a horseradish peroxidase study. **Muscle Nerve** 5: 654–660, 1982. doi:10.1002/mus.880050811.

Rossignol S, Dubuc R, Gossard JP. Dynamic sensorimotor interactions in locomotion. **Physiol Rev** 86: 89–154, 2006. doi:10.1152/physrev.00028.2005.

Schomburg ED, Kalezic I, Dibaj P, Steffens H. Reflex transmission to lumbar α-motoneurones in the mouse similar and different to those in the cat. **Neurosci Res** 76: 133–140, 2013. doi:10.1016/j.neures.2013.03.011.

Sherrington CS. Flexion-reflex of the limb, crossed extension-reflex, and reflex stepping and standing. **J Physiol** 40: 28–121, 1910. doi:10.1113/jphysiol.1910.sp001362.

Steffens H, Dibaj P, Schomburg ED. In vivo measurement of conduction velocities in afferent and efferent nerve fibre groups in mice. **Physiol Res** 61: 203–214, 2012.

Stubbs PW, Mrachacz-Kersting N. Short-latency crossed inhibitory responses in the human soleus muscle. **J Neurophysiol** 102: 3596–3605, 2009. doi:10.1152/jn.00667.2009.

Stubbs PW, Nielsen JF, Sinkjær T, Mrachacz-Kersting N. Phase modulation of the short-latency crossed spinal response in the human soleus muscle. **J Neurophysiol** 105: 503–511, 2011. doi:10.1152/jn.00786.2010.

Talpalar AE, Bouvier J, Borgius L, Fortin G, Pierani A, Kiehn O. Dual-mode operation of neuronal networks involved in left-right alternation. **Nature** 500: 85–88, 2013. doi:10.1038/nature12286.

Vanderhorst VGJM, Holstege G. Organization of lumbosacral motoneuronal cell groups innervating hindlimb, pelvic floor, and axial muscles in the cat. **J Comp Neurol** 382: 46–76, 1997. doi:10.1002/(SICI)1096-9861(19970526)382:1<46::AID-CNE4>3.0.CO;2-K.

Zhang Y, Narayan S, Geiman E, Lanuza GM, Velasquez T, Shanks B, Akay T, Dyck J, Pearson K, Gosgnach S, Fan CM, Goulding M. V3 spinal neurons establish a robust and balanced locomotor rhythm during walking. **Neuron** 60: 84–96, 2008. doi:10.1016/j.neuron.2008.09.027.

Chapter 3. Crossed reflex responses to flexor nerve stimulation in mice

Contribution statement

The work presented in this chapter was published in the Journal of Neurophysiology.

Laflamme OD, Ibrahim M, Akay T. Crossed reflex responses to flexor nerve stimulation in mice. ***J Neurophysiology*** 127: 493–503, 2022.

I would like to acknowledge Marwan Ibrahim for assisting with the experiments and data analysis. I would like to thank Brenda Ross for her technical assistance with the mouse colony.

3.1 ABSTRACT

Motor responses in one leg to sensory stimulation of the contralateral leg have been named “crossed reflexes” and are extensively investigated in cats and humans. Despite this effort, a circuit-level understanding of the crossed reflexes has remained missing. In mice, advances in molecular genetics enabled insights into the “commissural spinal circuitry” that ensures coordinated leg movements during locomotion. Despite some common features between the commissural spinal circuitry and the circuit for the crossed reflexes, the degree to which they overlap has remained obscure. Here, we describe excitatory crossed reflex responses elicited by electrically stimulating the common peroneal nerve that mainly innervates ankle flexor muscles and the skin on the anterolateral aspect of the hind leg. Stimulation of the peroneal nerve with low current intensity evoked low-amplitude motor responses in the contralateral flexor and extensor muscles. At higher current strengths, stimulation of the same nerve evoked stronger and more synchronous responses in the same contralateral muscles. In addition to the excitatory crossed reflex pathway indicated by muscle activation, we demonstrate the presence of an inhibitory crossed reflex pathway, which was modulated when the motor pools were active during walking. The results are compared with the crossed reflex responses initiated by stimulating proprioceptors from extensor muscles and cutaneous afferents from the posterior part of the leg. We anticipate that these findings will be essential for future research combining the in vivo experiments presented here with mouse genetics to understand crossed reflex pathways at the network level in vivo.

3.2 INTRODUCTION

Stimulation of the somatosensory afferents from one leg has been shown to elicit motor responses in the contralateral leg which was termed “crossed reflex” (Sherrington, 1910). These crossed reflex responses were shown to be elicited by the stimulation of proprioceptive sensory afferents (*groups I* and *II*) and cutaneous afferents, as well as flexor reflex afferents (FRAs), a term defining high-threshold afferents from joints, muscles, and skin involved in ipsilateral limb flexion and contralateral limb extension (Jankowska et al. 1968). Activation of all these afferents generates excitatory and inhibitory responses in

contralateral flexor and extensor muscles in cats (Perl, 1957; Jankowska et al. 1967; Arya et al. 1991; Aggelopoulos et al. 1996; Edgley and Aggelopoulos, 2006; Hurteau et al. 2017).

Neurons whose axons cross the spinal cord from one side to the other (commissural interneurons, CINs) involved in crossed reflexes have been described in cats (Arya et al. 1991; Aggelopoulos and Edgley, 1995; Edgley et al. 2003). In mice, genetically and physiologically distinct classes of CINs that are important in left-right coordination during locomotion have been identified (Lanuza et al. 2004; Zhang et al. 2008; Talpalar et al. 2013). However, further research is required to provide insights into whether or not the CINs identified in cats and those identified in mice share common pathways. A promising approach is to conduct crossed reflex experiments with mice whose CIN pathways have been genetically manipulated. A thorough description of the crossed reflex responses in normal wild-type mice is essential for this to happen.

Crossed reflex experiments have been performed, to a limited degree, in rodents using in vitro spinal cord preparations (Bagust and Kerkut, 1987; Jiang et al. 1999) or in vivo decerebrate adult mouse preparations (Nakanishi and Whelan, 2012). We have recently demonstrated a new in vivo technique to record excitatory and inhibitory crossed reflex pathways elicited by stimulating two peripheral nerves (Laflamme and Akay, 2018). First, the tibial nerve was stimulated electrically at different intensities to activate sensory afferents from ankle extensor muscles (e.g., gastrocnemius, plantaris, and soleus) or the posterior and distal aspects of the hind leg (Cain et al. 2011). Second, we stimulated the main trunk of the sural nerve that predominantly carries afferents from the hind leg's cutaneous regions that are more lateral (Kambiz et al. 2014). However, it is not known whether the motor responses of one leg are different depending on the target of the afferents stimulated.

Here, we aimed to extend our investigation of normal crossed reflexes by measuring crossed reflex responses elicited by electrical stimulation of muscle afferents from flexor muscles and afferents from a cutaneous region on the anterior aspect of the hind leg. To do this, we recorded electromyogram (EMG) activity from up to five hindlimb muscles,

whereas we stimulated the common peroneal nerve in the contralateral hind leg to activate either proprioceptive afferents from ankle flexor muscles (tibialis anterior, peroneus longus, extensor digitorum longus, etc.) or cutaneous afferents from the anterior aspect of the hind leg (Zimmermann et al. 2009) (Fig. 3.1*A*). Our data suggest that during resting, the overall pattern of crossed reflexes initiated by the common peroneal nerve stimulation is similar to the pattern previously shown when the tibial nerve was stimulated. Furthermore, when crossed reflexes are initiated during walking, we observed a downregulation of the inhibitory crossed reflexes in knee extensor and ankle flexor muscles, similar to when the tibial nerve is stimulated. However, we also observed the downregulation of the inhibitory crossed reflex in the ankle extensor muscle when we stimulated the common peroneal nerve. These experiments add to the groundwork in the mouse model to identify the neuronal pathways involved in crossed reflexes and the role of these crossed reflex pathways during motor behaviour.

3.3 MATERIAL AND METHODS

Experiments were conducted on 20 adult wild-type (WT) mice (2–4 mo old) of either sex from the C57Bl6 background mouse. None of the mice were trained on the treadmill before the experiments. All studies were performed according to the Canadian Council on Animal Care (CCAC) guidelines and approved by the local council on animal care of Dalhousie University.

3.3.1 Construction of the electrodes

The electrodes were made using multistranded, Teflon-coated annealed stainless steel wire (A-M systems, Cat. No. 793200). The construction of the EMG electrode and nerve cuff was previously described in detail (Akay, 2014; Pearson et al. 2005; Akay et al. 2006). One or two nerve cuff electrodes and six EMG recording electrodes were attached to the headpiece pin connector (female, SAM1153-12; Digi-Key Electronics, Thief River Falls, MN) and covered with epoxy (Devcon 5 min Epoxy Gel).

3.3.2 Electrode implantation surgeries

All surgeries were performed in aseptic conditions and on a warm water-circulated heating pad maintained at 42°C. Each mouse received an electrode implantation surgery,

as previously described (Laflamme and Akay, 2018). Briefly, the animals were anesthetized with isoflurane (5% for inductions, 2% for maintenance of anesthesia), ophthalmic eye ointment was applied to the eyes, and the skin of the mice was sterilized with three-part skin scrub using hibitane, alcohol, and povidone-iodine. Before each surgery, buprenorphine (0.03 mg/kg) and ketoprofen (5 mg/kg)/meloxicam (5 mg/kg) were injected subcutaneously as analgesics, whereas the animals were still under anesthesia. Additional buprenorphine injections were performed in 12-h intervals for 48 h.

A set of six bipolar EMG electrodes and one or two nerve stimulation cuffs were implanted in a total of 20 wild-type mice, as previously described (Pearson et al. 2005; Akay et al. 2006). Small incisions were made on the shaved areas (neck and both hind legs), and each bipolar EMG electrode and the nerve cuff electrodes were led under the skin from the neck incisions to the leg incisions, and the headpiece connector was stitched to the skin around the neck incision. The EMG recording electrodes were implanted into the right (ipsilateral) hip flexor (iliopsoas, Ip_r), knee flexor (semitendinosus, St_r) and extensor (vastus lateralis, VL_r), and ankle flexor (tibialis anterior, TA_r) and extensor (gastrocnemius, Gs_r) as well as the left ankle flexor (tibialis anterior, TA_l) or the left ankle extensor (gastrocnemius, Gs_l) depending on whether the common peroneal (13 mice; 8 males and 5 females) or the main trunk of the tibial nerve (7 mice; all males) were stimulated, respectively. Nerve stimulation electrodes were implanted in the left common peroneal or tibial nerves to activate proprioceptive and cutaneous feedback that produces crossed reflexes and the right sural nerve (the main trunk) to evoke ipsilateral cutaneous reflexes. The anesthetic was discontinued, and mice were placed in a heated cage for 3 days before returning to a regular mouse rack. Food mash and hydrogel were provided for the first 3 days after the surgery. Any mouse handling was avoided until mice were fully recovered, and the first recording session started at least 10 days after the electrode implantation surgeries.

3.3.3 Crossed reflex recording sessions

After the animals fully recovered (~10 days) from the electrode implantation surgeries, crossed reflexes were recorded as follows: under brief anesthesia with isoflurane, a wire to connect the headpiece connector with the amplifier, and the stimulation insulation

units (ISO-FLEX; AMPI, Jerusalem, Israel, or the DS4; Digitimer, Hertfordshire, UK) were attached to the mouse. The anesthesia was discontinued, and the mouse was placed on a mouse treadmill (model 802; custom built in the workshop of the Zoological Institute, University of Cologne, Germany). The electrodes were connected to an amplifier (model 102; custom built in the workshop of the Zoological Institute, University of Cologne, Germany) and a stimulus isolation unit. After the animal fully recovered from anesthesia (at least 5 min), the minimal (threshold) current necessary to elicit local monosynaptic reflex responses was determined. This was done by injecting single impulses of 0.2 ms duration into the peroneal nerve or the tibial nerve while recording the EMG response in the tibialis anterior or the gastrocnemius muscle, respectively (average ±SD threshold current: 111.8 ±82.3 μA; range: 22.5–250 μA). Following the determination of threshold currents, the current injected into the common peroneal nerve was set as either 1.2 times the monosynaptic reflex threshold current (1.2 × threshold) or five times the monosynaptic reflex threshold current (5 × threshold).

EMG signals from five muscles of the right leg and the tibialis anterior or gastrocnemius muscle of the left leg were simultaneously recorded (sampling rate: 10,000 kHz), whereas the common peroneal or tibial nerve of the left leg was electrically stimulated with five brief impulses (impulse duration: 0.2 ms, frequency: 500 Hz) using the ISO-FLEX (AMPI, Jerusalem, Israel) and DS4 (Digitimer, Hertfordshire, UK) stimulation insulation units. In some experiments, the right sural nerve was also stimulated in combination with contralateral tibial or sural nerve stimulation. The crossed reflexes were recorded while the mice were resting on the treadmill or moving at 0.2 m/s constant speed. The EMG signals were amplified (gain 100), band-pass filtered from 400 Hz to 5 kHz, and stored on the computer using the Power1410 interface and Spike2 software (Cambridge Electronic Design, Cambridge, UK).

3.3.4 Statistical analysis

All graphical representations of data were made using GraphPad Prism 5 and processed using Illustrator CS5 (Adobe). All data are presented as means ± standard deviation. One-to-one statistical comparisons of the data were made with the t-test or Mann-Whitney test using GraphPad Prism 5 depending on whether the normality was

present (t-test) or not (Mann-Whitney test) using omnibus K^2 or Kolmogorov-Smirnov tests. All statistical tests were two-tailed, and differences were considered statistically significant when the P-value was <0.05.

3.4 RESULTS

3.4.1 Crossed reflex motor activity in flexor and extensor muscles

First, the left common peroneal nerve was electrically stimulated with a single pulse (0.2 ms) at different current intensities to determine the threshold current that would elicit motor responses on the ipsilateral TA muscle (Fig. 3.1*B*). Following the determination of the threshold current, currents at 1.2 × T and 5 × T were used to deliver five pulses at 500 Hz to investigate the role of proprioceptive and cutaneous afferents in crossed reflexes in the mouse, respectively (Fig. 3.1*C*). In these experiments, the low-current stimulation (1.2 × threshold) would predominantly activate group Ia (from muscle spindles) and Ib (from Golgi tendon organs) proprioceptive afferents from ankle flexor muscles (Jack, 1978; Schomburg et al. 2013). Our results showed that low-amplitude motor responses were evoked in all contralateral leg's recorded flexor or extensor muscles (Fig. 3.1*Ci*). High-current stimulation (5 × threshold), which activated proprioceptive afferents (the Group Ia, Ib, and II), flexor reflex afferents, and cutaneous afferents (groups βand γ) (Schomburg et al. 2013) from the anterolateral aspect of the leg, evoked more robust motor responses simultaneously in right flexor and extensor muscles (Fig. 3.1*Cii*). Overall, the observed muscle activity pattern, as a response to the common peroneal nerve stimulation at different intensities, was qualitatively similar to the observations with tibial nerve stimulation (Laflamme and Akay, 2018).

We then investigated the crossed reflex responses by analyzing the rectified EMG signals and averaging them over multiple trials at either 1.2 × T (Fig. 3.2*i*, Supplemental Fig. S3.1) or 5 × T (Fig. 3.2*ii*). Stimulation of the common peroneal nerve elicited crossed reflex responses in every recorded muscle, regardless of stimulation intensity. However, we noticed that low-current stimulation elicited considerably weaker responses when the common peroneal nerve was stimulated compared with when the tibial nerve was stimulated. This weaker response in the average EMG traces was due to less robust

responses in individual muscles (Supplemental Fig. S3.1). Therefore, we next analysed the probabilities of contralateral muscle activation with the common peroneal nerve stimulation and compared them with the probabilities of muscle response to tibial nerve stimulation (Fig. 3.3). Confirming the observations described in Fig. 3.2, the occurrence of activity in all contralateral muscles was lower when the common peroneal nerve was stimulated at 1.2 × T compared with the tibial nerve. It is noteworthy that the differences were only statistically significant for St, TA, and Gs (Fig. 3.3*A*). We observed no difference in the occurrence of local reflex response in the ipsilateral TA for the common peroneal nerve stimulation and Gs for the tibial nerve stimulation. In contrast, the occurrences of crossed reflex responses in any recorded muscles were not different when the common peroneal nerve and tibial nerves were stimulated at 5 × T (Fig. 3.3*B*). These data suggest that proprioceptive afferent activation from flexor muscles elicits weaker crossed reflex responses than proprioceptive afferents from extensor muscles.

3.4.2 Temporal characteristics of muscle activation pattern during crossed reflex initiated by the common peroneal nerve stimulation

We next compared the muscle activation pattern during crossed reflexes by measuring the delays between the stimulation onset and the on- and offsets of activities in each recorded muscle when the common peroneal nerve (Fig. 3.4, *A* and *B*) or the tibial nerve (Fig. 3.4, *C* and *D*) was stimulated. When we compared the pattern at 1.2 × T in both nerves, the onsets of activity did not exhibit considerable differences (Fig. 3.4*E*). In contrast, the duration of activities in all muscles was shorter when the common peroneal nerve was stimulated than when the tibial nerve was stimulated with 1.2 × T stimulation (Fig. 3.4*Fi*). The pattern at 5 × T was primarily similar regardless of which nerve was stimulated (Fig 3.4, *Eii* and *Fii*). Moreover, we observed a silent period with no activity in any EMG recordings after common peroneal nerve stimulation (Fig. 3.4, *A* and *B*) and tibial nerve stimulation (Fig. 3.4, *C* and *D*). This was similar to our previously reported observations (Laflamme and Akay, 2018). Overall, the muscle activation pattern during crossed reflex was qualitatively similar regardless of the nerve-stimulated or stimulation intensity, with minor differences mainly reflected in the duration of activities.

3.4.3 Short-latency inhibition in crossed reflex initiated by the common peroneal nerve stimulation

The observation of a silent period after the common peroneal nerve stimulation at 5 × T indicated the presence of an inhibitory crossed reflex pathway. To investigate this possibility further, we used a paired stimulation protocol where peripheral nerves on both legs were stimulated with different delays, as previously shown (Laflamme and Akay, 2018). For this, nerve stimulation electrodes were implanted on the common peroneal nerves of the left leg to evoke crossed reflex motor responses. In addition to the five EMG recording electrodes in the right hind leg, we implanted a nerve stimulation electrode to the right sural nerve to evoke local cutaneous reflex (Fig. 3.5*A*). As shown previously (Laflamme and Akay, 2018), we reasoned that an inhibitory crossed reflex pathway should cause decreased activity with a constant delay after contralateral nerve stimulation regardless of the presence of EMG activity initiated by local reflex.

First, we stimulated the right sural nerve with a high current (5 × threshold) to obtain a local reflex response (Fig. 3.5, *B* and *C*, red traces). Then, we stimulated the left common peroneal nerve simultaneously with the right sural nerve at varying delays (Fig. 3.5, *B* and *C*, black traces). We detected a period of decreased EMG activity immediately after the left common peroneal nerve stimulation (Fig. 3.5, *B* and *C*, blue arrows). This response could be detected consistently in all recorded flexor (Fig. 3.5*B*) and extensor (Fig. 3.5*C*) muscles. This finding suggested that similar to the previous reports, with tibial and sural nerve stimulations (Laflamme and Akay, 2018), inhibitory crossed reflex pathways were also activated with the common peroneal nerve stimulation.

3.4.4 Long-latency crossed reflex responses initiated by the common peroneal nerve stimulation

One qualitative difference between the crossed reflex responses initiated by the common peroneal or the tibial nerve was the presence of a long-latency response observed when the common peroneal nerve was stimulated but not when the tibial nerve was stimulated (Fig. 3.6). The 75-ms timeframe following the contralateral tibial and the common peroneal nerves are illustrated in Fig. 3.6, *A* and *B*, respectively. We consistently

detected a long-latency response in all recorded muscles only when the common peroneal nerve was stimulated but not when the tibial nerve was stimulated.

3.4.5 Modulation of crossed reflex responses during locomotion initiated by the common peroneal nerve stimulation

Are the crossed reflex responses to the common peroneal nerve stimulation similar when the animal is moving compared with when the animal is resting? To address this question, we stimulated the left common peroneal nerve when the animals were moving on a treadmill and recorded EMG activity from the right leg muscles (Fig. 3.7*A*). We evoked crossed reflexes by stimulating the common peroneal nerve at a high current (5 × T) separately during each muscle's active or inactive phase (Fig. 3.7, *B* and *C*). We observed that the crossed reflex responses during locomotion depended on the timing of the nerve stimulation relative to the activity of the muscle before the stimulation. We consistently detected the silent period after nerve stimulation when all muscles were inactive before nerve stimulation, as described during resting above. However, the silent period was absent when the contralateral nerve stimulation occurred while the Gs_r, VL_r, and TA_r muscles were active (Fig. 3.7). In contrast, in the EMG activity profile of Ip_r and St_r, a short latency silent period was always observed after stimulation regardless of the muscle activity before nerve stimulation (Fig. 3.7). These data reveal that the crossed inhibitory reflex pathway is downregulated during locomotion selectively for Gs_r, VL_r, and TA_r muscles depending on the activity before the contralateral common peroneal nerve stimulation.

3.5 DISCUSSION

Here, we presented a detailed analysis of the crossed reflex responses evoked by the common peroneal nerve stimulation in awake mice in vivo at rest and during locomotion. In the following, the results are compared with crossed reflex responses evoked by tibial nerve stimulation or sural nerve stimulation (Laflamme and Akay, 2018). Our data indicate that crossed reflex responses are mostly similar regardless of which nerve is stimulated, with mainly two qualitative differences. First, the common peroneal nerve stimulation elicits a long-latency crossed reflex response that is absent when the tibial nerve [in this paper and the study by Laflamme and Akay, (2018)] or sural nerve (Laflamme and

Akay, 2018) is stimulated. Second, when the crossed reflex responses are elicited with the common peroneal nerve stimulation while the animal is walking, we observed the downregulation of inhibitory crossed reflex responses in TA, VL, and Gs muscles. This downregulation of the inhibitory crossed reflex responses was only observed in TA and VL, but not in Gs, when tibial or sural nerves were stimulated (Laflamme and Akay, 2018). These findings will be essential and serve as a starting point for future research combining the type of experiments presented here with mouse genetics to understand the spinal network underlying the crossed reflexes.

3.5.1 Short-latency crossed reflex responses are widely similar regardless of the stimulated nerve

Our results in this article indicate that short-latency activation patterns, as a response to the stimulation of different nerves of the contralateral sites, are widely similar when the animal is resting. The similarity of the response to the common peroneal nerve stimulation, with the tibial and sural nerve stimulation, is especially interesting when considering the muscles or cutaneous regions these nerves innervate. First, the common peroneal nerve innervates mostly the flexor muscles of the ankle joint, namely the tibial anterior and the extensor digitorum longus. In contrast, the tibial nerve innervates ankle extensor muscles, such as gastrocnemius muscles, soleus, and plantaris muscles. Second, the cutaneous sensory fibers that run through the common peroneal nerve originate mainly from the anterior aspect of the leg. In contrast, the cutaneous sensory fibers that run through the tibial and the sural nerves originate from the posterior aspects of the leg (Bernard et al. 2007). The similarities of the crossed reflex responses to these nerves indicate that the spinal network that conveys the afferent information is widely similar despite the difference in the afferent's origin.

The similarity of a crossed reflex response to the stimulation of cutaneous afferents originating from different leg regions is especially interesting because clear differences are observed at the local reflex level. When cutaneous afferents from the anterior aspect of the leg are activated by electrically stimulating the superficial peroneal nerve (Quevedo et al. 2005) or the saphenous nerve (Mayer and Akay, 2018), a well-defined reflex response called the stumbling corrective reaction is elicited (Forssberg et al. 1975; Prochazka et al.

1978; Forssberg, 1979). This stumbling corrective reaction is not observed when the tibial nerve or the sural nerve carrying cutaneous afferent fibers from the posterior aspect of the leg is stimulated. These observations indicate that even if the sensory afferents stimulated are completely different, the crossed reflex responses can be similar. This suggests that the divergence of spinal function or circuitry in one reflex (the ipsilateral reflex) can be absent in another reflex (the crossed reflex).

Apart from observing muscle activation patterns indicating excitatory crossed reflex pathways, we could find evidence of inhibitory crossed reflex pathways similar to when the tibial or the sural nerve is stimulated (Laflamme and Akay, 2018). Two observations indicated this. First, the stimulation of the common peroneal nerve at low intensity (1.2xT) initiated a staggering muscle activation on the contralateral side. When the stimulation strength was increased to recruit cutaneous afferents in addition to proprioceptive afferents, the muscle activation was more simultaneous with a ∼10-ms delay after the stimulation offset. Second, contralateral cutaneous afferent stimulation could suppress local reflex response initiated by ipsilateral cutaneous afferent stimulation. These data support the previous findings of inhibitory crossed reflex pathways activated by cutaneous afferents in cats (Edgley and Aggelopoulos, 2006) and humans (Gervasio et al. 2017) and mice shown with tibial and sural nerve stimulation (Laflamme and Akay, 2018).

Collectively, our results, together with our previous data (Laflamme and Akay, 2018), suggest that proprioceptive and non-nociceptive cutaneous afferent activation initiate crossed reflex responses in mice. This is in agreement with results from research conducted on cats and humans that muscle afferents (Arya et al. 1991; Aggelopoulos and Edgley, 1995; Stubbs and Mrachacz-Kersting, 2009; Jankowska and Edgley, 2010; Stubbs et al. 2011; Gervasio et al. 2017), as well as cutaneous afferents (Perl, 1957; Gauthier and Rossignol, 1981; Edgley and Aggelopoulos, 2006; Stubbs and Mrachacz-Kersting, 2009), mediate crossed reflex responses.

3.5.2 Long-latency crossed reflex responses are only observed when the common peroneal nerve Is stimulated

One of the most striking qualitative differences in the crossed reflex response in the resting mouse was a long-latency response only observed when the common peroneal nerve was stimulated but not when the tibial or the sural nerve was stimulated. We believe that these long-latency motor responses could be explained by the presence of a longer pathway that would involve the supraspinal centers (Kurtzer, 2015). These pathways could involve main ascending pathways that carry proprioceptive and low-threshold cutaneous mechanoinformation, such as the dorsal column lemniscus pathways and the dorsal spinocerebellar pathway (Hantman and Jessell, 2010; Tuthill and Azim, 2018). Clarification of this issue needs further experimentation in the future.

3.5.3 Crossed reflex during locomotion

Our data demonstrate that similar to the tibial and sural nerve stimulation (Laflamme and Akay, 2018), the crossed inhibitory reflex is downregulated when the animal walks selectively for the knee extensor (VL) and the ankle flexor (TA) muscles. In addition, the inhibitory crossed reflex is also downregulated in the Gs muscle during walking, only with the common peroneal nerve stimulation but not with tibial or sural nerve stimulation. This observation extends the previous observations that the inhibitory crossed reflex selectively for the VL muscle during locomotion in the cat when the superficial peroneal nerve and the tibial nerve were stimulated (Frigon and Rossignol, 2008). Our present and previous (Laflamme and Akay, 2018) results add to this data that crossed inhibition is also downregulated during walking in TA muscle. We also show that during locomotion, crossed inhibition is downregulated in the ankle extensor muscle. Our present data extend previous data on inhibitory crossed reflex changes during walking to further describe crossed reflex modulation during locomotion.

Previously, it was suggested that the absence of crossed inhibitory influence in the VL was due to the more rostral location of the motor neuron pool in the spinal cord than the other muscles (Frigon and Rossignol, 2008). However, our previous (Laflamme and Akay, 2018) and present results show that the inhibitory crossed reflex influence is also downregulated in TA (motor neurons located in lumbar 3–4 spinal segments) and only for

the common peroneal nerve stimulation in Gs (motor neurons located mainly in lumbar 4 spinal segments) in addition to VL (motor neuron cell bodies located between lumbar spinal segments 1–3) (McHanwell and Biscoe, 1981). Therefore, our data do not support the view that the absence of the state-dependent modulation of the inhibitory crossed reflex response is due to motor neuron pool location.

Commissural interneurons mediating crossed reflexes from group II muscle spindle afferents have been shown to depend on the presence of serotonin. When group II muscle afferents were stimulated, short-latency inhibition of contralateral extensor motor neurons was observed when the spinal cord was intact, but excitation was observed when the animal was spinalized (Arya et al. 1991; Aggelopoulos and Edgley, 1995). The inhibition of motor neurons in spinalized cats could be restored following the activation of 5-HT receptors (Aggelopoulos et al. 1996). In addition, monoaminergic inputs are also known to interact with commissural interneuron located in lamina VIII of the spinal cord (Hammar et al. 2004; 2007), and they are also involved in rhythmic motor activities such as locomotion (Schmidt and Jordan, 2000). Therefore, it is likely that monoaminergic modulation might be the regulating factor of inhibitory crossed reflex in the VL, TA, and Gs during locomotion.

In this study, we provide a detailed description of the motor response to the stimulation of contralateral sensory afferents innervating the ankle flexor muscles, and the skin covering the anterolateral aspect in mice in vivo. Our results demonstrate that crossed reflexes regardless of the stimulated nerves are mostly similar with slight differences. These differences are limited to the downregulation of the inhibitory crossed reflexes to particular muscles during walking. Moreover, we found the existence of long-latency crossed reflex responses when the common peroneal nerve is stimulated, but not when the tibial or sural nerve is stimulated (Laflamme and Akay, 2018). These data will be important for our future efforts to disclose the role of genetically distinct classes of commissural interneurons (Lanuza et al. 2004; Zhang et al. 2008; Talpalar et al. 2013) in crossed reflexes.

3.6 FIGURES

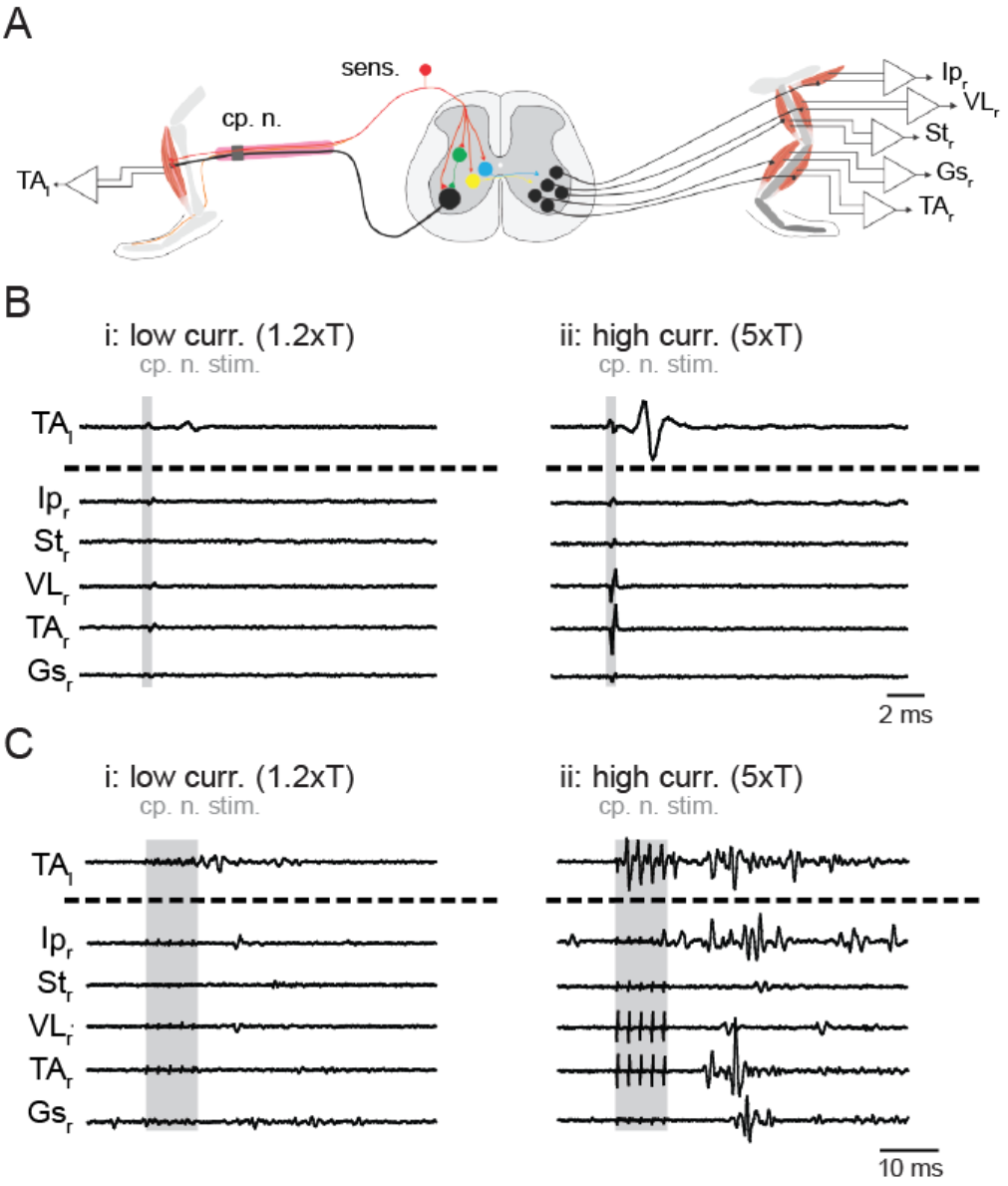

Figure 3.1. Schematic of experimental design used to investigate crossed reflex in vivo. *A*: the experimental design used to investigate crossed reflex in vivo. Example of EMG recording at low- (1.2 × T; *i*) and high- (5 × T; *ii*) current stimulation from one mouse after stimulation (stim.) of the common peroneal nerve (cp. n.) using a single pulse (*B*) or five-pulse train (*C*). Shaded areas indicate stimulation. Gs_r, right gastrocnemius; Ip_r, right iliopsoas; sens., sensory neurons; St_r, right semitendinosus; TA_l, left tibialis anterior; TA_r, right tibialis anterior; VL_r, right vastus lateralis.

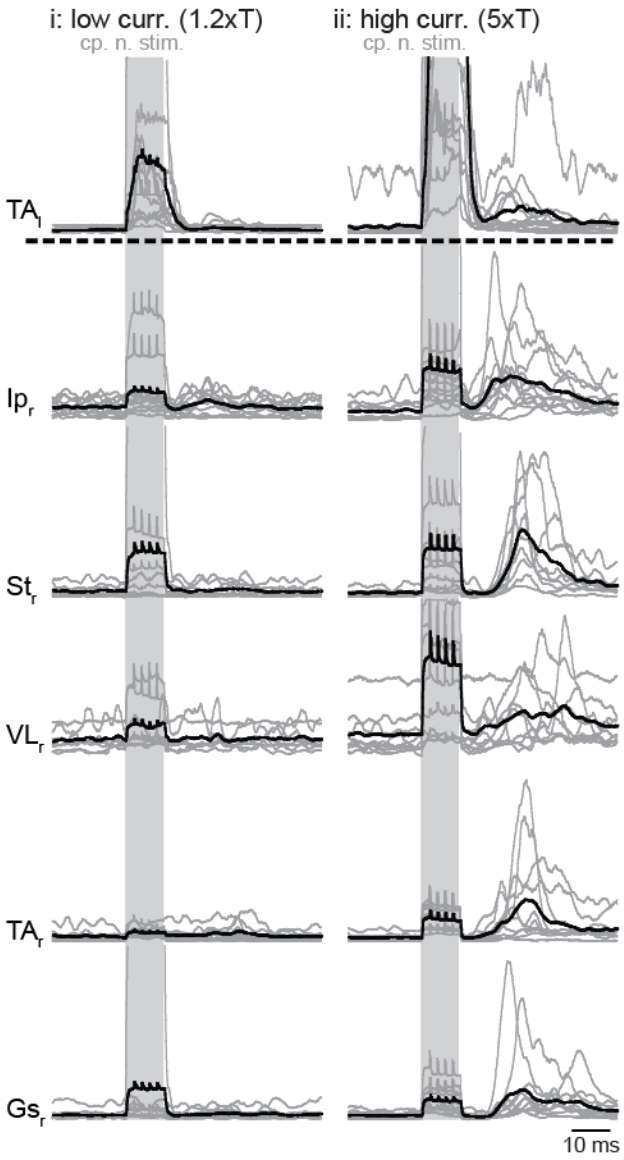

Figure 3.2. Average crossed reflex responses from different muscles after stimulation of the common peroneal nerve. *i*: low (1.2 × T) current stimulation. *ii*: high (5 × T) current stimulation. The gray lines are averages of 20–40 stimulations in each animal. The black lines correspond to the average across all animals. Shaded areas indicate stimulation. cp. n. stim., stimulation of the common peroneal nerve; Gs_r, right gastrocnemius; Ip_r, right iliopsoas; St_r, right semitendinosus; TA_l, left tibialis anterior; TA_r, right tibialis anterior; VL_r, right vastus lateralis. From 13 animals (8 males and 5 females).

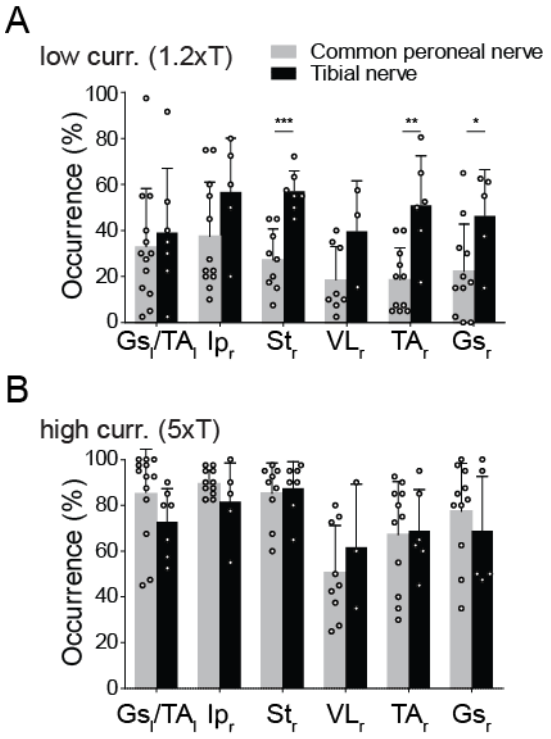

Figure 3.3. Occurrence of motor responses following the common peroneal. Bar graph showing the percentage of time a motor response was triggered following stimulation of either the common peroneal nerve (gray) or tibial nerve (black) at low current (*A*) and high current (*B*). The occurrence was calculated using 40 nerve stimulations for the same current strength. Each dot represents one animal. GS_l, left gastrocnemius; Gs_r, right gastrocnemius; Ip_r, right iliopsoas; St_r, right semitendinosus; TA_l, left tibialis anterior; TA_r, right tibialis anterior; VL_r, right vastus lateralis. Statistical comparisons were made using Student's t-test if normality was present. Otherwise, the Mann-Whitney test was applied. Open circles on the bars indicate averages from individual animals. (n = 13; 8 males, 5 females) and tibial nerve (n = 7; all males) stimulation.

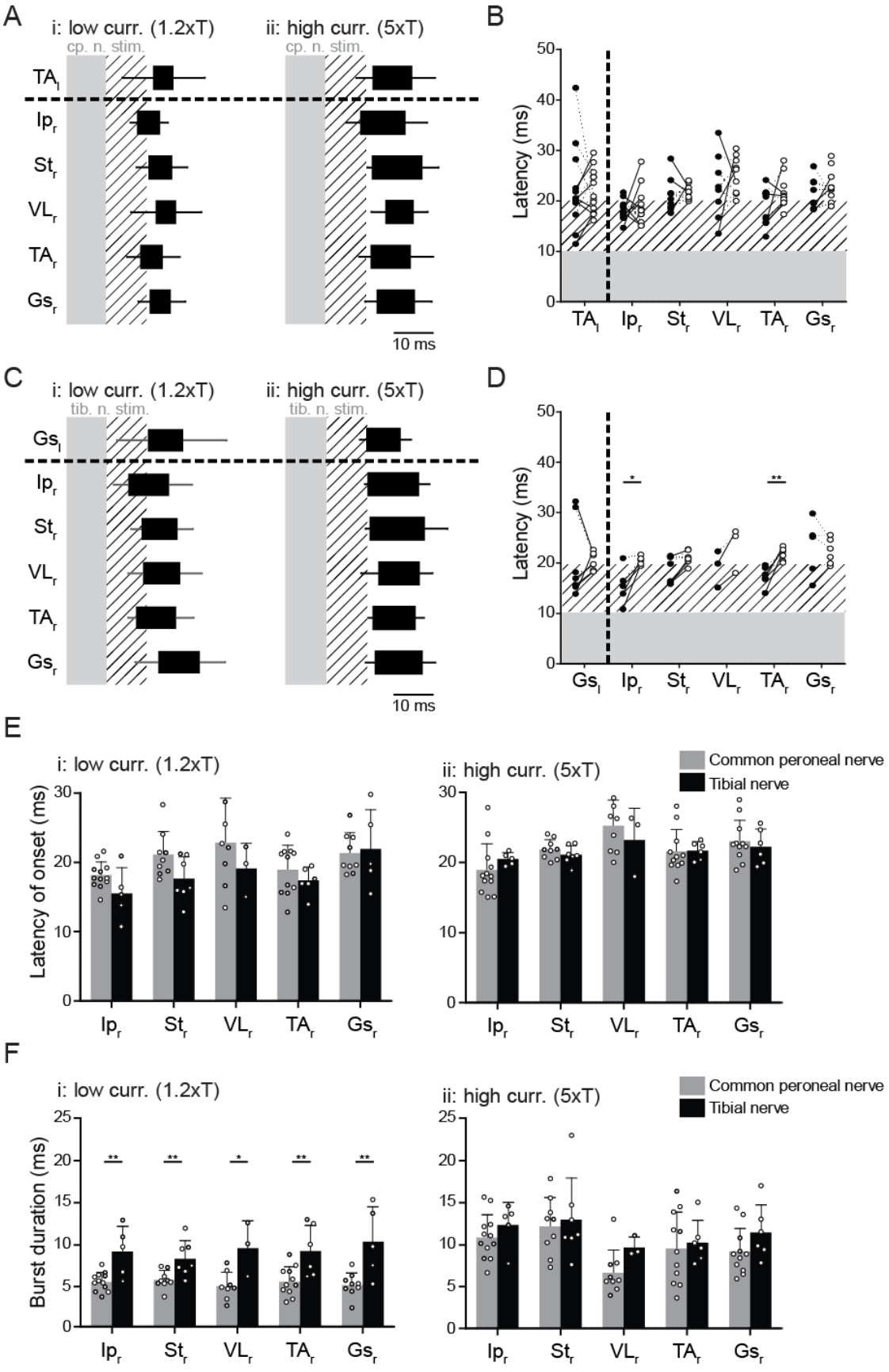
A
i: low curr. (1.2xT)
ii: high curr. (5xT)
cp. n. stim.
TA_l
Ip_r
St_r
VL_r
TA_r
Gs_r
10 ms
B
Latency (ms)
C
tib. n. stim.
Gs_l
D
*
**
E
Latency of onset (ms)
Common peroneal nerve
Tibial nerve
F
Burst duration (ms)

Figure 3.4. Crossed reflex muscle activation pattern. *A*: the muscle activation pattern at low- and high-current stimulation following the common peroneal nerve stimulation (data from 13 experiments; 8 males and 5 females). *B*: latencies of activity onset in different muscles at low- and high-current stimulation following the common peroneal nerve stimulation. *C*: the pattern of muscle activation at low- and high-current stimulation following tibial nerve stimulation summarizing data from seven experiments (all male). *D*: latencies of onsets of activity in the recorded muscles following tibial nerve stimulation. *E* and *F*: latencies of onset and duration of activities in each recorded muscle as a response to common peroneal nerves (gray bars) or the tibial nerve (black bars) at low (*i*) and high (*ii*) current. Open circles on the bars indicate averages from individual animals. The shaded area in *A–D* represents the stimulation area. The striped area represents 10 ms after the stimulation. Filled and empty circles represent latency onset at low and high currents, respectively. In *B* and *D–F*, statistical comparisons were made using Student's t-test if normality was present. Otherwise, Mann–Whitney test was applied. cp. n. stim., common peroneal nerve stimulation; Gs_l, left gastrocnemius; Gs_r, right gastrocnemius; Ip_r, right iliopsoas; St_r, right semitendinosus; TA_l, left tibialis anterior; TA_r, right tibialis anterior; tib. n. stim., tibial nerve stimulation; VL_r, right vastus lateralis.

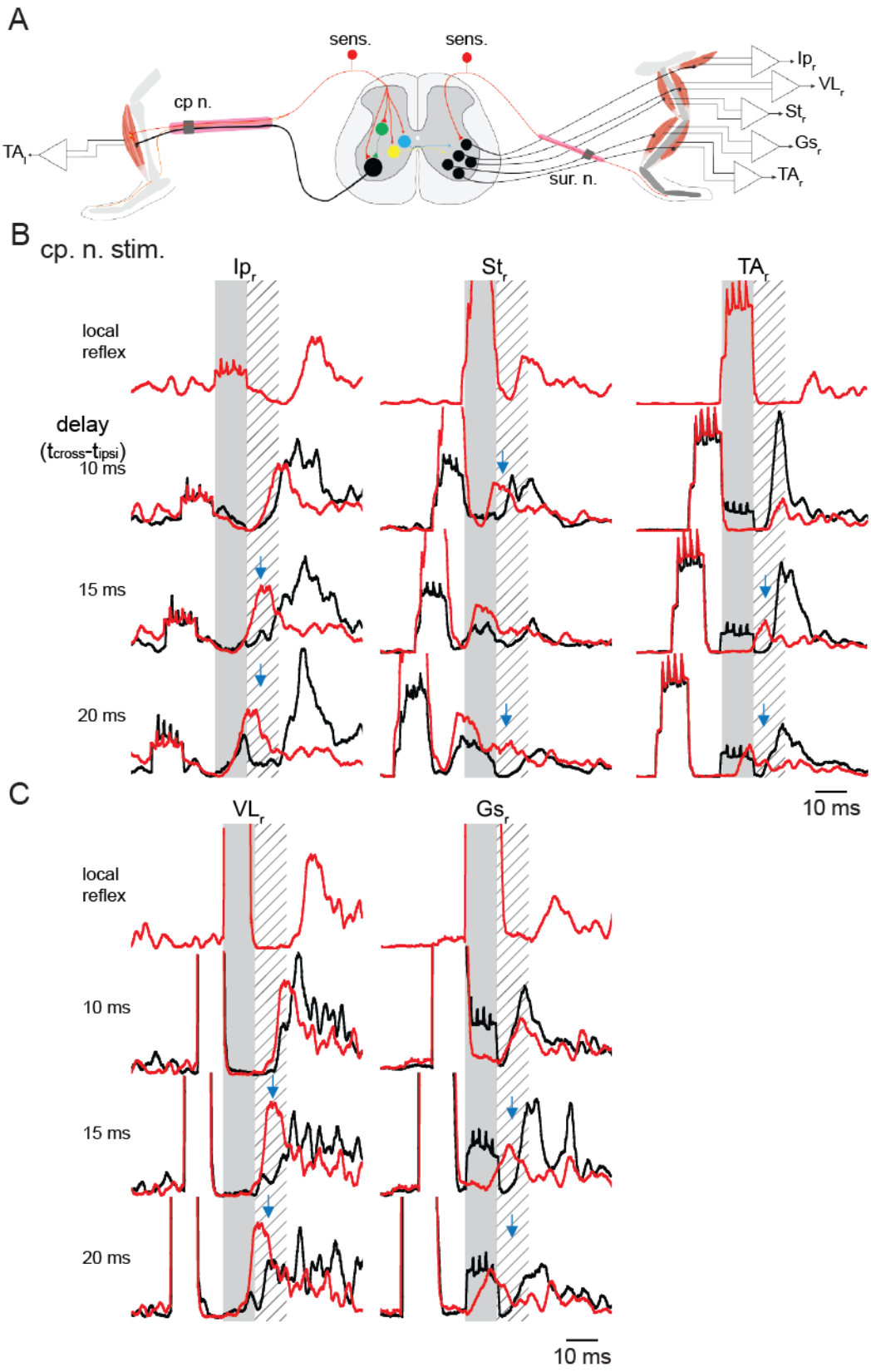
A
sens.
sens.
cp n.
TA$_l$
Ip$_r$
VL$_r$
St$_r$
Gs$_r$
TA$_r$
sur. n.
B
cp. n. stim.
Ip$_r$
St$_r$
TA$_r$
local reflex
delay
(t$_{cross}$-t$_{ipsi}$)
10 ms
15 ms
20 ms
10 ms
C
VL$_r$
Gs$_r$
local reflex
10 ms
15 ms
20 ms
10 ms

Figure 3.5. Short-latency inhibition in crossed reflex initiated by tibial nerve stimulation. *A*: schematic presentation of the paired stimulation of the left common peroneal nerve (cp. n.) and right sural nerve (sur. n.) at different delays. The existence of a decreased electromyogram (EMG) activity immediately after cp. n. stimulation (black traces) regardless of expected activity due to sur. n. stimulation (red traces) is evidence for the existence of an inhibitory crossed reflex pathway. Data are representative examples from 20 stimulations for each muscle for a total of six experiments (3 males and 3 females). The traces are average EMG recordings from the contralateral flexor (*B*) and the extensor (*C*) muscles. Shaded areas represent stimulation of the contralateral common peroneal nerve to evoke a crossed reflex. Hatched areas represent the silent period detected previously. Red traces represent the average EMG response to local reflex activation initiated by ipsilateral sural nerve stimulation. Black traces indicate the EMG response when the ipsilateral sural nerve is stimulated with the contralateral tibial nerve with a delay indicated on the left of each set of recordings. Blue arrows represent the suppression of local cutaneous reflex by contralateral sensory stimulation. Gs_r, right gastrocnemius; Ip_r, right iliopsoas; St_r, right semitendinosus; TA_l, left tibialis anterior; TA_r, right tibialis anterior; VL_r, right vastus lateralis.

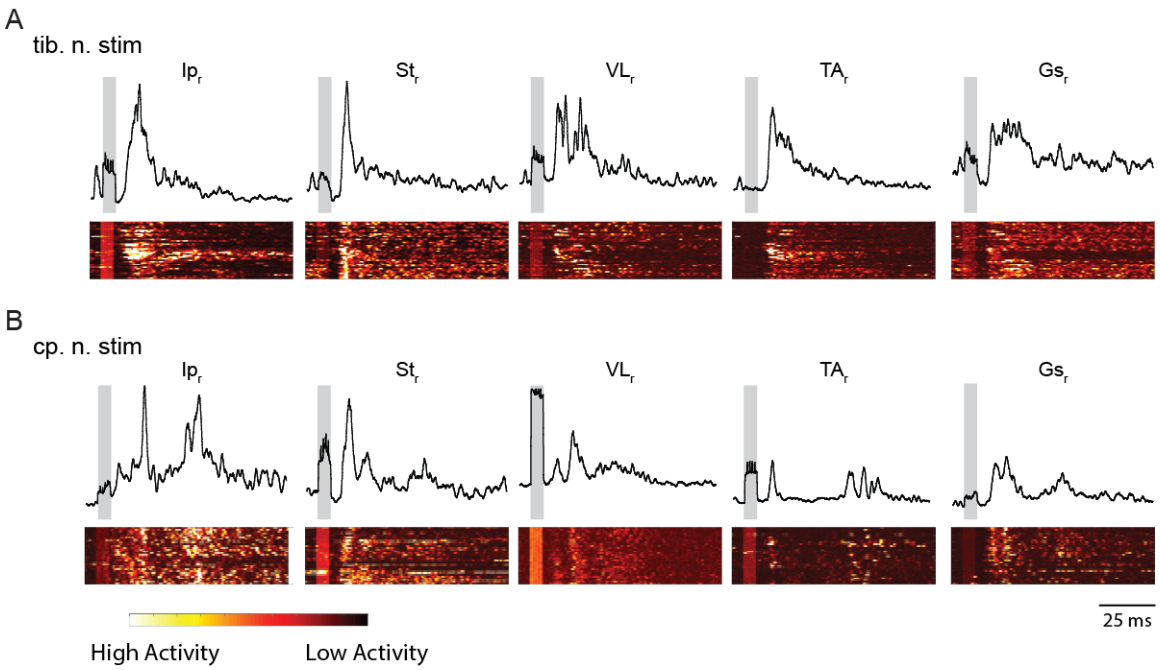

Figure 3.6. Long-latency motor responses in the common peroneal but not tibial nerve stimulation. Example of average crossed reflex responses from different muscles after the stimulation of the tibial nerve representing similar results from seven animals (*A*) or the common peroneal nerve representing similar results from 13 animals (8 males and 5 females) (*B*). Heat diagrams of muscle activity are shown underneath each average. Muscle response to each of 40 nerve stimulations from 1 experiment is staggered on the vertical axis as a function of time. The brighter color indicates higher muscle Gs_r, right gastrocnemius; Ip_r, right iliopsoas; St_r, right semitendinosus; TA_r, right tibialis anterior; VL_r, right vastus lateralis. common peroneal (cp. n.), tibial nerve (tib. n.), stimulation (stim).

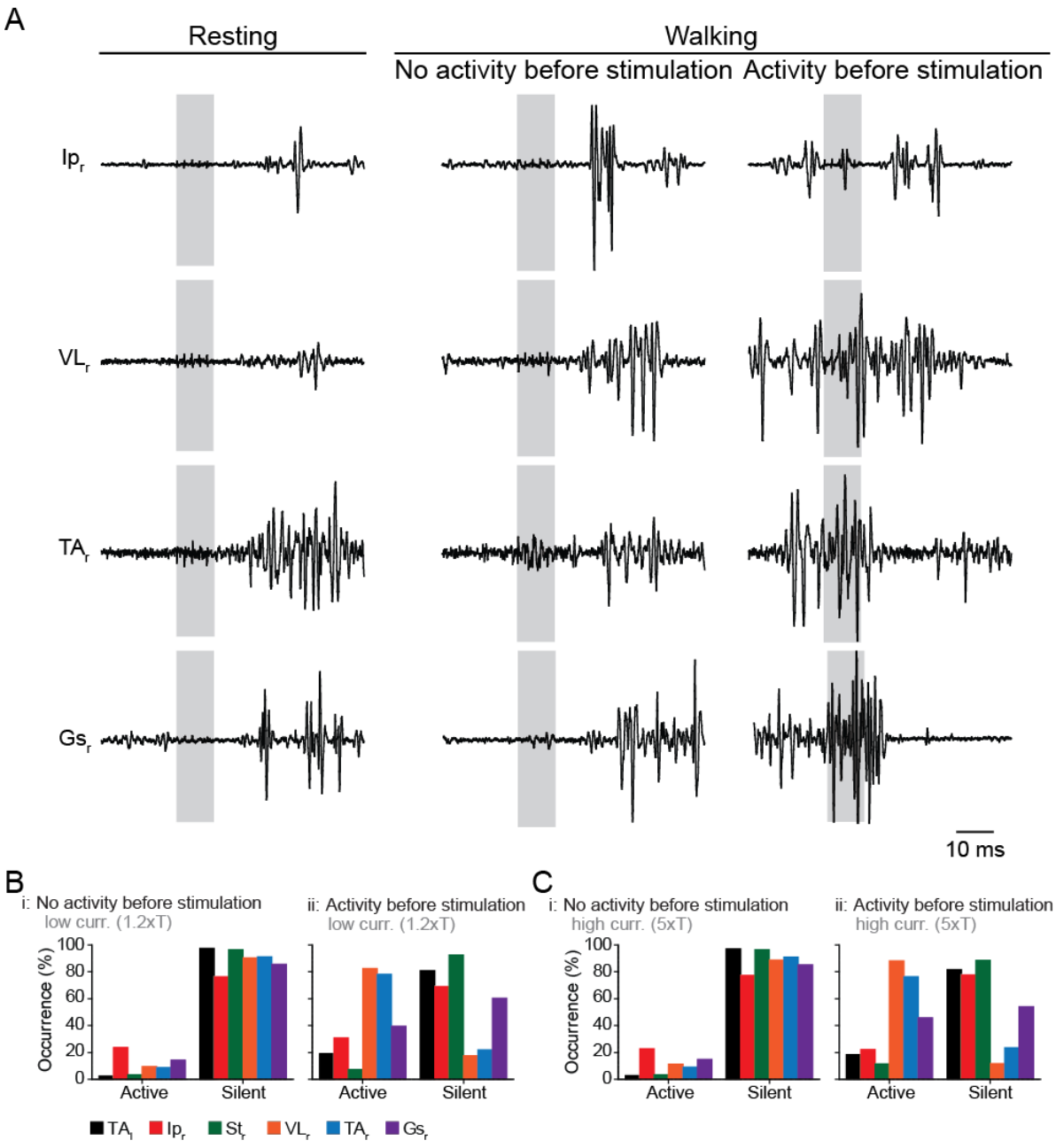
A
Resting
Walking
No activity before stimulation
Activity before stimulation
Ip$_r$
VL$_r$
TA$_r$
Gs$_r$
10 ms
B
i: No activity before stimulation
low curr. (1.2xT)
ii: Activity before stimulation
low curr. (1.2xT)
Occurrence (%)
100
80
60
40
20
0
Active
Silent
TA$_l$ Ip$_r$ St$_r$ VL$_r$ TA$_r$ Gs$_r$
C
i: No activity before stimulation
high curr. (5xT)
ii: Activity before stimulation
high curr. (5xT)

Figure 3.7. Crossed reflex response selectively in right vastus lateralis (VL_r), right tibialis anterior (TA_r), and right gastrocnemius (Gs_r) depends on muscle activity status before nerve stimulation during walking. *A*: electromyogram (EMG) recordings from the right iliopsoas (Ip_r), VL_r, TA_r, and Gs_r at rest and the two different states during walking when the muscle was not active or active before the stimulation. These examples are representative of nine experiments (5 males and 2 females). Occurrences of muscle responses, as active or silent within the first 5 ms after stimulation of the common peroneal nerve at low current (*B*) or high current (*C*). The graphs in *B* and *C* illustrate the data from nine animals (5 males and 2 females). St_r, right semitendinosus; TA_l, left tibialis anterior.

3.7 SUPPLEMENTAL FIGURE

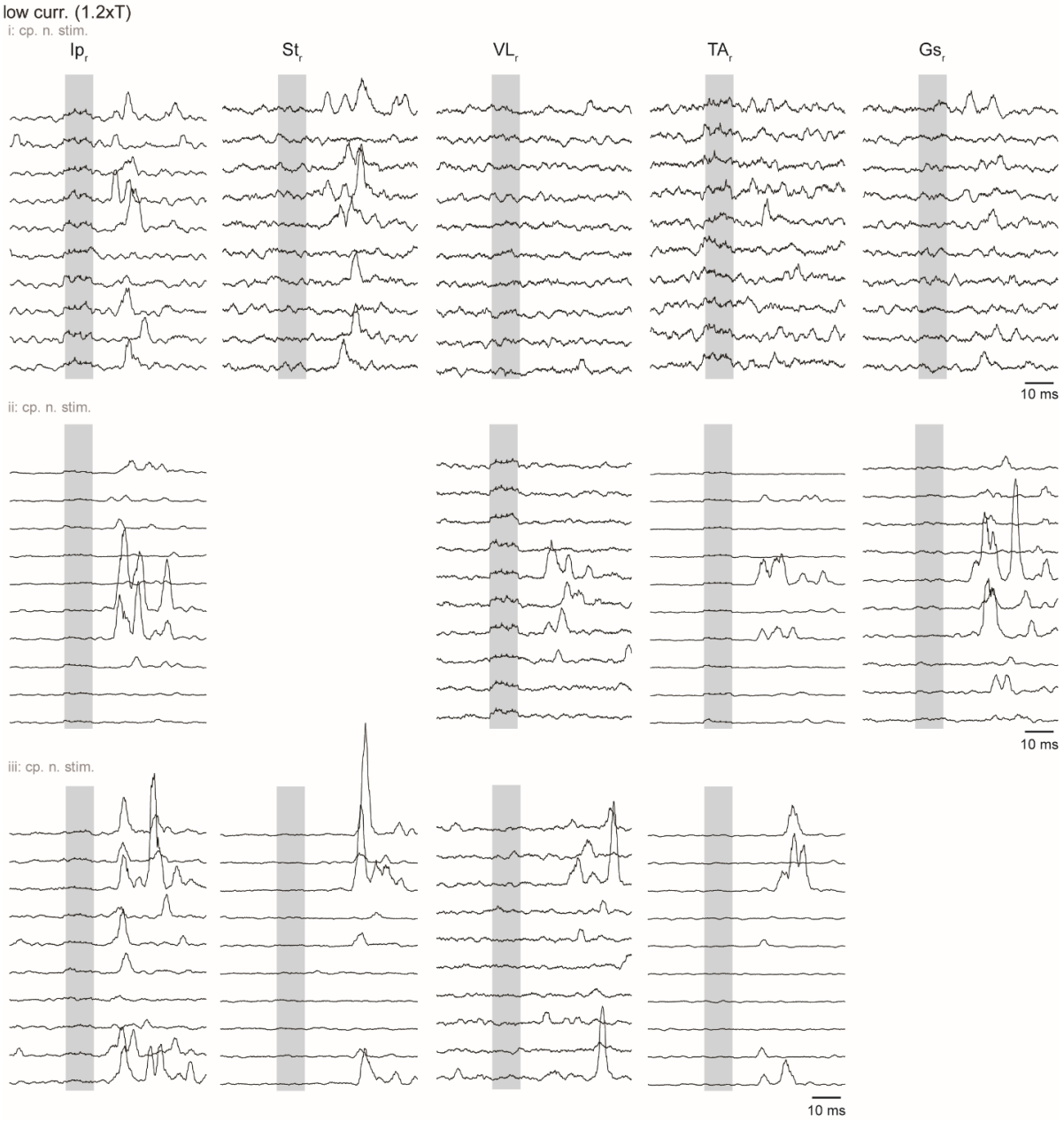

Supplemental figure S3.1. Crossed reflex responses from different muscles after stimulation of the common peroneal nerve at low current (1.2 xT). Each line represents EMG responses to individual stimulations of the common peroneal nerve (cp. n. stim.) at a low current (1.2 xT) in three animals. Shaded areas indicate stimulation. Right iliopsoas (Ip_r), right semitendinosus (St_r), right vastus lateralis (VL_r), right tibialis anterior (TA_r), and right gastrocnemius (Gs_r). Functional St_r and Gs_r recordings were missing in the animal presented in the middle and bottom, respectively.

3.8 REFERENCES

Aggelopoulos NC, Burton MJ, Clarke RW, Edgley SA. Characterization of a descending system that enables crossed group II inhibitory reflex pathways in the cat spinal cord. **J Neurosci** 16: 723–729, 1996. doi:10.1523/JNEUROSCI.16-02-00723.1996.

Aggelopoulos NC, Edgley SA. Segmental localisation of the relays mediating crossed inhibition of hindlimb motoneurones from group II afferents in the anaesthetized cat spinal cord. **Neurosci Lett** 185: 60–64, 1995. doi:10.1016/0304-3940(94)11225-8.

Akay T. Long-term measurement of muscle denervation and locomotor behavior in individual wild-type and ALS model mice. **J Neurophysiol** 111: 694–703, 2014. doi:10.1152/jn.00507.2013.

Akay T, Acharya HJ, Fouad K, Pearson KG. Behavioral and electromyographic characterization of mice lacking EphA4 receptors. **J Neurophysiol** 96: 642–651, 2006. doi:10.1152/jn.00174.2006.

Arya T, Bajwa S, Edgley SA. Crossed reflex actions from group II muscle afferents in the lumbar spinal cord of the anaesthetized cat. **J Physiol** 444: 117–131, 1991. doi:10.1113/jphysiol.1991.sp018869.

Bagust J, Kerkut GA. Crossed reflex activity in an entire, isolated, spinal cord preparation taken from juvenile rodents. **Brain Res** 411: 397–399, 1987. doi:10.1016/0006-8993(87)91094-8.

Bernard G, Bouyer L, Provencher J, Rossignol S. Study of cutaneous reflex compensation during locomotion after nerve section in the cat. **J Neurophysiol** 97: 4173–4185, 2007. doi:10.1152/jn.00797.2006.

Cain DM, Khasabov SG, Simone DA. Response properties of mechanoreceptors and nociceptors in mouse glabrous skin: an in vivo study. **J Neurophysiol** 85: 1561–1574, 2001. doi:10.1152/jn.2001.85.4.1561.

Edgley SA, Aggelopoulos NC. Short latency crossed inhibitory reflex actions evoked from cutaneous afferents. **Exp Brain Res** 171: 541–550, 2006. doi:10.1007/s00221-005-0302-9.

Edgley SA, Jankowska E, Krutki P, Hammar I. Both dorsal horn and lamina VIII interneurones contribute to crossed reflexes from feline group II muscle afferents. **J Physiol** 552: 961–974, 2003. doi:10.1113/jphysiol.2003.048009.

Forssberg H. Stumbling corrective reaction: a phase-dependent compensatory reaction during locomotion. **J Neurophysiol** 42: 936–953, 1979. doi:10.1152/jn.1979.42.4.936.

Forssberg H, Grillner S, Rossignol S. Phase dependent reflex reversal during walking in chronic spinal cats. **Brain Res** 85: 103–107, 1975. doi:10.1016/0006-8993(75)91013-6.

Frigon A, Rossignol S. Adaptive changes of the locomotor pattern and cutaneous reflexes during locomotion studied in the same cats before and after spinalization. **J Physiol** 586: 2927–2945, 2008. doi:10.1113/jphysiol.2008.152488.

Hurteau M-F, Thibaudier Y, Dambreville C, Danner SM, Rybak IA, Frigon A. Intralimb and interlimb cutaneous reflexes during locomotion in the intact cat. **J Neurosci** 38: 4104–4122, 2018. doi:10.1523/JNEUROSCI.3288-17.2018.

Gauthier L, Rossignol S. Contralateral hindlimb responses to cutaneous stimulation during locomotion in high decerebrate cats. **Brain Res** 207: 303–320, 1981. doi:10.1016/0006-8993(81)90366-8.

Gervasio S, Voigt M, Kersting UG, Farina D, Sinkjær T, Mrachacz-Kersting N. Sensory feedback in interlimb coordination: contralateral afferent contribution to the short-latency crossed response during human walking. **PLoS One** 12: e0168557–24, 2017. doi:10.1371/journal.pone.0168557.

Hammar I, Bannatyne BA, Maxwell DJ, Edgley SA, Jankowska E. The actions of monoamines and distribution of noradrenergic and serotoninergic contacts on different subpopulations of commissural interneurons in the cat spinal cord. **Eur J Neurosci** 19: 1305–1316, 2004. doi:10.1111/j.1460-9568.2004.03239.x.

Hammar I, Stecina K, Jankowska E. Differential modulation by monoamine membrane receptor agonists of reticulospinal input to lamina VIII feline spinal commissural interneurons. **Eur J Neurosci** 26: 1205–1212, 2007. doi:10.1111/j.1460-9568.2007.05764.x.

Hantman AW, Jessell TM. Clarke's column neurons as the focus of a corticospinal corollary circuit. **Nat Neurosci** 13: 1233–1239, 2010. doi:10.1038/nn.2637.

Jack JJB. Some methods for selective activation of muscle afferent fibres. In: **Studies in Neurophysiology: Presented to A. K. McIntryre**, edited by Porter R. London, New York, Melbourne: Cambridge University Press, 1978, p. 155–176.

Jankowska E, Edgley SA. Functional subdivision of feline spinal interneurons in reflex pathways from group Ib and II muscle afferents; an update. **Eur J Neurosci** 32: 881–893, 2010. doi:10.1111/j.1460-9568.2010.07354.x.

Jankowska E, Jukes MGM, Lund S, Lundberg A. The effect of DOPA on the spinal cord 5. Reciprocal organization of pathways transmitting excitatory action to alpha motoneurones of flexors and extensors. **Acta Physiol Scand** 70: 369–388, 1967. doi:10.1111/j.1748-1716.1967.tb03636.x.

Jankowska E, Jukes MG, Lund S, Lundberg A. The effect of DOPA on the spinal cord 6. Half-centre organization of interneurones transmitting effects from the flexor reflex afferents. **Acta Physiol Scand** 70: 389–402, 1968. doi:10.1111/j.1748-1716.1967.tb03637.x.

Jiang Z, Carlin KP, Brownstone RM. An in vitro functionally mature mouse spinal cord preparation for the study of spinal motor networks. **Brain Res** 816: 493–499, 1999. doi:10.1016/S0006-8993(98)01199-8.

Kambiz S, Baas M, Duraku LS, Kerver AL, Koning AHJ, Walbeehm ET, Ruigrok TJH. Innervation mapping of the hind paw of the rat using Evans Blue extravasation, optical surface mapping and CASAM. **J Neurosci Methods** 229: 15–27, 2014. doi:10.1016/j.jneumeth.2014.03.015.

Kurtzer IL. Long-latency reflexes account for limb biomechanics through several supraspinal pathways. **Front Integr Neurosci** 8: 99, 2015. doi:10.3389/fnint.2014.00099.

Laflamme OD, Akay T. Excitatory and inhibitory crossed reflex pathways in mice. **J Neurophysiol** 120: 2897–2907, 2018. doi:10.1152/jn.00450.2018.

Lanuza GM, Gosgnach S, Pierani A, Jessell TM, Goulding M. Genetic identification of spinal interneurons that coordinate left-right locomotor activity necessary for walking movements. **Neuron** 42: 375–386, 2004. doi:10.1016/s0896-6273(04)00249-1.

Mayer WP, Akay T. Stumbling corrective reaction elicited by mechanical and electrical stimulation of the saphenous nerve in walking mice. **J Exp Biol** 221: jeb.178095, 2018. doi:10.1242/jeb.178095.

McHanwell S, Biscoe T. The localization of the motoneurons supplying the hindlimb muscles of the mouse. **Philos Trans R Soc Lond B Biol Sci** 293: 477–508, 1981. doi:10.1098/rstb.1981.0082.

Nakanishi ST, Whelan PJ. A decerebrate adult mouse model for examining the sensorimotor control of locomotion. **J Neurophysiol** 107: 500–515, 2012. doi:10.1152/jn.00699.2011.

Pearson KG, Acharya H, Fouad K. A new electrode configuration for recording electromyographic activity in behaving mice. **J Neurosci Methods** 148: 36–42, 2005. doi:10.1016/j.jneumeth.2005.04.006.

Perl ER. Crossed reflexes of cutaneous origin. **Am J Physiol** 188: 609–615, 1957. doi:10.1152/ajplegacy.1957.188.3.609.

Prochazka A, Sontag KH, Wand P. Motor reactions to perturbations of gait: proprioceptive and somesthetic involvement. **Neurosci Lett** 7: 35–39, 1978. doi:10.1016/0304-3940(78)90109-x.

Quevedo J, Stecina K, Gosgnach S, McCrea DA. Stumbling corrective reaction during fictive locomotion in the cat. **J Neurophysiol** 94: 2045–2052, 2005. doi:10.1152/jn.00175.2005.

Schomburg ED, Kalezic I, Dibaj P, Steffens H. Reflex transmission to lumbar α-motoneurones in the mouse similar and different to those in the cat. **Neurosci Res** 76: 133–140, 2013. doi:10.1016/j.neures.2013.03.011.

Sherrington CS. Flexion-reflex of the limb, crossed extension-reflex, and reflex stepping and standing. **J Physiol** 40: 28–121, 1910. doi:10.1113/jphysiol.1910.sp001362.

Schmidt BJ, Jordan LM. The role of serotonin in reflex modulation and locomotor rhythm production in the mammalian spinal cord. **Brain Res Bull** 53: 689–710, 2000. doi:10.1016/s0361-9230(00)00402-0.

Stubbs PW, Mrachacz-Kersting N. Short-latency crossed inhibitory responses in the human soleus muscle. **J Neurophysiol** 102: 3596–3605, 2009. doi:10.1152/jn.00667.2009.

Stubbs PW, Nielsen JF, Sinkjær T, Mrachacz-Kersting N. Phase modulation of the short-latency crossed spinal response in the human soleus muscle. **J Neurophysiol** 105: 503–511, 2011 [Erratum in *J Neurophysiol* 106: 1600, 2011]. doi:10.1152/jn.00786.2010.

Talpalar AE, Bouvier J, Borgius L, Fortin G, Pierani A, Kiehn O. Dual-mode operation of neuronal networks involved in left-right alternation. **Nature** 500: 85–88, 2013. doi:10.1038/nature12286.

Tuthill JC, Azim E. Proprioception. **Curr Biol** 28: R187–R207, 2018. doi:10.1016/j.cub.2018.01.064.

Zhang Y, Narayan S, Geiman E, Lanuza GM, Velasquez T, Shanks B, Akay T, Dyck J, Pearson K, Gosgnach S, Fan CM, Goulding M. V3 spinal neurons establish a robust and balanced locomotor rhythm during walking. **Neuron** 60: 84–96, 2008. doi:10.1016/j.neuron.2008.09.027.

Zimmermann K, Hein A, Hager U, Kaczmarek JS, Turnquist BP, Clapham DE, Reeh PW. Phenotyping sensory nerve endings in vitro in the mouse. **Nat Protoc** 4: 174–196, 2009. doi:10.1038/nprot.2008.223.

Chapter 4. Segregated spinal commissural pathways for central versus peripheral information

Contribution statement

I would like to acknowledge Rachel Banks for assisting with the experiments and data analysis of the $V3^{off}$ mice. I would like to thank Brenda Ross for her technical assistance with the mouse colony. I also want to acknowledge the work of Dr. Simon Danner and Dr. Sergey Markin on the quantification of the inhibitory pathway and help throughout the data analysis. I would like to thank Dr. Ying Zhang for providing the Sim1::Cre mouse and her input and help from her laboratory on this project throughout my Ph.D. I would also thank Dr. Hanns Ulrich Zeilhofer and Dr. Arthur Kania for providing the HoxB8::Cre breeder mice.

4.1 ABSTRACT

Commissural pathways coordinating the activities of spinal locomotor circuits during locomotion have been characterized in mice but the involvement of the same commissural pathways in transmitting sensory information is not known. Here we use mouse genetics and *in vivo* electrophysiology to investigate the involvement of the two main groups of commissural interneurons (CINs) important for locomotion, the V0, and the V3 CINs, in the crossed reflex pathways. We show that the V0 CINs that include inhibitory CINs, although important for the left-right coordination during locomotion are not involved in inhibitory crossed reflex. In contrast, the exclusively excitatory V3 CINs, although not necessary for the left-right alternation, but necessary for the regularity of the pattern, are involved in inhibitory crossed reflex responses. Thus, we provide evidence for segregated pathways for coordinating the activity of the central locomotor circuit and crossed reflex pathways important for left-right alternation of leg movements during locomotion.

4.2 INTRODUCTION

Coordinated movement of the legs on both sides of the body is a hallmark of locomotor behaviour. Quadrupedal animals change their gaits depending on the speed of locomotion. Gaits with alternating movements of the left and right limbs are commonly used at low speeds, while gaits with synchronous or nearly synchronous left and right limb movements are commonly used at high speeds (Hildebrand, 1989). Mice use alternating gaits to walk and trot at lower speeds and synchronous gaits gallop and bound at higher speeds (Bellardita and Kiehn, 2015; Lemieux et al. 2016). With the advances in mouse developmental genetics and genetic engineering, it was possible to describe the spinal neuronal circuitry that controls the movement of the left and right hindlimbs during locomotion at different speeds (Bellardita and Kiehn, 2015; Kiehn, 2016). However, whether and how this circuitry processes somatosensory information remains still obscure.

Two main cardinal groups of commissural interneurons, the V0, and the V3 have been shown to emerge from two ventrally located progenitor domains, the p0, and the p3, of the embryonic spinal cord (Pierani et al. 2001; Lanuza et al. 2004; Zhang et al. 2008).

While the V0 further diverges into dorsal inhibitory CINs ($V0_d$) and ventral excitatory CINs ($V0_v$), the V3 CINs are exclusively excitatory (Lanuza et al. 2004; Zhang et al. 2008). Previous research provided evidence that these interneurons constitute a neuronal network that coordinates the left-right movement by providing excitation and inhibition to the contralateral site of the spinal cord (Lanuza et al. 2004; Zhang et al. 2008). The excitation is provided by the V3 CINs while the inhibition is provided by a dual pathway; either directly through the inhibitory $V0_d$ CINs or indirectly through the excitatory $V0_v$ and V3 CINs (Zhang et al. 2008; 2022; Kiehn, 2011; Talpalar et al. 2013; Shevtsova et al. 2015; Danner et al. 2019). Furthermore, it has been shown that the removal of the V0 CINs from the spinal network using mouse genetics severely disrupts the left-right alternation during locomotion in a speed-dependent manner (Talpalar et al. 2013). In contrast, genetically silencing V3 CIN output does not eliminate the left-right alternation during locomotion, but it compromises the stability of coordination (Zhang et al. 2008; 2022). Despite this large amount of information, the involvement of the V0 and the V3 CINs in crossed reflexes is not known.

Crossed reflexes are defined as the reflex response of one limb to somatosensory stimuli coming from the contralateral limb. The spinal circuitry that mediates crossed reflexes transduced by muscle proprioceptive afferents, as well as cutaneous afferents, has been investigated in detail in cats (Sherrington, 1905; Perl, 1957; Gauthier and Rossignol, 1981; Arya et al. 1991; Aggelopoulos and Edgley, 1995; Edgley et al. 2003; Jankowska, 2008; Jankowska and Edgley, 2010). Despite, many interneurons including CINs that are involved in crossed reflexes have been identified using physiological and histological criteria in the cat model, the cellular structure of the spinal circuitry is still obscure. The significance of sensorimotor integration through commissural interneurons lies in its importance for interlimb coordination, and gait stability, for example during stumbling correction (Jankowska, 2013; 2016; Kiehn, 2016). These gait properties are compromised following various motor disorders (Dietz et al. 1995; Plotnik et al. 2007; 2008; Tseng and Morton, 2010; Meijer et al. 2011; Tester et al. 2012) as well as in the elderly (Krasovsky et al. 2012). Indeed, impairment of crossed reflex and its inhibitory component has been shown in individuals with stroke or when transcranial magnetic stimulation was performed on healthy participants (Stubbs et al. 2012; Mrachacz-Kersting et al. 2018). Especially, in

light of the insights gained using the mouse model, it is not clear how the V0 and the V3 CINs relate to crossed reflexes. A better understanding of the spinal commissural pathways is crucial as they are very likely to be a crucial part of a spinal network to maintain stability during standing and locomotion in a natural environment in the presence of external perturbations.

In the present study, we investigated the involvement of the V0 and V3 commissural interneurons in the crossed reflexes by combining mouse genetics and in vivo methodology we recently developed (Laflamme and Akay, 2018; Laflamme et al. 2022). We tested the hypothesis that the spinal commissural pathways controlling the left-right coordination of limb movements during locomotion and the commissural pathways involved in crossed reflexes are segregated. Our data provide evidence that 1) the V3 CINs although not necessary for the left-right alternation of leg movements during locomotion are involved in excitatory crossed reflexes and necessary for the inhibitory crossed reflexes. 2) Although necessary for left-right coordination during locomotion, the V0 CINs are not necessary for crossed reflexes but modulate crossed reflex actions during locomotion. 3) The spinal commissural pathways controlling the coordinated movement of the left-right legs during locomotion and the commissural pathways involved in crossed reflexes are segregated.

4.3 METHODS

4.3.1 Animals

All experiments were performed according to the Canadian Council on Animal Care guidelines and approved by the Dalhousie University Committee on Laboratory Animals. Experiments were done on 19 wild-type, 14 $V0^{kill}$ mice, and 19 $V3^{off}$ mice. $V0^{kill}$ mice (Hoxb8::Cre;Dbx1::DTA) were obtained by crossing the HoxB8::Cre mouse (Witschi et al., 2010) provided as a courtesy of Dr. Hanns Ulrich Zeilhofer (University of Zurich) and the Dbx1::DTA mice obtained from Infrafrontier EMMA (Stock # EM 01926) as previously described (Talpalar et al. 2013). The $V3^{off}$ mice (Sim1::Cre;$Vglut2^{flox/flox}$) were obtained by crossing the Sim1::Cre mouse (Zhang et al. 2008) with the $Vglut2^{flox/flox}$ moue (Tong et al. 2007) obtained from the Jackson Laboratories (Stock # 012898) as

previously described (Chopek et al. 2018). All mice were housed on a 12-hour light/dark cycle (light from 07:00 to 19:00) with access to laboratory chow and water ad libitum.

4.3.2 Surgery

All adult mice (>6 weeks of age) were anesthetized with isoflurane (5% isoflurane with a constant flow rate of 1 l/min at 0.1 bar). Following the deep anesthesia indicated by a slow and regular breathing rate, the anesthesia was maintained with 1.5-2% isoflurane throughout the surgery. At the onset of each surgery, ophthalmic eye ointment was applied to the eyes, and the skin was sterilized by using a three-part skin scrub using Hibitane (Chlorhexidine gluconate 4%), alcohol, and povidone-iodine. At the beginning of the surgery buprenorphine (0.03 mg/kg) and ketoprofen (5 mg/kg) or meloxicam (5 mg/kg) were injected subcutaneously. A set of six bipolar EMG electrodes and one or two nerve stimulation cuffs were implanted in all experimental mice (Laflamme and Akay, 2018) as follows: small incisions were made on the shaved areas (neck and both hindlimbs), and each bipolar EMG electrode and the nerve cuff electrodes were led under the skin from the neck incision to the leg incisions, and the headpiece connector was attached to the skin around the neck incision using suture. The EMG recording electrodes were implanted into the right hip flexor (iliopsoas, Ip_r), knee flexor (semitendinosus, St_r) and extensor (vastus lateralis, VL_r), and ankle flexor (tibialis anterior, TA_r) and extensor (gastrocnemius, Gs_r), as well as the left ankle extensor (gastrocnemius, Gs_l). Nerve stimulation electrodes were implanted in the left leg to activate contralateral proprioceptive and cutaneous feedback (tibial nerve) or predominantly cutaneous afferents (sural nerve), as well as in the right leg to activate ipsilateral cutaneous afferents (sural nerve). After the incisions on the skin for electrode implantations were closed, anesthesia was discontinued, and mice were placed in a heated cage for at least 3 days before being returned to a regular mouse rack. Food mash and hydrogel were provided until full recovery after the surgery. Any handling of the mouse was avoided until the animal was fully recovered. The first recording session started at least 10 days after electrode implantation surgeries.

4.3.3 Recording sessions

After the mice fully recovered from the implantation surgeries, the animals were briefly anesthetized with isoflurane, and a custom-made wire to connect the headpiece

connector with the amplifier and the stimulation insulation units was attached to the mouse. The mice were removed from anesthesia and placed on a mouse treadmill (model 802; custom-built in the workshop of the Zoological Institute, University of Cologne, Germany). The electrodes were connected to an amplifier (model 102; custom-built in the workshop of the Zoological Institute, University of Cologne, Germany) and a stimulus isolation unit (ISO-FLEX; A.M.P.I., Jerusalem, Israel or DS4; Digitimer, Welwyn Garden City, UK). After the animal fully recovered from anesthesia (at least 5 min), we first determined the minimal (threshold) current necessary to initiate local reflex responses. To do this, we injected single impulses lasting 0.2 ms into the tibial nerve and double impulses each lasting 0.2 ms with 2 ms intervals into the sural nerve. These threshold currents were then used to set the current to either 1.2 times the threshold current (1.2xT, low current) or five times the threshold (5xT, high current) which was further used to elicit crossed reflex responses. These values were chosen because 1.2xT stimulation in mice activates group Ia and Ib afferents and 5xT stimulation additionally activates the group II muscle afferents from muscle spindles and cutaneous low-threshold mechanosensitive afferents (Steffens et al. 2012; Schomburg et al. 2013).

Following the determination of threshold currents, the EMG signal from the five muscles of the right hindlimb was recorded (sampling rate: 10 kHz for each muscle) while the right peripheral nerves, tibial nerve or the sural nerve, were stimulated at 1.2xT and 5xT with five brief impulses (impulse duration: 0.2 ms, frequency: 500 Hz) during resting (treadmill off and animal is either resting or calmly exploring the treadmill) or locomoting at a constant speed set by the treadmill. The treadmill was set at 0.2 m/s for all wild-type mice as all wild-type mice consistently locomoted at this speed. Because both mutant mice could not locomote steadily at higher speeds we set the treadmill speed for $V3^{off}$ mice at 0.1 m/s, and for $V0^{kill}$ mice at 0.05 m/s. In some experiments, the right sural nerve was also stimulated in combination with contralateral tibial or sural nerve stimulation (wild type: 9 mice; $V0^{kill}$: 13 mice; $V3^{off}$: 12 mice). The EMG signals were amplified (gain 100), bandpass filtered and stored on the computer using Power1410 interface and Spike2 software (Cambridge Electronic Design, Cambridge, UK).

4.3.4 Data analysis

To investigate the V0 or the V3 CIN involvement in excitatory crossed reflexes, we measured the area under the average rectified EMG traces from 12-50 ms post-stimulation onset after each contralateral (left) tibial and sural nerve stimulations at 1.2xT and 5xT in wild type, $V0^{kill}$, and $V3^{off}$ mice. We then calculated a generalized linear mixed model for each recorded muscle in each mouse line (wild-type, $V3^{off}$, and $V0^{kill}$). This was performed for each stimulated nerve (sural and tibial) and stimulation intensity (1.2xT and 5xT), as well as their interactions as fixed effects. A per-animal random offset and a full-factorial dispersion model were included. To account for non-normality a Gamma-distribution with a log-link function was used. The statistical model was fit using glmmTMB.

To test if the inhibition of the local reflexes by the crossed reflexes differed between the wild-type, $V3^{off}$, and $V0^{kill}$ mice, we calculated two parameters. First, we measured the average of the rectified and smoothened EMG traces within 12-18 ms after the contralateral nerve stimulation onset. Second, we measured the EMG activity only when the local reflex was activated, in the absence of contralateral nerve stimulation. That is, we measured the average of the rectified and smoothened EMG traces activated by the local reflex that would have corresponded to a 12-18 ms if the contralateral nerve stimulation onset had occurred. In both conditions, a generalized linear mixed model on these data was applied. To ensure reliable reflex recordings and avoid variability in data due to extended recording sessions, we developed exclusion criteria to only include recordings in which the reflex responses were stable through the experiments. Individual EMG recordings were excluded if: 1) there was persistent background activity (n=3 EMG recordings); 2) the crossed reflex (n=73 EMG recordings) was absent [defined as having an amplitude smaller than three times mean baseline activity (50 ms to 1 ms before the stimulation)]; 3) the local reflex was absent (n=11 EMG recordings); 4) the crossed (n=7 EMG recordings) or the local reflex (n=8 EMG recordings) were absent in the control recording after the protocol; and 5) finally, if either the crossed or local reflex size was larger than twice the size of the other reflex (n=22 EMG recordings). Thus, from a total of 190 recordings, 66 were included (WT: n=19, 11 sural, 8 tibial; $V3^{off}$: n=23, 9 sural, 14 tibial; $V0^{kill}$: n=24, 3 sural, 21 tibial). The stimulation type, stimulated nerve (sural or tibial nerve), and mouse model (WT, $V3^{off}$, $V0^{kill}$) as well as all second and third-order interaction effects were modeled as fixed effects

and a nested per mouse and muscle random offset was included. To account for non-normality, a Gamma-distribution with a log-link was used; to account for heteroskedasticity, a full-factorial dispersion model was used. The model was fit using Template Model Builder (Kristensen et al. 2016), interfaced through the glmmTMB R package (Brooks et al. 2017).

4.3.5 Statistical tests

All graphical representations of data in figures 4.3, 4.4, and 4.6 were made using GraphPad Prism 5 and processed using Illustrator CS5 (Adobe). All data are presented as means ± standard deviation. One-to-one statistical comparisons of the data were made with the t-test or Mann–Whitney test using GraphPad Prism 5 depending on whether the normality was present or absent, respectively, using omnibus K^2 or Kolmogorov–Smirnov tests. ANOVA with Tukey post-hoc test when the data exhibited normal distribution or Kruskall-Wallis with Dunns comparison post-hoc test when data did not exhibit normal distribution was used to compare more than two groups. All statistical tests were two-tailed, and differences were considered statistically significant when the *P* value was <0.05.

For the data presented in figures 2 and 5, post-hoc tests were calculated using estimated marginal means (EMM) and Tukey's method was used to account for alpha-inflation due to multiple comparisons. Model assumptions were tested using the DHARMa package for R (distribution, dispersion, outliers, and quantile deviation tests were performed). Quantile–quantile (Q–Q) plots and histograms of residuals were inspected. Violation of assumptions led us to test different error distributions and link function. A Gamma-distribution with log-link function satisfied the assumptions of both models and was hence used. An alpha-error of $p<0.05$ was regarded as significant.

4.4 RESULTS

4.4.1 Involvement of V0 and V3 CINs in the excitatory crossed reflex pathways

To measure the crossed reflex responses of different leg muscles to afferent activation on the contralateral leg, we recorded electromyogram (EMG) activities from multiple muscles of the right hindlimb while we electrically stimulated either the tibial nerve or the sural nerve of the left hindlimb (Fig. 4.1*a*). Stimulation of the nerves was

carried out either at low (1.2xT) or high (5xT) threshold intensity necessary to elicit a local reflex response in the left gastrocnemius muscle (Gs). Based on previous research, it is to be expected that 1.2xT stimulation of the tibial nerve will activate mostly proprioceptive afferent fiber of groups Ia and Ib that innervate the triceps surae muscles and the 5xT stimulation would activate in addition to the groups Ia and Ib afferents, the group II afferents that include proprioceptive group II afferents from muscles and cutaneous low threshold mechanoreceptors (Steffens et al. 2012; Schomburg et al. 2013). Stimulation of the sural nerves is rather likely to activate cutaneous afferent fibers of large caliber at 1.2xT and of intermediate to large caliber at 5xT. However, it has to be considered that the sural nerve harbors minor motor fibers to the flexor digiti minimi muscle in rodents (Peyronnard and Charron, 1982; Steffens et al. 2012). Therefore, the contribution of minimal proprioceptive afferent during sural nerve stimulation cannot be excluded. These experiments were carried out on wild-type mice and in mutant mice where either V0 CINs were killed ($V0^{kill}$) (Talpalar et al. 2013), or the synaptic outputs of V3 CINs were silenced ($V3^{off}$) (Chopek et al. 2018).

In wild-type mice, stimulation of the left tibial nerve or the sural nerve at 1.2xT or 5xT activated all recorded muscles (Fig. 4.1*b* and 4.1*c*). Visual comparison of average rectified EMG activities from all muscles in $V0^{kill}$, and $V3^{off}$ mice could be elicited, and the overall activity pattern qualitatively resembled the responses recorded in wild type mice when the contralateral tibial (Fig. 4.2*a*) or the sural (Fig. 4.2*b*) nerve was stimulated. Next, we sought to quantify the muscle responses in all mice, all muscles, and after both nerve stimulations. To do this, we measured the area underneath the average rectified EMG traces within a 12-50 ms time window after the stimulation onset. With increasing intensity from 1.2xT to 5xT responses increased ($p<0.0001$); the extend of the increase did not differ between WT, $V0^{kill}$ and $V3^{off}$ mice (interaction effect: $p=0.603$). There was significant effect of mouse type ($p=0.0045$): across muscles, nerves, and stimulation intensities, $V3^{off}$ mice exhibited significantly smaller muscle activities than $V0^{kill}$ mice ($p=0.0065$) and their wild-type counterparts ($p=0.0327$) (Fig. 4.2*e*). All second and third order interaction effects involving mouse type and nerve and/or stimulation intensity were not significant (all $p>0.6$), indicating that the reduction of amplitudes in $V3^{off}$ mice compared to WT and $V0^{kill}$ mice was present independently of stimulated nerve and stimulation intensity. The

interaction between mouse type and muscle was significant indicating that the effect of mouse type was different between muscle groups. Indeed, responses in $V3^{off}$ mice was were significantly smaller than in WT mice only in IP, VL, and St (all $p<0.0071$); and smaller than in $V0^{kill}$ mice in St and TA (all $p<0.0180$). This data suggested that V3 CINs, but not the V0 CINs, might have a minor role in mediating excitatory crossed reflex responses.

To further elaborate on this, we next investigated the likelihood of eliciting a muscle response with stimulation of the contralateral tibial nerve and sural nerve (Fig. 4.3) stimulation. This was done by visually inspecting EMG traces immediately after the nerve stimulation. The relative frequency of occurrence of muscle activity after nerve stimulation was calculated as the number of nerve stimuli that were followed by a muscle response over the total number of stimulations. Across muscles, stimulated nerves, and mouse types, the frequency of muscle activity in response to stimulation was significantly higher at 5xT than at 1.2xT [odds ratio (OR)=5.66, $p<0.0001$, Fig. 4.3*a*]. While there wasn't a significant difference of the frequency of responses between WT, $V0^{kill}$, and $V3^{off}$ mice ($p=0.0698$), the interaction effect between with stimulation intensity was significant ($p<0.0001$), indicating that influence of stimulation intensity differed between the mouse types (Fig. 4.3*b*). Indeed, at 1.2xT significantly fewer responses were recorded in $V3^{off}$ mice than in WT (OR=0.467, $p=0.0292$) or $V0^{kill}$ mice (OR=0.404, $p=0.0171$). The lack of a significant three-way interaction effect with nerve type ($p=0.2084$) indicates that this effect is not influenced by whether tibial (Fig. 4.3*c*) or sural nerve (Fig. 4.3*d*) was stimulated. Together, these data suggest that V3 CINs but not V0 CINs contribute to the excitatory components of the crossed reflexes, since both, the EMG activities in response to contralateral nerve stimulation and the reliability of these responses at low stimulation intensities, were lower in $V3^{off}$ mice than in their wild-type counterparts.

Next, we asked whether there are temporal differences in the muscle activity patterns during crossed reflex responses in the three groups of mice. To do this, we detected the delays from the stimulation onset to the on and offsets of muscle activity responses to the tibial (Fig. 4.4, *a* and *b*) or sural (Fig. 4.4, *c* and *d*) nerve stimulations at 1.2xT and 5xT. Comparisons of the onset latencies of the muscle activities overall were similar (ANOVA, $p>0.05$) in all groups with large inter-animal variability (Fig. 4.4, *b* and *d*). Only in

occasional cases did the difference reach statistical significance (ANOVA, $p<0.05$). Overall, these data suggest that the temporal structure of the crossed reflex responses of the recorded muscles was similar in all groups of mice.

In short, two of our observations presented above suggests that V3 CINs contribute to the excitatory crossed reflexes: first, the overall EMG activity (Fig. 4.2e) as a response to contralateral nerve stimulation is lower in amplitude in $V3^{off}$ mice compared to wild type and $V0^{kill}$ mice. Second, the decreased occurrences of reflex responses at low current stimulation (Fig. 4.3c and 4.3d) in $V3^{off}$ mice following contralateral nerve stimulation is lower in $V3^{off}$ mice than the overall activity in WT and $V0^{kill}$ mice. No indication for V0 CIN contribution to the excitatory crossed reflex action could be detected. This suggests the V3 but not V0 CINs are likely to be part of the excitatory crossed reflex pathway.

4.4.2 Involvement of V0 and V3 CINs in the inhibitory crossed reflex pathways

Next, we aimed to investigate the contribution of the V0 and the V3 CINs to the inhibitory crossed reflexes, using the double nerve stimulation technique we recently developed (Laflamme and Akay, 2018; Laflamme et al. 2022). To do this, we elicited muscle activity by stimulating the ipsilateral sural nerve at 4-5xT and stimulating at a varying delay with the contralateral nerve crossed reflex to investigate the interaction of the local and the crossed reflexes (Fig. 4.5). The delay between the two stimulation was chosen so that the center of the activity of the local reflex occurred in the silent period of the crossed reflex. We reasoned that if there is an inhibitory crossed reflex response, we should always see a decreased EMG activity of the local reflex immediately after the contralateral nerve stimulation (Fig. 4.5*a*,). This inhibition was present in all recorded muscles regardless of whether the crossed reflex was initiated by the tibial nerve (Supplemental Fig. S.4.1) or sural nerve stimulation (Supplemental Fig. S.4.2). This observation indicated an inhibitory crossed reflex response.

Interestingly, we observed that this inhibitory effect was preserved in $V0^{kill}$ mice but was absent in $V3^{off}$ mice (Fig. 4.5*b*). To confirm our observations quantitatively, we activated the local reflex along with the crossed reflex, averaged the EMG activity within 12-18 ms time window from the onset of contralateral stimulation and compared it to the average EMG activity of the local reflex only in the same time window (Fig. 4.5*c*). The

ratio of these two parameters was used quantify for the amount of inhibition of the local reflex by the contralateral stimulation (values lower than 1 indicate inhibition). The generalized linear mixed model showed that there was a significant interaction effect between stimulation type (conditioning test vs. local reflexes only) and mouse type (WT, $V3^{off}$, $V0^{kill}$; $F_{2,2244}$=116.655, p<0.0001), indicating that the amount of modulation of the local reflex by the crossed reflex in the 12-18 ms post-stimulation interval was different between the different mouse types (Fig. 4.5*diii*). Post-hoc tests revealed that paired stimulation led to a significant reduction in the activity of the local reflex in WT [odds ratio (OR)=0.839±0.040, p=0.0002] and $V0^{kill}$ mice (OR=0.264±0.020, p<0.0001) but not in $V3^{off}$ mice (OR=1.053±0.053, p=0.306). Interestingly, we observed that the inhibition was more pronounced in $V0^{kill}$ mice than in the wild-type mice, suggesting that V0 CINs, although not directly involved, have a modulatory effect on crossed reflexes. Furthermore, an almost significant three-way interaction effect between stimulation type, mouse type, and stimulated nerves ($F_{2,2244}$=2.640, p=0.0716) suggests that the modulation of the local reflex activities by the crossed reflexes in WT, $V3^{off}$, and $V0^{kill}$ mice differed depending on whether sural or tibial nerve stimulation was applied (Fig. 4.5*di-ii*). Indeed, post-hoc tests showed that the reduction of local reflex activities by the crossed reflexes in WT mice was only significant with sural nerve stimulation and not with tibial nerve stimulation. In the case of $V0^{kill}$ and $V3^{off}$ mice, there were no differences between the nerves; the inhibition was present in $V0^{kill}$ mice and absent in $V3^{off}$ mice regardless of which nerve was stimulated. These data suggest the presence of the inhibitory crossed reflex component in WT and $V0^{kill}$ mice and that this inhibitory component was lost in $V3^{off}$ mice.

Our data provide evidence that the inhibitory crossed reflex action elicited by tibial nerve or sural nerve stimulation is mediated by the V3 CINs that are exclusively excitatory. Interestingly, the V0 CINs which constitute excitatory as well as inhibitory CINs are not part of the inhibitory crossed reflex pathway.

4.4.3 Involvement of V0 and V3 CINs in the crossed reflex actions during locomotion.

Previously, we demonstrated that during locomotion in mice that the inhibitory crossed reflex response is downregulated specifically for the vastus lateralis (VL, knee extensor) and the tibialis anterior (TA, ankle flexor) (Laflamme and Akay, 2018). We

further sought to provide additional evidence for the involvement of the V3 CINs in inhibitory crossed reflex pathways by investigating crossed reflex responses in the presence of muscle activity prior to reflex activation. Furthermore, we investigated if the V0 or the V3 CINs played any role in the regulation of the crossed reflexes during locomotion. To do this, we recorded the crossed reflex action during locomotion on a treadmill at a constant speed. All wild-type mice were most comfortable moving at 0.2 m/s, therefore this speed was chosen for all wild-type mice. However, because the limited capability of locomotion is a main phenotypical characteristic of the $V0^{kill}$ and $V3^{off}$ mice, the locomotion for $V3^{off}$ mice was set to 0.1 m/s, and for $V0^{kill}$ mice was set to 0.05 m/s. It should be noted, that the $V0^{kill}$ mice exhibited severe postural abnormalities making locomotion experiments especially challenging, but whenever they did stepping movements, the left and right hindlimbs always stepped synchronously as previously described (Talpalar et al. 2013).

In accordance with our observation during the reflex response in non-locomoting animals, the data during locomotion provided evidence that V3 CINs are necessary for the inhibitory crossed reflex action, but the V0 CINs are not. To do this we visually inspected all cases in which the right sural (Fig. 4.6*a*) or tibial (Supplemental Fig. 4.3*a*) nerve when there was activity in that particular muscle prior to nerve stimulation. We then right sural calculated the occurrence of inhibition the ongoing EMG activity as number of cases in which there were no activity in each left muscle within the 5 ms time window following the right sural (Fig. 4.6b) or the right tibial nerve stimulation. In wild-type and in $V3^{off}$ mice ongoing activity of muscles was suppressed by sural (Fig. 4.6*a* and 4.6*bi*) or by tibial (Supplemental Fig. 4.3*a* and 4.3*bi*) nerve stimulations except for VL and TA. The same was true for $V0^{kill}$ mice when the tibial nerve was stimulated (Supplemental Fig. 4.3*biii*). Strikingly, during sural nerve stimulation, the inhibition was preserved in all muscles indicating the down-regulatory effect of the inhibitory crossed reflex was diminished in the absence of V0 CINs (Fig. 4.6*bii*), suggesting that the downregulation of the inhibitory crossed reflex was compromised. Confirming the results presented in non-locomotion animals above, the termination of ongoing muscle activity after contralateral sural (Fig. 4.6*biii*) or tibial (Supplemental Fig 4.3*biii*) nerve stimulation was severely disrupted indicating that V3 CINs are also necessary for the inhibitory crossed reflex during locomotion. This observation was also confirmed when we quantified the temporal

structure of the muscle activation pattern after contralateral sural (Fig. 4.6*c*) or tibial (Supplemental Fig. 4.3*c*) nerve stimulation. The onsets of muscle activity occurred on average around the 10 ms delay from stimulation onset, sometimes even closer to zero indicating muscle activation as soon as stimulation started, in the absence of V3 CINs indicating no silent period after nerve stimulation (Fig. 4.6*d* and Supplemental Fig. 4.3*d*). In the absence of V0 CINs however, the onset latency was consistently closer to 20 ms in all recorded muscles, including the TA and VL, indicating the selective downregulation of inhibitory crossed reflex influence on TA and VL muscles was missing. Together, these data provide additional evidence that V3 CINs mediate the inhibitory crossed reflex response, and that V0 CINs are not involved in inhibitory crossed reflexes but are important for their modulation during locomotion, as our data with resting animals suggested above.

4.5 DISCUSSION

The current study uncovers the basic network structure that controls the excitatory and inhibitory crossed reflex pathways in mice. Our data suggest that the excitatory crossed reflex pathway is activated by proprioceptive afferents from muscle (1.2xT stimulation of the tibial nerve) as well as cutaneous afferent activation through sural nerve stimulation. In contrast, the inhibitory crossed reflex pathways were consistently activated by low threshold cutaneous afferents as indicated by 5xT stimulation of both nerves. We showed that the V0 CINs, which play a crucial role in the left-right alternation of leg movement during locomotion, do not have a significant contribution to the crossed reflexes. In contrast, we provided evidence that the V3 CINs contribute to the excitatory crossed reflex response and are an essential part of the inhibitory crossed reflex pathway. Moreover, even though the V0 CINs are not involved in crossed reflexes at rest, they exert a modulatory effect on the crossed reflex pathway during locomotion. These observations suggest that commissural pathways underlying crossed reflexes are segregated from the pathway that coordinates left-right alternation during locomotion.

Commissural circuitry that transmits the activity status of the CPG during locomotion and necessary for left-right coordination during locomotion has been described by combining electrophysiological recording and mouse genetics (Lanuza et al. 2004; Kiehn, 2011; 2016; Talpalar et al. 2013; Bellardita and Kiehn, 2015). Our data suggest that

spinal commissural pathways that are essential for the left-right coordination during locomotion, and the commissural pathways that control crossed reflexes are segregated. Previously, it was shown that V0 CINs are necessary for the alternating activity in the spinal cord during fictive locomotion in spinal cords of neonatal mice or alternating stepping of the left and right hindlimb during locomotion in adult mice (Lanuza et al. 2004; Talpalar et al. 2013; Bellardita and Kiehn, 2015). On the other hand, experiments have shown that in the absence of V3 CINs alternating activity is maintained during fictive locomotion in spinal cords of neonatal mice as well as the alternating stepping of the left and right hindlimbs during locomotion in adult mice is preserved, although with more variable rhythmicity (Zhang et al. 2008). Interestingly, our data here provide evidence that the V3 CINs are an essential part of the crossed reflex pathways but V0 CINs are not. This suggests that the commissural pathways that control left-right coordination during locomotion and the commissural pathways for crossed reflexes are segregated pathways. This kind of network segregation was previously suggested considering connectivity patterns of commissural interneurons with supraspinal centers and proprioceptive signals from muscles (Jankowska et al. 2005). Our data here provides the direct evidence for segregated pathways for leg coordination during locomotion and crossed reflexes.

An interesting observation in our experiments was that the inhibitory crossed reflex actions transduced by cutaneous afferent signals were exclusively transmitted by excitatory CINs, the V3 CINs. This is in accordance with observations in cats that excitatory commissural interneurons synapse with local inhibitory interneurons, including the group Ia interneurons that mediate the reciprocal inhibitory stretch reflex response (Jankowska et al. 2005). A similar circuit was also suggested in humans (Mrachacz-Kersting et al. 2017). Our data provide evidence for a similar network design in mice regarding cutaneous afferent signals. That is, cutaneous sensory signals are conveyed by the exclusively excitatory V3 CINs to the contralateral side of the spinal cord to synapse with local inhibitory interneurons that in turn exert their inhibitory influence on the motor neurons. Supporting this idea comes from previous histological experiments showing that the V3 CINs indeed synapse with the local inhibitory interneurons including the V1 and V2b interneurons that among others, give rise to the group Ia interneurons and the Renshaw cells (Alvarez et al. 2005; Zhang et al. 2014). Future experiments will have to reveal the

identity of these local inhibitory interneurons that are involved in the inhibitory crossed reflex action. Nevertheless, our data add to the observation that inhibitory crossed reflex action is transmitted by excitatory commissural interneurons.

Crossed reflexes have been shown to be modulated during behavioural states or when the spinal circuitry is severed from the supraspinal centers (Perl, 1957; Duysens et al. 1980; Aggelopoulos and Edgley, 1995; Aggelopoulos et al. 1996). In our previous investigation, we have shown also in mice, that the inhibitory crossed reflex action is downregulated when the animal is moving (Laflamme and Akay, 2018). Confirming the previous observations done on cats (Frigon and Rossignol, 2008). However, the network underlying this modulation is not known. Our data provide evidence that the V3 CINs are the main CINs involved in the inhibitory crossed reflex pathways and the modulation of this pathway during locomotion involves the V0 CINs, as in the absence of V0 CINs, the downregulation of the inhibitory crossed reflex during locomotion is absent. Furthermore, quantification of the inhibitory crossed reflex responses was consistently stronger in $V0^{kill}$ mice, also indicating the down-regulatory effect of V0 CINs on the inhibitory crossed reflex pathway. This is indicated in figure 4.7 as the dashed arrow from the V0 CINs to the inhibitory crossed reflex pathway. These results provide the first insights into the identities of interneurons involved in the state-dependent modulation of the crossed reflex responses.

The spinal circuitry that controls left-right coordination during locomotion is well understood in mice, due to advances in mouse genetics and electrophysiological techniques applicable to mice (Kiehn, 2016). Based on in vitro and in vivo experiments, a network design has been suggested that constitutes a dual inhibitory commissural pathway involving the V0 and the V3 CINs to coordinate left-right stepping in a speed-dependent manner (Talpalar et al. 2013). Despite this considerable advance in understanding the spinal locomotor circuitry, it is not known what the involvements of V0 and the V3 CINs are in crossed reflex. Our data provide the first insights into the spinal circuitry that controls crossed reflexes in mice and identifies genetically defined classes of commissural interneurons as part of it (Fig. 4.7). While V0 CINs transmit information on the activity status of the CPG to the contralateral site, the V3 CINs transmit excitatory as well as inhibitory crossed reflex actions. As the V3 CINs are exclusively excitatory interneurons,

there must be at least one inhibitory local interneuron interconnected between the V3 CINs and the motor neurons. In addition, the V0 CINs exert a modulatory influence on the inhibitory crossed reflex action when the animal is moving. We provide evidence that the spinal commissural pathways consist of two segregated pathways: one transmitting the central CPG information to the contralateral side involving V0 CINs, and the other transmitting sensory information involving the V3 CINs.

4.6 FIGURES

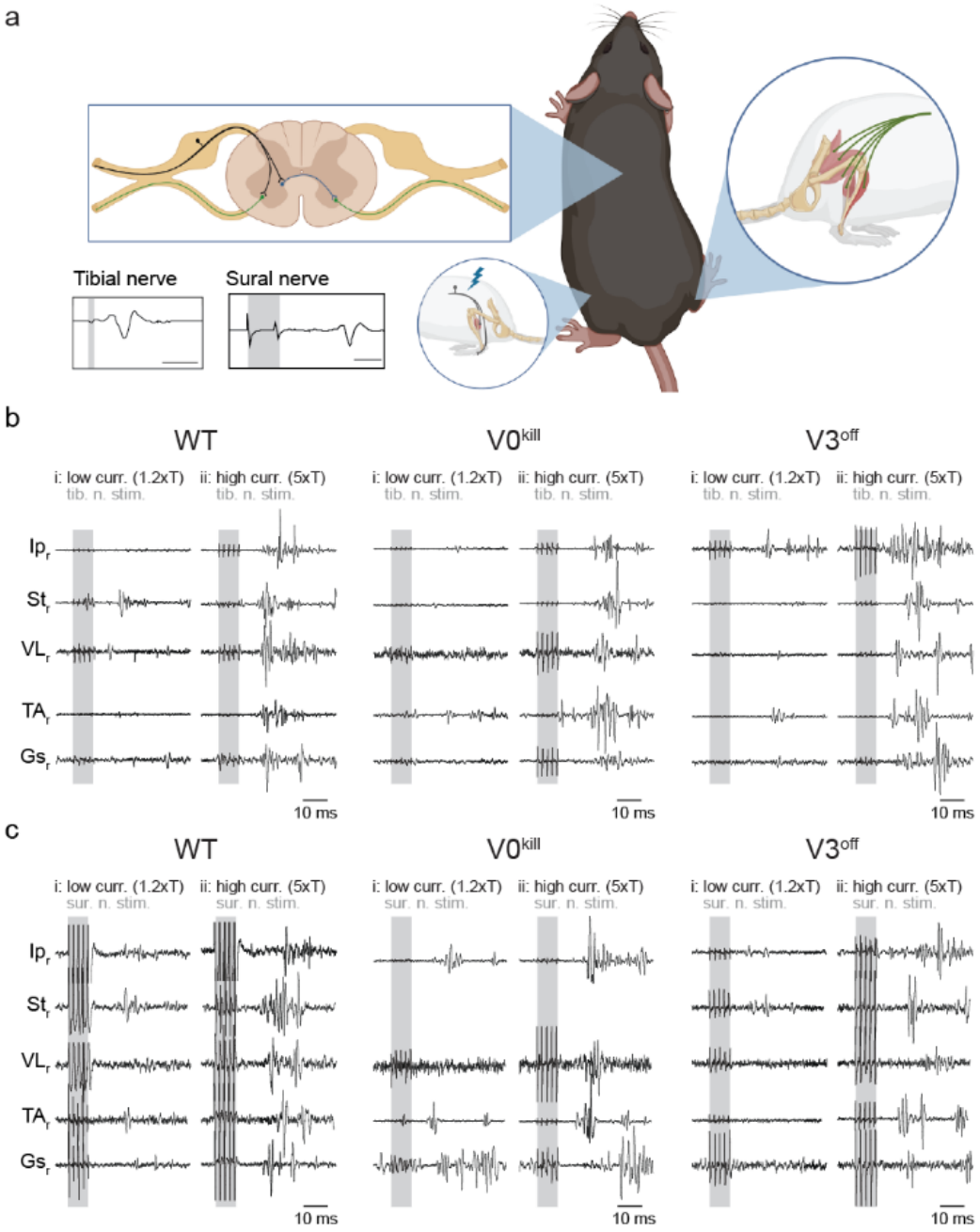
a
Tibial nerve
Sural nerve
b
WT
V0kill
V3off
i: low curr. (1.2xT)
tib. n. stim.
ii: high curr. (5xT)
tib. n. stim.
Ipr
Str
VLr
TAr
Gsr
10 ms
c
WT
V0kill
V3off
i: low curr. (1.2xT)
sur. n. stim.
ii: high curr. (5xT)
sur. n. stim.
Ipr
Str
VLr
TAr
Gsr
10 ms

Figure 4.1. Crossed reflex responses in wild-type, $V0^{kill}$, and $V3^{off}$ mice. a) Schematic of the experimental setup. Nerve cuff electrodes to the left tibial or sural nerve along with one EMG recording electrode into the left Gs were implanted to determine the threshold current to activate local reflex. In addition, EMG recording electrodes to five muscles of the left leg were implanted to record crossed reflex responses. **b)** EMG responses of all recorded muscles of the right leg to left tibial nerve stimulation at 1.2xT (i) and 5xT (ii) in wild-type, $V0^{kill}$, and $V3^{off}$ mice. The shaded area indicates nerve stimulation. **c)** Same as in **b)** but the responses are shown to the left sural nerve stimulation.

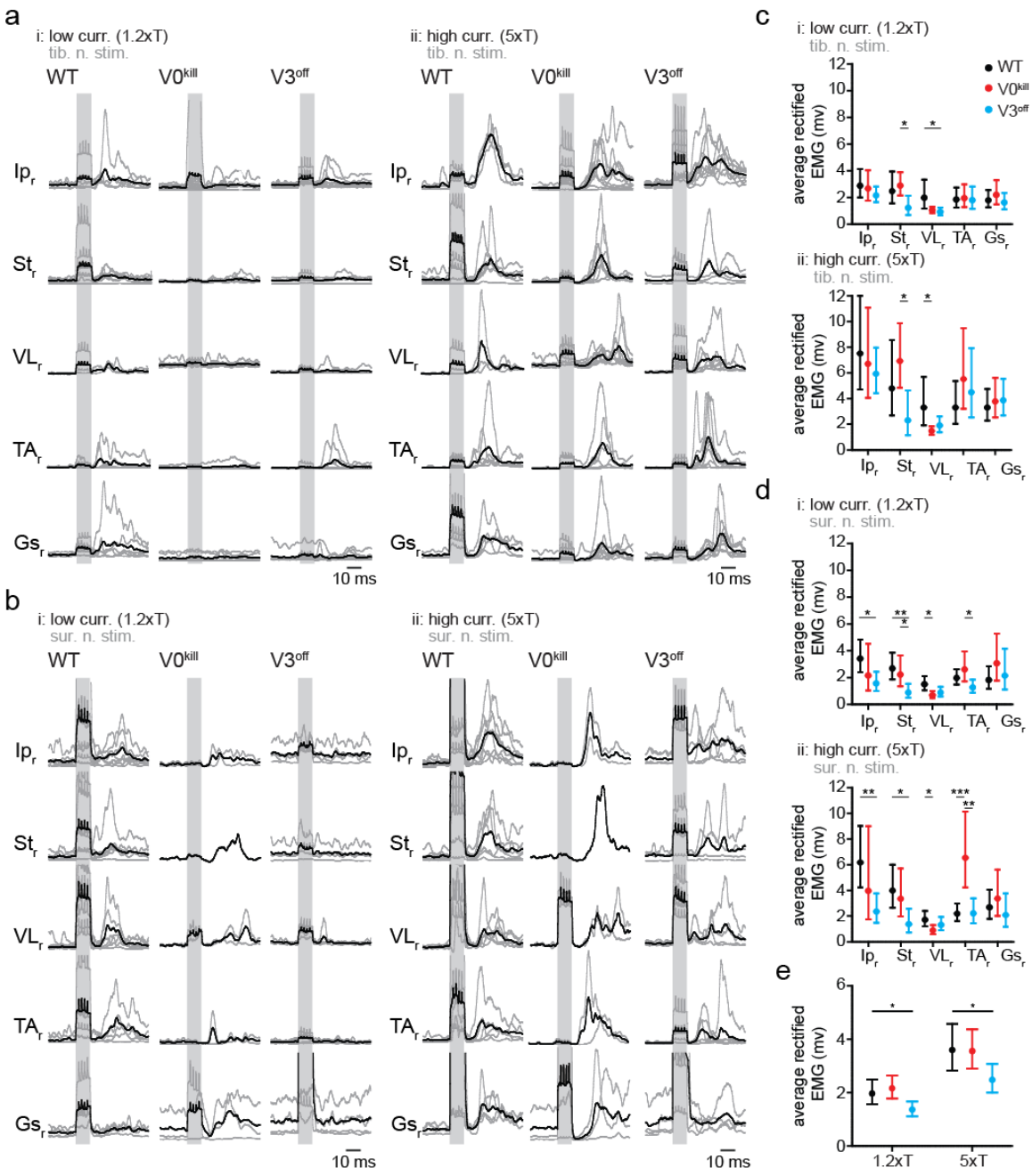
a
i: low curr. (1.2xT)
tib. n. stim.
ii: high curr. (5xT)
tib. n. stim.
WT
V0kill
V3off
Ipr
Str
VLr
TAr
Gsr
10 ms
b
i: low curr. (1.2xT)
sur. n. stim.
ii: high curr. (5xT)
sur. n. stim.
c
i: low curr. (1.2xT)
tib. n. stim.
ii: high curr. (5xT)
tib. n. stim.
average rectified EMG (mv)
d
i: low curr. (1.2xT)
sur. n. stim.
ii: high curr. (5xT)
sur. n. stim.
e
1.2xT
5xT

Figure 4.2. Average EMG responses of muscles as a response to contralateral nerve stimulation. a) Average traces of rectified and filtered EMG activities from right leg muscles as a response to left tibial nerve stimulation at 1.2xT (i) and 5xT (ii) in wild-type, $V0^{kill}$, and $V3^{off}$ mice. **b)** Same as in a but for sural nerve stimulation. **c)** Graphs showing the average area underneath the average rectified EMG traces from 12-50 ms delays from the stimulation onset for 1.2xT (top) and 5xT (bottom) stimulation of the tibial nerve. **d)** Same as in c but for sural nerve stimulation. **e)** Graphs illustrating the combined averages from all EMG traces for 1.2xT and 5xT stimulation of the tibial and the sural nerves combined.

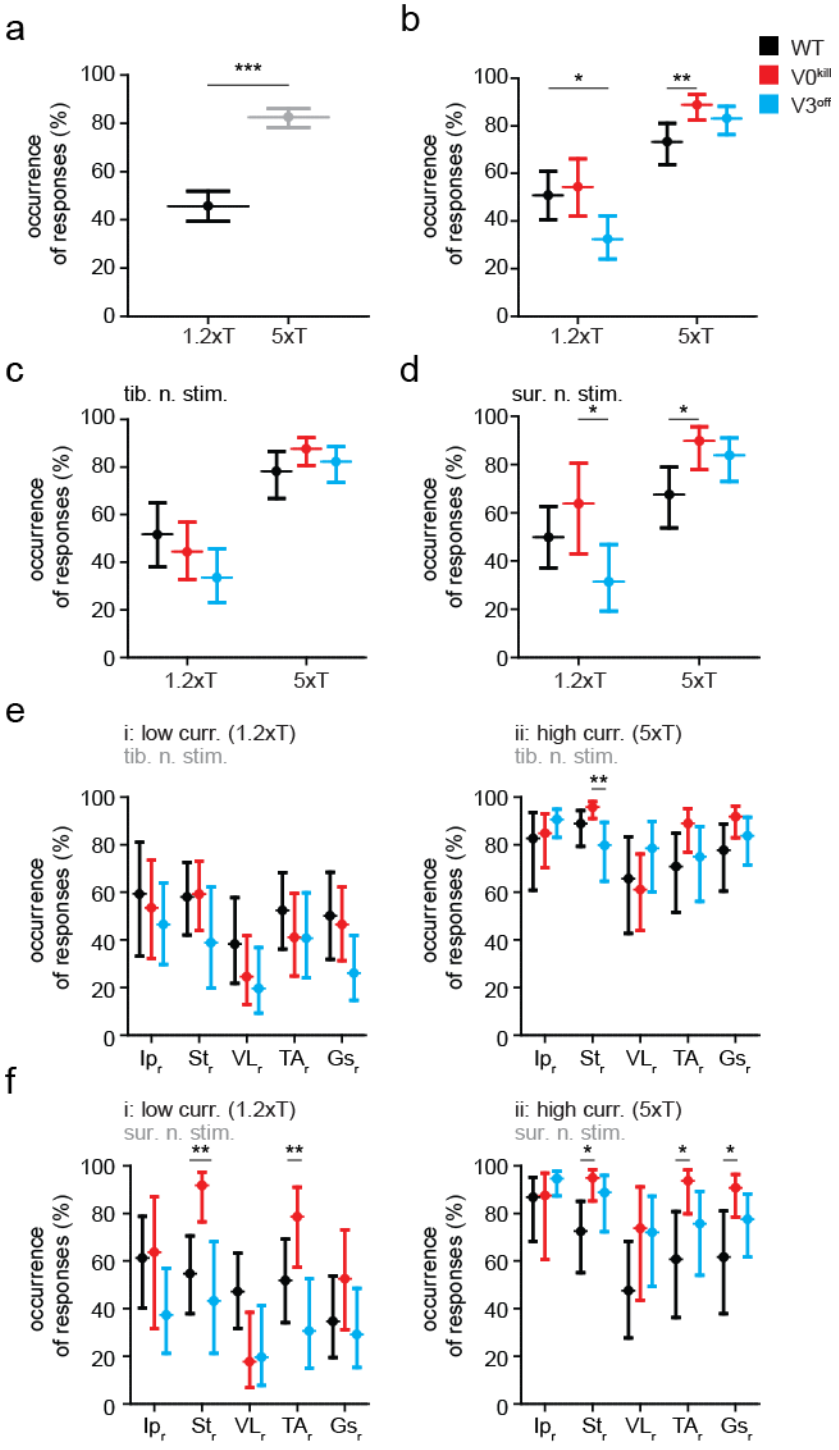
a
b
c
d
e
f
WT
V0kill
V3off
occurrence of responses (%)
1.2xT
5xT
tib. n. stim.
sur. n. stim.
i: low curr. (1.2xT)
ii: high curr. (5xT)
Ipr
Str
VLr
TAr
Gsr

Figure 4.3. The probability of muscle activation does not change in the presence or absence of V0 or the V3 CINs. a) Probabilities of observed crossed reflex responses, defined as the presence of muscle activation, across muscles, stimulated nerves, and mouse types. **b)** Probabilities of observed crossed reflex responses across muscles and stimulated nerves separated by mouse type. Probabilities of observed crossed reflex responses across muscles separated by mouse type when the tibial **(c)** or sural nerve **(d)** is stimulated. **e)** Probabilities of observed crossed reflex responses defined as the presence of muscle activation out of all contralateral tibial nerve stimulation at 1.2xT (i) or 5xT (ii) stimulation. **f)** Same as in **e)** but for the contralateral sural nerve stimulation.

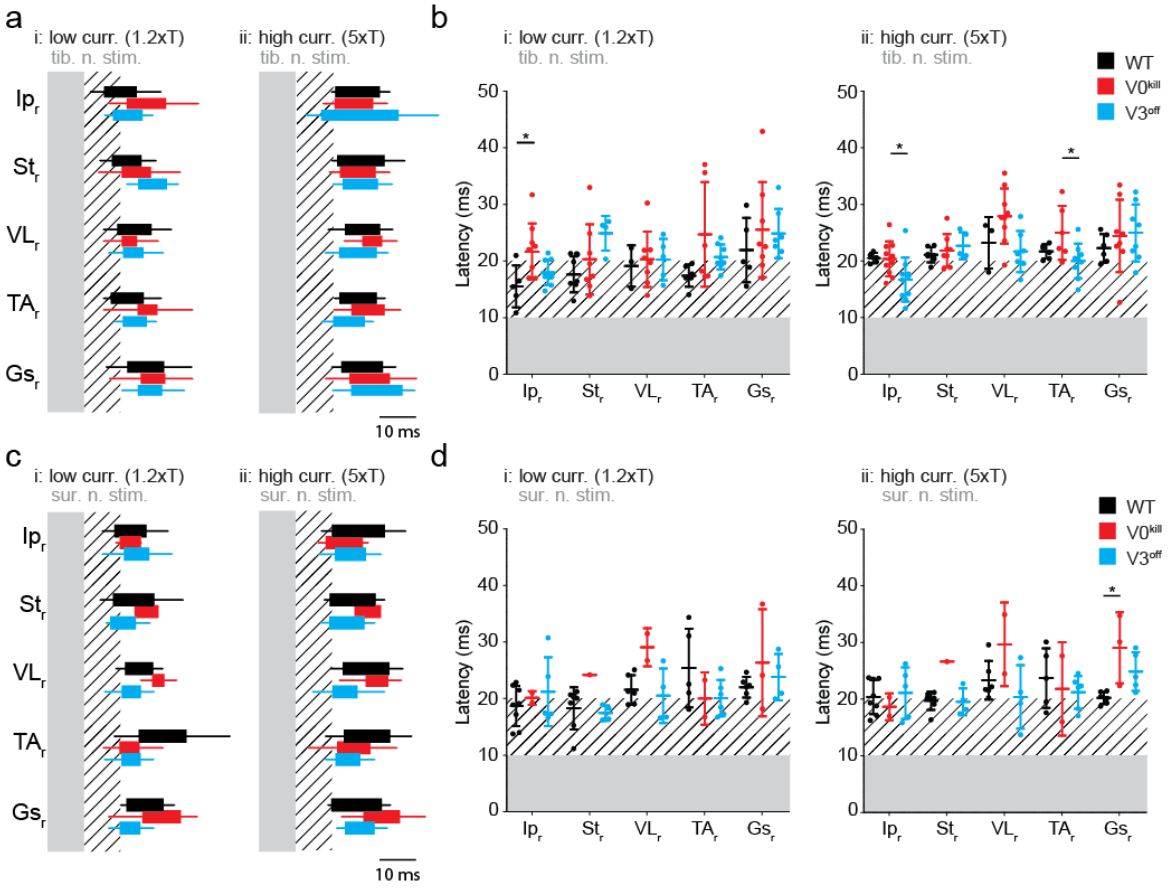

Figure 4.4. Crossed reflex response patterns are comparable in the presence or absence of V0 or V3 commissural interneurons. a) Box diagrams showing the average (+/- standard deviation) on and offsets of right muscle activities in response to the left tibial nerve stimulation at 1.2xT (i) and 5xT (ii) (indicated by the shaded area) when the animals were resting. Hatched area indicates a 10 ms time window after nerve stimulation. Black bar: wild type, red bar: $V0^{kill}$, and blue bar: $V3^{off}$. **b)** Diagrams illustrating the onset latencies of muscle activities in a bar: wild type (black), $V0^{kill}$ (red), and $V3^{off}$ (blue) mice. Circles are averages from individual mice, and the horizontal lines indicate group averages (+/- standard deviation). **c) and d)** Same as in a and b but investigating the response pattern to the left sural nerve.

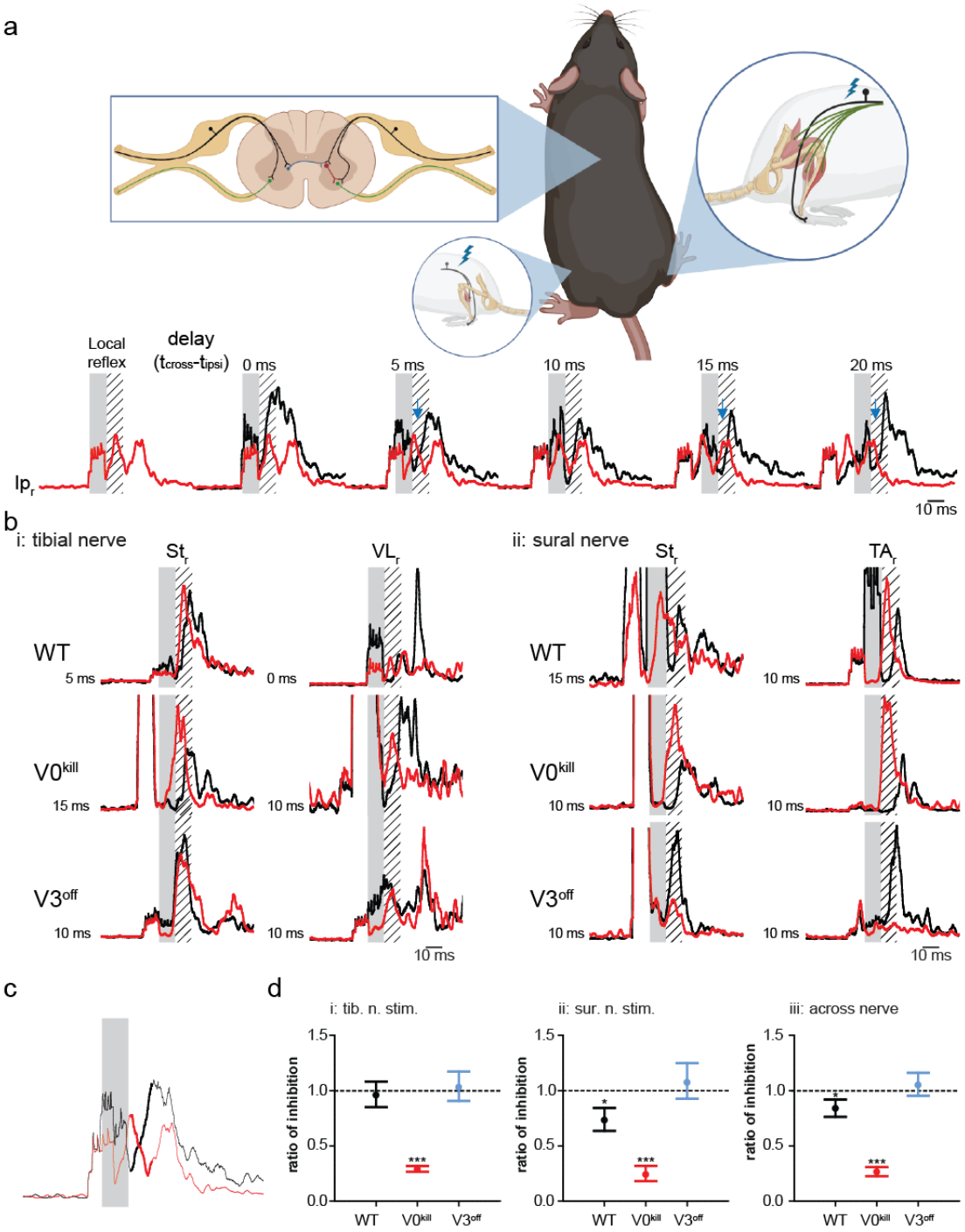
a
Local reflex
delay (tcross-tipsi)
0 ms
5 ms
10 ms
15 ms
20 ms
Ipr
10 ms
b
i: tibial nerve
Str
VLr
ii: sural nerve
Str
TAr
WT
V0kill
V3off
5 ms
0 ms
15 ms
10 ms
10 ms
10 ms
10 ms
10 ms
10 ms
10 ms
10 ms
c
d
i: tib. n. stim.
ii: sur. n. stim.
iii: across nerve
ratio of inhibition
1.5
1.0
0.5
0.0
***
*
WT
V0kill
V3off

Figure 4.5. V3 CINs but not V0 CINs are necessary for the inhibitory crossed reflex. **a)** Schematic of the experimental setup. The experimental setup is as presented in **Fig. 4.1a** with the addition of one nerve stimulation electrode to the right sural nerve. The stimulation of the right sural nerve allowed us to elicit a local reflex response (red trace) that was used to detect inhibitory influence when nerves on both sides were stimulated with varying delays (black trace). Lower activity in black traces and then red traces (blue arrows) indicated inhibitory crossed reflex action. **b)** inhibitory effect was detected in the majority of EMG recordings in wild-type and $V0^{kill}$ mice but not in $V3^{off}$ mice. **c)** to quantify the inhibitory crossed reflex, we averaged the red and black traces in the area indicated by the bold line (12 -18 ms delay from stimulation onset) and took the ratio of these averages. A smaller number than 1 indicated an inhibition. **d)** Graphs of ratios described in **b** for contralateral tibial (i) or sural (ii) nerve were stimulated. The graph in iii is when the data in i and ii are pooled together. These graphs illustrate statistically, that inhibition was preserved in $V0^{kill}$ mice, but not in $V3^{off}$ mice.

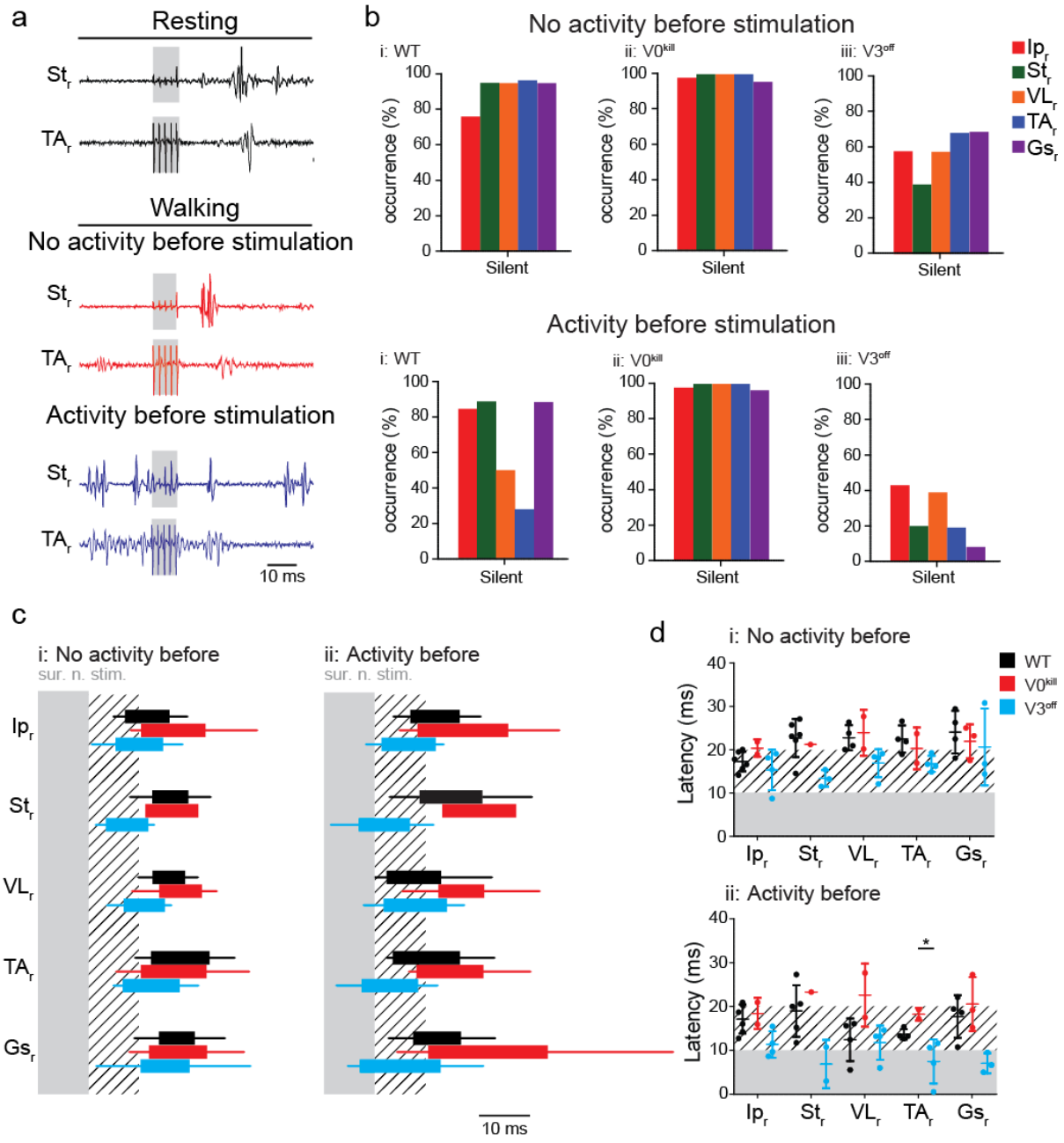
a
Resting
St$_r$
TA$_r$
Walking
No activity before stimulation
St$_r$
TA$_r$
Activity before stimulation
St$_r$
TA$_r$
10 ms
b
No activity before stimulation
i: WT
ii: V0^{kill}
iii: V3^{off}
occurrence (%)
Silent
Ip$_r$
St$_r$
VL$_r$
TA$_r$
Gs$_r$
Activity before stimulation
i: WT
ii: V0^{kill}
iii: V3^{off}
occurrence (%)
Silent
c
i: No activity before
sur. n. stim.
ii: Activity before
sur. n. stim.
Ip$_r$
St$_r$
VL$_r$
TA$_r$
Gs$_r$
10 ms
d
i: No activity before
WT
V0^{kill}
V3^{off}
Latency (ms)
Ip$_r$ St$_r$ VL$_r$ TA$_r$ Gs$_r$
ii: Activity before
*
Latency (ms)
Ip$_r$ St$_r$ VL$_r$ TA$_r$ Gs$_r$

Figure 4.6. V3 CINs but not the V0 CINs are necessary for inhibitory crossed reflex during locomotion. a) Example EMG recordings from right St and TA muscles as a response to the left sural nerve stimulation during resting (top), and during locomotion when the muscle was either inactive (middle) or active (bottom) prior to the stimulation in a wild-type mouse. **b)** Bar diagrams illustrating the probability of occurrence of a silent period in all recorded muscles of the right leg within the 5 ms window immediately after left sural nerve stimulation when there was no muscle activity (top) or there was activity (bottom) prior to nerve stimulation. **c)** Box diagrams showing the average (+/- standard deviation) on and offsets of right muscle activities as a response to the left sural nerve stimulation at 1.2xT (i) and 5xT (ii) (indicated by the shaded area) during locomotion. Hatched area indicates a 10 ms time window after nerve stimulation. Black bar: wild type, red bar: $V0^{kill}$, and blue bar: $V3^{off}$. **d)** Diagrams illustrating the onset latencies of muscle activities in a bar: wild type (black), $V0^{kill}$ (red), and $V3^{off}$ (blue) mice during locomotion. Circles are averages from individual mice, and the horizontal lines indicate group averages (+/- standard deviation).

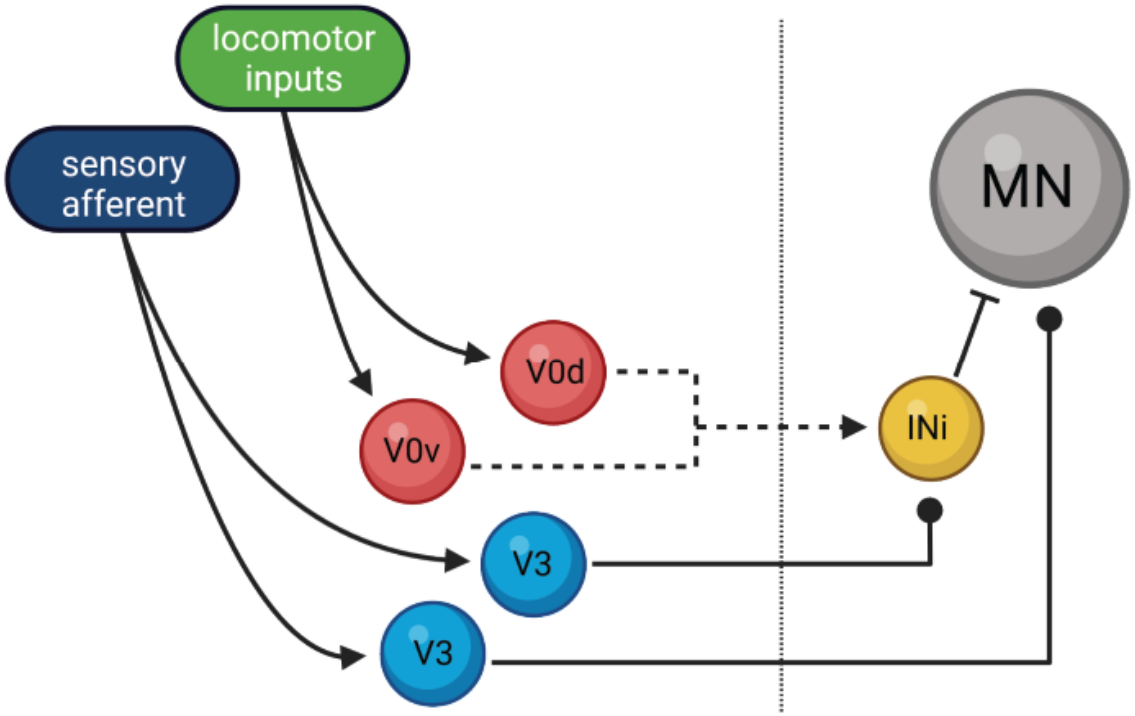

Figure 4.7. Commissural pathways transmitting information about the CPG activity status and the sensory information from the contralateral side are segregated. Our findings suggest that the spinal commissural pathways for crossed reflexes that involve V3 CINs are segregated from the spinal commissural pathway necessary for left-right alternation during locomotion that involves the V0 CINs. INi: Local inhibitory interneuron.

4.7 SUPPLEMENTAL FIGURES

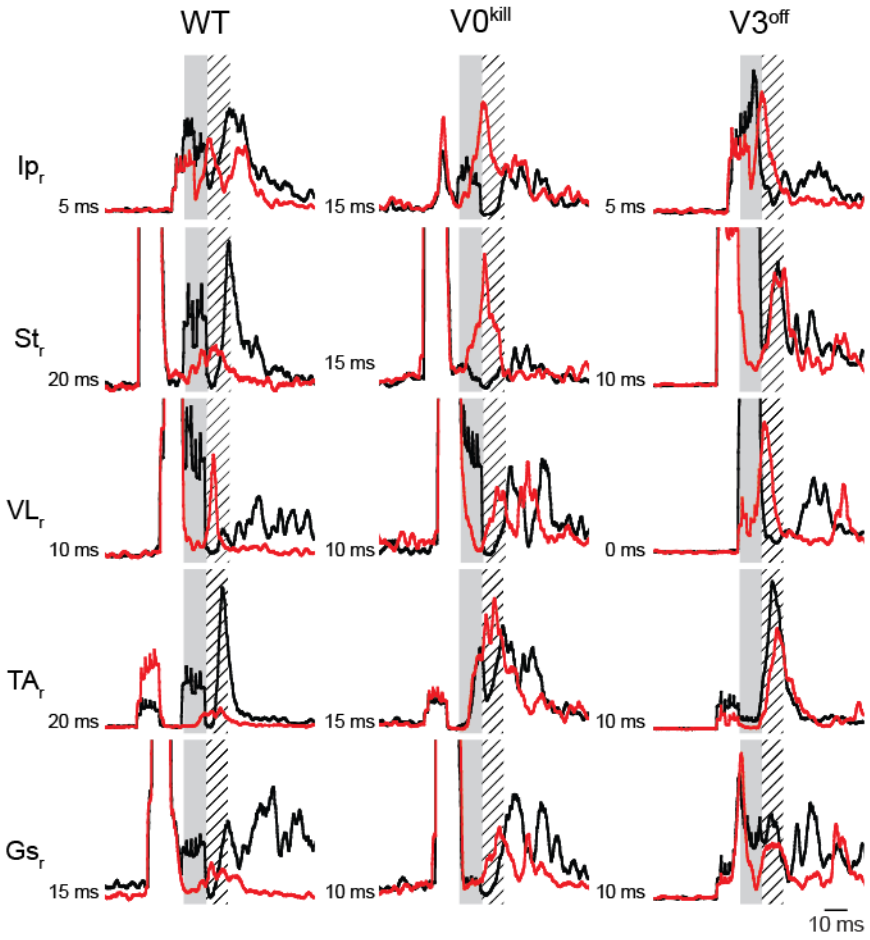

Supplemental Figure S4.1. V3 CINs but not V0 CINs are necessary for the inhibitory crossed reflex initiated by the contralateral tibial nerve stimulation. The inhibitory effect was detected in the majority of all EMG recordings in wild-type and $V0^{kill}$ mice but not in $V3^{off}$ mice, when the contralateral tibial nerve was stimulated.

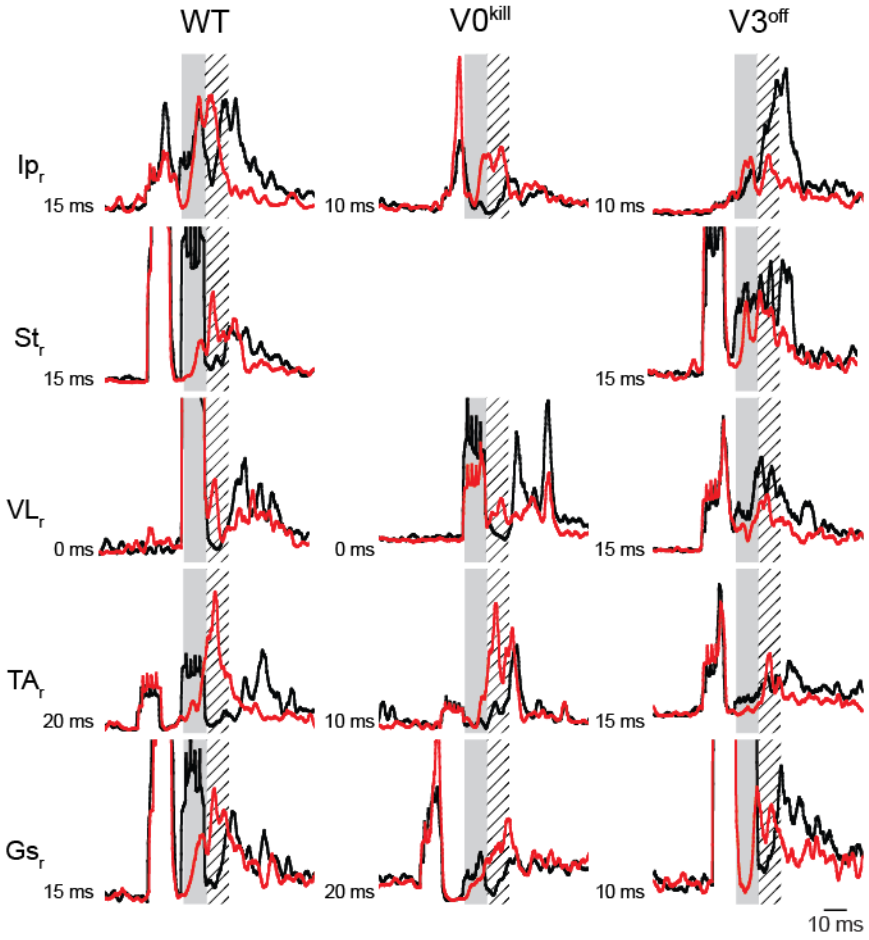

Supplemental Figure S4.2: V3 CINs but not V0 CINs are necessary for the inhibitory crossed reflex initiated by the contralateral sural nerve stimulation. The inhibitory effect was detected in the majority of all EMG recordings in wild-type and $V0^{kill}$ mice but not in $V3^{off}$ mice, when the contralateral sural nerve was stimulated.

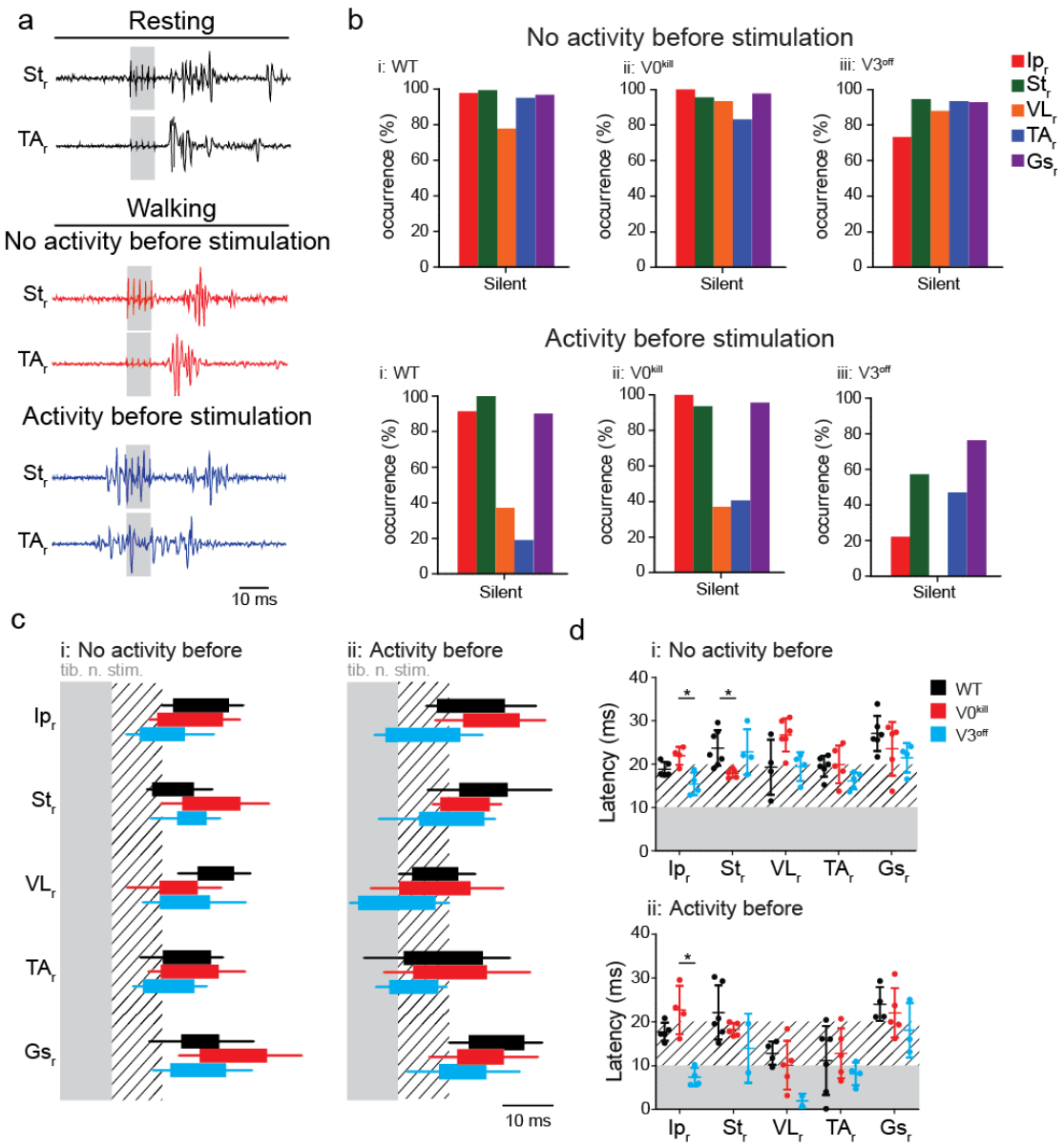
a
Resting
St_r
TA_r
Walking
No activity before stimulation
St_r
TA_r
Activity before stimulation
St_r
TA_r
10 ms
b
No activity before stimulation
i: WT
ii: V0kill
iii: V3off
occurrence (%)
Silent
Ip_r
St_r
VL_r
TA_r
Gs_r
Activity before stimulation
i: WT
ii: V0kill
iii: V3off
occurrence (%)
Silent
c
i: No activity before
tib. n. stim.
ii: Activity before
tib. n. stim.
Ip_r
St_r
VL_r
TA_r
Gs_r
10 ms
d
i: No activity before
ii: Activity before
Latency (ms)
WT
V0kill
V3off
Ip_r
St_r
VL_r
TA_r
Gs_r

Supplemental Figure S4.3: Crossed reflex responses to tibial nerve stimulation during locomotion. a) Example EMG recordings from right St and TA muscles as a response to the left tibial nerve stimulation during resting (top), and during locomotion when the muscle was either inactive (middle) or active (bottom) prior to the stimulation in a wild-type mouse. **b)** Bar diagrams illustrating the probability of occurrence of a silent period in all recorded muscles of the right leg within the 5 ms window immediately after left tibial nerve stimulation when there was no muscle activity (top) or there was activity (bottom) prior to nerve stimulation. **c)** Box diagrams showing the average (+/- standard deviation) on and offsets of right muscle activities in response to the left tibial nerve stimulation at 1.2xT (i) and 5xT (ii) (indicated by the shaded area) during locomotion. Hatched area indicates a 10 ms time window after nerve stimulation. Black bar: wild type, red bar: $V0^{kill}$, and blue bar: $V3^{off}$. **d)** Diagrams illustrating the onset latencies of muscle activities in a bar: wild type (black), $V0^{kill}$ (red), and $V3^{off}$ (blue) mice during locomotion. Circles are averages from individual mice, and the horizontal lines indicate group averages (+/- standard deviation).

4.8 REFERENCES

Aggelopoulos NC, Burton MJ, Clarke RW, Edgleyl SA. Characterization of a Descending System that Enables Crossed Group II Inhibitory Reflex Pathways in the Cat Spinal Cord. **J Neurosci** 16: 723–729, 1996.

Aggelopoulos NC, Edgley SA. Segmental localisation of the relays mediating crossed inhibition of hindlimb motoneurones from group II afferents in the anaesthetized cat spinal cord. **Neurosci Lett** 185: 60–64, 1995.

Akay T, Tourtellotte WG, Arber S, Jessell TM. Degradation of mouse locomotor pattern in the absence of proprioceptive sensory feedback. **Proc Natl Acad Sci U S A** 111: 16877–16882, 2014.

Alvarez FJ, Jonas PC, Sapir T, Hartley R, Berrocal MC, Geiman EJ, Todd AJ, Goulding M. Postnatal phenotype and localization of spinal cord V1 derived interneurons. **J Comp Neurol** 493: 177–192, 2005.

Arya T, Bajwa S, Edgley SA. Crossed reflex actions from group II muscle afferents in the lumbar spinal cord of the anaesthetized cat. **J Physiol** 444: 117–131, 1991.

Bellardita C, Kiehn O. Phenotypic Characterization of Speed-Associated Gait Changes in Mice Reveals Modular Organization of Locomotor Networks. **Curr Biol** 25: 1426–1436, 2015.

Brooks ME, Kristensen K, van Benthem KJ, Magnusson A, Berg CW, Nielsen A, Skaug HJ, Mächler M, Bolker BM. glmmTMB Balances Speed and Flexibility Among Packages for Zero-inflated Generalized Linear Mixed Modeling. **R J** 9: 378–400, 2017.

Chopek JW, Nascimento F, Beato M, Brownstone RM, Zhang Y. Sub-populations of Spinal V3 Interneurons Form Focal Modules of Layered Pre-motor Microcircuits. **Cell Rep** 25: 146-156.e3, 2018.

Danner SM, Zhang H, Shevtsova NA, Borowska-Fielding J, Deska-Gauthier D, Rybak IA, Zhang Y. Spinal V3 Interneurons and Left-Right Coordination in Mammalian Locomotion. **Front Cell Neurosci** 13: 516, 2019.

Dietz V, Colombo G, Jensen L, Baumgartner L. Locomotor capacity of spinal cord in paraplegic patients. **Ann Neurol** 37: 574–582, 1995.

Duysens J, Loeb GE, Weston BJ. Crossed flexor reflex responses and their reversal in freely walking cats. **Brain Res** 197: 538–542, 1980.

Edgley SA, Jankowska E, Krutki P, Hammar I. Both dorsal horn and lamina VIII interneurones contribute to crossed reflexes from feline group II muscle afferents. **J Physiol** 552: 961–974, 2003.

Frigon A, Rossignol S. Short-latency crossed inhibitory responses in extensor muscles during locomotion in the cat. **J Neurophysiol** 99: 989–998, 2008.

Gauthier L, Rossignol S. Contralateral hindlimb responses to cutaneous stimulation during locomotion in high decerebrate cats. **Brain Res** 207: 303–320, 1981.

Hildebrand M. The Quadrupedal Gaits of Vertebrates. **Bioscience** 39: 766–775, 1989.

Jankowska E. Spinal interneuronal networks in the cat: Elementary components. **Brain Res Rev** 57: 46–55, 2008.

Jankowska E. Spinal interneurons. In: **Neuroscience in the 21st Century: From Basic to Clinical,** edited by Pfaff DW. New York, NY: Springer Science+Business Media, 2013, p. 11063–1099.

Jankowska E. Spinal Reflexes. In: **Neuroscience in the 21st Century,** edited by Pfaff DW, Volkow ND. New York: Springer Science+Business Media, 2016, p. 1599–1621.

Jankowska E, Edgley SA. Functional subdivision of feline spinal interneurons in reflex pathways from group Ib and II muscle afferents ; an update. **Eur J Neurosci** 32: 881–893, 2010.

Jankowska E, Krutki P, Matsuyama K. Relative contribution of Ia inhibitory interneurones to inhibition of feline contralateral motoneurones evoked via commissural interneurones. **J Physiol** 568.2: 617–628, 2005.

Kiehn O. Development and functional organization of spinal locomotor circuits. **Curr Opin Neurobiol** 21: 100–109, 2011.

Kiehn O. Decoding the organization of spinal circuits that control locomotion. **Nat Rev Neurosci** 17: 224–238, 2016.

Krasovsky T, Baniña MC, Hacmon R, Feldman AG, Lamontagne A, Levin MF. Stability of gait and interlimb coordination in older adults. **J Neurophysiol** 107: 2560–2569, 2012.

Kristensen K, Nielsen A, Berg CW, Skaug H, Bell BM. TMB: Automatic Differentiation and Laplace Approximation. **J Stat Softw** 70: 1–21, 2016.

Laflamme OD, Akay T. Excitatory and inhibitory crossed reflex pathways in mice. **J Neurophysiol** 120: 2897–2907, 2018.

Laflamme OD, Ibrahim M, Akay T. Crossed reflex responses to flexor nerve stimulation in mice. **J Neurophysiology** 127: 493–503, 2022.

Lanuza GM, Gosgnach S, Pierani A, Jessell TM, Goulding M. Genetic Identification of Spinal Interneurons that Coordinate Left-Right Locomotor Activity Necessary for Walking Movements. **Neuron** 42: 375–386, 2004.

Lemieux M, Josset N, Roussel M, Couraud S, Bretzner F. Speed-dependent modulation of the locomotor behavior in adult mice reveals attractor and transitional gaits. **Front Neurosci** 10: 42, 2016.

Meijer R, Plotnik M, Zwaaftink EG, va Lummel RC, Ainsworth E, Martina JD, Hausdorff JM. Markedly impaired bilateral coordination of gait in post-stroke patients : Is this deficit distinct from asymmetry ? A cohort study. **J Neuroeng Rehabil** 8: 23, 2011.

Mrachacz-Kersting N, Geertsen SS, Stevenson AJT, Nielsen JB. Convergence of ipsi- and contralateral muscle afferents on common interneurons mediating reciprocal inhibition of ankle plantar flexors in humans. **Exp Brain Res** 235: 1555–1564, 2017.

Perl ER. Crossed Reflexes of Cutaneous Origin. **Am J Physiol** 188: 609–615, 1957.

Peyronnard J-M, Charron L. Motor and sensory neurons of the rat sural nerve: A horseradish peroxide study. **Muscle Nerve** 5: 664–660, 1982.

Pierani A, Moran-Rivard L, Sunshine MJ, Littman DR, Goulding M, Jessell TM. Control of Interneuron Fate in the Developing Spinal Cord by the Progenitor Homeodomain Protein Dbx1. **Neuron** 29: 367–384, 2001.

Plotnik M, Giladi N, Hausdorff JM. A new measure for quantifying the bilateral coordination of human gait: effects of aging and Parkinson's disease. **Exp Brain Res** 181: 561–570, 2007.

Plotnik M, Giladi N, Hausdorff JM. Bilateral coordination of walking and freezing of gait in Parkinson's disease. **Eur J Neurosci** 27: 1999–2006, 2008.

Schomburg ED, Kalezic I, Dibaj P, Steffens H. Reflex transmission to lumbar α-motoneurones in the mouse similar and different to those in the cat. **Neurosci Res** 76: 133–140, 2013.

Sherrington CS. On Reciprocal Innervation of Antagonistic Msucles.-Eighth Note. **Proc R Soc B** 76: 269–297, 1905.

Shevtsova NA, Talpalar AE, Markin SN, Harris-Warrick RM, Kiehn O, Rybak IA. Organization of left-right coordination of neuronal activity in the mammalian spinal cord : Insights from computational modelling Key points. **J Physiol** 11: 2403–2426, 2015.

Steffens H, Dibaj P, Schomburg ED. In Vivo Measurement of Conduction Velocities in Afferent and Efferent Nerve Fibre Groups in Mice. **Physiol Res** 61: 203–214, 2012.

Stubbs PW, Nielsen JF, Sinkjær T, Mrachacz-Kersting N. Short-latency crossed spinal responses are impaired differently in sub-acute and chronic stroke patients. **Clin Neurophysiol** 123: 541–549, 2012.

Talpalar AE, Bouvier J, Borgius L, Fortin G, Pierani A, Kiehn O. Dual-mode operation of neuronal networks involved in left-right alternation. **Nature** 500: 85–88, 2013.

Tester NJ, Barbeau H, Howland DR, Cantrell A, Behrman AL. Arm and leg coordination during treadmill walking in individuals with motor incomplete spinal cord injury : A preliminary study. **Gait Posture** 36: 49–55, 2012.

Tong Q, Ye C, McCrimmon RJ, Dhillon H, Choi B, Kramer MD, Yu J, Yang Z, Christiansen LM, Lee CE, Choi CS, Zigman JM, Shulman GI, Sherwin RS, Elmquist JK, Lowell BB. Synaptic Glutamate Release by Ventromedial Hypothalamic Neurons Is Part of the Neurocircuitry that Prevents Hypoglycemia. **Cell Metab** 5: 383–393, 2007.

Tseng S, Morton SM. Impaired Interlimb Coordination of Voluntary Leg Movements in Poststroke Hemiparesis. **J Neurophysiology** 104: 248–257, 2010.

Witschi R, Johansson T, Morscher G, Scheurer L, Deschamps J, Zeilhofer HU. Hoxb8-Cre mice: A tool for brain-sparing conditional gene deletion. **Genesis** 48: 596–602, 2010.

Zhang H, Shevtsova NA, Deska-Gauthier D, Cackay C, Dougherty KJ, Danner SM, Zhang Y, Rybak IA. The role of V3 neurons in speed-dependent interlimb coordination during locomotion in mice. **Elife** 11: e73424, 2022.

Zhang J, Lanuza GM, Britz O, Wang Z, Siembab VC, Zhang Y, Velasquez T, Alvarez FJ, Frank E, Goulding M. V1 and V2b Interneurons Secure the Alternating Flexor-Extensor Motor Activity Mice Require for Limbed Locomotion. **Neuron** 82: 138–150, 2014.

Zhang Y, Narayan S, Geiman E, Lanuza GM, Velasquez T, Shanks B, Akay T, Dyck J, Pearson K, Gosgnach S, Fan CM, Goulding M. V3 Spinal Neurons Establish a Robust and Balanced Locomotor Rhythm during Walking. **Neuron** 60: 84–96, 2008.

Chapter 5. Inhibitory interneurons within the deep dorsal horn integrate convergent sensory input to regulate motor performance

Contribution statement

This work comes from the collaboration with Dr. Victoria Abraira's laboratory to which a lot of people contributed. The work presented in this chapter represents a reduced version of a much broader work that was recently submitted on Biorxiv as a preprint.

Ozeri-Engelhard N, Gradwell MA, Laflamme OD, Upadhyay A, Aoki A, Shrier T, Gandhi M, Gonzalez M, Eisdorfer JT, Abbas-Zadeh G, Yusuf N, Katz J, Haas M, Akay T, Abraira V. Inhibitory interneurons within the deep dorsal horn integrate convergent sensory input to regulate motor performance. **bioRxiv** 2022.05.21.492933.

I would like to give special thanks to Dr. Mark A Gradwell, and Nofar Ozeri-Engelhard for their major role in this project. From all the experiments performed to their leadership role demonstrated in this project. I would also like to acknowledge Dr. Abraira for allowing me to participate in this project. I would like to thank every member of Dr. Abraira's laboratory for their contribution to this work Aman Upadhyay, Adin Aoki, Tara Shrier, Melissa Gandhi, Melissa Gonzalez, Jaclyn T Eisdorfer, Gloria Abbas- Zadeh, Nusrath Yusuf, Jordan Katz, and Michael Haas.

5.1 ABSTRACT

To achieve smooth motor performance in a rich and changing sensory environment, the motor output must be constantly updated in response to sensory feedback. Although proprioception and cutaneous information are known to modulate motor output, it is unclear whether they work together in the spinal cord to shape complex motor actions such as locomotion. Here we identify the medial deep dorsal horn (mDDH) as a "hot zone" of convergent proprioception and cutaneous input for locomotion. Due to increased responsiveness to sensory input, inhibitory interneurons in the mDDH area are preferentially recruited in locomotion. To study inhibitory interneurons in this area, we utilize an intersectional genetic strategy to isolate and ablate a population of parvalbumin-expressing glycinergic interneurons in the mDDH (dPVs). Using histological and electrophysiological methods we find that dPVs integrate convergent proprioceptive and cutaneous inputs while targeting diffuse ventral horn motor networks. dPV ablation paired with behavioural testing reveals a role for dPVs in the timing and controlling step-cycle transition, suggesting a role in multimodal sensory processing for locomotion. Finally, we use EMG muscle recordings to directly show that dPVs are part of a cutaneous-motor pathway. Together, our results suggest convergent sensory inputs work in concert to coordinate the activity of dPVs, and in-turn regulate motor output in a contextually relevant manner. Our results indicate that dPVs form a critical node in the spinal sensorimotor circuitry.

5.2 INTRODUCTION

The ability to locomote is fundamental to almost every living creature, making it one of the most robust motor behaviours across the animal kingdom. Whether by searching for food, escaping a predator, or migrating due to climate change, animals use locomotion for survival. It is thus not surprising that the study of locomotion can be dated back to Aristotle, among other philosophers and Greek physicians during the 3rd century (*Aristotle's De Motu Animalium*, 1986). However, it was the experiments performed by Charles Sherrington and Graham Brown during the 20th century that shaped our current views about the circuits involved in locomotion. Sherrington proposed that locomotion is

organized as a “chain” of reflexes, requiring the participation of sensory feedback (Sherrington, 1906). However, Brown’s pioneering experiments, recording fictive locomotion in decerebrated and deafferented cats, demonstrated that locomotion persists in the absence of sensory feedback (Brown and Sherrington, 1911). These studies led to the dogma most accepted today of “Central Pattern Generator” (CPGs), intrinsic spinal networks generating the rhythmic and alternating activity controlling locomotion. Although not required for its generation, sensory input plays an important role in locomotion. In humans, permanent loss of large sensory fibers leads to a complete inability to walk, which is only regained following long training and visual guidance (Lajoie et al. 1996; Tuthill and Azim, 2018).

Two main sensory inputs “disturb” the rhythmic pattern of locomotion. The first is proprioception, the sense of one’s own body position and movement, detected by receptors embedded in muscles, joints, and tendons. The second is cutaneous input, relaying information about skin distortion and detected by low threshold mechanoreceptors (LTMRs) innervating it. Studies show that both proprioceptive and cutaneous afferents can initiate, arrest, reset, and enhance locomotion (Sherrington, 1910; Grillner and Rossignol, 1978; Duysens and Pearson, 1980). Furthermore, experiments evoking proprioceptive or cutaneous reflexes during locomotion demonstrate modulated muscle responses. For example, inducing the stumbling reflex with mechanical perturbations to the dorsum of the foot triggers knee flexion followed by flexion of the ankle and hip to clear the obstacle and place the foot in front of it (Forssberg, 1979). Similar experiments (Forssberg et al. 1975; Schillings et al. 1996), as well as modeling studies (Prochazka and Yakovenko, 2007), conclude that the main role of proprioceptive and cutaneous input is in tuning locomotion to environmental changes.

For efficient modulation of locomotion, information from both proprioceptors and cutaneous receptors must be integrated and processed by motor networks. In the cat spinal cord, the medial part of the deep dorsal horn (DDH) was found to be an area of convergent proprioceptive and cutaneous inputs, suggesting that interneurons (INs) located in this area process multimodal sensory input for locomotion. Additionally, the same area was

identified in the mouse as a hot zone of premotor interneurons, indicating these INs might participate in multimodal sensorimotor processing.

Over the last decade, striking progress in the development of mouse genetic tools enabled precise access to spinal cord interneuron populations defined by their common gene expression (Abraira et al. 2017). Using these tools, both excitatory and inhibitory DDH INs were found to perform multimodal sensorimotor processing. For example, the excitatory dl3 pre-motor interneuron integrates proprioceptive and LTMR input and regulates grasping in response to a change in the environment (Bui et al. 2013). Inhibitory neurons expressing the satb2 transcription factor integrate proprioception and nociception and play an appropriate role in the modulation of locomotion and pain withdrawal reflex (Hilde et al. 2016). Inhibitory RORβ expressing neurons mainly integrate proprioceptive input and modulate locomotion in a phase-dependent manner by exerting presynaptic inhibition on proprioceptive afferents (Koch et al. 2017).

While we have a better understanding of the role of DDH INs in sensorimotor control, a broader characterization of this area, as well as the identification of new uncharacterized populations is still lacking. Here we find that the highest convergence of proprioception and cutaneous input in the mouse is localized to the medial portion of laminas 4-5 (laminas 4-5m). Inhibitory INs within this region are more excitable and are preferentially recruited during locomotion. We identify an inhibitory IN population localized to the medial DDH, deep parvalbumin-expressing INs (dPVs), and hypothesize that they integrate multimodal sensory input and relay it to spinal cord motor networks to modulate locomotion. With colocalization experiments, we show that dPVs represent a new and uncharacterized population, originating from the dorsal Lbx1 lineage. Utilizing intersectional genetics we assess the function of dPVs and examine their underlying input/output circuits to define their importance in sensorimotor control. We reveal a new model by which sensory convergence produces a surprisingly divergent influence on motor networks, thereby increasing the diversity of mechanisms by which sensory input can shape movement.

5.3 METHODS

5.3.1 Experimental model and subject details

Mouse lines used to target DRG neuron populations include *TH*^{2aCreER} (Jax#025614), *vGlut3*^{iresCre} (Jax#028534), *TrkB*^{CreER} (Jax#027214), PTGFR^{CreER} (Zheng et al. 2019; Lehnert et al. 2021), *Ret*^{CreER} (Luo et al. 2009), Split^{Cre} (Rutlin et al. 2014), *Advillin*^{Cre} (Jax#032536), Advillin^{CreER} (Jax#032027) and *PV*^{2aCreER} (Jax#028580). Mouse lines used to target spinal cord interneurons include *vGAT*^{irescre} (Jax#028862), *GAD2*^{Cherry} (Jax#023140), GAD67^{GFP} (Tamamaki et al. 2003), GlyT2^{GFP} (Miranda et al. 2022), RoRB^{FlpO} (Jax#029590), RorB^{CreER}*,Satb2*^{CreER} (Hilde et al. 2016), *vGlut2*^{iresCre}(Jax#016963), *islet1*^{iresCre} (Jax#024242), Sim1^{iresCre} (Jax#006395), CCK^{iresCre} (Jax#012706), vGluT2^{YFP} (Jax#017978), and *Lbx1*^{Cre} (Sieber et al. 2007). To target Parvalbumin interneurons we used PV^{Tdtomato} (Jax#027395) and PV^{FlpO} (Jax#022730) mouse lines. For visualization, and manipulation of target populations the following mouse lines were used: *R26*$^{LSL\text{-}FSF\text{-}tdTomato}$ (Ai65, Jax#021875), *R26*$^{LSL\text{-}FSF\text{-}synaptophysin\text{-}GFP}$ (*RC::FPSit,* Jax#030206), R26$^{\mathbf{FSF\text{-}SynGFP}}$ (derived from RC::FPSit), *R26*^{LSL}-synaptophysin-tdTomato (Ai34, Jax#012570), *R26*$^{LSL\text{-}tdTomato}$ (Ai9, Jax#007909), *R26*$^{LSL\text{-}tdTomato}$ (Ai14, Jax#007914), Tau$^{LSL\text{-}LacZ\text{-}FSF\text{-}DTR}$ (Gatto et al. 2021) *R26*$^{LSL\text{-}ChR2\text{-}YFP}$(Ai32, Jax#024109); *R26*$^{LSL\text{-}FSF\text{-}ChR2\text{-}YFP}$(Ai80, Jax#025109). ChAT^{eGFP} (Jax#007902) was used to target cholinergic interneurons and motor neurons, *Emx1*^{Cre} (Jax#005628) was used to target cortical neurons, and *Lbx1*^{Cre} (Acton et al. 2019) was used to identify dPVs genetic lineage and restrict PV expression to the deep dorsal horn. Transgenic mouse strains were used and maintained on a mixed genetic background (129/C57BL/6). Experimental animals used were of both sexes. Except for EMG recordings, housing, surgery, behavioural experiments, and euthanasia were performed in compliance with Rutgers University Institutional Animal Care and Use Committee (IACUC; protocol #: 201702589). All mice used in experiments were housed in a regular light cycle room (lights on from 08:00 to 20:00) with food and water available ad libitum.

EMG recordings were performed at the lab of Dr. Turgay Akay (Dalhousie, Canada) according to the Canadian Council on Animal Care (CCAC) guidelines and approved by the local council on animal care of Dalhousie University. All mice used in

experiments were housed in a regular light cycle room (lights on from 07:00 to 19:00) with food and water available ad libitum.

5.3.2 Tamoxifen treatment

Tamoxifen was dissolved in ethanol (20 mg/ml), mixed with an equal volume of sunflower seed oil (Sigma), vortexed for 5-10 min, and centrifuged under vacuum for 20-30 min to remove the ethanol. The solution was kept at −80°C and delivered via oral gavage to pregnant females for embryonic or postnatal treatment. For all analyses, the morning after coitus was designated as E0.5 and the day of birth as P0.

5.3.3 Immunohistochemistry and free-floating sections

Male and female P30-P37 mice were anesthetized with isoflurane and perfused transcardially (using an in-house gravity driven-perfusion system) with Heparinized- saline (~30 sec) followed by 15-20 minutes of 4% paraformaldehyde (PFA) in PBS at room temperature (RT). Vertebral columns were dissected and post-fixed in 4% PFA at 4°C for 2 hours (for c-Fos and PV staining) or 24 hr. Sections were collected using a vibrating microtome (Leica VT1200S) and processed for immunohistochemistry (IHC) as described previously (Hughes et al. 2012). Unless otherwise mentioned, transverse sections (50-60 thick) were taken from the limb level lumbar spinal cord (LIV-VI). Free-floating sections were rinsed in 50% ethanol (30 min) to increase antibody penetration, followed by three washes in a high salt PBS buffer (HS-PBS), each lasting 10 min. The tissue was then incubated in a cocktail of primary antibodies made in HS-PBS containing 0.3% Triton X-100 (HS-PBSt) for 48 at 4°C. Next, tissue was washed 3 times (10 minutes each) with HS-PBSt, then incubated in a secondary antibody solution made in HS-PBSt for 24 hr at 4°C. Immunostained tissue was mounted on positively charged glass slides (41351253, Worldwide Medical Products) and coverslipped (48393-195, VWR) with Fluoromount-G mounting medium (100241-874, VWR).

5.3.4 Image acquisition and analysis

Images were captured with a Zeiss LSM 800 confocal or a Zeiss axiovert 200M fluorescence microscope. Images for cell counts were taken with 10x or 20x air objectives, and images of synaptic contacts were taken with a 40x oil objective. ImageJ (cell count

plug-in) was used for colocalization analysis of cell bodies. Imaris was used for synaptic analysis. For synaptic analysis of proprioceptive and cutaneous input onto dPVs, the fraction of each input was calculated relative to their sum. For synaptic analysis of dPVs output to target neurons, input was normalized to cell body area or dendrite length. Only puncta apposing a postsynaptic marker (Homer1 and Gephyrin for excitatory and inhibitory synapses, respectively) were included for analysis. Synaptic analysis was performed separately for somas and proximal dendrites (up to 50 um from the cell body). Imaris software was additionally used for the measurement of the cell body/synaptic terminal's spatial coordinates (using the central canal and dorsal edge of the spinal cord as references). This data was then used to generate density plots (custom MatLab script).

5.3.5 c-Fos induction

To decrease stress, at least 7 days prior to the experiment, mice were transferred to a holding area adjacent to the testing room. 6-8 weeks old $vGAT^{Cre}$;$Tau^{LSL\text{-}LacZ}$ mice were randomly placed in one of three groups: control (n=4), swim (n=4), and walk (n=5). All mice were habituated to the testing room for 30 minutes. Control mice were kept in their home cage for 60 minutes. The "walk" group walked on a treadmill (Mouse Specifics, Inc, Boston, MA, USA) at 20 cm/s for 2 x 20 minutes with a 5-minute break. The "swim" group was kept in a swim tank for 4 x 10 minutes with 5 minutes breaks. 60 minutes following the completion of the task, mice were anesthetized with isoflurane and perfused for immunohistochemistry. Sections stained with chicken- ß-galactosidase (ab9361, Abcam), mouse-NeuN (MAB377, Millipore), and rabbit-c-Fos (226003, Synaptic Systems) were used to acquire 20x images of the entire hemisection, stitches with zen. These images were used for quantification of c-Fos expressing neurons (normalized to total NeuN) by lamina (Fig. 5.1) and c-Fos expressing inhibitory (vGAT+c-Fos+NeuN+) and excitatory (vGAT-c-Fos+NeuN-) neurons in the medial portion of laminas 4-5 (Fig. 5.2). Alternate sections from the same animals stained with Guinea pig-PV (PV-GP-Af1000, frontier institute) and c-Fos, were used to acquire 20x images of the deep dorsal horn to quantify the fraction of dPVs that express c-Fos in each of the 3 conditions. All images were acquired with the Zeiss LSM 800 confocal microscope. 3-6 images from each mouse were used for quantification.

5.3.6 Electrophysiology

Recordings were made from male and female mice. Mice were anesthetized with ketamine (100 mg/kg i.p.), decapitated, and the lumbar enlargement of the spinal cord rapidly removed in ice-cold sucrose substituted artificial cerebrospinal fluid (sACSF) containing (in mM): 250 sucrose, 25 $NaHCO_3$, 10 glucose, 2.5 KCl, 1 NaH_2PO_4, 6 $MgCl_2$, and 1 $CaCl_2$. Sagittal or transverse slices (200µm thick) were prepared using a vibrating microtome (Leica VT1200S). Slices were incubated for at least 1hr at 22-24°C in an interface chamber holding oxygenated ACSF containing (in mM): 118 NaCl, 25 $NaHCO_3$, 10 glucose, 2.5 KCl, 1 NaH_2PO_4, 1 $MgCl_2$, and 2.5 $CaCl_2$.

Following incubation, slices were transferred to a recording chamber and continually superfused with ACSF bubbled with Carbogen (95% O_2 and 5% CO_2) to achieve a pH of 7.3-7.4. All recordings were made at room temperature (22-24°C) and neurons were visualized using a Zeiss Axiocam 506 color camera. Recordings were acquired in cell-attached (holding current = 0mV), voltage-clamp (holding potential -70mV), or current-clamp (maintained at −60mV). Patch pipettes (3-7 MΩ) were filled with a potassium gluconate-based internal solution containing (in mM): 135 $C_6H_{11}KO_7$, 8 NaCl, 10 HEPES, 2 Mg_2ATP, 0.3 Na_3GTP, and 0.1 EGTA, (pH 7.3, adjusted with KOH, and 300 mOsm) to examine AP discharge and excitatory synaptic transmission. A cesium chloride-based internal solution containing (in mM): 130 CsCl, 10 HEPES, 10 EGTA, 1 $MgCl_2$, 2 Na-ATP, 2 Na-GTP, and 5 QX-314 bromide (pH 7.3, adjusted with CsOH, and 280 mOsm) was used to record inhibitory synaptic transmission. No liquid junction potential correction was made, although this value was calculated at 14.7 mV (22°C). Slices were illuminated using an X-CITE 120LED Boost High-Power LED Illumination System that allowed visualization of Td-Tomato expressing dPVs with TRITC filters and visualization of GFP fluorescence and ChR2 photostimulation using FITC filter set.

AP discharge patterns were assessed in the current clamp from a membrane potential of −60 mV by delivering a series of depolarizing current steps (1 s duration, 20 pA increments, 0.1 Hz), with rheobase defined as the first current step that induced AP discharge. For optogenetic circuit mapping, photostimulation intensity was suprathreshold (24 mW), duration 1 ms (controlled by transistor-transistor logic pulses), and 0.1 Hz. This

ensured the generation of action potential discharge in presynaptic populations and allowed confident assessment of postsynaptic currents in recorded neurons.

All data were amplified using a MultiClamp 700B amplifier, digitized online (sampled at 20 kHz, filtered at 5 kHz) using an Axon Digidata 1550B, acquired and stored using Clampex software. After obtaining the whole-cell recording configuration, series resistance, input resistance, and membrane capacitance were calculated (averaged response to -5mV step, 20 trials, holding potential -70mV).

5.3.7 Electrophysiology analysis

All data were analysed offline using AxoGraph X software. AP discharge was classified according to previously published criteria (Browne et al. 2020). In the analysis of AP discharge, individual APs elicited by step-current injection were captured using a derivative threshold method (dV/dt > 15 V/second) with the inflection point during spike initiation defined as the AP threshold. Individual AP properties for each neuron were assessed from the first spike generated at rheobase. AP latency was measured as the time difference between the stimulus onset and the AP threshold. The difference between the AP threshold and its maximum positive peak was defined as the AP peak. AP half-width was measured at 50% of the AP peak. AP rise and decay time were measured from 10-90% of peak. AP afterhyperpolarization (AHP) amplitude was taken as the difference between the AP threshold and the maximum negative peak following the AP. AHP half-width was measured at 50% of the AHP peak. AP threshold adaptation was determined by dividing the AP threshold of the last AP by the AP Threshold of the first AP evoked by a step-current. AP number was the number of spikes discharged in the entire response. Instantaneous frequency was the average instantaneous frequency across a step-current.

Optogenetically-evoked excitatory postsynaptic currents (oEPSCs) and inhibitory postsynaptic currents (oIPSCs) were measured from baseline, just before photostimulation. The peak amplitude of responses was calculated from the average of 10 successive trials. Several parameters were considered for determining whether a photostimulation-evoked synaptic input was monosynaptic or polysynaptic. The latency of oPSCs was measured as the time from photostimulation to the onset of the evoked current. The “jitter” in latency

was measured as the standard deviation in latency of 10 successive trials. Importantly, the latency of monosynaptic inputs was much shorter, there was minimal jitter in the onset of responses between trials, and reliability (percentage of photostimulation trials to evoke a response) was higher than those deemed polysynaptic inputs. To assess the contribution of different neurotransmitter systems to photostimulation responses, various synaptic blockers were sequentially applied.

5.3.8 Diphtheria Toxin preparation and delivery

DTx was dissolved in 1xPBS to 100 ug/ml and kept as 15 ul aliquot at −20°C. On the day of injection, DTx was diluted 1:10 in a hyperbaric solution (filtered 0.9% NaCl, 8% dextrose) as described in (Albisetti et al. 2019). P21-P28 mice carrying the PV^{FlpO};Lbx^{1Cre};$Tau^{LSL\text{-}FSF\text{-}DTR}$ (dPVs^{abl}) or PV^{FlpO};$Tau^{LSL\text{-}FSF\text{-}DTR}$ (dPVs^{norm}) alleles, received Diphtheria Toxin (DTx, D0564-1MG, Sigma) on day 1 and 3 (5 ul of 10 ug/ml DTx, overall 50 ng) through intrathecal (I.T.) injection to the L5-L6 intervertebral space. DTx was delivered with a 25 ul Hamilton syringe (72310-388) with a 30 G needle and performed as previously described (Li et al. 2019). Briefly, mice were anesthetized with isoflurane and the hair above their lower back was removed with Nair. Under anesthesia, exposed skin was wiped with 70% ethanol. Next, mice were held firmly by the pelvic girdle with their skin taut in one hand, while the other hand was used to gently rotate the base of the tail to find the midline of the spine. A needle was inserted through the skin along the midline, between the pelvic girdles to the L5-L6 intervertebral space. An occurrence of a sudden tail indicated successful entry into the intradural space.

5.3.9 Quantification of DTx-mediated ablation

Following behavioural testing, 9 PV^{FlpO};Lbx^{1Cre};$Tau^{LSL\text{-}FSF\text{-}DTR}$ and 6 PV^{FlpO};$Tau^{LSL\text{-}FSF\text{-}DTR}$ mice were perfused, their spinal cord and cerebellum were dissected, and sectioned using a vibrating microtome (Leica VT1200S). For consistency, sections were collected at the levels of the mid-cervical enlargement, mid-thoracic, mid-lumbar enlargement, and the midline of the cerebellum. Sections were immunostained with Guinea pig-PV and mouse-NeuN, and 20x images were taken using the Zeiss axiovert 200M fluorescence microscope. For quantification, 3 spinal cord and 2 cerebellum images were used. PV neurons were counted in the superficial dorsal horn (sPVs), deep dorsal horn (dPVs), and molecular layer

of the cerebellum. sPVs were normalized to NeuN, dPVs were normalized to sPVs (to account for the difference in staining success), and PV neurons in the molecular layer were normalized to the area.

5.3.10 Behavioural testing

7-12 weeks old male and female PV^{FlpO};Lbx^{1Cre};$Tau^{LSL\text{-}FSF\text{-}DTR}$ and PV^{FlpO};$Tau^{LSL\text{-}FSF\text{-}DTR}$ mice were used for behaviour testing following DTx injection (P21-P28). The experimenter was blind to the genotype of the animals. For all behaviour assays, mice were transferred to the holding area adjacent to the behaviour rooms at least 7 days prior to testing. On the day of training/testing, mice were transferred to the behaviour room for 30-minute habituation.

Mice were forced to walk on a motorized treadmill (Mouse specifics, inc.) with a transparent belt at speeds of 5-100 cm/s for 2 days. Each mouse had to exhibit a minimum of 3 seconds of walk at a certain speed for it to be included in the analysis. On day 2, mice were given one more chance to walk at speeds they failed at on the first day. A high-speed camera (165 fps) located underneath the belt, was used to record mice' paw placement. A custom-developed software was used to calculate the area paw in contact with the belt, for each paw, in each video frame, as described in Hampton et al. (2004). We then used this data to calculate (in-house MatLab script) the duration of stance (when paw area>0), swing (paw area=0), stride (summed swing and stance duration), and the stride frequency (the number of strides per second) of each limb.

5.3.11 Construction of EMG electrodes

EMG electrodes were made using multi-stranded, Teflon-coated annealed stainless-steel wire (A-M systems, catalog number 793200). The construction of the EMG electrode and nerve cuff was previously described in detail (Pearson et al. 2005; Akay et al. 2006; 2014). Two nerve cuff electrodes and six EMG recording electrodes were attached to the headpiece pin connector (female, SAM1153-12; DigiKey Electronics Thief River Falls, MN) and covered with 3D printed cap.

5.3.12 EMG electrode implantation surgeries

Experiments were conducted on males and females (4-5 month-old), PV^{FlpO}/Lbx^{1Cre};$Tau^{LSL\text{-}FSF\text{-}DTR}$ (dPVs^{norm}, n=9) and PV^{FlpO};Lbx^{1Cre};$Tau^{LSL\text{-}FSF\text{-}DTR}$ (dPVs^{abl}, n=6) mice. All surgeries were performed in aseptic conditions and on a warm water-circulated heating pad maintained at 42°C. Each mouse received an electrode implantation surgery as previously described (Laflamme and Akay, 2018; Laflamme et al. 2022). Briefly, animals were anesthetized with isoflurane (5% for inductions, 2% for maintenance of anesthesia), ophthalmic eye ointment was applied to the eyes, and the skin of the mice was sterilized with three-part skin scrub using hibitane, alcohol, and povidone-iodine. Prior to each surgery, buprenorphine (0.03 mg/kg) and meloxicam (5 mg/kg) were injected subcutaneously as analgesics while the animals were still under anesthesia. Additional buprenorphine injections were performed in 12-hour intervals for 48 hours.

A set of six bipolar EMG electrodes and two nerve stimulation cuffs were implanted in each mouse as the following: small incisions were made on the shaved areas (neck and both hind legs), and each bipolar EMG electrode and the nerve cuff electrodes were led under the skin from the neck incisions to the leg incisions, and the headpiece connector was stitched to the skin around the neck incision. EMG recording electrodes were implanted into the left knee flexor (semitendinosus, St_l), ankle flexor (tibialis anterior, TA_l), and extensor (gastrocnemius, Gs_l) as well as the right knee flexor (semitendinosus, St_r) and extensor (Vastus Lateralis, VL_r) and the left ankle extensor (gastrocnemius, Gs_r). Nerve stimulation electrodes were implanted in the left saphenous nerve and right sural nerve to evoke cutaneous feedback. After surgery, the anesthetic was discontinued, and mice were placed in a heated cage for three days before returning to a regular mouse rack. Food mash and hydrogel were provided for the first three days after the surgery. Any mouse handling was avoided until mice were fully recovered, and the first recording session started at least ten days after electrode implantation surgeries.

5.3.13 EMG recording sessions

After animals fully recovered (~10 days) from electrode implantation surgeries, the recording session went as follows: Under brief anesthesia with isoflurane, a wire to connect the headpiece connector with the amplifier, and the stimulation insulation units (ISO-

FLEX-AMPI, Jerusalem, Israel or the DS4-Digitimer, Hertfordshire, United Kingdom) was attached to the mouse. The anesthesia was discontinued, and the mouse was placed on a mouse treadmill (model 802; custom built in the workshop of the Zoological Institute, University of Cologne, Germany). The electrodes were connected to an amplifier (model 102; custom built in the workshop of the Zoological Institute, University of Cologne, Germany) and a stimulus isolation unit. After the animal fully recovered from anesthesia (at least five minutes), the minimal (threshold) current necessary to elicit local reflex responses in the ipsilateral leg was determined by injecting a double impulse of 0.2 ms duration into the saphenous nerve (average ±SD threshold current: 436.4 µA ±396; range: 120-1300 µA) and the sural nerve (average ±SD threshold current: 117.6 µA ±83.4; range: 28-230 µA) of $dPVs^{norm}$, and the saphenous nerve (average ±SD threshold current: 215 µA ±157.9; range: 64-450 µA) and the sural nerve (average ±SD threshold current: 253.3 µA ±127.5; range: 130-500 µA) of $dPVs^{abl}$. Following the determination of threshold currents, the current injected into the sural and saphenous nerve was set as either 1.2 times the local reflex threshold current (1.2 X threshold) or five times the local reflex threshold current (5 X threshold).

EMG signals from six muscles of the right and left leg were simultaneously recorded (sampling rate: 10,000 kHz). For the 1- nerve stimulation assay, saphenous or sural nerves were electrically stimulated, while for the 2- nerve stimulation assay, both nerves were stimulated at varying delays (0,5,15,15,20,25,30,35,40,45, or 50 ms). Paired stimulation of both legs at different delays provides evidence of an inhibitory period if there is a suppression of the motor responses from one leg following stimulation of the other leg. Nerve stimulations (five 0.2ms impulses at 500 Hz) were applied using the ISO-FLEX (AMPI, Jerusalem, Israel) and DS4 (Digitimer, Hertfordshire, United Kingdom) stimulation insulation units. Stimulation protocols were recorded while the mice were resting on the treadmill. EMG signals were amplified (gain 100), band-pass filtered from 400 Hz to 5 kHz, and stored on the computer using Power1410 interface and Spike2 software (Cambridge Electronic Design, Cambridge, United Kingdom).

5.3.14 Analysis of EMG responses

EMG analysis response was done using Spike2 software (Cambridge Electronic Design, Cambridge, United Kingdom). Response latency was quantified for each stimulation and then averaged for each mouse. Inhibition quantification was performed on a delay in which the peak amplitude of the expected response is located between 10-20ms after the second nerve stimulation as latency is shown to involve an inhibitory pathway (Laflamme and Akay, 2018; Laflamme et al. 2022). Every muscle inside a single mouse was treated separately to provide the best delay for each case. The average expected response was then compared to single paired stimulation of the selected delay. When the average expected response possesses a higher amplitude than the paired stimulation, it was categorized as an inhibition.

5.3.15 Quantification and statistical analysis

All data are reported as mean values ± s.e.m. Behavioural assays were repeated several times (3 to 10 times depending on the experiment) and averaged per animal. Statistical analysis was performed in GraphPad Prism (USA) or MatLab, using two-sided paired or unpaired Student's t-tests, one-way ANOVA for neuromorphological evaluations with more than two groups, and one- or two-way repeated-measures ANOVA for functional assessments, when data were distributed normally. Post-hoc Tukey's or Bonferroni's test was applied when appropriate. The significance level was set as $p < 0.05$. The nonparametric Mann-Whitney or Wilcoxon signed-rank tests were used in comparisons of <5 mice. Statistics were performed over the mean of animals. For the analyses of step cycles, all cycles from all mice were used and statistical analysis was performed with a linear mixed-effects regression model with mouse ID as a random effect.

5.4 RESULTS

5.4.1 Deep dorsal horn inhibitory neurons exhibit preferred excitability and responsiveness to sensory input

Integration of proprioceptive and cutaneous information is essential to normal locomotion and motor adaptation. To identify spinal regions that process convergent proprioceptive and cutaneous inputs, we first visualized the terminal endings of these

populations using $PV^{2aCreER}$;$Advillin^{FlpO}$;$Rosa^{LSL\text{-}FSF\text{-}TdTomato}$;$Rosa^{LSL\text{-}SynGFP}$ mice (Fig. 5.1, *A-B*). We found that cutaneous inputs (green) are restricted to the superficial and deep dorsal horn (LI-IV), while proprioceptive inputs (yellow) span the deep dorsal and ventral horns (LIV-X). Of particular interest, convergent sensory input (green + yellow) was largely restricted to the medial deep dorsal horn (mDDH) (Fig. 5.1*B*). This finding suggests that the mDDH plays an important role in integrating convergent proprioceptive and cutaneous sensory inputs.

Given that inhibitory and excitatory neurons are functionally divergent, we separately examined their c-Fos expression in the DDH, using $vGAT^{Cre}$;$Tau^{LSL\text{-}LacZ}$ mice. Quantification of c-Fos in inhibitory (c-Fos$^+$/LacZ$^+$) and excitatory (c-Fos$^+$/LacZ$^-$) neurons suggested that increased c-Fos expression following swim and walk is attributed to enhanced activity in inhibitory, but not excitatory neurons (Fig. 5.1, *C-E*). The preferred recruitment of inhibitory neurons suggests distinct roles for DDH excitatory and inhibitory neurons, with a prevalent role for inhibition in sensorimotor control.

To further explore the functional properties of these two populations, we performed an electrophysiological characterization of randomly sampled excitatory and inhibitory neurons within the DDH using the $vGluT2^{Cre}$;$Rosa^{LSL\text{-}TdTomato}$, and $vGAT^{Cre}$;$Rosa^{LSL\text{-}TdTomato}$ lines, respectively (Fig. 5.1*F*). Cell-attached recordings showed that significantly more inhibitory neurons exhibit spontaneous action potential (sAP) discharge than excitatory neurons (Fig. 5.1, *G-H*). Of the spontaneously active neurons, inhibitory neurons showed higher sAP frequency with a lower coefficient of variation (Fig. 5.1, *I-J*). These findings suggest that inhibitory neurons are more active than their excitatory counterparts and are a likely source of tonic inhibition. To further explore the intrinsic excitability of these two populations, we next examined their responsiveness to depolarizing current injection. Using previously established AP discharge phenotypes (Browne et al. 2020), we found that the majority of excitatory and inhibitory neurons within the DDH exhibit tonic firing (TF) AP discharge patterns (Fig. 5.1*K*). TF Ins could be further classified into 2 subcategories: TF-non-accommodating (TF_{Na}) and TF accommodating (TF_{Ac}). TF_{Na} was more frequently observed in inhibitory neurons whereas TF_{Ac} was more present in excitatory neurons. Inhibitory neurons showed a lower latency to the first AP (Fig. 5.1*L*) and an increased

number of Aps (Fig. 5.1*M*). Together, these data suggest inhibitory neurons possess more excitable intrinsic properties that promote spontaneous AP discharge and increased responsiveness to sensory input.

In summary, this data demonstrates that inhibitory neurons exhibit more excitable properties compared to their excitatory counterparts, allowing for their preferential recruitment. This preferential recruitment of inhibitory neurons within the mDDH, along with the convergence of proprioceptive and cutaneous input to this region, suggests a particularly important role for inhibitory Ins within the mDDH in the processing of sensory information during locomotion. We, therefore, used genetic strategies to target inhibitory mDDH interneurons and study their role in motor performance.

5.4.2 Parvalbumin-expressing inhibitory interneurons are confined to the medial deep dorsal horn

The calcium-binding protein parvalbumin (PV) is a known marker of inhibitory Ins in the brain and spinal cord (Kim et al. 2016; Boyle et al. 2019; Nahar et al. 2021). Using the $PV^{TdTomato}$ mouse line, we identified a population of PV-Ins confined to the medial portion of the DDH (Fig. 5.2*A*), previously identified as the region receiving convergent sensory input. We named these Ins deep dorsal horn parvalbumin-expressing interneurons (dPVs) and found that they represent 18±5.45% of LIV-V. Given that PV-Ins within LIIi-III of the spinal cord are a mixed excitatory/inhibitory population, we investigated the neurochemical phenotype of dPVs using excitatory and inhibitory markers (Figure 5.2*B*, Supplemental Fig. S5.1, *A-D*). We found that dPVs are largely inhibitory, with the majority being purely glycinergic (Supplemental Fig. S5.1, *A-D*). We also compared the dPV population to two previously characterized inhibitory DDH IN populations defined by the transcription factor Satb2 and the orphan nuclear hormone receptor RORβ. Colocalization analysis showed that dPVs show limited co-expression with Satb2 and RORβ (Supplemental Fig. S5.1, *E-G*) suggesting that dPVs represent a substantial population of uncharacterized inhibitory Ins confined to the mDDH.

To determine whether dPVs are active during locomotion, we again examined c-Fos expression following rest, swimming, and walking behavioural tasks. In line with our

previous data showing enhanced activity in inhibitory neurons of the mDDH, we found a significant increase in c-Fos expression in dPVs following locomotor activity (Fig. 5.2*C*). Furthermore, dPVs electrophysiological characteristics were similar to those of inhibitory Ins within the same region (Fig. 5.2, *D-E*) Together, these data show that dPVs are recruited during locomotor activity, are a source of tonic inhibitory control, and are therefore likely to play an important role as modulators of locomotor output. Given the wide expression of PV throughout the brain, spinal cord, and dorsal root ganglia (DRG), we next sought to devise an experimental approach to specifically target and manipulate the activity of the dPV population.

5.4.3 dPV ablation alters stride frequency

To study the function of dPVs we devised an intersectional genetic approach. First, we found preferential recombination within the DDH when using the PV^{FlpO} mouse line, avoiding the more dorsal PV-IN population. To restrict expression to the spinal cord, we then examined the co-expression of dPVs with known genetic lineages. As dPVs lie in the dorsoventral interface, we chose to focus on Islet1, and Lbx1 that give rise to dorsal lineages and Sim1, the genetic origin of the ventral V3 population (Gross et al. 2002; Lu et al. 2015). As dPVs are almost exclusively derived from the Lbx1-lineage (Supplemental Fig. S5.1, *H-K*), we generated a $Lbx1^{Cre}$;PV^{FlpO} intersectional approach to target dPVs throughout the rostrocaudal axis of the spinal cord (Fig. 5.2*F*), while avoiding recombination within the more superficial dorsal horn, ventral horn, and DRG. To specifically ablate the dPV population we utilized an intersection of PV^{FlpO};$Lbx1^{Cre}$;$Tau^{LSL\text{-}FSF\text{-}DTR}$ with intrathecal (I.T.) injection of Diphtheria toxin (DTx), prepared in a hyperbaric solution, shown to restrict DTx to the spinal cord (Albisetti et al. 2019). We therefore generated mice with ablated dPVs (dPV^{abl}: PV^{FlpO};$Lbx1^{Cre}$;$Tau^{LSL\text{-}FSF\text{-}DTR}$ injected with DTx) and non-manipulated dPVs (dPV^{norm}: PV^{FlpO}/$Lbx1^{Cre}$;$Tau^{LSL\text{-}FSF\text{-}DTR}$ injected with DTx) (Fig. 5.2, *F-G*).

After developing an approach to specifically target dPVs, control (dPV^{norm}) and dPV ablated (dPV^{abl}) mice were run on a treadmill at different speeds. A high-speed camera located underneath the transparent belt was used to record paw placement and calculate basic locomotion parameters. dPV ablation caused an increase in stride frequency, and a

decrease in swing time, without major changes to stance (Fig. 5.2, *I-J*). To increase stride frequency, animals shorten their stance time with minimal changes to swing (Goslow Jr. et al. 1973; Halbertsma, 1983). We, therefore, hypothesize that dPVs primary role is to modulate step timing, with changes to swing time a secondary effect. In line with this hypothesis, we observed a change in the phase of the transition from stance to swing, with dPV^{abl} mice transitioning later in the step cycle (Fig. 5.2*K*). We next sought to dissect dPVs circuit connectivity that underlies their role in the behaving animal.

5.4.4 dPVs integrate proprioceptive and cutaneous inputs

The location of dPVs in the mDDH and their role in locomotion suggest they integrate proprioceptive and cutaneous inputs, in particular from the paw. To assess the contribution of proprioception and cutaneous inputs to dPV sensory inputs, we utilized our genetic strategy to label both modalities. High-resolution imaging revealed that both proprioceptive and cutaneous terminals contact dPVs (Fig. 5.3*A*), with significantly more cutaneous input onto dPV dendrites (Fig. 5.3*B*). To both validate inputs' functionality and reveal possible polysynaptic connections, we next performed slice electrophysiology where dPVs activity was recorded in response to optogenetic stimulation of sensory afferents. We found that most monosynaptic input to dPVs originates from proprioceptors, Aß-RA, and Aß-field (Fig. 5.3, *C-E*). Additionally, we found that dPVs receive polysynaptic input from proprioceptors, Aß-, C-, and Aδ- LTMR (Fig. 5.3, *F-G*). Taken together, dPVs input connections support the integration of proprioceptive and cutaneous inputs from the paw through direct and indirect pathways. We next teased out some of the dPVs output targets that support their role in sensorimotor processing.

5.4.5 dPVs form a diffuse inhibitory circuit with spinal cord motor networks

What are dPVs output targets that support their role in motor action? To address this question, we visualized dPVs axon terminals using the intersection *PV^{FlpO}*;Lbx1^{Cre};*Rosa$^{LSL\text{-}FSF\text{-}SynGFP}$*. Our map shows a diffuse pattern of dPVs axon terminals through the deep dorsal and ventral horn laminas, suggesting output divergence (Fig. 5.3*H*). We next used immunohistochemistry tools to dissect some of the dPVs' targets. We found dPV contacts onto other dPVs, pre-motor neurons such as Renshaw cells and V0cs, as well as motor neurons (Fig. 5.3*I*). Next, we performed slice electrophysiology and

recorded potential postsynaptic targets while optically stimulating dPVs. Consistent with our histological findings, we found monosynaptic inhibitory inputs onto other dPVs, V0cs, MNs within the medial motor pool, MNs within the lateral motor pool, and putative foot MNs. While dPV-mediated inhibition was most frequent and strongest on other dPVs, the incidence and amplitude of dPV-mediated inhibition in other populations were relatively equal (Fig. 5.3, *J-K*). Taken together, our results show that dPVs integrate proprioceptive and cutaneous inputs and innervate MNs and pre-motor Ins in the deep and ventral horns. To directly test if dPVs form a sensorimotor circuit, we next performed electromyogram activity from flexor and extensor muscles in response to stimulation of sensory nerves.

5.4.6 dPVs mediate cutaneous-evoked muscle inhibition

To perform sensorimotor processing for locomotion, dPVs must relay sensory inputs to motor networks where their activity will affect motor response. We thus proceeded by studying the role of dPVs in muscle response evoked by the activation of paw cutaneous inputs. $dPVs^{abl}$ and $dPVs^{norm}$ were implanted with nerve cuffs on 2 cutaneous nerves: the right sural and left saphenous nerves, innervating the ventral and dorsal paw. Electromyogram (EMG) electrodes were implanted in the right and left semitendinosus (St, knee flexor), right vastus lateralis (VL, knee extensor), right and left gastrocnemius (Gs, ankle extensor), and left tibialis anterior (ankle flexor). Following the stimulation of each nerve, activity was recorded in both ipsi and contralateral muscle (Fig. 5.4, *A-B*). We found that ablation of dPVs decreased response latency of the muscle activity (Fig. 5.4*B*); this was evident in both flexors and extensors, mostly in ipsilateral muscles, but also in contralateral muscles (Fig. 5.4, *C-D*).

These faster responses in $dPVs^{abl}$ could suggest a loss of inhibition following dPVs ablation. To directly test this, we designed a 2-nerve assay paradigm (Fig. 5.5, *A-top*) in which local cutaneous inputs will suppress a motor response if inhibitory pathways are present. Nerve cuffs and EMG electrodes were implanted as described above. We started by stimulating a single nerve and calculated the average expected response (black trace, Fig. 5.5*B*). Next, both nerves were stimulated at varying delays (see Supplemental Fig. S5.2 and methods for further explanation) and the summed response (yellow trace, Fig. 5.5*B*) was compared to the expected response. If the response to the 2-nerve stimulation

was lower than the expected response, we concluded that the trial includes an inhibition component. Figure 5.5B shows an example of this process, where inhibition was detected in dPV^{norm} but not in dPV^{abl}. The experimental setup allowed us to explore the participation of dPVs in both local inhibition (when the second nerve stimulated is ipsilateral to the recorded muscle) and contralateral inhibition (when the second nerve stimulated is contralateral to the recorded muscle). Quantifying percent inhibition (the percentage of trials in which inhibition was detected), revealed that ablation of dPVs resulted in the loss of ipsilateral inhibition from the saphenous nerve to the knee flexor St, and from the sural nerve to the ankle extensor Gs (Fig. 5.5*C*). Additionally, $dPVs^{abl}$ showed a loss of contralateral inhibition from the sural nerve to the ankle flexor TA (Fig. 5.5*D*)

Together, these data suggest that dPVs mediate cutaneous-evoked inhibition of motor circuits to delay muscle response. Following the ablation of dPVs, this cutaneous evoked inhibition is lost, and muscle response is faster. The source of inhibition is shown to be primarily ipsilateral. Further, loss of ipsilateral inhibition could underlie the change in ipsilateral coupling interlimb coordination following dPV ablation. We find that ablation of dPVs results in decreased inhibition of both flexor and extensor muscles.

5.5 DISCUSSION

In this paper, we characterize the role of the DDH in the multimodal integration of proprioceptive and cutaneous inputs for locomotion. We identify the medial deep dorsal horn as the epicenter of sensory convergence and highlight inhibitory Ins within this region as key players in sensorimotor processing. We find a new population of inhibitory interneurons, dPVs, that receive convergent sensory input and are a source of divergent inhibitory control over premotor and motor circuits. Abolition of dPVs revealed that dPVs modulate locomotion suggesting that dPVs are involved in dynamic sensorimotor interaction. Indeed, by characterizing their connectivity we find that dPVs integrate proprioceptive and cutaneous input to inhibit DDH and ventral horn neurons, including pre-motor and motor neurons. Lastly, we directly demonstrate a loss of sensory-evoked muscle inhibition following the ablation of dPVs.

5.5.1 Convergence of proprioceptive and cutaneous input by deep dorsal horn interneurons for the modulation of locomotion

With the growing development of molecular and genetic tools, studies are rushing to tease out the distinct functions of neuronal subsets. However, it is important to recognize, as shown by a recent study (Gatto et al. 2021), that the dorsal horn of the spinal cord displays a laminar organization, where molecularly heterogeneous Ins show overlapping roles. In a similar fashion, the DDH, suggested to integrate proprioceptive and cutaneous inputs (Orlovskiĭ and Fel'dman, 1972; Brown and Fyffe, 1981; Edgley and Jankowska, 1987; Hongo et al. 1989; Moschovakis et al. 1992; Abraira et al. 2017) and shown to harbor premotor Ins (Moschovakis et al. 1992; Levine et al. 2014), is thought to play a significant role in sensorimotor processing. Here we use new genetic tools and show that indeed, the medial portion of laminas 4-5 of the DDH integrates multimodal proprioceptive and cutaneous inputs. We focus our attention on dPV interneurons, representing a large portion of laminas 4-5, and by functionally characterizing their input-output connectivity, we provide evidence for the role of the DDH interneuron in sensorimotor processes. Further, although their existence has been assumed from studies demonstrating a role for cutaneous input in the modulation of motor output, dPVs are genetically identified inhibitory Ins shown to form a spinal cord cutaneous-motor circuit.

This paper and others, identify Ins that integrate multimodal sensory input (Hilde et al. 2016; Koch et al. 2017; Bui et al. 2013). Why is it beneficial that such convergence occurs on Ins as opposed to the output neurons, in this case, the motor neuron? We propose two reasons why such "early" convergence is beneficial for motor performance. First, it reduces the amount of processing required to be performed by motor neurons. As the last-order neuron in the motor pathway, motor neurons must consider multiple information. Early processing can thus reduce the load on motor neurons. Second, locomotion requires the coordination of muscles across all limb joints, and between all limbs. Thus, incoming sensory input must modulate the activity of several muscles in parallel. Sensory input convergence on Ins as opposed to motor neurons offers the opportunity for output convergence to multiple motor and pre-motor neurons that can modulate the activity of several muscles in parallel.

5.5.2 Dynamic modulation of locomotion by sensory inputs

In this study, we identify the DDH parvalbumin-expressing Ins (dPVs) that functionally integrate direct multimodal sensory inputs from proprioceptors and Aß-LTMRs as well as indirect input from Aδ-LTMR, and C-LTMRs. Detailed analysis of high-speed videos of treadmill walking revealed changes to locomotion that were more pronounced at high speeds. At high speeds, swing duration was shorter, and stride frequency increased. Under normal conditions, mice increase their walking speed by decreasing stance duration, with minimal change to swing duration. However, this phase dependency is consistent with other studies showing different roles of sensory inputs during the different phases of locomotion. For example, similar to our results, Bouyer and Rossignol showed that removal of hindpaw cutaneous afferents in otherwise intact results in faster swing, but no change in stance duration (Bouyer and Rossignol, 1998). Experiments, where cutaneous or proprioceptive reflexes were entrained during locomotion, showed interesting results suggesting dynamic modulation of reflex response depending on the locomotion phase. For example, electrical or mechanical stimulation of the dorsum of the foot during the swing phase produces a similar pattern of muscle activation involving activation of knee flexors, as well as ankle and hip extensors to move the leg away from and over the obstacle (Forssberg et al. 1975; 1977; Forssberg, 1979; Schillings et al. 1996; Mayer and Akay, 2021). On the other hand, stimulation during stance does not recruit flexors but instead results in a short latency amplitude increase of already active ankle and knee extensor muscles (Forssberg et al. 1975). dPVs dynamic role in the modulation of locomotion is consistent with previous literature on the role of sensory afferents in locomotion. While further experiments are needed to better understand the mechanisms for this dynamic modulation, our results show that dPVs firing rate has a wide dynamic range in response to current injections, suggesting that their activity can be up and down-regulated as necessary.

5.5.3 The role of inhibition in the spinal cord

We found that inhibitory INs located in the medial DDH are preferentially recruited during weight-bearing locomotion, requiring the integration of cutaneous and

proprioceptive inputs. The role of inhibition has been extensively studied, in both the brain and spinal cord. Studies show that experimentally disrupting excitation-inhibition balance leads to aberrant neural states (Dudek and Sutula, 2007). Further, it was demonstrated in various brain sensory systems, that a change in the excitatory drive leads to a concomitant change in the inhibitory drive to maintain the balance (Anderson et al. 2000; Poo and Isaacson, 2009; Wehr and Zador, 2003; Wilent and Contreras, 2005; Li et al. 2003). Evidence for this balance was also demonstrated in the spinal cord. In turtles, recordings from motor neurons during scratching revealed that changes in neuronal conductance were accompanied by a simultaneous increase in rhythmic inhibition and excitation (Berg et al. 2007; Petersen et al. 2014). This simultaneous inhibition and excitation has been termed "push-pull", and is thought to be a mechanism for gain control, i.e. to induce a divisive change in the input-output relationship of neurons (Johnson et al. 2012). This was demonstrated in ankle extensor motor neurons of the feline where inhibitory and excitatory inputs from flexor and extensor Ia proprioceptive afferents, respectively, behaved in a push-pull manner and provided tonic inhibition and excitation to motor neurons. As a result of this background "noise", response gain to phasic sensory input from the same afferents was increased. Here we identify dPVs that relay cutaneous information to motor neurons. While dPVs show phasic responses to proprioceptive and cutaneous input, they are also tonically active. Additionally, we show that excitatory INs in the DDH similarly integrate cutaneous and proprioceptive input and are mostly tonically active. Thus, dPVs might act in tandem with an excitatory component that receives the same inputs and excite the same motor neurons to maintain their inhibition-excitation balance in order to "sharpen" motor neuron response to the sensory input. Additionally, decreasing the dPVs firing frequency by modulation of CPGs or neuromodulators can be used to decrease the motor neuron gain so it is less sensitive to incoming sensory input, which can explain dPVs dynamic role.

5.6 FIGURES

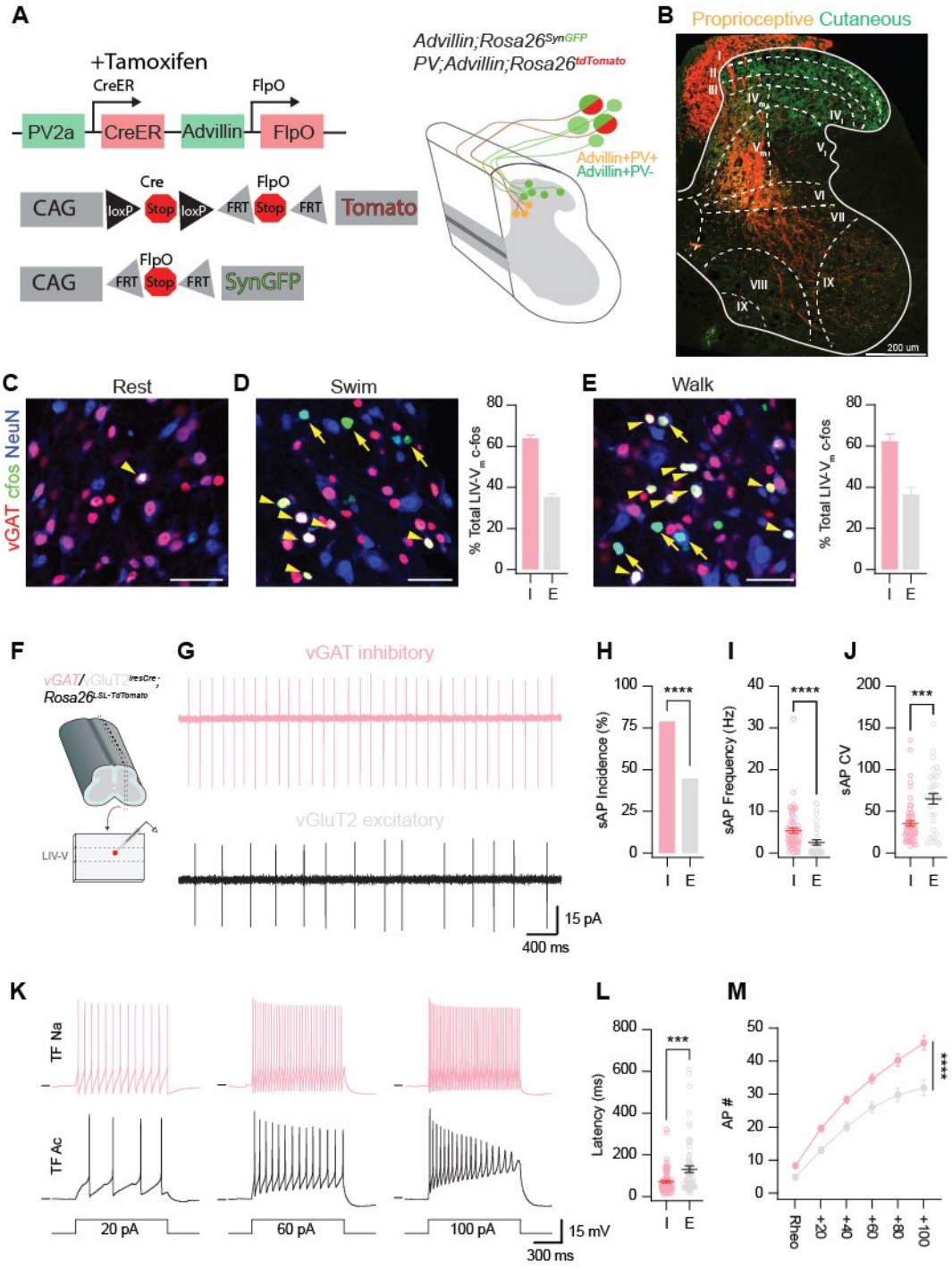
A
+Tamoxifen
CreER
FlpO
PV2a
CreER
Advillin
FlpO
Cre
FlpO
CAG
loxP
Stop
loxP
FRT
Stop
FRT
Tomato
CAG
FlpO
FRT
Stop
FRT
SynGFP
Advillin;Rosa26SynGFP
PV;Advillin;Rosa26tdTomato
Advillin+PV+
Advillin+PV-
B
Proprioceptive Cutaneous
200 um
C
Rest
vGAT cfos NeuN
D
Swim
% Total LIV-Vm c-fos
E
Walk
% Total LIV-Vm c-fos
F
vGAT/vGluT2IresCre;
Rosa26LSL-TdTomato
LIV-V
G
vGAT inhibitory
vGluT2 excitatory
15 pA
400 ms
H
sAP Incidence (%)
I
sAP Frequency (Hz)
J
sAP CV
K
TF Na
TF Ac
20 pA
60 pA
100 pA
15 mV
300 ms
L
Latency (ms)
M
AP #
Rheo
+20
+40
+60
+80
+100

Figure 5.1. The medial deep dorsal horn, a region for convergence proprioceptive and cutaneous input, is active during locomotion and exhibits excitable electrophysiological profiles. A) Left- intersectional genetic approach to label cutaneous and proprioceptive input in the mouse. **Right-** $PV^{2aCreER};Advillin^{FlpO};Rosa^{LSL\text{-}FSF\text{-}Tomato}/Rosa^{FSF\text{-}SynGFP}$ mice have proprioceptor fibers (PV+Advillin+) labelled in red and all sensory terminals (Advillin+) in green. In the spinal cord, proprioceptor terminals are identified by both green and red fluorescence (yellow), while cutaneous terminals are identified by green fluorescence alone. **B)** Representative transverse section of limb level lumbar spinal cord from the genetic intersection in A, showing the convergence of cutaneous and proprioceptive input in the medial part of laminas IV-V. scale bar: 200 **C-E*)*** Mice performed one of 3 tasks: rest (A), swimming (B), or walking (C), and their tissue was processed for c-Fos (green), vGAT (red), and NeuN (blue) immunostaining. **C,D-left, E-left)** Representative 20x confocal images, zoomed-in on LIV-V_{Medial}, show c-Fos expressing inhibitory (c-Fos+vGAT+NeuN+, yellow arrowheads) and excitatory (c-Fos+vGAT-NeuN+, yellow arrows) neurons in the rest (A), swim (B-left), and walk (C-left) conditions. scale bars: 40 μm. **D-right, E-right)** Percentage c-Fos expressing neurons that are inhibitory (I) and excitatory (E) in the swim (left) and walk (right) conditions. **F)** Schematic of conditions for electrophysiological comparison of inhibitory and excitatory neurons. **G)** Cell-attached voltage-clamp recording showing spontaneous AP discharge in inhibitory (pink) and excitatory (black) neurons. **H)** Inhibitory neurons exhibited higher sAP incidence. **I)** higher sAP frequency. **J)** and lower sAP coefficient of variation. **K)** Representative responses of inhibitory (pink, top) and excitatory (black, bottom) to depolarizing current injection. **L)** Inhibitory interneurons exhibited lower latency to 1st AP. **M)** and fired more APs in response to the current injection. 2-way ANOVA, ****$p < 0.0001$. Graphs show average +S.E.M. Statistical analysis was done using Mann Witney test or two-way ANOVA (N), with *$p<0.05$, **$p<0.005$, ****$p < 0.0005$ and ****$p < 0.0001$.

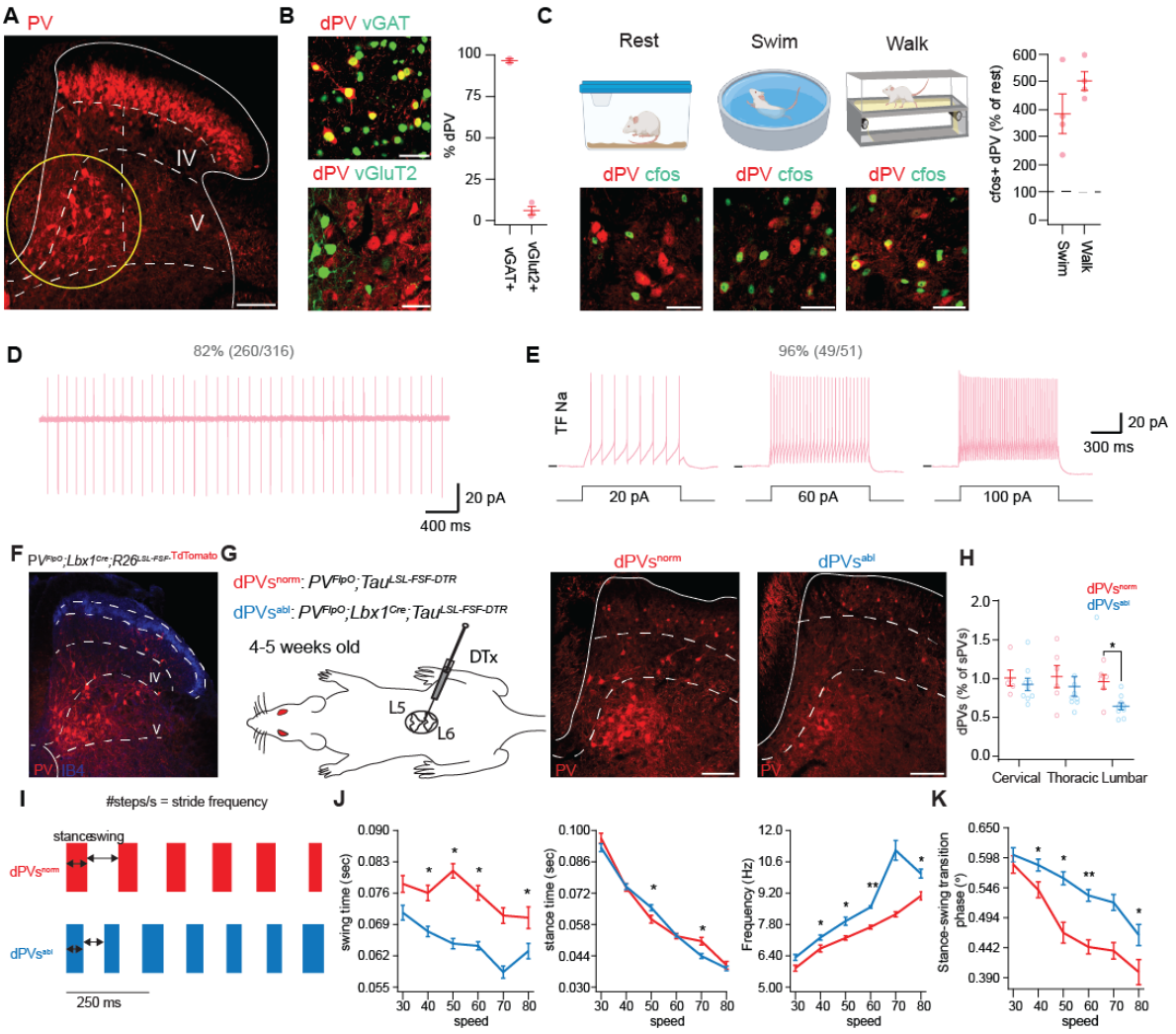
A PV
IV
V
B dPV vGAT
dPV vGluT2
% dPV
vGAT+
vGlut2+
C Rest
Swim
Walk
dPV cfos
dPV cfos
dPV cfos
cfos+ dPV (% of rest)
Swim
Walk
D 82% (260/316)
20 pA
400 ms
E 96% (49/51)
TF Na
20 pA
300 ms
20 pA
60 pA
100 pA
F PVFlpO;Lbx1Cre;R26LSL-FSF-TdTomato
PV
TB4
G dPVsnorm: PVFlpO;TauLSL-FSF-DTR
dPVsabl: PVFlpO;Lbx1Cre;TauLSL-FSF-DTR
4-5 weeks old
DTx
L5
L6
dPVsnorm
dPVsabl
PV
PV
H
dPVsnorm
dPVsabl
dPVs (% of sPVs)
Cervical
Thoracic
Lumbar
I #steps/s = stride frequency
stance
swing
dPVsnorm
dPVsabl
250 ms
J
swing time (sec)
stance time (sec)
Frequency (Hz)
speed
speed
speed
K
Stance-swing transition phase (°)
speed

Figure 5.2. dPVs are active during locomotion. A) Transverse lumbar section of $PV^{TdTomato}$ BAC transgenic shows the presence of PV expressing interneurons in the deep dorsal horn (dPVs, in yellow circle). Scale bar: 100 µm. **B)** dPVs are inhibitory neurons. Left- representative images demonstrating colocalization of dPVs (PV+, red) with the inhibitory marker vGAT (green, top image) and the excitatory marker vGluT2+ (green, bottom image). Scale bar: 40 µm. **C) Left, top-** schematic of c-Fos experiment used to quantify c-Fos expressing dPVs in different tasks. **Left, bottom-** 20x confocal images zoomed-in on LIV-V_{Medial} show dPVs (red) and c-Fos (green) in the rest (left), swim (middle) walk (right) conditions. Scale bar: 40 µm. **Right-** Quantification of c-Fos expressing dPVs in swim and walk. C-Fos is shown as a percentage of rest. **D)** Cell-attached voltage-clamp recording showing dPVs (82%) exhibit spontaneous AP discharge. **E)** Representative traces of dPV response to depolarizing current injection. **F**) Strategy for dPVs ablation. PV^{FlpO};$Lbx1^{Cre}$;$Tau^{LSL\text{-}FSF\text{-}DTR}$ and PV^{FlpO};$Tau^{LSL\text{-}FSF\text{-}DTR}$ were injected with 50 ng Diphtheria toxin (DTx), delivered intrathecally (I.T.) into the L5-L6 intervertebral space to generate animals with ablated dPVs (dPV^{abl}) and non-ablated dPVs (dPV^{norm}). **G)** Transverse section demonstrating PV neurons in L4 spinal cord of dPV^{norm} (left) and dPV^{abl} (right). Scale bar: 100 µm. **H)** Quantification of dPVs (normalized to superficial PVs) in dPV^{abl} and dPV^{norm} throughout the cervical, thoracic and lumbar segments. dPV^{abl} shows a decrease in lumbar dPVs. **I-K)** Comparison of step cycle parameters of dPV^{norm} and dPV^{abl}, calculated from the data extracted by DigiGait™. **I)** Example stepping of the lateral hindlimb at 60 cm/s shows a shorter swing and increased step frequency in dPV^{abl}. **J)** Swing duration (left), stance duration (middle) and step frequency (right) of the hindlimbs vs speed (30-80 cm/s). **K)** Stance-to-swing transition phase vs speed (30-80 cm/s, data from right hindlimb). Graphs show average +S.E.M. Statistical analysis was done using paired t-test (F,G), with *p<0.05, **p<0.005, ****p < 0.0005 and ****p < 0.0001. Blue and red denote dPV^{norm} and dPV^{abl}, respectively. Statistical analysis of step cycle (J-K) parameters was performed with a linear mixed-effects regression model with mouse ID as a random effect, with *p < 0.05 and **p < 0.005.

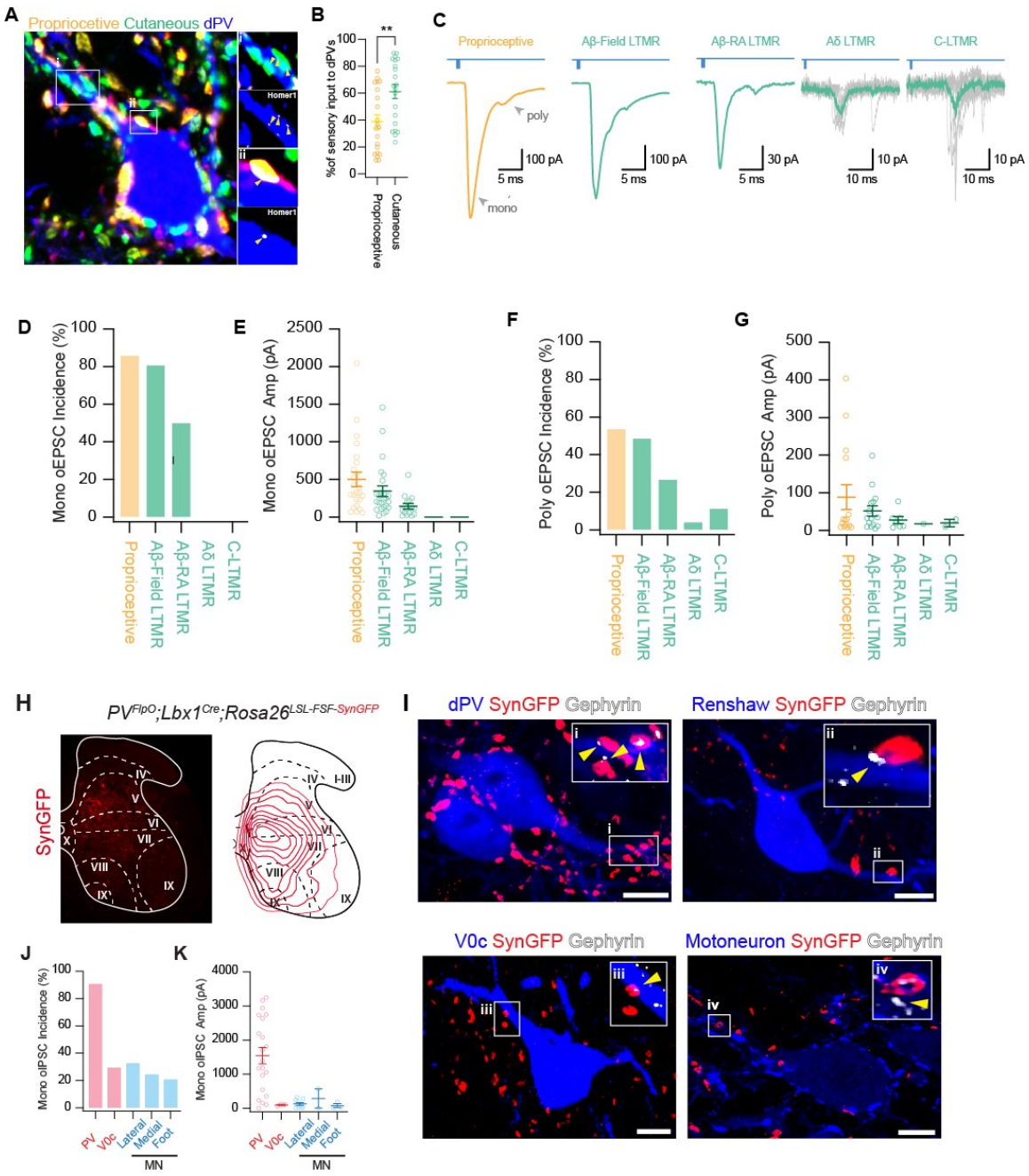
A
Proprioceptive Cutaneous dPV
Homer1
Homer1
B
**
%of sensory input to dPVs
Proprioceptive
Cutaneous
C
Proprioceptive
Aβ-Field LTMR
Aβ-RA LTMR
Aδ LTMR
C-LTMR
poly
mono
100 pA
5 ms
100 pA
5 ms
30 pA
5 ms
10 pA
10 ms
10 pA
10 ms
D
Mono oEPSC Incidence (%)
Proprioceptive
Aβ-Field LTMR
Aβ-RA LTMR
Aδ LTMR
C-LTMR
E
Mono oEPSC Amp (pA)
F
Poly oEPSC Incidence (%)
G
Poly oEPSC Amp (pA)
H
PVFlpO;Lbx1Cre;Rosa26LSL-FSF-SynGFP
SynGFP
I
dPV SynGFP Gephyrin
Renshaw SynGFP Gephyrin
V0c SynGFP Gephyrin
Motoneuron SynGFP Gephyrin
J
Mono oIPSC Incidence (%)
PV
V0c
Lateral
Medial
Foot
MN
K
Mono oIPSC Amp (pA)

Figure 5.3. dPVs process convergent proprioceptive and cutaneous sensory inputs. A) 40x confocal image demonstrates a single dPV neuron surrounded and in contact with cutaneous (green) and proprioceptive (yellow) puncta. Scale bar: 10µm. i,ii) cutaneous (i) and proprioceptive (ii) puncta that are in contact with dPV soma and dendrite are shown to be in apposition to the postsynaptic marker Homer1 (yellow arrows). Scale bars: 2µm. **B)** Quantification of cutaneous (green) and proprioceptive (yellow) input as a percentage of the total sensory input to dPVs. Cutaneous input shows higher innervation of dPVs. Mann-Whitney test, **p < 0.005. **C)** Representative traces from dPVs showing 10 consecutive sweeps with average oEPSC overlaid of oEPSCs following activation of proprioceptive afferents, Aβ-Field LTMRs, Aβ-RA LTMRs, Aδ-LTMRs, and C-LTMRs. **D)** Grouped data of monosynaptic oEPSC incidence. **E)** Grouped data of monosynaptic oEPSC amplitude. **F)** Grouped data showing polysynaptic oEPSC amplitude. **G)** Representative trace from dPV showing 10 consecutive sweeps with average overlaid of oEPSCs following activation of CCK+INs. **H) Left-** representative image from limb level lumbar cord from the intersection PV^{FlpO};$Lbx1^{Cre}$;$Rosa^{LSL\text{-}FSF\text{-}SynGFP}$ showing dPVs axon terminals in pseudo-red. Scale bar: 200 µm. **Right-** density map showing the distribution of dPVs axon terminals throughout the dorso-ventral axis of the lumbar spinal cord. **I)** 40x confocal images demonstrating direct contact between dPVs terminals (SynGFP, red) and deep dorsal horn and ventral horn interneurons (blue). dPVs are shown to contact other dPVs, Renshaw cells (top right), V0c interneurons (bottom left), and motor neurons (bottom right). Scale bar: 10 µm. i,ii,iii,iv,v) dPVs' terminals are shown to be in apposition to the inhibitory postsynaptic marker Gephyrin (white, yellow arrows). Scale bar: 2 µm **J)** Grouped data of monosynaptic oEPSC incidence. **K)** Grouped data of monosynaptic oEPSC amplitude. Graphs show average +S.E.M.

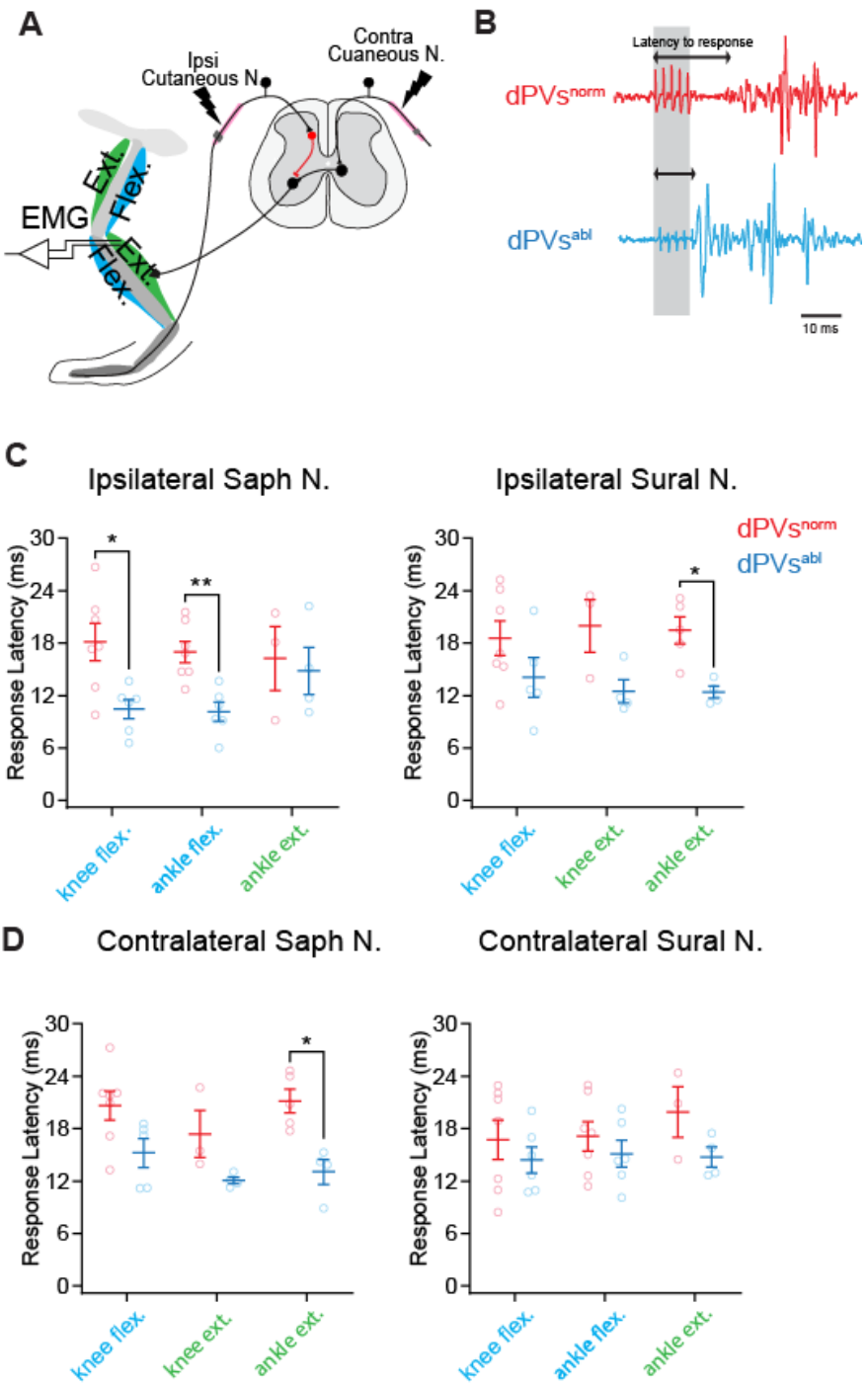
A
Ipsi Cutaneous N.
Contra Cuaneous N.
EMG
Ext.
Flex.
Ext.
Flex.
B
Latency to response
dPVs^norm
dPVs^abl
10 ms
C
Ipsilateral Saph N.
Ipsilateral Sural N.
dPVs^norm
dPVs^abl
Response Latency (ms)
knee flex.
ankle flex.
ankle ext.
knee ext.
D
Contralateral Saph N.
Contralateral Sural N.

Figure 5.4. dPVs mediate cutaneous-evoked muscle activation. A) Diagram depicting the single nerve stimulation assay designed to reveal the contribution of dPVs to motor activity evoked by stimulation of ipsilateral cutaneous nerves. Nerve cuffs were implanted on the right sural nerve and left saphenous nerve. EMG electrodes were implanted into the right and left semitendinosus (St, knee flexor), right vastus lateralis (VL, knee extensor), left tibialis anterior (TA, ankle flexor), and right and left gastrocnemius (Gs, ankle extensor). EMG responses were recorded from ipsilateral hindlimb flexors and extensors following stimulation of cutaneous nerves (saphenous/sural nerve). **B)** Example St EMG responses to stimulation of the right saphenous nerve at 5 times threshold (see methods) in dPV^{norm} (top) and dPV^{abl} (bottom), during the experiment described in D. **C)** Response latency of ipsilateral hindlimb muscles to stimulation of the saphenous (left) or sural (right) nerves during the experiment depicted in **A**. dPV^{abl} show decreased response latency in St and TA in response to stimulation of the ipsilateral saphenous nerve and in Gs in response to stimulation of the ipsilateral sural nerve. **D)** Response latency of contralateral hindlimb muscles to stimulation of the saphenous (left) or sural (right) nerves during the experiment depicted in A. dPV^{abl} showed decreased response latency in Gs muscle contralateral to the saphenous nerve. Statistical analysis was done Mann-Whitney test or Student's test as appropriate, with *$p<0.05$ and, **$p<0.005$.

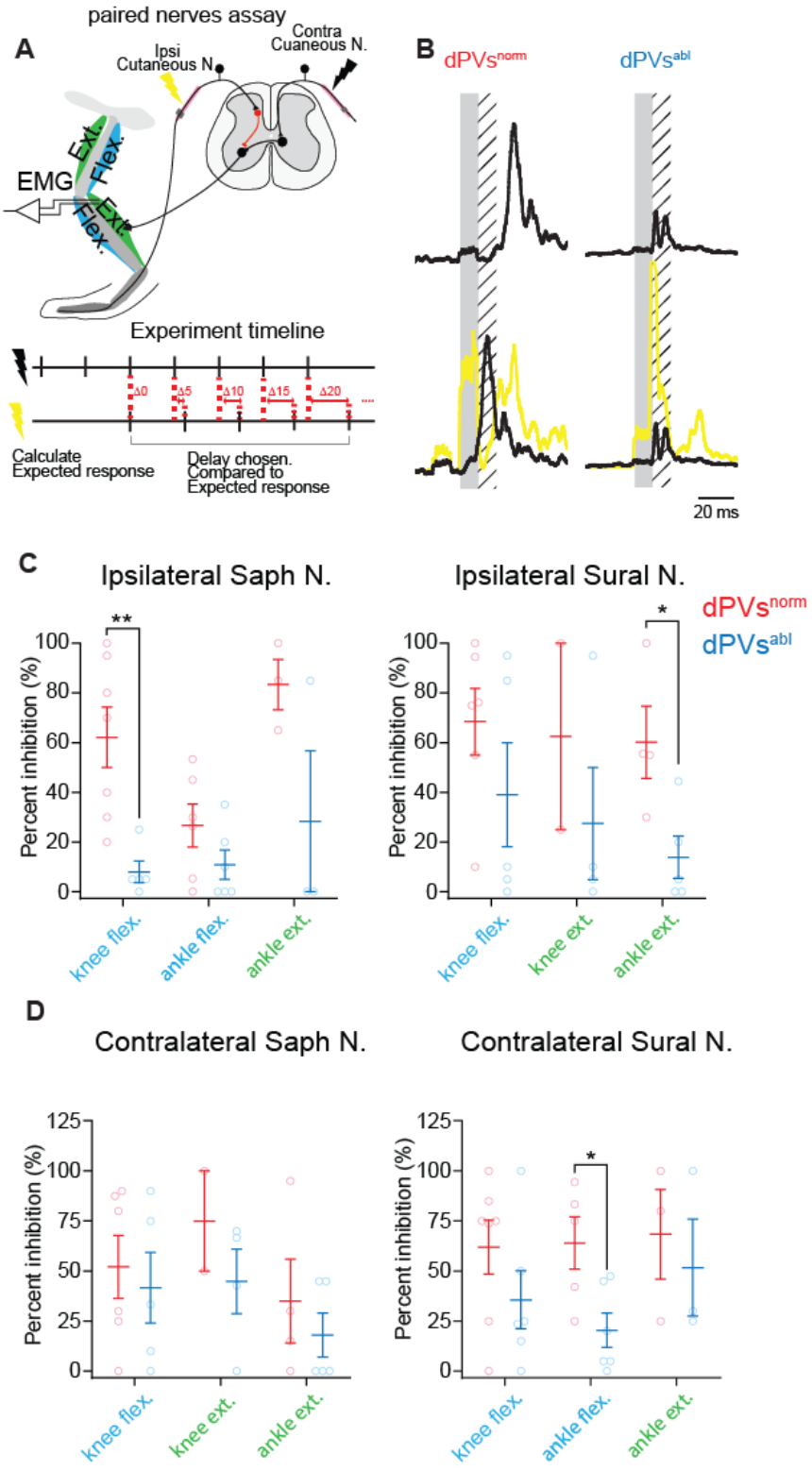
paired nerves assay
A
Ipsi Cutaneous N
Contra Cuaneous N.
EMG
Ext.
Flex.
Ext.
Flex.
Experiment timeline
Δ0
Δ5
Δ10
Δ15
Δ20
Calculate Expected response
Delay chosen. Compared to Expected response
B
dPVsnorm
dPVsabl
20 ms
C
Ipsilateral Saph N.
Ipsilateral Sural N.
dPVsnorm
dPVsabl
Percent inhibition (%)
knee flex.
ankle flex.
ankle ext.
knee ext.
D
Contralateral Saph N.
Contralateral Sural N.

Figure 5.5. dPVs mediate cutaneous-evoked muscle inhibition. A) Top- diagram of paired nerves assay applied to reveal if dPVs mediate sensory-evoked ipsilateral inhibition. **Bottom-** experiment timeline. Nerve cuffs and EMG electrodes were placed as in A. Stimulation of the contralateral cutaneous nerve (saphenous/ sural) alone (black lightning) was used to calculate the expected response in the absence of sensory-evoked ipsilateral inhibition. Following, both nerves were stimulated (yellow lightning), with variable delays, and compared to the expected response to reveal ipsilateral inhibition. **B) Top-** expected Gs EMG response to stimulation of a single cutaneous nerve in dPV^{abl} (left) and dPV^{norm} (right), averaged over 20 responses. **Bottom-** expected responses (black) superimposed on single trial responses to stimulation of both cutaneous nerves (yellow). **Left-** response to stimulation of both nerves (15 ms delay), shows a "dip" that is absent in the expected response, indicating ipsilateral inhibition. **Right-** no "dip" is seen (0 ms delay), suggesting a loss of inhibition. For each mouse and each muscle, the delay in which responses were best aligned was chosen for further analysis. **C)** Percent inhibition (the percentage of trials where inhibition was detected) in hindlimb muscles, mediated by ipsilateral saphenous (left) and ipsilateral sural (right) nerves, calculated from the results of the experiment depicted in A. dPV^{abl} show a decrease in percent inhibition in St in response to stimulation of the ipsilateral saphenous nerve, and in Gs in response to the ipsilateral sural nerve. **D)** Percent inhibition (the percentage of trials where inhibition was detected) in hindlimb muscles, mediated by contralateral saphenous (left) and contralateral sural (right) nerves, quantified from results of the experiment in A. dPV^{abl} showed a decrease in percent inhibition in TA muscle contralateral to the sural nerve. Graphs show average +S.E.M. Blue and red denote dPV^{norm} and dPV^{abl}, respectively. Statistical analysis was done Mann-Whitney test or Student's test as appropriate, with *$p<0.05$ and, **$p<0.005$.

5.7 SUPPLEMENTAL FIGURES

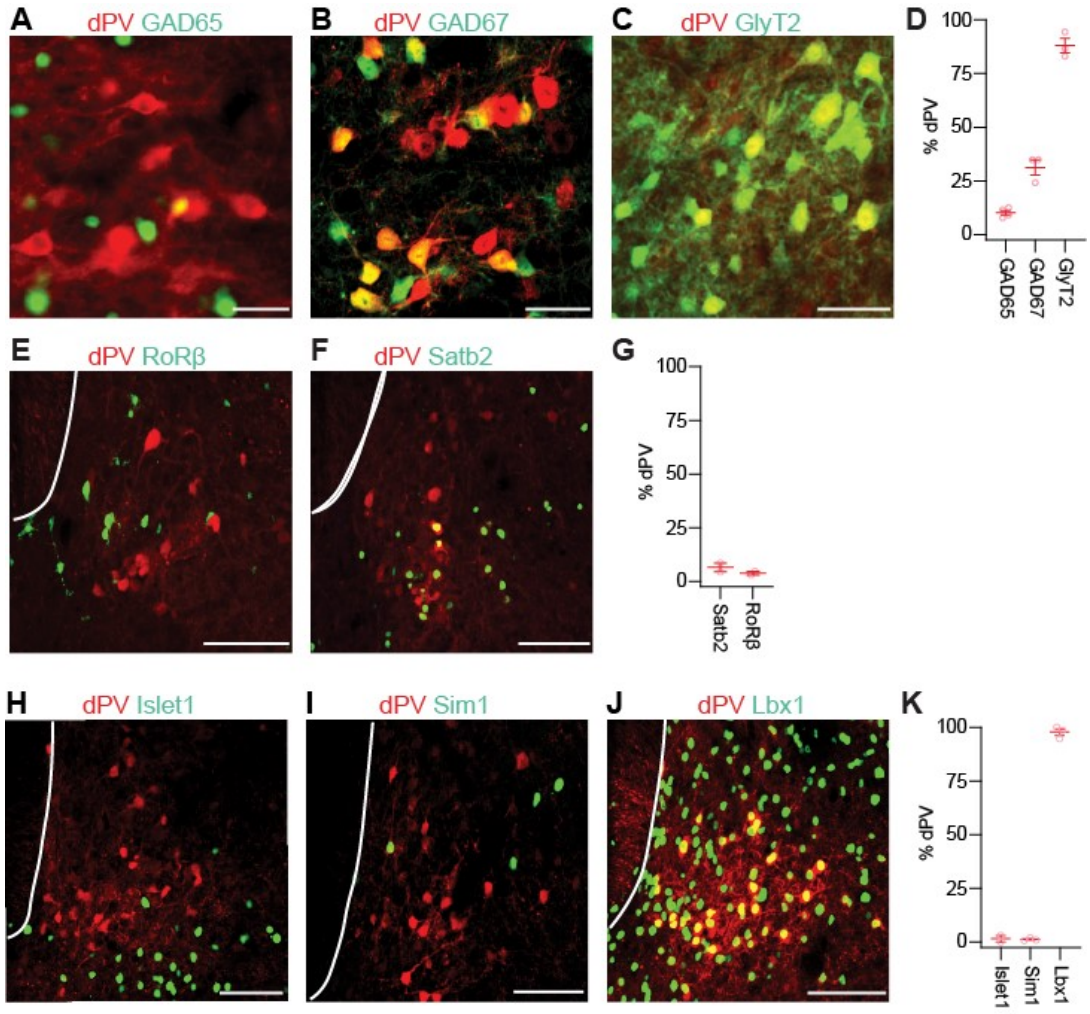

Supplemental Figure S5.1. Lbx1-derived glycinergic dPVs represent an uncharacterized population with excitable intrinsic properties. **A-C**) Representative images demonstrating colocalization of dPVs (red) with interneurons identified by their neurotransmitter expression (green). Colocalization is shown with **A)** GAD65 (*PV*^{FlpO};*R26*$^{FSF\text{-}GFP}$;*GAD2*^{mcherry}), **B)** GAD67 (GAD67^{GFP};PV^{TdTomato}) and **C)** GlyT2 (GlyT2^{GFP}, stained with Guinea-pig-PV). Scale bar: 40 µm. **D)** Quantification of percent dPVs expressing GAD65, GAD67, or GlyT2, shows that dPVs are predominantly glycinergic. Analysis was performed using 12 images from 4 *PV*^{FlpO};*RosaFSF-GFP*;*GAD2*^{mcherry} mice; 7 images from 3 GAD67^{GFP};PV^{TdTomato} mice; and 11 images from 3 GlyT2^{GFP} mice **E-F)** Representative images demonstrating colocalization of dPVs (red) with characterized inhibitory interneurons of the deep dorsal horn (green). Colocalization is shown with **E)** RoRβ (Rorb^{FlpO};*Rosa*$^{LSL\text{-}Tomato}$, stained with Guinea-pig-PV), and **F)** Satb2 (*Satb2*^{Cre};*Tau*$^{LSL\text{-}LacZ}$;PV^{TdTomato}). Scale bar: 100 µm. **G)** Quantification of percent dPVs expressing SatB2 or RoRβ, shows that dPVs are mostly uncharacterized. Analysis was performed using 6 images from 2 Rorb^{FlpO};*R26*$^{LSL\text{-}Tomato}$ mice; and 12 images from 2 *Satb2*^{CreER};*R26*$^{LSL\text{-}TdTomato}$ (stained with Guinea-pig-PV) mice. **H-K)** Representative images demonstrating colocalization of dPVs (red) with genetic lineages identified by transcription factor expression (green). Colocalization is shown with **H)** islet1 (*islet1*^{Cre};*Tau*$^{LSL\text{-}LacZ}$;PV^{TdTomato}), **I**) Sim1 (*sim1*^{Cre};*Tau*$^{LSL\text{-}LacZ}$;PV^{TdTomato}), and **J**) Lbx1 (*Lbx1*^{Cre};*Tau*$^{LSL\text{-}LacZ}$;PV^{TdTomato}). Scale bar: 100 µm. **K**) Quantification of percent dPVs expressing islet1, Sim1, or Lbx1 shows that dPVs originate from the Lbx1 lineage. Analysis was performed using 15 images from 2 *islet1*^{Cre};*Tau*$^{LSL\text{-}LacZ}$;PV^{TdTomato}mice; 9 images from 3 *sim1*^{Cre};*Tau*$^{LSL\text{-}LacZ}$;PV^{TdTomato} mice; and 9 images from 3 *Lbx1*^{Cre};*Tau*$^{LSL\text{-}LacZ}$;PV^{TdTomato} mice.

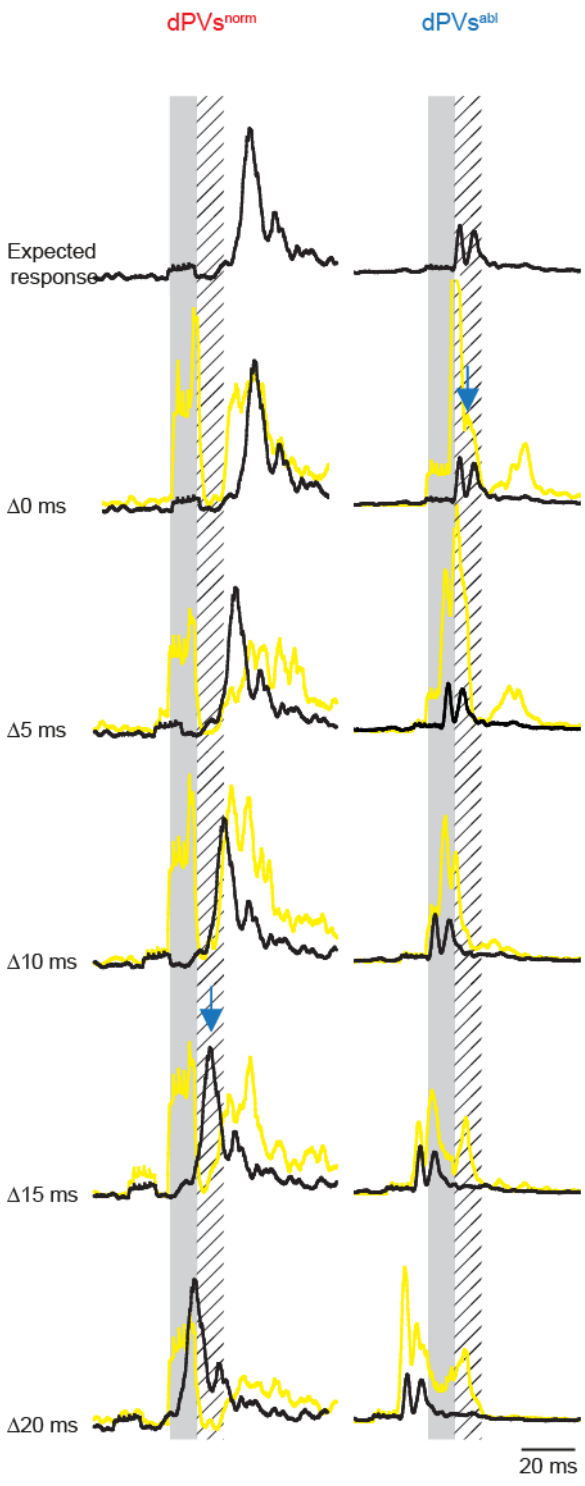
dPVs^norm
dPVs^abl
Expected response
Δ0 ms
Δ5 ms
Δ10 ms
Δ15 ms
Δ20 ms
20 ms

Supplemental Figure S5.2. Use of variable delays in the paired nerves assay. Examples of EMG responses were recorded in the right gastrocnemius (Gs) muscle. Left and right columns show responses in control (PV^{FlpO};$Tau^{LSL\text{-}FSF\text{-}DTR}$), and experimental ($PV^{FlpO}$;$Lbx1^{Cre}$;$Tau^{LSL\text{-}FSF\text{-}DTR}$) animals, respectively. The top row shows the "expected response" in the Gs muscle to stimulation of the left saphenous nerve (black), averaged over 20 trials. Rows 2-5 show responses (yellow) to paired stimulation of the left saphenous and right sural nerves with a delay of 0, 5, 10, 15, and 20 ms respectively. Different delays are applied to account for differences in response latencies within muscles and animals. Responses to the paired stimulation are overlaid on the expected response, aligned to the onset of stimulus artifact or its expected time. For each animal, and each muscle a single delay is chosen for quantification of percent inhibition (Fig. 5.5*B*, Supplemental Fig. S5.2*D*). The delay on which the peak of the expected response occurs 10-20 ms following the stimulation of the second nerve is chosen for analysis of percent inhibition (in this example, 15 ms for dPV^{norm}, and 0 ms for dPV^{abl}).

5.8 REFERENCES

Abraira, VE, Kuehn ED, Chirila AM, Springel MW, Toliver AA, Zimmerman AL, Orefice LL, Boyle KA. Bai L, Song BJ, Bashista KA, O'Neill TG, Zhuo J, Tsan C, Hoynoski J, Rutlin M, Kus L, Niederkofler V, Watanabe M, Dymecki SM, Nelson SB, Heintz N, Hughes DI, Ginty DD. The Cellular and Synaptic Architecture of the Mechanosensory Dorsal Horn. **Cell** 168 (1–2): 295-310.e19, 2017.

Acton D, Ren X, Di Costanzo S, Dalet A, Bourane S, Bertocchi I, Eva C, and Goulding M. Spinal Neuropeptide Y1 Receptor-Expressing Neurons Form an Essential Excitatory Pathway for Mechanical Itch. **Cell Reports** 28 (3): 625-639.e6, 2019. https://doi.org/10.1016/j.celrep.2019.06.033.

Akay T, Acharya HJ, Fouad K, and Pearson KG. Behavioral and Electromyographic Characterization of Mice Lacking EphA4 Receptors. **Journal of Neurophysiology** 96 (2): 642–51, 2006. https://doi.org/10.1152/jn.00174.2006.

Akay T, Tourtellotte WG, Arber S, and Jessell TM. Degradation of Mouse Locomotor Pattern in the Absence of Proprioceptive Sensory Feedback. **Proceedings of the National Academy of Sciences of the United States of America** 111 (47): 16877–82, 2014. https://doi.org/10.1073/pnas.1419045111.

Albisetti GW, Pagani M, Platonova E, Hösli L, Johannssen HC, Fritschy J-M, Wildner H, and Zeilhofer HU. Dorsal Horn Gastrin-Releasing Peptide Expressing Neurons Transmit Spinal Itch But Not Pain Signals. **The Journal of Neuroscience: The Official Journal of the Society for Neuroscience** 39 (12): 2238–50, 2019.

Anderson, J, Lampl I, Reichova I, Carandini M, and Ferster D. Stimulus Dependence of Two-State Fluctuations of Membrane Potential in Cat Visual Cortex. **Nature Neuroscience** 3 (6): 617–21, 2000. https://doi.org/10.1038/75797.

Andersson O, and Grillner S. Peripheral Control of the Cat's Step Cycle. II. Entrainment of the Central Pattern Generators for Locomotion by Sinusoidal Hip Movements during 'Fictive Locomotion.' **Acta Physiologica Scandinavica** 118 (3): 229–39, 1983. https://doi.org/10.1111/j.1748-1716.1983.tb07267.x.

Aristotle's De Motu Animalium. 1986. https://press.princeton.edu/books/paperback/9780691020358/aristotles-de-motu-animalium.

Berg RW, Alaburda A, and Hounsgaard J. Balanced Inhibition and Excitation Drive Spike Activity in Spinal Half-Centers. **Science** (New York, N.Y.) 315 (5810): 390–93, 2007. https://doi.org/10.1126/science.1134960.

Bouyer LJ, and Rossignol S. The Contribution of Cutaneous Inputs to Locomotion in the Intact and the Spinal Cat. **Annals of the New York Academy of Sciences** 860 (November): 508–12, 1998. https://doi.org/10.1111/j.1749-6632.1998.tb09090.x.

Boyle KA, Gradwell MA, Yasaka T, Dickie AC, Polgar E, Ganley RP, Orr DPH, Watanabe M, Abraira VE, Kuehn ED, Zimmerman AL, Ginty DD, Callister RJ, Graham BA, and Hughes DI. Defining a Spinal Microcircuit That Gates Myelinated Afferent Input: Implications for Tactile Allodynia. **Cell Reports** 28 (2): 526-540.e6, 2019. https://doi.org/10.1016/j.celrep.2019.06.040.

Brown AG, and Fyffe RE. Direct Observations on the Contacts Made between Ia Afferent Fibres and Alpha-Motoneurones in the Cat's Lumbosacral Spinal Cord. **The Journal of Physiology** 313: 121–40, 1981.

Brown TG, and Sherrington CS. The Intrinsic Factors in the Act of Progression in the Mammal. **Proceedings of the Royal Society of London**. Series B, Containing Papers of a Biological Character 84 (572): 308–19, 1911. https://doi.org/10.1098/rspb.1911.0077.

Browne TJ, Gradwell MA, Iredale JA, Maden JF, Callister RJ, Hughes DI, Dayas CV, and Graham BA. Transgenic Cross-Referencing of Inhibitory and Excitatory Interneuron Populations to Dissect Neuronal Heterogeneity in the Dorsal Horn. **Frontiers in Molecular Neuroscience** 13: 32, 2020. https://doi.org/10.3389/fnmol.2020.00032.

Brownstone RM, and Chopek JW. Reticulospinal Systems for Tuning Motor Commands. **Frontiers in Neural Circuits** 12: 30, 2018. https://doi.org/10.3389/fncir.2018.00030.

Bui TV, Akay T, Loubani O, Hnasko TS, Jessell TM, and Brownstone RM. Circuits for Grasping: Spinal DI3 Interneurons Mediate Cutaneous Control of Motor Behavior. **Neuron** 78 (1): 191–204, 2013. https://doi.org/10.1016/j.neuron.2013.02.007.

Caggiano V, Leiras R, Goñi-Erro H, Masini D, Bellardita C, Bouvier J, Caldeira V, Fisone G, and Kiehn O. Midbrain Circuits That Set Locomotor Speed and Gait Selection. **Nature** 553 (7689): 455–60, 2018. https://doi.org/10.1038/nature25448.

Capelli P, Pivetta C, Esposito MS, and Arber S. Locomotor Speed Control Circuits in the Caudal Brainstem. **Nature** 551 (7680): 373–77, 2017.

Donelan MJ, McVea DA, and Pearson KG. Force Regulation of Ankle Extensor Muscle Activity in Freely Walking Cats. **Journal of Neurophysiology** 101 (1): 360–71, 2009. https://doi.org/10.1152/jn.90918.2008.

Donelan, MJ, and Pearson KG. Contribution of Force Feedback to Ankle Extensor Activity in Decerebrate Walking Cats. **Journal of Neurophysiology** 92 (4): 2093–2104, 2004. https://doi.org/10.1152/jn.00325.2004.

Donelan, MJ, and Pearson KG. Contribution of Sensory Feedback to Ongoing Ankle Extensor Activity during the Stance Phase of Walking. **Canadian Journal of Physiology and Pharmacology** 82 (8–9): 589–98, 2004. https://doi.org/10.1139/y04-043.

Dubuc R, Brocard F, Antri M, Fénelon K, Gariépy J-F, Smetana R, Ménard A, Le Ray D, Di Prisco GV, Pearlstein E, Sirota MG, Derjean D, St-Pierre M, Zielinski B, Auclair F, Veilleux D. Initiation of Locomotion in Lampreys. **Brain Research Reviews** 57 (1): 172–82, 2008. https://doi.org/10.1016/j.brainresrev.2007.07.016.

Dudek EF, and Sutula TP. Epileptogenesis in the Dentate Gyrus: A Critical Perspective. **Progress in Brain Research** 163: 755–73, 2007. https://doi.org/10.1016/S0079-6123(07)63041-6.

Duysens J, Clarac F, and Cruse H. Load-Regulating Mechanisms in Gait and Posture: Comparative Aspects. **Physiological Reviews** 80 (1): 83–133, 2000. https://doi.org/10.1152/physrev.2000.80.1.83.

Edgley SA, and Jankowska E. Field Potentials Generated by Group II Muscle Afferents in the Middle Lumbar Segments of the Cat Spinal Cord. **The Journal of Physiology** 385 (April): 393–413, 1987. https://doi.org/10.1113/jphysiol.1987.sp016498.

Forssberg H. Stumbling Corrective Reaction: A Phase-Dependent Compensatory Reaction during Locomotion. **Journal of Neurophysiology** 42 (4): 936–53, 1979. https://doi.org/10.1152/jn.1979.42.4.936.

Forssberg H, Grillner S, and Rossignol S. Phase Dependent Reflex Reversal during Walking in Chronic Spinal Cats. **Brain Research** 85 (1): 103–7, 1975. https://doi.org/10.1016/0006-8993(75)91013-6.

Forssberg H, Grillner S, and Rossignol S. Phasic Gain Control of Reflexes from the Dorsum of the Paw during Spinal Locomotion. **Brain Research** 132 (1): 121–39, 1977. https://doi.org/10.1016/0006-8993(77)90710-7.

Garcia-Rill E, Skinner RD, and Fitzgerald JA. Chemical Activation of the Mesencephalic Locomotor Region. **Brain Research** 330 (1): 43–54, 1985. https://doi.org/10.1016/0006-8993(85)90006-x.

Gatto G, Bourane S, Ren X, Di Costanzo S, Fenton PK, Halder P, Seal RP, and Goulding MD. A Functional Topographic Map for Spinal Sensorimotor Reflexes. **Neuron** 109 (1): 91-104.e5, 2021. https://doi.org/10.1016/j.neuron.2020.10.003.

Goldberger ME. Locomotor Recovery after Unilateral Hindlimb Deafferentation in Cats. **Brain Research** 123 (1): 59–74, 1977. https://doi.org/10.1016/0006-8993(77)90643-6.

Goslow Jr GE, Reinking RM, and Stuart DG. The Cat Step Cycle: Hind Limb Joint Angles and Muscle Lengths during Unrestrained Locomotion. **Journal of Morphology** 141 (1): 1–41, 1973. https://doi.org/10.1002/jmor.1051410102.

Grillner S, and Rossignol S. On the Initiation of the Swing Phase of Locomotion in Chronic Spinal Cats. **Brain Research** 146 (2): 269–77, 1978. https://doi.org/10.1016/0006-8993(78)90973-3.

Gross MK, Dottori M, and Goulding M. Lbx1 Specifies Somatosensory Association Interneurons in the Dorsal Spinal Cord. **Neuron** 34 (4): 535–49, 2002. https://doi.org/10.1016/S0896-6273(02)00690-6.

Gruner JA, and Altman J. Swimming in the Rat: Analysis of Locomotor Performance in Comparison to Stepping. **Experimental Brain Research** 40 (4): 374–82, 1980. https://doi.org/10.1007/BF00236146.

Halbertsma JM. The Stride Cycle of the Cat: The Modelling of Locomotion by Computerized Analysis of Automatic Recordings. **Acta Physiologica Scandinavica. Supplementum** 521: 1–75, 1983.

Hampton TG, Stasko MR, Kale A, Amende I, and Costa ACS. Gait Dynamics in Trisomic Mice: Quantitative Neurological Traits of Down Syndrome. **Physiology & Behavior** 82 (2–3): 381–89, 2004. https://doi.org/10.1016/j.physbeh.2004.04.006.

Hilde KL, Levine AJ, Hinckley CA, Hayashi M, Montgomery JM, Gullo M, Driscoll SP, Grosschedl R, Kohwi Y, Kohwi-Shigematsu T, and Pfaff SL. Satb2 Is Required for the Development of a Spinal Exteroceptive Microcircuit That Modulates Limb Position. **Neuron** 91 (4): 763–76, 2016. https://doi.org/10.1016/j.neuron.2016.07.014.

Hongo T, Kitazawa S, Ohki Y, and Xi M. Functional Identification of Last-Order Interneurones of Skin Reflex Pathways in the Cat Forelimb Segments. **Brain Research**, December, 1989.

Hunt, SP, Pini A, and Evan G. Induction of C-Fos-like Protein in Spinal Cord Neurons Following Sensory Stimulation. **Nature** 328 (6131): 632–34, 1987. https://doi.org/10.1038/328632a0.

Duysens J, and Pearson KG. Inhibition of Flexor Burst Generation by Loading Ankle Extensor Muscles in Walking Cats. **Brain Research** 187 (2), 1980. https://doi.org/10.1016/0006-8993(80)90206-1.

Johnson MD, Hyngstrom AS, Manuel M, and Heckman CJ. Push-Pull Control of Motor Output**. The Journal of Neuroscience: The Official Journal of the Society for Neuroscience** 32 (13): 4592–99, 2012. https://doi.org/10.1523/JNEUROSCI.4709-11.2012.

Hoseok K, Ährlund-Richter S, Wang X, Deisseroth K, and Carlén M. Prefrontal Parvalbumin Neurons in Control of Attention. **Cell** 164 (1–2): 208–18, 2016. https://doi.org/10.1016/j.cell.2015.11.038.

Koch SC, Del Barrio MG, Dalet A, Gatto G, Günther T, Zhang J, Seidler B, Saur D, Schüle R, and Goulding M. RORβ Spinal Interneurons Gate Sensory Transmission during Locomotion to Secure a Fluid Walking Gait. **Neuron** 96 (6): 1419-1431.e5, 2017. https://doi.org/10.1016/j.neuron.2017.11.011.

Laflamme OD, and Akay T. Excitatory and Inhibitory Crossed Reflex Pathways in Mice. **Journal of Neurophysiology** 120 (6): 2897–2907, 2018.

Laflamme OD, Ibrahim M, and Akay T. Crossed Reflex Responses to Flexor Nerve Stimulation in Mice. **Journal of Neurophysiology** 127 (2): 493–503, 2022. https://doi.org/10.1152/jn.00385.2021.

Lajoie Y, Teasdale N, Cole JD, Burnett M, Bard C, Fleury M, Forget R, Paillard J, and Lamarre Y. Gait of a Deafferented Subject without Large Myelinated Sensory Fibers below the Neck. **Neurology** 47 (1): 109–15, 1996. https://doi.org/10.1212/wnl.47.1.109.

Lehnert BP, Santiago C, Huey EL, Emanuel AJ, Renauld S, Africawala N, Alkislar I, Zheng Y, Bai L, Koutsioumpa C, Hong JT, Magee AR, Harvey CD, and Ginty DD. Mechanoreceptor Synapses in the Brainstem Shape the Central Representation of Touch." **Cell** 184 (22): 5608-5621.e18, 2021. https://doi.org/10.1016/j.cell.2021.09.023.

Levine AJ, Hinckley CA, Hilde KL, Driscoll SP, Poon TH, Montgomery JM, and Pfaff SL. Identification of a Cellular Node for Motor Control Pathways. **Nature Neuroscience** 17 (4): 586–93, 2014. https://doi.org/10.1038/nn.3675.

Li D, Li Y, Tian Y, Xu Z, and Guo Y. Direct Intrathecal Injection of Recombinant Adeno-Associated Viruses in Adult Mice. **JoVE** (Journal of Visualized Experiments), no. 144 (February): e58565, 2019. https://doi.org/10.3791/58565.

Li Z, Tan AY, Schreiner CE, and Merzenich MM. Topography and Synaptic Shaping of Direction Selectivity in Primary Auditory Cortex. **Nature** 424 (6945), 2003. https://doi.org/10.1038/nature01796.

Lu DC, Niu T, and Alaynick WA. Molecular and Cellular Development of Spinal Cord Locomotor Circuitry. **Frontiers in Molecular Neuroscience** 8 (June): 25, 2015. https://doi.org/10.3389/fnmol.2015.00025.

Luo W, Enomoto H, Rice FL, Milbrandt J, and Ginty DD. Molecular Identification of Rapidly Adapting Mechanoreceptors and Their Developmental Dependence on Ret Signaling. **Neuron** 64 (6): 841–562009. https://doi.org/10.1016/j.neuron.2009.11.003.

Martinez LM, and Alonso J-M. Complex Receptive Fields in Primary Visual Cortex. **The Neuroscientist: A Review Journal Bringing Neurobiology, Neurology and Psychiatry** 9 (5): 317–312003. https://doi.org/10.1177/1073858403252732.

Mathis A, Mamidanna P, Cury KM, Abe T, Murthy VN, Mathis MW, and Bethge M. DeepLabCut: Markerless Pose Estimation of User-Defined Body Parts with Deep Learning. **Nature Neuroscience** 21 (9): 1281–89, 2018. https://doi.org/10.1038/s41593-018-0209-y.

McClellan AD., and Grillner S. Activation of 'fictive Swimming' by Electrical Microstimulation of Brainstem Locomotor Regions in an in Vitro Preparation of the Lamprey Central Nervous System. **Brain Research** 300 (2): 357–611984. https://doi.org/10.1016/0006-8993(84)90846-1.

Miranda CO, Hegedüs K, Wildner H, Zeilhofer HU, and Antal M. Morphological and Neurochemical Characterization of Glycinergic Neurons in Laminae I-IV of the Mouse Spinal Dorsal Horn. **The Journal of Comparative Neurology** 530 (3): 607–26, 2022. https://doi.org/10.1002/cne.25232.

Morgan JI, and Curran T. Role of Ion Flux in the Control of C-Fos Expression. **Nature** 322 (6079): 552–551986. https://doi.org/10.1038/322552a0.

Mori S. Integration of Posture and Locomotion in Acute Decerebrate Cats and in Awake, Freely Moving Cats. **Progress in Neurobiology** 28 (2): 161–95, 1987. https://doi.org/10.1016/0301-0082(87)90010-4.

Moschovakis AK, Solodkin M, and. Burke RE. Anatomical and Physiological Study of Interneurons in an Oligosynaptic Cutaneous Reflex Pathway in the Cat Hindlimb. **Brain Research** 586 (2): 311–18, 1992. https://doi.org/10.1016/0006-8993(92)91641-q.

Muir GD, and Steeves JD. Phasic Cutaneous Input Facilitates Locomotor Recovery after Incomplete Spinal Injury in the Chick. **Journal of Neurophysiology** 74 (1): 358–68, 1995. https://doi.org/10.1152/jn.1995.74.1.358.

Nahar L, Delacroix BM, and Nam HW. The Role of Parvalbumin Interneurons in Neurotransmitter Balance and Neurological Disease. **Frontiers in Psychiatry** 12, 2021. https://www.frontiersin.org/article/10.3389/fpsyt.2021.679960.

Orlovskiĭ GN, and Fel'dman AG. [Classification of the neurons of the lumbo-sacral region of the spinal cord in accordance with their discharge patterns during provoked locomotion]. **Neirofiziologiia** = Neurophysiology 4 (4): 410–17, 1972.

Pearson KG, Acharya H, and Fouad K. A New Electrode Configuration for Recording Electromyographic Activity in Behaving Mice. **Journal of Neuroscience Methods** 148 (1): 36–42, 2005. https://doi.org/10.1016/j.jneumeth.2005.04.006.

Petersen PC, Vestergaard M, Jensen KHR, and Berg RW. Premotor Spinal Network with Balanced Excitation and Inhibition during Motor Patterns Has High Resilience to Structural Division. **The Journal of Neuroscience: The Official Journal of the Society for Neuroscience** 34 (8): 2774–84, 2014. https://doi.org/10.1523/JNEUROSCI.3349-13.2014.

Poo C, and Isaacson JS. Odor Representations in Olfactory Cortex: 'Sparse' Coding, Global Inhibition, and Oscillations. **Neuron** 62 (6): 850–61, 2009. https://doi.org/10.1016/j.neuron.2009.05.022.

Prochazka A, and Yakovenko S. The Neuromechanical Tuning Hypothesis. **Progress in Brain Research** 165: 255–65, 2007. https://doi.org/10.1016/S0079-6123(06)65016-4.

Ringach DL. Mapping Receptive Fields in Primary Visual Cortex. **The Journal of Physiology** 558 (Pt 3): 717–28, 2004. https://doi.org/10.1113/jphysiol.2004.065771.

Rutlin M, Ho C-Y, Abraira VE, Cassidy C, Bai L, Woodbury JC, and Ginty DD. The Cellular and Molecular Basis of Direction Selectivity of Aδ-LTMRs. **Cell** 159 (7): 1640–51, 2014. https://doi.org/10.1016/j.cell.2014.11.038.

Schillings AM, Van Wezel BM, and Duysens J. Mechanically Induced Stumbling during Human Treadmill Walking. **Journal of Neuroscience Methods** 67 (1): 11–17, 1996. https://doi.org/10.1016/0165-0270(95)00149-2.

Sherrington CS. The Integrative Action of the Nervous System, 1906.

Sherrington CS. Remarks on the Reflex Mechanism of the Step **Brain** 33: 1–25, 1910.

Sieber, MA, Storm R, Martinez-de-la-Torre M, Müller T, Wende H, Reuter K, Vasyutina E, and Birchmeier C. Lbx1 Acts as a Selector Gene in the Fate Determination of Somatosensory and Viscerosensory Relay Neurons in the Hindbrain. **Journal of Neuroscience** 27 (18): 4902–9, 2007. https://doi.org/10.1523/JNEUROSCI.0717-07.2007.

Takakusaki K, Habaguchi T, Ohtinata-Sugimoto J, Saitoh K, and Sakamoto T. Basal Ganglia Efferents to the Brainstem Centers Controlling Postural Muscle Tone and Locomotion: A New Concept for Understanding Motor Disorders in Basal Ganglia Dysfunction. **Neuroscience** 119 (1): 293–308, 2003. https://doi.org/10.1016/s0306-4522(03)00095-2.

Tamamaki N, Yanagawa Y, Tomioka R, Miyazaki J-I, Obata K, and Kaneko T. Green Fluorescent Protein Expression and Colocalization with Calretinin, Parvalbumin, and Somatostatin in the GAD67-GFP Knock-in Mouse. **The Journal of Comparative Neurology** 467 (1): 60–79, 2003. https://doi.org/10.1002/cne.10905.

Tripodi M, Stepien AE, and Arber S. Motor Antagonism Exposed by Spatial Segregation and Timing of Neurogenesis. **Nature** 479 (7371): 61–66, 2011. https://doi.org/10.1038/nature10538.

Tuthill JC, and Azim E. Proprioception. **Current Biology** 28 (5): R194–203, 2018. https://doi.org/10.1016/j.cub.2018.01.064.

Wehr M, and Zador AM. Balanced Inhibition Underlies Tuning and Sharpens Spike Timing in Auditory Cortex. **Nature** 426 (6965): 442–46, 2003. https://doi.org/10.1038/nature02116.

Wetzel MC, Atwater AE, Wait JV, and Stuart DG. Kinematics of Locomotion by Cats with a Single Hindlimb Deafferented. **Journal of Neurophysiology** 39 (4): 667–78, 1976. https://doi.org/10.1152/jn.1976.39.4.667.

Wilent BW, and Contreras D. Dynamics of Excitation and Inhibition Underlying Stimulus Selectivity in Rat Somatosensory Cortex. **Nature Neuroscience** 8 (10): 1364–70, 2005. https://doi.org/10.1038/nn1545.

Wu H, Petitpré C, Fontanet P, Sharma A, Bellardita C, Quadros RM, Jannig PR, Wang Y, Heimel AJ, Cheung KKY, Wanderoy S, Xuan Y, Meletis K, Ruas J, Gurumurthy CB, Kiehn O, Hadjab S & Lallemend F. Distinct Subtypes of Proprioceptive Dorsal Root Ganglion Neurons Regulate Adaptive Proprioception in Mice. **Nature Communications** 12 (1): 1026, 2021. https://doi.org/10.1038/s41467-021-21173-9.

Zheng Y, Liu P, Bai L, Trimmer JS, Bean BP, and Ginty DD. Deep Sequencing of Somatosensory Neurons Reveals Molecular Determinants of Intrinsic Physiological Properties. **Neuron** 103 (4): 598-616.e7, 2019.

Chapter 6: Conclusions

6.1 SUMMARY OF RESULTS

This thesis aimed to provide insights into the spinal circuitry that controls crossed reflexes in awake mice in vivo at rest and during locomotion. In general, crossed reflex responses were elicited through activation of different afferent types, achieved by electrical stimulation of different peripheral nerves (chapters 2 and 3). We combined these crossed reflex experiments with the well-established genetic mouse models in which defined classes of interneurons were either silenced or killed by genetic engineering, to investigate the spinal circuitry involved in crossed reflexes (chapters 4 and 5).

In chapter 2, I investigated crossed reflex responses elicited by the stimulation of the contralateral tibial and sural nerves. My results show that the stimulation of the tibial and sural nerves induced crossed reflex responses in all recorded muscles, indicating an excitatory crossed reflex action. I also uncovered the presence of a short-latency crossed inhibitory pathway in all muscles using a conditioning paired stimulation paradigm. Finally, I demonstrated that the crossed inhibitory response was downregulated selectively in the knee extensor (VL) and ankle flexor (TA) when the muscle was active before the stimulation during locomotion. This investigation provided the first detailed description of a muscle activity pattern during crossed reflex responses in adult awake mice at rest or in locomotion.

In chapter 3, I aimed to understand the impact that different sensory afferent inputs could have on the modulation of crossed reflexes. To do this, I recorded crossed reflex responses in muscles elicited by the stimulation of the common peroneal nerve, which carries proprioceptive afferent fibers mainly from flexor muscles and cutaneous afferent fibers innervating mostly the anterior aspect of the leg. The muscle activation pattern was then compared with those elicited by the stimulation of the tibial nerve, mainly carrying proprioceptive afferent fibers from extensor muscles and cutaneous afferent fibers innervating mostly the posterior aspect of the leg. My results suggested that both nerves offered similar contralateral responses, with mainly two qualitative differences. First, the

common peroneal nerve elicited a long-latency crossed motor response that was absent when the tibial or sural nerve was stimulated. Second, when the animal was locomoting and the common peroneal nerve was stimulated, the modulation of the inhibitory crossed reflex was also observed in the ankle extensor (Gs), in addition to the VL and TA. This project extended the observations presented in Chapter 2 by showing that the differences in muscle activation patterns elicited by nerves carrying proprioceptive afferent fibers from antagonist muscles or different skin regions are present but subtle.

In chapter 4, I investigated the involvement of the V0 and V3 commissural interneurons in the transmission of sensory input to the contralateral side. To do this, I used genetically engineered mice with manipulated (killed or silenced) V0 and V3 commissural interneurons, respectively. My data suggests that V0 interneurons are not involved in crossed reflexes at rest. In mice without V0 CINs, both excitatory and inhibitory pathways are present and modulated during locomotion, similar to what was found in wild-type mice following tibial nerve stimulation. Interestingly, following sural nerve stimulation during locomotion, even though the inhibitory crossed reflex is still present, its modulation is absent. On the other hand, crossed inhibitory responses were mostly absent in V3 silenced mice. This research suggests that while the V3 commissural interneurons are part of the crossed reflex pathways, the V0 commissural interneurons are not.

Finally, in chapter 5, in collaboration with the laboratory of Dr. Victoria Abraira at Rutgers University, I investigated the role of a newly identified interneuron population located in the deep dorsal horn that expresses the calcium-binding protein parvalbumin (dPVs). To test whether dPVs are involved in crossed inhibitory pathways, I used the conditioning-test paradigm on a mouse line in which the dPVs were genetically silenced (dPV^{abl}). In dPV^{abl} mice, the occurrence of crossed inhibitory reflex was mostly similar to control except for the TA after stimulation of the sural nerve, suggesting that dPVs interneurons are mostly not involved in crossed inhibitory reflex pathways. However, complementary sets of experiments provided evidence of their involvement in local inhibitory reflex pathways.

6.2 EXCITATORY CROSSED REFLEX

This thesis aimed to uncover the spinal circuitry underlying crossed reflex. My results show that crossed reflex in mice involves a short-latency inhibitory pathway and an excitatory pathway. In the ventral spinal cord, only three cardinal populations of interneurons have been discovered to project their axons to the contralateral side, namely the dI6, V0, and V3 populations (Lanuza et al. 2004; Zhang et al. 2008; Andersson et al. 2012). From these, only the V0 and V3 interneurons have been shown to be excitatory. As dI6 interneurons constitute a mostly inhibitory population, I hypothesize that either V0 or V3 interneurons would be involved in the excitatory pathways. However, experiments carried out on mice lines with selective removal of V0 or V3 interneurons did not cause significant changes in the overall muscle activity, suggesting that V0 and V3 commissural interneurons have a minor role, if any, in the excitatory crossed reflex responses. The lack of clear results could have three explanations:

First, our technique limitations prevented us from quantifying the changes in the excitatory pathway. The electrode used for EMG recording consists of a bipolar electrode that is inserted as a pair into the small muscle of the mouse (Pearson et al. 2005). The electrode is custom-made before each experiment and consists of two components: a nerve stimulation cuff and the EMG recording electrode. The quality of the recorded EMG is affected by small, unavoidable differences in the fabrication of the electrode and surgical implantation as well as the quality of the post-surgical recovery of the animal. Therefore, a comparison of the raw muscle amplitude between animals to quantify the excitatory pathway should be avoided as too many external factors can influence it. Considering this, it is still interesting to note that the overall EMG activity measured using the area under the curve of the rectified response in $V3^{off}$ mice was in general smaller compared to WT or $V0^{kill}$ mice. However, comparing the ratio of motor recruitment activity between 1.2xT and 5xT stimulation strength for each animal demonstrated that no difference was found between WT, $V0^{kill}$, and $V3^{off}$ mice. This could suggest that the overall excitatory pathway is reduced in $V3^{off}$ mice without affecting motor recruitment activity. Further experiments will be needed to determine the role of V3 interneurons in the excitatory pathway.

Nevertheless, the limitations of the technique severely impaired our ability to quantify the excitatory pathway.

Another possibility might come from the compensatory modulation of the spinal circuitry following the suppression of either the V0 or V3 subpopulations. As seen with V1 and V2b interneurons, flexor-extensor muscle alternation is preserved when only one neuronal population is removed (Wang et al. 2008; Zhang et al. 2014; Britz et al. 2015). Removal of both interneuronal populations is necessary to disturb the flexor and extensor alternation (Zhang et al. 2014). Therefore, V0 and V3 interneurons may be modulated in a similar fashion when it comes to the transmission of sensory afferents. The removal of either interneuronal population does not significantly alter the excitation pathway in crossed reflex as the remaining population compensates for the missing one.

Finally, it is also possible that the excitatory pathway does not go through V0 or V3 interneurons. In this case, the excitatory pathway would most likely involve other contralaterally projecting excitatory interneurons. As the only other ventral commissural interneurons (dI6) are mainly inhibitory (Andersson et al. 2012), it is unlikely that ventral commissural interneurons would be involved in the excitatory pathway. In the dorsal horn, excitatory contralateral projecting interneurons could include dI1 and dI2 interneurons, which are involved in proprioception and smooth movement (Wilson et al. 2008; Mieseagaes et al. 2009; Avraham et al. 2009; 2010; Sakai et al. 2012; Goetz et al. 2015; Yuengert et al. 2015). More experiments would be needed before concluding on the role of these interneurons in crossed reflexes.

6.3 INHIBITORY CROSSED REFLEX

Several observations provided evidence for a crossed inhibitory pathway in wild-type mice. First, stimulation of the tibial nerve initiated muscle activity at a longer latency with simultaneous activation of all muscles at ~20 ms after stimulation onset when current strength was increased, suggesting the existence of an inhibitory crossed reflex pathway opening at higher current strength. This was later confirmed using a conditioning-paired stimulation paradigm in which the local reflex was suppressed by the crossed reflex. This crossed inhibitory pathway was also found to be disrupted in $V3^{off}$ mice but remained intact

in $V0^{kill}$ mice. These results suggest that while the V3 interneurons are a necessary part of the inhibitory crossed reflex pathway, the V0 interneurons are not.

During locomotion, V0 commissural interneurons are involved in the alternating stepping between both legs (Lanuza et al. 2004; Talpalar et al. 2013). In contrast, V3 commissural interneurons' role during locomotion remains more elusive. V3 interneurons are implicated in the balance and rhythmicity between both legs but are not necessary for the left-right alternation (Zhang et al. 2008). Furthermore, these mice displayed higher step-to-step variability in the left-right leg coordination (Zhang et al. 2022). Overall, these results suggest that V3 interneurons are important for left-right coordination by securing a balanced movement between distinct limbs. Similarly, sensory afferents' role during locomotion has long been associated with the modulation of the CPG to provide a robust locomotor pattern (Rossignol et al. 2006; Akay et al. 2014; Santuz et al. 2019; Mayer and Akay, 2021). Therefore, I propose that the role of V0 interneurons during locomotion is mainly to carry the information from the CPG that controls left-right alternation. In contrast, the V3 interneurons' main role is to carry sensory afferent information to coordinate smooth movement across different limbs (Fig. 4.7).

6.4 COMPARISON TO PREVIOUS CROSSED REFLEX MODEL

V0 and V3 interneurons form two functionally distinct populations regarding their role in crossed reflexes. These results are similar to those obtained in cats on the role of various commissural interneurons. For instance, in cat experiments, commissural interneurons involved in proprioceptive crossed reflexes that target contralateral motoneurons fall into two main subpopulations, those with monosynaptic input from reticulospinal neurons, vestibulospinal neurons, and group I afferents, and those with monosynaptic input from group II muscle afferents (Jankowska et al. 2005a, 2005b). Commissural interneurons monosynaptically excited by reticulospinal neurons are also rhythmically activated when stimulation is applied to the MLR (Matsuyama et al. 2004a; 2004b), suggesting that they are also incorporated into the locomotor network. On the other hand, the population with monosynaptic input from group II muscle afferents is important to determine the different patterns in crossed reflex (Jankowska et al. 2005b) and is

modulated by supraspinal input (Arya et al. 1991). Furthermore, their axonal projection indicates that they seem to target the same population of premotor interneurons that mediate the actions of ipsilateral group Ia, Ib, and II muscle afferents on motoneurons (Jankowska, 2010).

The effect of supraspinal input on V0 and V3 commissural interneurons remains unknown. It is therefore challenging to associate V0 and V3 populations to CINs discovered in cats. The results from this thesis suggest that V3 interneurons present more similarities with the commissural interneuron population that receives input from group II afferents. Although the impact of supraspinal input on V3 interneurons remains unknown, it was recently demonstrated that the activity of V3 interneurons is modulated following spinal cord injury (Lin et al. 2019). Spinal cord injury often leads to uncontrolled spastic activity in muscles innervated by motoneurons below the injury, including prolonged muscle spasms triggered by brief sensory inputs (Bennett et al. 1999; Heckman et al. 2005; Kulhn and Macht, 1949; Li et al. 2007; Nielsen et al. 2007; Steldt and Schmit, 2004). Optogenetic activation or inhibition of V3 interneurons reduces or increases spasms after spinal cord injury, respectively. Furthermore, stimulation of V3 neurons by themselves can trigger coordinated spasm-like motor activity very similar to actual sensory-evoked spasms. (Lin et al. 2019). Overall, these results suggest that the V3 interneuron's action might be modulated by supraspinal input. Considering the results from this thesis on the role of V3 interneurons in crossed reflex and their potential modulation from supraspinal inputs, V3 interneurons present several similarities associated with the commissural interneurons receiving monosynaptic input from group II muscle afferents discovered in the cat. However, further investigation is required to test this hypothesis as the two CINs groups described in cats were based on proprioceptive input and the result from this thesis emphasizes the role of cutaneous afferents in crossed reflex.

6.5 LONG-LATENCY MOTOR RESPONSES

In this thesis, I investigated the role of various sensory afferent inputs in the generation of crossed reflexes. As mentioned previously in chapters 2 and 3, the origin of the sensory information seems to have little impact on the resulting contralateral motor

response. This was surprising, considering that the tibial and common peroneal nerves innervate opposite proprioceptive and cutaneous areas of the leg (Bernard et al. 2007). Nevertheless, one major qualitative difference between these two stimulations was the presence of a long-latency motor response that was present in the common peroneal nerve stimulation but not following tibial nerve stimulation. Two hypotheses could explain the origin of this motor response.

First, these long-latency motor responses could involve main ascending pathways that carry proprioceptive and low-threshold cutaneous information, such as the dorsal column lemniscus pathways and the dorsal spinocerebellar pathway (Hantman and Jessell, 2010; Tuthill and Azim, 2018). To test this hypothesis, I did preliminary experiments in which I lesioned the dorsal column lemniscus pathway and stimulated the common peroneal nerve to elicit a crossed motor response. My results showed that long-latency responses persisted after the lesion of the dorsal column lemniscus pathway (Fig. 6.1). However, it is important to note that the extent of the lesion was not measured. Therefore, it is possible that part of the pathway remained intact in these mice. More experiments are needed before any conclusion can be said about the involvement of supraspinal structures in the long-lasting motor response.

Another hypothesis is that these long-lasting motor responses come from activity within the CPG. Previously, a proposed flexor-driven concept (also called the swing generator model) by Pearson and Duysens (1976) and Duysens (2006; 2013) emphasized the role of flexor muscles in the rhythm generation of the CPG. In this model, only the flexor half-center is intrinsically rhythmic, while the extensor half-center shows sustained activity if uncoupled and only exhibits rhythmic bursting through rhythmic inhibition from the flexor half-center. The common peroneal nerve innervates primarily the flexor muscles of the ankle joint, specifically the tibialis anterior and extensor digitorum longus, as well as cutaneous afferents originating primarily from the anterior aspect of the leg (Bernard et al. 2007). Therefore, in our experiments, stimulation of different sensory afferents could have a different output on an asymmetric CPG. Flexor-related sensory afferents would have a greater impact on the flexor CPG half-center, creating a long-latency response compared to the extensor sensory afferent on the extensor CPG half-

center. Furthermore, as we proposed previously, V0 interneurons might be the main interneurons involved in the transmission of locomotor information in the spinal cord. Therefore, to test if the long-lasting motor responses originate from the CPG circuitry, stimulating the common peroneal nerve in $V0^{kill}$ mice could represent an interesting approach to answering this question.

6.6 LOCAL INHIBITORY INTERNEURONS

My results in $V3^{off}$ mice suggest that V3 interneurons are involved in the crossed inhibitory pathway. However, V3 interneurons represent a glutamatergic population (Zhang et al. 2008), suggesting that V3 interneurons connect to at least one inhibitory interneuron on the contralateral side. In chapter 5, we investigated which neurons could be involved in the crossed inhibitory pathway. One hypothesis coming from cat and human experiments was the involvement of Ia inhibitory interneuron as a potential candidate (Harrison and Zytnicki, 1984; Jankowska et al. 2009; Stubbs and Mrachacz-Kersting, 2009; Mrachacz-Kersting et al. 2017). Ia inhibitory interneurons are involved in the reciprocal inhibition of the flexor and extensor MNs. Primarily identified by their physiological features (Feldman and Orlovsky, 1975), a subpopulation of the Ia inhibitory interneuron was later found to be included in the V1 interneuron population (Alvarez et al. 2005). V2b has also been shown to be involved in the flexor-extensor reciprocal inhibition (Zhang et al. 2014), suggesting that either V1 or V2b interneuron could be good candidates to mediate the crossed inhibitory pathway. Experiments using mice lacking V1 or V2b interneurons would provide invaluable knowledge to understand the local inhibitory circuitry mediating crossed inhibitory pathways.

Another possibility is the involvement of dorsal interneurons in the inhibitory crossed reflex pathway. The dorsal horn is home to several interneuronal populations that are involved in the somatosensory system and corrective reflexes (Gatto et al. 2021). For instance, dI1-dI3 interneurons and some dI4/dIL_A interneurons are involved in the sensory transmission or are part of motor pathways involved in the smooth movement (Wilson et al. 2008; Mieseagaes et al. 2009; Avraham et al. 2009; 2010; Sakai et al. 2012; Bui et al. 2013; Goetz et al. 2015; Yuengert et al. 2015). dPVs interneurons represent a newly

investigated population of glycinergic interneurons discovered in the deep dorsal horn of the spinal cord that functionally integrate touch and proprioceptive information. Lumbar dPVs interneurons are directly innervated by proprioceptors and cutaneous afferents from the hindpaw, and ablation of dPVs interneurons alters the step transition. In vitro electrophysiological recordings demonstrated that dPVs interneurons form a diffuse inhibitory network in the ventral horn where they contact motor and pre-motor neurons. Overall, these data suggest that dPVs interneurons act as a node for sensorimotor integration and support their role in the modulation of motor output. Hence, I hypothesize that dPVs interneurons act as local inhibitory interneurons, receiving input from the contralateral side and mediating crossed inhibitory pathways.

My results show that dPVs interneurons were involved in the local inhibitory pathway, but their involvement in the crossed inhibitory pathway was more difficult to assess. My findings suggest that dPVs are involved in the crossed inhibitory pathway selectively, inhibiting TA muscle activity only when the sural nerve is stimulated. However, it is important to consider that the crossed inhibitory pathway following sural nerve stimulation was difficult to characterize in control mice (dPV^{norm}) and experimental mice (dPV^{ablat}). Indeed, in some mice, stimulation at 5-time threshold induced jerking movements, sometimes accompanied by squeaking, suggesting the involvement of the pain pathway. In some rare instances, squeaking was heard as low as 3-4 times the threshold (unpublished observation). These observations were made in both control and experimental mice, suggesting that it was not associated with the lack of dPVs interneurons. Any wild-type or experimental mice obtained from our colony at Dalhousie University never displayed such behaviour. The lack of difference that we observed between the dPV^{norm} and dPV^{ablat} mice comes from the fact that the crossed inhibitory pathway was not always present in control mice after stimulation of the sural nerve. As the saphenous nerve was never studied in mice from Dalhousie University, it is not possible to comment on the involvement of crossed inhibitory pathways following saphenous nerve stimulation.

For now, the main local inhibitory interneuron population involved in crossed inhibitory pathways remains to be discovered. Further experiments with dPVs interneurons could provide invaluable insights in combination with other techniques such as in vitro

recording to clearly assess their role in crossed reflex. Furthermore, the role of other important interneurons such as the V1 and V2b interneurons could provide a lot of information about the sensory circuits proposed in this thesis.

6.7 LIMITATIONS

In this thesis, the main approach used to investigate crossed reflexes was to stimulate sensory afferents in awake mice. This approach offers a great opportunity to study crossed reflexes in unrestrained, non-anesthetized mice. However, it also presents some important limitations. Inhibitory crossed reflex actions cannot be directly measured using EMG recording. Indeed, EMG recording can only indicate motor neuron activation through the activity of the muscles but not their inhibition. Therefore, in this thesis, all the evidence of an inhibitory pathway comes from indirect methods. For instance, I used a conditioning-paired stimulation paradigm to demonstrate the presence of an inhibitory pathway. In this paradigm, I used a custom-made electrode in which I could independently stimulate a crossed reflex coming from one leg and a local cutaneous reflex in the same muscle. This allows us to determine the expected motor response following each stimulation independently from the other. It is also possible to stimulate both reflex pathways simultaneously and with various delays between them. If the response evoked by the crossed reflex includes an inhibitory component, the summation of the two responses (local + crossed) will reveal a “dip” when compared to the single nerve response. On the other hand, if no inhibitory pathway exists, both curves will become two distinct motor responses as they separate without revealing a “dip” (Fig. 6.2). Overall, paired stimulation of both legs at different delays provides evidence of an inhibition period if there is a consistent suppression of the motor responses from one leg following stimulation of the other leg.

Another clue to the involvement of an inhibition phase could be seen during locomotion. Indeed, when the muscle was active as a result of the animal walking on the treadmill, a silent phase following the crossed reflex stimulation could be observed. In this situation, we used normal mouse behaviour to activate the muscle prior to the stimulation. Our results showed that the inhibition was modulated differently depending on the muscle

but was still present in the contralateral iliopsoas, semitendinosus, and gastrocnemius muscles. Although these two methods strongly suggest the presence of an inhibitory pathway in mice, we never recorded direct evidence of it. To do this, we must use other techniques in which we can directly measure inhibitory post-synaptic potential (IPSP) in motoneurons. One such technique could involve the use of intracellular motoneuron recording in which we could stimulate the contralateral sensory afferent.

Another limitation of our study is the great variability present in every group. Multiple factors could explain the discrepancies that increase variability inside one group. First, as the animals are awake for the recording, they are free to explore their environment. This can result in stimulation being applied when the animal was doing various behaviours. To mitigate this problem, mice were placed on the treadmill for a few minutes before the experiments began. This was for two reasons. First, to make sure that all the anesthesia administered to attach the mouse to the apparatus was fully removed from the body, and second, to let the animal explore its surroundings. Experiments were performed only when the mice became more comfortable with their new environment. Typically, once the exploration phase was completed, mice mostly remained calm in one corner of the treadmill while the experiments were underway. Although precautionary measure was taken, we can't exclude the fact that the mice occasionally performed certain movements, such as scratching, reaching, short bouts of walking, or grooming. When the animals were doing such activities, good care was taken to pause the experiments so that these movements would not affect the reflex responses.

As presented above, the main technique used in this thesis presents some methodological restrictions that must be considered. However, the fact that it was possible to record motor activity from intact and awake mice represents a great opportunity to study crossed reflexes in an almost normal physiological approach. Furthermore, this technique allows for the recording of multiple muscles during a variety of behaviours with little interference with leg movement. Therefore, in vivo EMG recording represents a great avenue to describe reflex action in mice.

6.8 CONCLUDING REMARKS

More than a century of research on cats and humans has described important aspects of crossed reflexes, but the spinal network that controls the crossed reflexes remained obscure (Sherrington, 1910; Duysens and Loeb, 1980; Aggelopoulos and Edgley, 1995; Gervasio et al. 2015; Mrachacz-Kersting et al. 2017). More recent research on mice has described commissural pathways that control the left and right hind leg coordination during walking (Pierani et al. 2001; Lanuza et al. 2004; Zhang et al. 2008; Borowska et al. 2013; Talpalar et al. 2013). However, the role of these commissural pathways in crossed reflexes was not known. The primary aim of this project was to gain insights into the spinal neuronal network that underlies crossed reflexes in mice and to describe how the previously described commissural interneurons are important for locomotion related to crossed reflexes. Subsequently, I aimed to provide the first framework to draw a spinal circuitry for the transmission of sensory afferent information in the spinal cord.

My data suggest that interneurons involved in left-right alternation (V0 interneurons) are not important for the transmission of sensory afferents. Instead, commissural interneurons involved in maintaining balanced left-right activity (V3 interneurons) are the main conductors of sensory information. As such, I suggest that motor and sensory information are transmitted using different interneuron populations. V0 interneurons are involved in the transmission of motor information leading to left-right alternation (Lanuza et al. 2004; Talpalar et al. 2013). Meanwhile, V3 interneurons are important for modulating motor information by transmitting sensory information to the contralateral side.

Although much remains to be discovered about the somatosensory circuit and how it can modulate motor activity, the data presented in this thesis represents the first step in allowing the convergence of century-long-accumulated knowledge with the more recent insights gained by using mouse genetics. The results presented in this thesis combined with recent discovery about the functional recuperation of locomotion after spinal cord injury could open new avenues to help patients with impaired locomotion after trauma.

6.9 FIGURES

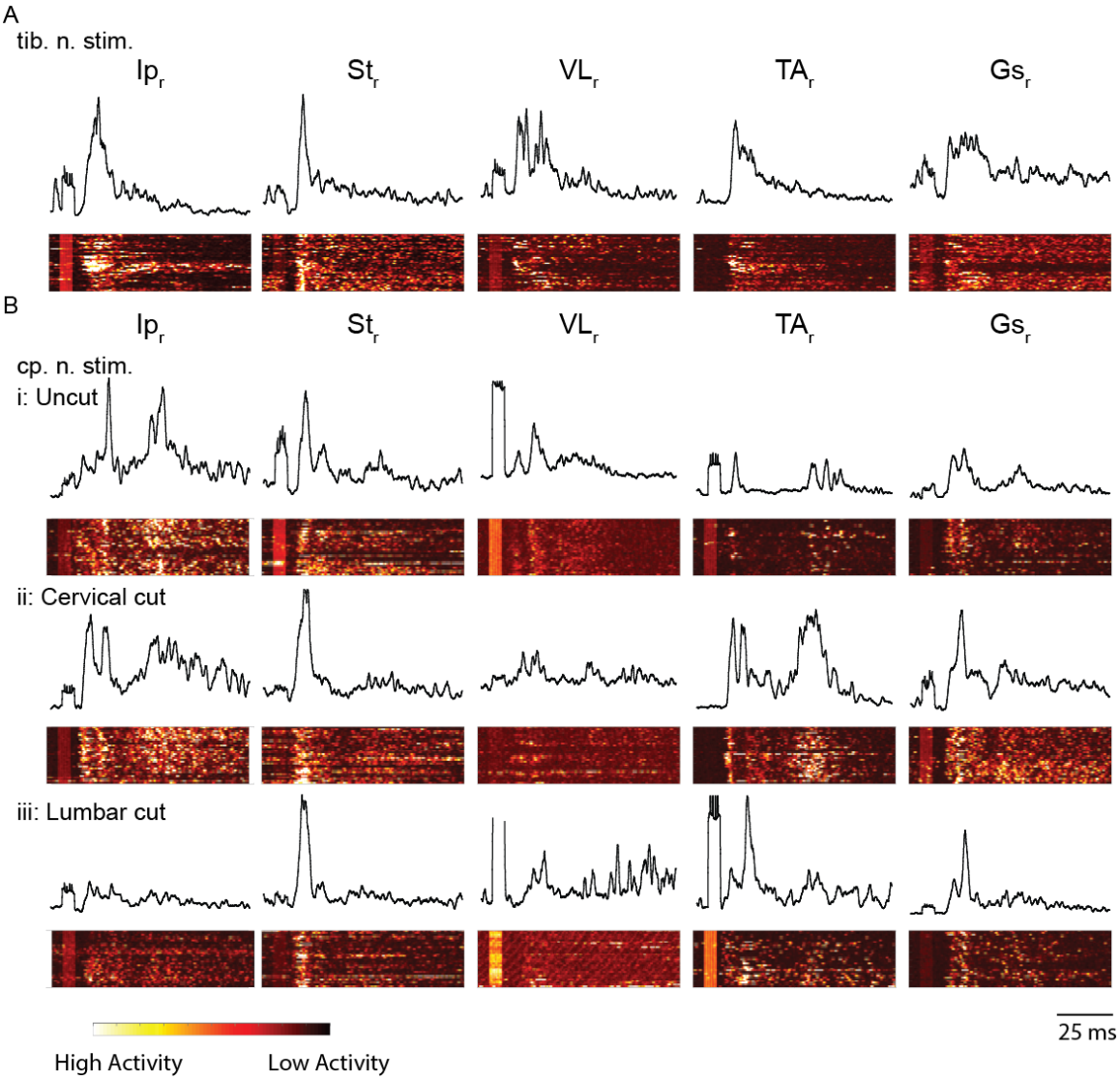

Figure 6.1. Long-latency motor responses in the common peroneal are preserved after a lesion of the spinal cord. Example of average crossed reflex responses from different muscles after the stimulation of the tibial nerve (*A*) or the common peroneal nerve (*B*). Heat diagrams of muscle activity are shown underneath each average. Muscle response to each of 40 nerve stimulations from 1 experiment is staggered on the vertical axis as a function of time. The brighter color indicates higher muscle. Lesion of the dorsal column-medial lemniscus pathways was performed at the lumbar and cervical level was performed to cut supraspinal input. Gs_r, right gastrocnemius; Ip_r, right iliopsoas; St_r, right semitendinosus; TA_r, right tibialis anterior; VL_r, right vastus lateralis.

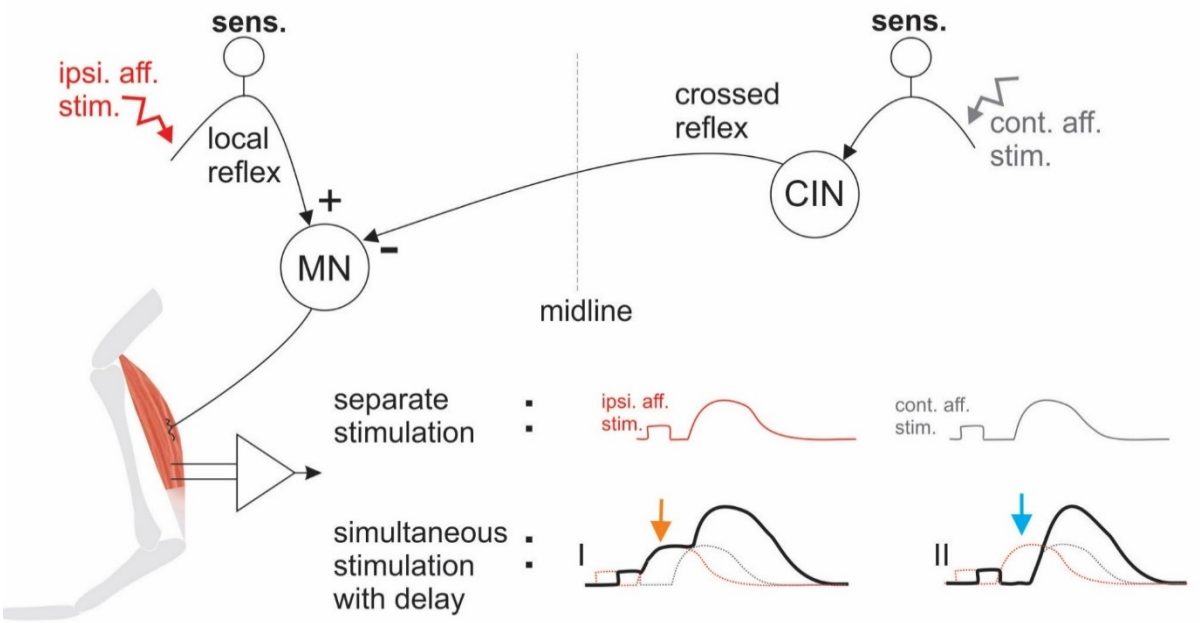

Figure 6.2. Conditioning paired stimulation paradigm. If ipsilateral afferents (ipsi. aff. stim., red) or the contralateral afferents (cont. aff. stim., grey) are stimulated separately, single responses are observed in the EMG recordings. If both afferents are stimulated simultaneously either they will sum up if the crossed reflex is excitatory (I, orange arrow) or there will be a silent period right after cont. aff. stim. observed as a black line below the red dotted line if the crossed reflex is inhibitory (II, blue arrow). CIN: commissural interneuron, and MN: motor neurons.

BIBLIOGRAPHY

Abraira VE, Ginty DD. The sensory neurons of touch. **Neuron** 79:618–639, 2013

Abraira, VE, Kuehn ED, Chirila AM, Springel MW, Toliver AA, Zimmerman AL, Orefice LL, Boyle KA. Bai L, Song BJ, Bashista KA, O'Neill TG, Zhuo J, Tsan C, Hoynoski J, Rutlin M, Kus L, Niederkofler V, Watanabe M, Dymecki SM, Nelson SB, Heintz N, Hughes DI, Ginty DD. The Cellular and Synaptic Architecture of the Mechanosensory Dorsal Horn. **Cell** 168 (1–2): 295-310.e19, 2017.

Acton D, Ren X, Di Costanzo S, Dalet A, Bourane S, Bertocchi I, Eva C, and Goulding M. Spinal Neuropeptide Y1 Receptor-Expressing Neurons Form an Essential Excitatory Pathway for Mechanical Itch. **Cell Reports** 28 (3): 625-639.e6, 2019. https://doi.org/10.1016/j.celrep.2019.06.033.

Aggelopoulos NC, Burton MJ, Clarke RW, Edgley SA. Characterization of a descending system that enables crossed group II inhibitory reflex pathways in the cat spinal cord. **J Neurosci** 16:723–729, 1996.

Aggelopoulos NC, Edgley SA. Segmental localisation of the relays mediating crossed inhibition of hindlimb motoneurones from group II afferents in the anaesthetized cat spinal cord. **Neurosci Lett** 185:60–64, 1995.

Akay T. Sensory Feedback Control of Locomotor Pattern Generation in Cats and Mice. **Neuroscience** 450:161–167, 2020. https://doi.org/10.1016/j.neuroscience.2020.05.008.

Akay T, Acharya HJ, Fouad K, Pearson KG. Behavioral and electromyographic characterization of mice lacking EphA4 receptors. **J Neurophysiol** 96: 642–651, 2006. doi:10.1152/jn.00174.2006.

Akay T, Tourtellotte WG, Arber S, Jessell TM. Degradation of mouse locomotor pattern in the absence of proprioceptive sensory feedback. **Proc Natl Acad Sci U S A** 111:16877–16882, 2014.

Alaynick WA, Jessell TM, Pfaff SL SnapShot : Spinal Cord Development. **Cell** 146:178-178.e1, 2011.

Albisetti GW, Pagani M, Platonova E, Hösli L, Johannssen HC, Fritschy J-M, Wildner H, and Zeilhofer HU. Dorsal Horn Gastrin-Releasing Peptide Expressing Neurons Transmit Spinal Itch But Not Pain Signals. **The Journal of Neuroscience: The Official Journal of the Society for Neuroscience** 39 (12): 2238–50, 2019. https://doi.org/10.1523/JNEUROSCI.2559-18.2019.

Alvarez FJ, Jonas PC, Sapir T, Hartley R, Berrocal MC, Geiman EJ, Todd AJ, Goulding M. Postnatal phenotype and localization of spinal cord V1 derived interneurons. **J Comp Neurol** 493: 177–192, 2005.

Anderson, J, Lampl I, Reichova I, Carandini M, and Ferster D. Stimulus Dependence of Two-State Fluctuations of Membrane Potential in Cat Visual Cortex. **Nature Neuroscience** 3 (6): 617–21, 2000. https://doi.org/10.1038/75797.

Andersson O, and Grillner S. Peripheral Control of the Cat's Step Cycle. II. Entrainment of the Central Pattern Generators for Locomotion by Sinusoidal Hip Movements during 'Fictive Locomotion.' **Acta Physiologica Scandinavica** 118 (3): 229–39, 1983. https://doi.org/10.1111/j.1748-1716.1983.tb07267.x.

Andersson LS, Larhammar M, Memic F, Wootz H, Schwochow D, Rubin C-J, Patra K, Arnason T, Wellbring L, Hjälm G, Imsland F, Petersen JL, McCue ME, Mickelson JR, Cothran G, Ahituv N, Roepstorff L, Mikko S, Vallstedt A, Lindgren G, Andersson L, Kullander K. Mutations in DMRT3 affect locomotion in horses and spinal circuit function in mice. **Nature** 488: 642–6, 2012.

Arber S. Motor Circuits in Action: Specification, Connectivity, and Function. **Neuron** 74: 975–989, 2012.

Aristotle's De Motu Animalium. 1986. https://press.princeton.edu/books/paperback/9780691020358/aristotles-de-motu-animalium.

Arya T, Bajwa S, Edgley SA. Crossed reflex actions from group II muscle afferents in the lumbar spinal cord of the anaesthetized cat. **J physiology** 444: 117–131, 1991.

Avraham O, Hadas Y, Vald L, Hong S, Song MR, Klar A. Motor and dorsal root ganglion axons serve as choice points for the ipsilateral turning of dI3 axons. **J Neurosci** 30:15546–15557, 2010.

Avraham O, Vald L, Zisman S, Schejter A, Visel A. Transcriptional control of axonal guidance and sorting in dorsal interneurons by the Lim-HD proteins Lhx9 and Lhx1. **Neural Dev** 4:2, 2009

Bagust J, Kerkut GA. Crossed reflex activity in an entire, isolated, spinal cord preparation taken from juvenile rodents. **Brain Res** 411: 397–399, 1987.

Bannatyne BA. Differential Projections of Excitatory and Inhibitory Dorsal Horn Interneurons Relaying Information from Group II Muscle Afferents in the Cat Spinal Cord. **J Neurosci** 26: 2871–2880, 2006.

Bannatyne BA, Edgley SA, Hammar I, Jankowska E, Maxwell DJ. Networks of inhibitory and excitatory commissural interneurons mediating crossed reticulospinal actions. **Eur J Neurosci** 18: 2273–2284, 2003.

Bellardita C, Kiehn O. Phenotypic Characterization of Speed-Associated Gait Changes in Mice Reveals Modular Organization of Locomotor Networks. **Curr Biol** 25: 1426–1436, 2015.

Bennett DJ, Gorassini M, Fouad K, Sanelli L, Han Y, Cheng J. Spasticity in rats with sacral spinal cord injury. **J Neurotrauma** 16:69–84, 1999

Berg RW, Alaburda A, and Hounsgaard J. Balanced Inhibition and Excitation Drive Spike Activity in Spinal Half-Centers. **Science** (New York, N.Y.) 315 (5810): 390–93, 2007. https://doi.org/10.1126/science.1134960.

Bernard G, Bouyer L, Provencher J, Rossignol S. Study of cutaneous reflex compensation during locomotion after nerve section in the cat. **J Neurophysiol** 97: 4173–4185, 2007. doi:10.1152/jn.00797.2006.

Blacklaws J, Deska-Gauthier D, Jones CT, Petracca YL, Liu M, Zhang H, Fawcett JP, Glover JC, Lanuza GM, Zhang Y. Sim1 is required for the migration and axonal projections of V3 interneurons in the developing mouse spinal cord. **Dev Neurobiol** 75: 1003–1017, 2015.

Böhm UL, Wyart C. Spinal sensory circuits in motion. **Curr Opin Neurobiol** 41: 38–43, 2016. doi:10.1016/j.conb.2016.07.007.

Borowska J, Jones CT, Deska-Gauthier D, Zhang Y. V3 interneuron subpopulations in the mouse spinal cord undergo distinctive postnatal maturation processes. **Neuroscience** 295: 221–228, 2015.

Borowska J, Jones CT, Zhang H, Blacklaws J, Goulding M, Zhang Y. Functional subpopulations of V3 interneurons in the mature mouse spinal cord. **J Neurosci** 33: 18553–65, 2013.

Bouyer LJ, and Rossignol S. The Contribution of Cutaneous Inputs to Locomotion in the Intact and the Spinal Cat. **Annals of the New York Academy of Sciences** 860 (November): 508–12, 1998. https://doi.org/10.1111/j.1749-6632.1998.tb09090.x.

Bouyer L, Rossignol S. Contribution of cutaneous inputs from the hindpaw to the control of locomotion in rats. **Behav Brain Res** 176: 193–201, 2003.

Boyle KA, Gradwell MA, Yasaka T, Dickie AC, Polgar E, Ganley RP, Orr DPH, Watanabe M, Abraira VE, Kuehn ED, Zimmerman AL, Ginty DD, Callister RJ, Graham BA, and Hughes DI. Defining a Spinal Microcircuit That Gates Myelinated Afferent Input: Implications for Tactile Allodynia. **Cell Reports** 28 (2): 526-540.e6, 2019. https://doi.org/10.1016/j.celrep.2019.06.040.

Briscoe J, Sussel L, Serup P, Hartigan-O'Connor D, Jessell TM, Rubenstein JLR, Ericson J. Homeobox gene Nkx2.2 and specification of neuronal identity by graded Sonic hedgehog signalling. **Nature** 398: 622–627, 1999.

Britz O, Zhang J, Grossmann KS, Dyck J, Kim JC, Dymecki S, Gosgnach S, Goulding M. A genetically defined asymmetry underlies the inhibitory control of flexor–extensor locomotor movements. **Elife** 4:1–22, 2013.

Brooks ME, Kristensen K, van Benthem KJ, Magnusson A, Berg CW, Nielsen A, Skaug HJ, Mächler M, Bolker BM. glmmTMB Balances Speed and Flexibility Among Packages for Zero-inflated Generalized Linear Mixed Modeling. **R J** 9: 378–400, 2017.

Brown AG, and Fyffe RE. Direct Observations on the Contacts Made between Ia Afferent Fibres and Alpha-Motoneurones in the Cat's Lumbosacral Spinal Cord. **The Journal of Physiology** 313: 121–40, 1981.

Brown TG, and Sherrington CS. The Intrinsic Factors in the Act of Progression in the Mammal. **Proceedings of the Royal Society of London**. Series B, Containing Papers of a Biological Character 84 (572): 308–19, 1911. https://doi.org/10.1098/rspb.1911.0077.

Browne TJ, Gradwell MA, Iredale JA, Maden JF, Callister RJ, Hughes DI, Dayas CV, and Graham BA. Transgenic Cross-Referencing of Inhibitory and Excitatory Interneuron Populations to Dissect Neuronal Heterogeneity in the Dorsal Horn. **Frontiers in Molecular Neuroscience** 13: 32, 2020. https://doi.org/10.3389/fnmol.2020.00032.

Brownstone RM, and Chopek JW. Reticulospinal Systems for Tuning Motor Commands. **Frontiers in Neural Circuits** 12: 30, 2018. https://doi.org/10.3389/fncir.2018.00030.

Bui TV, Akay T, Loubani O, Hnasko TS, Jessell TM, Brownstone RM. Circuits for grasping: spinal dI3 interneurons mediate cutaneous control of motor behavior. **Neuron** 78: 191–204, 2013. doi:10.1016/j.neuron.2013.02.007.

Caggiano V, Leiras R, Goñi-Erro H, Masini D, Bellardita C, Bouvier J, Caldeira V, Fisone G, and Kiehn O. Midbrain Circuits That Set Locomotor Speed and Gait Selection. **Nature** 553 (7689): 455–60, 2018. https://doi.org/10.1038/nature25448.

Cain DM, Khasabov SG, Simone DA. Response properties of mechanoreceptors and nociceptors in mouse glabrous skin: an in vivo study. **J Neurophysiol** 85: 1561–1574, 2001. doi:10.1152/jn.2001.85.4.1561.

Capelli P, Pivetta C, Esposito MS, and Arber S. Locomotor Speed Control Circuits in the Caudal Brainstem. **Nature** 551 (7680): 373–77, 2017.

Chopek JW, Nascimento F, Beato M, Brownstone RM, Zhang Y. Sub-populations of Spinal V3 Interneurons Form Focal Modules of Layered Pre-motor Microcircuits Article Sub-populations of Spinal V3 Interneurons Form Focal Modules of Layered Pre-motor Microcircuits. **CellReports** 25: 146-156.e3, 2018.

Danner SM, Zhang H, Shevtsova NA, Borowska-Fielding J, Deska-Gauthier D, Rybak IA, Zhang Y. Spinal V3 Interneurons and Left-Right Coordination in Mammalian Locomotion. **Front Cell Neurosci** 13: 516, 2019.

Deska-gauthier D, Zhang Y. The functional diversity of spinal interneurons and locomotor control. **Curr. Opin. Psychol.** (2019). doi: 10.1016/j.cophys.2019.01.005.

Dietz V, Colombo G, Jensen L, Baumgartner L. Locomotor capacity of spinal cord in paraplegic patients. **Ann Neurol** 37: 574–582, 1995.

Donelan MJ, McVea DA, and Pearson KG. Force Regulation of Ankle Extensor Muscle Activity in Freely Walking Cats. **Journal of Neurophysiology** 101 (1): 360–71, 2009. https://doi.org/10.1152/jn.90918.2008.

Donelan, MJ, and Pearson KG. Contribution of Force Feedback to Ankle Extensor Activity in Decerebrate Walking Cats. **Journal of Neurophysiology** 92 (4): 2093–2104, 2004. https://doi.org/10.1152/jn.00325.2004.

Donelan, MJ, and Pearson KG. Contribution of Sensory Feedback to Ongoing Ankle Extensor Activity during the Stance Phase of Walking. **Canadian Journal of Physiology and Pharmacology** 82 (8–9): 589–98, 2004. https://doi.org/10.1139/y04-043.

Dubuc R, Brocard F, Antri M, Fénelon K, Gariépy J-F, Smetana R, Ménard A, Le Ray D, Di Prisco GV, Pearlstein E, Sirota MG, Derjean D, St-Pierre M, Zielinski B, Auclair F, Veilleux D. Initiation of Locomotion in Lampreys. **Brain Research Reviews** 57 (1): 172–82, 2008. https://doi.org/10.1016/j.brainresrev.2007.07.016.

Dudek EF, and Sutula TP. Epileptogenesis in the Dentate Gyrus: A Critical Perspective. **Progress in Brain Research** 163: 755–73, 2007. https://doi.org/10.1016/S0079-6123(07)63041-6.

Duysens J. Reflex control of locomotion as revealed by stimulation of cutaneous afferents in spontaneously walking premammillary cats. **J Neurophysiol** 40: 737–751, 1977.

Duysens J. How deletions in a model could help explain deletions in the laboratory. **J Neurophysiol** 95:562–565, 2006.

Duysens J, Clarac F, and Cruse H. Load-Regulating Mechanisms in Gait and Posture: Comparative Aspects. **Physiological Reviews** 80 (1): 83–133, 2000.

Duysens J, De Groote F, Jonkers I. The flexion synergy, mother of all synergies and father of new models of gait. **Front Comput Neurosci** 7:1–9, 2013.

Duysens J, Loeb GE. Modulation of ipsi- and contralateral reflex responses in unrestrained walking cats. **J Neurophysiol** 44: 1024–1037, 1980.

Duysens J, Loeb GE, Weston BJ. Crossed flexor reflex responses and their reversal in freely walking cats. **Brain Res** 197: 538–42, 1980.

Duysens J, Pearson KG. The role of cutaneous afferents from the distal hindlimb in the regulation of the step cycle of thalamic cats. **Exp brain Res** 24:245–255, 1976.

Duysens J, and Pearson KG. Inhibition of Flexor Burst Generation by Loading Ankle Extensor Muscles in Walking Cats. **Brain Research** 187 (2), 1980. https://doi.org/10.1016/0006-8993(80)90206-1.

Duysens J, Stein RB. Reflexes induced by nerve stimulation in walking cats with implanted cuff electrodes. **Exp Brain Res** 32: 213–224, 1978.

Duysens J, Tax AAM, van der Doelen B, Trippel M, Dietz V. Selective activation of human soleus or gastrocnemius in reflex responses during walking and running. **Exp Brain Res** 87: 193–204, 1991.

Dyck J, Lanuza GM, Gosgnach S. Functional characterization of dI6 interneurons in the neonatal mouse spinal cord. **J Neurosci** 107: 3256–3266, 2012.

Ellaway P, Taylor A, Durbaba R, Rawlinson S. Role of the Fusimotor System in Locomotion. In: **Sensorimotor Control of Movement and Posture,** edited by Gandevia SC, Proske U, Stuart DG. Springer US, p. 335–342.

Edgley SA, Aggelopoulos NC. Short latency crossed inhibitory reflex actions evoked from cutaneous afferents. **Exp Brain Res** 171: 541–550, 2006. doi:10.1007/s00221-005-0302-9.

Edgley SA, and Jankowska E. Field Potentials Generated by Group II Muscle Afferents in the Middle Lumbar Segments of the Cat Spinal Cord. **The Journal of Physiology** 385 (April): 393–413, 1987. https://doi.org/10.1113/jphysiol.1987.sp016498.

Edgley SA, Jankowska E, Krutki P, Hammar I. Both dorsal horn and lamina VIII interneurones contribute to crossed reflexes from feline group II muscle afferents. **J Physiol** 552: 961–974, 2003. doi:10.1113/jphysiol.2003.048009.

Engberg I. Reflexes to Foot Muscles in the Cat. **Acta Physiol. Scand. Suppl**.1964

Feldman AG, Orlovsky GN. Activity of interneurons mediating reciprocal 1a inhibition during locomotion. **Brain Res** 84:181–194, 1975.

Forssberg H. Stumbling corrective reaction: a phase-dependent compensatory reaction during locomotion. **J Neurophysiol** 42: 936–953, 1979. doi:10.1152/jn.1979.42.4.936.

Forssberg H, Grillner S, Rossignol S. Phasic gain control of reflexes from the dorsum of the paw during spinal locomotion. **Brain Res** 132: 121–139, 1977.

Forssberg H, Grillner S, Rossignol S. Phase dependent reflex reversal during walking in chronic spinal cats. **Brain Res** 85: 103–107, 1975. doi:10.1016/0006-8993(75)91013-6.

Frigon A, Rossignol S. Adaptive changes of the locomotor pattern and cutaneous reflexes during locomotion studied in the same cats before and after spinalization. **J Physiol** 586: 2927–2945, 2008. doi:10.1113/jphysiol.2008.152488.

Frigon A, Rossignol S. Short-latency crossed inhibitory responses in extensor muscles during locomotion in the cat. **J Neurophysiol** 99: 989–998, 2008.

Garcia-Campmany L, Stam FJ, Goulding M. From circuits to behaviour: motor networks in vertebrates. **Curr Opin Neurobiol** 20: 116–125, 2010. doi:10.1016/j.conb.2010.01.002.

Garcia-Rill E, Skinner RD, and Fitzgerald JA. Chemical Activation of the Mesencephalic Locomotor Region. **Brain Research** 330 (1): 43–54, 1985. https://doi.org/10.1016/0006-8993(85)90006-x.

Gatto G, Bourane S, Ren X, Di Costanzo S, Fenton PK, Halder P, Seal RP, and Goulding MD. A Functional Topographic Map for Spinal Sensorimotor Reflexes. **Neuron** 109 (1): 91-104.e5, 2021. https://doi.org/10.1016/j.neuron.2020.10.003.

Gauthier L, Rossignol S. Contralateral hindlimb responses to cutaneous stimulation during locomotion in high decerebrate cats. **Brain Res** 207: 303–320, 1981. doi:10.1016/0006-8993(81)90366-8.

Gervasio S, Farina D, Sinkjær T, Mrachacz-Kersting N. Crossed reflex reversal during human locomotion. **J Neurophysiol** 109: 2335–2344, 2013. doi:10.1152/jn.01086.2012.

Gervasio S, Kersting UG, Farina D, Mrachacz-Kersting N. The effect of crossed reflex responses on dynamic stability during locomotion. **J Neurophysiol** 114: 1034–1040, 2015.

Gervasio S, Voigt M, Kersting UG, Farina D, Sinkjaer T, Mrachacz-Kersting N. Sensory feedback in interlimb coordination: Contralateral afferent contribution to the short-latency crossed response during human walking. **PLoS One** 12: 1–24, 2017.

Giuliani CA, Smith JL. Stepping behaviors in chronic spinal cats with one hindlimb deafferented. **J Neurosci** 7: 2537–2546, 1987.

Goetz C, Pivetta C, Arber S. Distinct Limb and Trunk Premotor Circuits Establish Laterality in the Spinal Cord. **Neuron** 85:131–145, 2015.

Heckman CJ, Gorassini MA, Bennett DJ. Persistent inward currents in motoneuron dendrites: Implications for motor output. **Muscle and Nerve** 31:135–156, (2005).

Goldberger ME. Locomotor recovery after unilateral hindlimb deafferentation in cats. **Brain Res** 123: 59–74, 1977.

Gosgnach S, Bikoff JB, Kimberly X, Dougherty J, Manira A El, Lanuza GM, Zhang Y. Delineating the Diversity of Spinal Interneurons in Locomotor Circuits. **J Neurosci** 37: 10835–10841, 2017.

Goslow Jr GE, Reinking RM, and Stuart DG. The Cat Step Cycle: Hind Limb Joint Angles and Muscle Lengths during Unrestrained Locomotion. **Journal of Morphology** 141 (1): 1–41, 1973. https://doi.org/10.1002/jmor.1051410102.

Goulding M. Circuits controlling vertebrate locomotion: moving in a new direction. **Nat Rev Neurosci** 10: 507–518, 2009.

Griener A, Zhang W, Kao H, Haque F, Gosgnach S. Anatomical and electrophysiological characterization of a population of dI6 interneurons in the neonatal mouse spinal cord. **Neuroscience** 362: 47–59, 2017.

Grillner S, El Manira A. Current principles of motor control, with special reference to vertebrate locomotion. **Physiol Rev** 100: 271–320, 2020.

Grillner S, and Rossignol S. On the Initiation of the Swing Phase of Locomotion in Chronic Spinal Cats. **Brain Research** 146 (2): 269–77, 1978. https://doi.org/10.1016/0006-8993(78)90973-3.

Grillner S, Zangger P. The effect of dorsal root transection on the efferent motor pattern in the cat's hindlimb during locomotion. **Acta Physiol Scand** 120: 393–405, 1984.

Gross MK, Dottori M, Goulding M. Lbx1 specifies somatosensory association interneurons in the dorsal spinal cord. **Neuron** 34: 535–549, 2002.

Gruner JA, and Altman J. Swimming in the Rat: Analysis of Locomotor Performance in Comparison to Stepping. **Experimental Brain Research** 40 (4): 374–82, 1980. https://doi.org/10.1007/BF00236146.

Halbertsma JM. The Stride Cycle of the Cat: The Modelling of Locomotion by Computerized Analysis of Automatic Recordings. **Acta Physiologica Scandinavica. Supplementum** 521: 1–75, 1983.

Hammar I, Bannatyne BA, Maxwell DJ, Edgley SA, Jankowska E. The actions of monoamines and distribution of noradrenergic and serotoninergic contacts on different subpopulations of commissural interneurons in the cat spinal cord. **Eur J Neurosci** 19: 1305–1316, 2004. doi:10.1111/j.1460-9568.2004.03239.x.

Hammar I, Stecina K, Jankowska E. Differential modulation by monoamine membrane receptor agonists of reticulospinal input to lamina VIII feline spinal commissural interneurons. **Eur J Neurosci** 26: 1205–1212, 2007.

Hampton TG, Stasko MR, Kale A, Amende I, and Costa ACS. Gait Dynamics in Trisomic Mice: Quantitative Neurological Traits of Down Syndrome. **Physiology & Behavior** 82 (2–3): 381–89, 2004. https://doi.org/10.1016/j.physbeh.2004.04.006.

Hantman AW, Jessell TM. Clarke's column neurons as the focus of a corticospinal corollary circuit. **Nat Neurosci** 13: 1233–1239, 2010. doi:10.1038/nn.2637.

Haque F, Rancic XV, Zhang W, Clugston XR, Ballanyi XK, Gosgnach XS. WT1 - Expressing Interneurons Regulate Left – Right Alternation during Mammalian Locomotor Activity. **J Neurosci** 38: 5666–5676, 2018.

Harrison PJ, Jankowska E, Zythicki D. Lamina VIII interneurones interposed in crossed reflex pathways in the cat. **J physiology**: 90–91, 1986.

Harrison PJ, Zytnicki D. Crossed actions of group I muscle afferents in the cat. **J Physiol** 356: 263–273, 1984.

Heckman CJ, Gorassini MA, Bennett DJ. Persistent inward currents in motoneuron dendrites: Implications for motor output. **Muscle and Nerve** 31:135–156, (2005).

Hilde KL, Levine AJ, Hinckley CA, Hayashi M, Montgomery JM, Gullo M, Driscoll SP, Grosschedl R, Kohwi Y, Kohwi-Shigematsu T, and Pfaff SL. Satb2 Is Required for the Development of a Spinal Exteroceptive Microcircuit That Modulates Limb Position. **Neuron** 91 (4): 763–76, 2016. https://doi.org/10.1016/j.neuron.2016.07.014.

Hildebrand M. The Quadrupedal Gaits of Vertebrates. **Bioscience** 39: 766–775, 1989.

Hongo T, Kitazawa S, Ohki Y, and Xi M. Functional Identification of Last-Order Interneurones of Skin Reflex Pathways in the Cat Forelimb Segments. **Brain Research**, December, 1989.

Hoseok K, Ährlund-Richter S, Wang X, Deisseroth K, and Carlén M. Prefrontal Parvalbumin Neurons in Control of Attention. **Cell** 164 (1–2): 208–18, 2016. https://doi.org/10.1016/j.cell.2015.11.038.

Houk J, Henneman E. Responses of Golgi tendon organs to active contractions of the soleus muscle of the cat. **J Neurophysiol** 30: 466–481, 1967.

Hulliger M. The mammalian muscle spindle and its central control. **Rev Physiol Biochem Pharmacol** 101: 1–110, 1984.

Hunt, SP, Pini A, and Evan G. Induction of C-Fos-like Protein in Spinal Cord Neurons Following Sensory Stimulation. **Nature** 328 (6131): 632–34, 1987. https://doi.org/10.1038/328632a0.

Hurteau M-F, Thibaudier Y, Dambreville C, Chraibi A, Desrochers E, Telonio A, Frigon A. Nonlinear Modulation of Cutaneous Reflexes with Increasing Speed of Locomotion in Spinal Cats. **J Neurosci** 37: 3896–3912, 2017.

Hurteau MF, Thibaudier Y, Dambreville C, Danner SM, Rybak IA, Frigon A. Intralimb and interlimb cutaneous reflexes during locomotion in the intact cat. **J Neurosci** 38: 4104–4122, 2018. doi:10.1523/JNEUROSCI.3288-17, 2018.

Jack JJ. Some methods for selective activation of muscle afferent fibres. In: **Studies in Neurophysiology: Presented to A. K. McIntyre**, edited by Porter R. London: Cambridge University Press, 1978, p. 155–176.

Jankowska E. Spinal interneuronal networks in the cat: elementary components. **Brain Res Brain Res Rev** 57: 46–55, 2008. doi:10.1016/j.brainresrev.2007.06.022.

Jankowska E. Spinal interneurons. In: **Neuroscience in the 21st Century: From Basic to Clinical,** edited by Pfaff DW. New York, NY: Springer Science+Business Media, 2013, p. 11063–1099.

Jankowska E. Spinal Reflexes. In: **Neuroscience in the 21st Century,** edited by Pfaff DW, Volkow ND. New York: Springer Science+Business Media, 2016, p. 1599–1621.

Jankowska E, Bannatyne BA, Stecina K, Hammar I, Cabaj A, Maxwell DJ. Commissural interneurons with input from group I and II muscle afferents in feline lumbar segments: Neurotransmitters, projections and target cells. **J Physiol** 587: 401–418, 2009.

Jankowska E, Edgley SA. Functional subdivision of feline spinal interneurons in reflex pathways from group Ib and II muscle afferents; an update. **Eur J Neurosci** 32: 881–893, 2010. doi:10.1111/j.1460-9568.2010.07354.x.

Jankowska E, Edgley S a, Krutki P, Hammar I. Functional differentiation and organization of feline midlumbar commissural interneurones. **J Physiol** 565: 645–658, 2005a.

Jankowska E, Jukes MGM, Lund S, Lundberg A. The effect of DOPA on the spinal cord 5. Reciprocal organization of pathways transmitting excitatory action to alpha motoneurones of flexors and extensors. **Acta Physiol Scand** 70: 369–388, 1967. doi:10.1111/j.1748-1716.1967.tb03636.x.

Jankowska E, Jukes MG, Lund S, Lundberg A. The effect of DOPA on the spinal cord 6. Half-centre organization of interneurones transmitting effects from the flexor reflex afferents. **Acta Physiol Scand** 70: 389–402, 1968. doi:10.1111/j.1748-1716.1967.tb03637.x.

Jankowska E, Krutki P, Matsuyama K. Relative contribution of Ia inhibitory interneurones to inhibition of feline contralateral motoneurones evoked via commissural interneurones. **J Physiol** 568.2: 617–628, 2005b.

Jankowska E, Noga BRR. Contralaterally projecting lamina VIII interneurones in middle lumbar segments in the cat. **Brain Res** 535: 327–330, 1990.

Jessell TM. Neuronal specification in the spinal cord: inductive signals and transcriptional codes. **Nat Rev Genet** 1: 20–29, 2000.

Jiang Z, Carlin KP, Brownstone RM. An in vitro functionally mature mouse spinal cord preparation for the study of spinal motor networks. **Brain Res** 816: 493–499, 1999.

Johnson MD, Hyngstrom AS, Manuel M, and Heckman CJ. Push-Pull Control of Motor Output**. The Journal of Neuroscience: The Official Journal of the Society for Neuroscience** 32 (13): 4592–99, 2012. https://doi.org/10.1523/JNEUROSCI.4709-11.2012.

Kambiz S, Baas M, Duraku LS, Kerver AL, Koning AHJ, Walbeehm ET, Ruigrok TJH. Innervation mapping of the hind paw of the rat using Evans Blue extravasation, optical surface mapping and CASAM. **J Neurosci Methods** 229: 15–27, 2014. doi:10.1016/j.jneumeth.2014.03.015.

Kiehn O. Decoding the organization of spinal circuits that control locomotion. **Nat Rev Neurosci** 17: 224–238, 2016.

Kiehn O. Decoding the organization of spinal circuits that control locomotion. **Nat Rev Neurosci** 17: 224–238, 2016.

Koch SC, Del Barrio MG, Dalet A, Gatto G, Günther T, Zhang J, Seidler B, Saur D, Schüle R, and Goulding M. RORβ Spinal Interneurons Gate Sensory Transmission during Locomotion to Secure a Fluid Walking Gait. **Neuron** 96 (6): 1419-1431.e5, 2017. https://doi.org/10.1016/j.neuron.2017.11.011.

Krasovsky T, Baniña MC, Hacmon R, Feldman AG, Lamontagne A, Levin MF. Stability of gait and interlimb coordination in older adults. **J Neurophysiol** 107: 2560–2569, 2012.

Kristensen K, Nielsen A, Berg CW, Skaug H, Bell BM. TMB: Automatic Differentiation and Laplace Approximation. **J Stat Softw** 70: 1–21, 2016.

Kudo N, Yamada T. N-Methyl-d,l-aspartate-induced locomotor activity in a spinal cord hindlimb muscles preparation of the newborn rat studied in vitro. **Neurosci Lett** 75: 43–48, 1987.

Kuhn RA, Macht MB. Some manifestations of reflex activity in spinal man with particular reference to the occurrence of extensor spasm. **Bull Johns Hopkins Hosp** 84:43–75, 1949.

Kurtzer IL. Long-latency reflexes account for limb biomechanics through several supraspinal pathways. **Front Integr Neurosci** 8: 99, 2015. doi:10.3389/fnint.2014.00099.

Laflamme OD, Akay T. Excitatory and inhibitory crossed reflex pathways in mice. **J Neurophysiol** 120: 2897–2907, 2018. doi:10.1152/jn.00450.2018.

Laflamme OD, Ibrahim M, Akay T. Crossed reflex responses to flexor nerve stimulation in mice. **J Neurophysiology** 127: 493–503, 2022.

Lai HC, Seal RP, Johnson JE. Making sense out of spinal cord somatosensory development. **Development** 143: 3434–3448, 2016.

Lajoie Y, Teasdale N, Cole JD, Burnett M, Bard C, Fleury M, Forget R, Paillard J, and Lamarre Y. Gait of a Deafferented Subject without Large Myelinated Sensory Fibers below the Neck. **Neurology** 47 (1): 109–15, 1996. https://doi.org/10.1212/wnl.47.1.109.

Lanuza GM, Gosgnach S, Pierani A, Jessell TM, Goulding M. Genetic identification of spinal interneurons that coordinate left-right locomotor activity necessary for walking movements. **Neuron** 42: 375–386, 2004.

Lehnert BP, Santiago C, Huey EL, Emanuel AJ, Renauld S, Africawala N, Alkislar I, Zheng Y, Bai L, Koutsioumpa C, Hong JT, Magee AR, Harvey CD, and Ginty DD. Mechanoreceptor Synapses in the Brainstem Shape the Central Representation of Touch." **Cell** 184 (22): 5608-5621.e18, 2021. https://doi.org/10.1016/j.cell.2021.09.023.
Lemieux M, Josset N, Roussel M, Couraud S, Bretzner F. Speed-dependent modulation of the locomotor behavior in adult mice reveals attractor and transitional gaits. **Front Neurosci** 10: 42, 2016.

Levine AJ, Hinckley CA, Hilde KL, Driscoll SP, Poon TH, Montgomery JM, and Pfaff SL. Identification of a Cellular Node for Motor Control Pathways. **Nature Neuroscience** 17 (4): 586–93, 2014. https://doi.org/10.1038/nn.3675.

Li D, Li Y, Tian Y, Xu Z, and Guo Y. Direct Intrathecal Injection of Recombinant Adeno-Associated Viruses in Adult Mice. **JoVE** (Journal of Visualized Experiments), no. 144 (February): e58565, 2019. https://doi.org/10.3791/58565.

Li X, Murray K, Harvey PJ, Ballou EW, Bennett DJ. Serotonin facilitates a persistent calcium current in motoneurons of rats with and without chronic spinal cord injury. **J Neurophysiol** 97:1236–1246, 2007.

Li Z, Tan AY, Schreiner CE, and Merzenich MM. Topography and Synaptic Shaping of Direction Selectivity in Primary Auditory Cortex. **Nature** 424 (6945), 2003. https://doi.org/10.1038/nature01796.

Lin S, Li Y, Lucas-Osma AM, Hari K, Stephens MJ, Singla R, Heckman CJ, Zhang Y, Fouad K, Fenrich KK, Bennett DJ. Locomotor-related V3 interneurons initiate and coordinate muscles spasms after spinal cord injury. **J Neurophysiol** 121:1352–1367, 2019.
Lu DC, Niu T, Alaynick WA. Molecular and cellular development of spinal cord locomotor circuitry. **Front Mol Neurosci** 8: 25, 2015.

Luo W, Enomoto H, Rice FL, Milbrandt J, and Ginty DD. Molecular Identification of Rapidly Adapting Mechanoreceptors and Their Developmental Dependence on Ret Signaling. **Neuron** 64 (6): 841–562009. https://doi.org/10.1016/j.neuron.2009.11.003.

Martinez LM, and Alonso J-M. Complex Receptive Fields in Primary Visual Cortex. **The Neuroscientist: A Review Journal Bringing Neurobiology, Neurology and Psychiatry** 9 (5): 317–312003. https://doi.org/10.1177/1073858403252732.

Mathis A, Mamidanna P, Cury KM, Abe T, Murthy VN, Mathis MW, and Bethge M. DeepLabCut: Markerless Pose Estimation of User-Defined Body Parts with Deep Learning. **Nature Neuroscience** 21 (9): 1281–89, 2018. https://doi.org/10.1038/s41593-018-0209-y.

Matsuyama K, Kobayashi S, Aoki M. Projection patterns of lamina VIII commissural neurons in the lumbar spinal cord of the adult cat: An anterograde neural tracing study. **Neuroscience** 140: 203–218, 2006.

Matsuyama K, Mori F, Nakajima K, Drew T, Aoki M, Mori S. Locomotor role of the corticoreticular-reticulospinal-spinal interneuronal system. **Prog Brain Res** 143: 239–249, 2004a.

Matsuyama K, Nakajima K, Mori F, Aoki M, Mori S. Lumbar commissural interneurons with reticulospinal inputs in the cat: Morphology and discharge patterns during fictive locomotion. **J Comp Neurol** 474: 546–561, 2004b.

Mayer WP, Akay T. Stumbling corrective reaction elicited by mechanical and electrical stimulation of the saphenous nerve in walking mice. **J Exp Biol** 221, 2018.

Mayer WP, Akay T. The role of muscle spindle feedback in the guidance of hindlimb movement by the ipsilateral forelimb during locomotion in mice. **eNeuro** 8: 1–13, 2021.

McClellan AD., and Grillner S. Activation of 'fictive Swimming' by Electrical Microstimulation of Brainstem Locomotor Regions in an in Vitro Preparation of the Lamprey Central Nervous System. **Brain Research** 300 (2): 357–611984. https://doi.org/10.1016/0006-8993(84)90846-1.

McCrea DA. Spinal circuitry of sensorimotor control of locomotion. **J Physiol** 533: 41–50, 2001. doi:10.1111/j.1469-7793.2001.0041b.x.

McHanwell S, Biscoe TJ. The localization of motoneurons supplying the hindlimb muscles of the mouse. **Philos Trans R Soc Lond B Biol Sci** 293: 477–508, 1981. doi:10.1098/rstb.1981.0082.

Meijer R, Plotnik M, Zwaaftink EG, va Lummel RC, Ainsworth E, Martina JD, Hausdorff JM. Markedly impaired bilateral coordination of gait in post-stroke patients : Is this deficit distinct from asymmetry ? A cohort study. **J Neuroeng Rehabil** 8: 23, 2011.

Miesegaes GR, Klisch TJ, Thaller C, Ahmad KA, Atkinson RC, Zoghbi HY. Identification and subclassification of new Atoh1 derived cell populations during mouse spinal cord development. **Dev Biol** 327:339–351, 2009.

Miles GB, Hartley R, Todd AJ, Brownstone RM. Spinal cholinergic interneurons regulate the excitability of motoneurons during locomotion. **Proc Natl Acad Sci U S A** 104: 2448–2453, 2007.

Miranda CO, Hegedüs K, Wildner H, Zeilhofer HU, and Antal M. Morphological and Neurochemical Characterization of Glycinergic Neurons in Laminae I-IV of the Mouse Spinal Dorsal Horn. **The Journal of Comparative Neurology** 530 (3): 607–26, 2022. https://doi.org/10.1002/cne.25232.

Morgan JI, and Curran T. Role of Ion Flux in the Control of C-Fos Expression. **Nature** 322 (6079): 552–551986. https://doi.org/10.1038/322552a0.

Mori S. Integration of Posture and Locomotion in Acute Decerebrate Cats and in Awake, Freely Moving Cats. **Progress in Neurobiology** 28 (2): 161–95, 1987. https://doi.org/10.1016/0301-0082(87)90010-4.

Moschovakis AK, Solodkin M, and. Burke RE. Anatomical and Physiological Study of Interneurons in an Oligosynaptic Cutaneous Reflex Pathway in the Cat Hindlimb. **Brain Research** 586 (2): 311–18, 1992. https://doi.org/10.1016/0006-8993(92)91641-q.

Mrachacz-Kersting N, Geertsen SS, Stevenson AJT, Nielsen JB. Convergence of ipsi- and contralateral muscle afferents on common interneurons mediating reciprocal inhibition of ankle plantarflexors in humans. **Exp Brain Res** 235: 1555–1564, 2017.

Muir GD, and Steeves JD. Phasic Cutaneous Input Facilitates Locomotor Recovery after Incomplete Spinal Injury in the Chick. **Journal of Neurophysiology** 74 (1): 358–68, 1995. https://doi.org/10.1152/jn.1995.74.1.358.

Nahar L, Delacroix BM, and Nam HW. The Role of Parvalbumin Interneurons in Neurotransmitter Balance and Neurological Disease. **Frontiers in Psychiatry** 12, 2021. https://www.frontiersin.org/article/10.3389/fpsyt.2021.679960.

Nakanishi ST, Whelan PJ. A decerebrate adult mouse model for examining the sensorimotor control of locomotion. **J Neurophysiol** 107: 500–515, 2012.

Nielsen JB, Crone C, Hultborn H. The spinal pathophysiology of spasticity - From a basic science point of view. **Acta Physiol** 189:171–180, 2007

Orlovskiĭ GN, and Fel'dman AG. [Classification of the neurons of the lumbo-sacral region of the spinal cord in accordance with their discharge patterns during provoked locomotion]. **Neirofiziologiia** = Neurophysiology 4 (4): 410–17, 1972.

Pearson KG. Generating the walking gait: role of sensory feedback. **Prog Brain Res** 143: 123–129, 2004. doi:10.1016/S0079-6123(03)43012-4.

Pearson KG, Acharya H, Fouad K. A new electrode configuration for recording electromyographic activity in behaving mice. **J Neurosci Methods** 148: 36–42, 2005. doi:10.1016/j.jneumeth.2005.04.006.

Perl ER. Crossed reflexes of cutaneous origin. **Am J Physiol** 188: 609–615, 1957. doi:10.1152/ajplegacy.1957.188.3.609.

Petersen PC, Vestergaard M, Jensen KHR, and Berg RW. Premotor Spinal Network with Balanced Excitation and Inhibition during Motor Patterns Has High Resilience to Structural Division. **The Journal of Neuroscience: The Official Journal of the Society for Neuroscience** 34 (8): 2774–84, 2014. https://doi.org/10.1523/JNEUROSCI.3349-13.2014.

Peyronnard JM, Charron L. Motor and sensory neurons of the rat sural nerve: a horseradish peroxidase study. **Muscle Nerve** 5: 654–660, 1982. doi:10.1002/mus.880050811.

Pierani A, Moran-Rivard L, Sunshine MJ, Littman DR, Goulding M, Jessell TM. Control of interneuron fate in the developing spinal cord by the progenitor homeodomain protein Dbx1. **Neuron** 29: 367–384, 2001.

Plotnik M, Giladi N, Hausdorff JM. A new measure for quantifying the bilateral coordination of human gait: effects of aging and Parkinson's disease. **Exp Brain Res** 181: 561–570, 2007.

Plotnik M, Giladi N, Hausdorff JM. Bilateral coordination of walking and freezing of gait in Parkinson's disease. **Eur J Neurosci** 27: 1999–2006, 2008.

Poo C, and Isaacson JS. Odor Representations in Olfactory Cortex: 'Sparse' Coding, Global Inhibition, and Oscillations. **Neuron** 62 (6): 850–61, 2009. https://doi.org/10.1016/j.neuron.2009.05.022.

Prochazka A, Sontag KH, Wand P. Motor reactions to perturbations of gait: proprioceptive and somesthetic involvement. **Neurosci Lett** 7: 35–39, 1978.

Prochazka A, and Yakovenko S. The Neuromechanical Tuning Hypothesis. **Progress in Brain Research** 165: 255–65, 2007. https://doi.org/10.1016/S0079-6123(06)65016-4.

Quevedo J, Stecina K, Gosgnach S, McCrea DA. Stumbling corrective reaction during fictive locomotion in the cat. **J Neurophysiol** 94: 2045–2052, 2005. doi:10.1152/jn.00175.2005.

Ringach DL. Mapping Receptive Fields in Primary Visual Cortex. **The Journal of Physiology** 558 (Pt 3): 717–28, 2004. https://doi.org/10.1113/jphysiol.2004.065771.

Rossignol S, Dubuc R, Gossard J-P, Dubuc J. Dynamic Sensorimotor Interactions in Locomotion. **Physiol Rev** 86: 89–154, 2006.

Ruffini A, Histology L, Uni- R. the Minute Anatomy of the Neuro- Their Physiological Significance. **J Physiol** 23: 190-208.3, 1898.

Rutlin M, Ho C-Y, Abraira VE, Cassidy C, Bai L, Woodbury JC, and Ginty DD. The Cellular and Molecular Basis of Direction Selectivity of Aδ-LTMRs. **Cell** 159 (7): 1640–51, 2014. https://doi.org/10.1016/j.cell.2014.11.038.

Sakai N, Insolera R, Sillitoe R V., Shi SH, Kaprielian Z. Axon sorting within the spinal cord marginal zone via Robo-mediated inhibition of N-cadherin controls spinocerebellar tract formation. **J Neurosci** 32:15377–15387, 2012.

Santuz A, Akay T, Mayer WP, Wells TL, Schroll A, Arampatzis A. Modular organization of murine locomotor pattern in the presence and absence of sensory feedback from muscle spindles. **J Physiol** 597: 3147–3165, 2019.

Schillings AM, Van Wezel BM, and Duysens J. Mechanically Induced Stumbling during Human Treadmill Walking. **Journal of Neuroscience Methods** 67 (1): 11–17, 1996. https://doi.org/10.1016/0165-0270(95)00149-2.

Schmidt BJ, Jordan LM. The role of serotonin in reflex modulation and locomotor rhythm production in the mammalian spinal cord. **Brain Res Bull** 53: 689–710, 2000. doi:10.1016/s0361-9230(00)00402-0.

Schomburg ED, Kalezic I, Dibaj P, Steffens H. Reflex transmission to lumbar α-motoneurones in the mouse similar and different to those in the cat. **Neurosci Res** 76: 133–140, 2013. doi:10.1016/j.neures.2013.03.011.

Sherrington CS. On Reciprocal Innervation of Antagonistic Msucles.-Eighth Note. **Proc R Soc B** 76: 269–297, 1905.

Sherrington CS. The Integrative Action of the Nervous System, 1906.

Sherrington CS. Remarks on the Reflex Mechanism of the Step **Brain** 33: 1–25, 1910.

Sherrington CS. Flexion-reflex of the limb crossed extension-reflex, and reflex stepping and standing. **J Physiol** 40: 28–121, 1910.

Shevtsova NA, Talpalar AE, Markin SN, Harris-Warrick RM, Kiehn O, Rybak IA. Organization of left-right coordination of neuronal activity in the mammalian spinal cord : Insights from computational modelling Key points. **J Physiol** 11: 2403–2426, 2015.

Sieber, MA, Storm R, Martinez-de-la-Torre M, Müller T, Wende H, Reuter K, Vasyutina E, and Birchmeier C. Lbx1 Acts as a Selector Gene in the Fate Determination of Somatosensory and Viscerosensory Relay Neurons in the Hindbrain. **Journal of Neuroscience** 27 (18): 4902–9, 2007. https://doi.org/10.1523/JNEUROSCI.0717-07.2007.

Smith JC, Feldman JL. In vitro brainstem-spinal cord preparations for study of motor systems for mammalian respiration and locomotion. **J Neurosci Methods** 21: 321–333, 1987.

Steffens H, Dibaj P, Schomburg ED. In vivo measurement of conduction velocities in afferent and efferent nerve fibre groups in mice. **Physiol Res** 61: 203–214, 2012.

Steldt RE, Schmit BD. Modulation of coordinated muscle activity during imposed sinusoidal hip movements in human spinal cord injury. **J Neurophysiol** 92:673–685, 2004.
Stubbs PW, Mrachacz-Kersting N. Short-latency crossed inhibitory responses in the human soleus muscle. **J Neurophysiol** 102: 3596–3605, 2009.

Stubbs PW, Nielsen JF, Sinkjaer T, Mrachacz-Kersting N. Phase Modulation of the Short-Latency Crossed Spinal Response in the Human Soleus Muscle. **J Neurophysiol** 105: 503–511, 2011.

Stubbs PW, Nielsen JF, Sinkjær T, Mrachacz-Kersting N. Short-latency crossed spinal responses are impaired differently in sub-acute and chronic stroke patients. **Clin Neurophysiol** 123: 541–549, 2012.

Takakusaki K, Habaguchi T, Ohtinata-Sugimoto J, Saitoh K, and Sakamoto T. Basal Ganglia Efferents to the Brainstem Centers Controlling Postural Muscle Tone and Locomotion: A New Concept for Understanding Motor Disorders in Basal Ganglia Dysfunction. **Neuroscience** 119 (1): 293–308, 2003. https://doi.org/10.1016/s0306-4522(03)00095-2.

Takeoka A, Arber S. Functional Local Proprioceptive Feedback Circuits Initiate and Maintain Locomotor Recovery after Spinal Cord Injury. **Cell Rep** 27: 71-85.e3, 2019.

Talpalar AE, Bouvier J, Borgius L, Fortin G, Pierani A, Kiehn O. Dual-mode operation of neuronal networks involved in left-right alternation. **Nature** 500: 85–8, 2013.

Tamamaki N, Yanagawa Y, Tomioka R, Miyazaki J-I, Obata K, and Kaneko T. Green Fluorescent Protein Expression and Colocalization with Calretinin, Parvalbumin, and Somatostatin in the GAD67-GFP Knock-in Mouse. **The Journal of Comparative Neurology** 467 (1): 60–79, 2003. https://doi.org/10.1002/cne.10905.

Taylor A, Durbaba R, Ellaway PH, Rawlinson S. Static and dynamic γ-motor output to ankle flexor muscles during locomotion in the decerebrate cat. **J Physiol** 571: 711–723, 2006.

Tester NJ, Barbeau H, Howland DR, Cantrell A, Behrman AL. Arm and leg coordination during treadmill walking in individuals with motor incomplete spinal cord injury : A preliminary study. **Gait Posture** 36: 49–55, 2012.

Tang JCY, Rudolph S, Dhande OS, Abraira VE, Choi S, Lapan SW, Drew IR, Drokhlyansky E, Huberman AD, Regehr WG, Cepko CL. Cell type-specific manipulation with GFP-dependent Cre recombinase. **Nat Neurosci** 18:1334–1341, 2015.

Tong Q, Ye C, McCrimmon RJ, Dhillon H, Choi B, Kramer MD, Yu J, Yang Z, Christiansen LM, Lee CE, Choi CS, Zigman JM, Shulman GI, Sherwin RS, Elmquist JK, Lowell BB. Synaptic Glutamate Release by Ventromedial Hypothalamic Neurons Is Part of the Neurocircuitry that Prevents Hypoglycemia. **Cell Metab** 5: 383–393, 2007.

Tourtellotte WG, Milbrandt J. Sensory ataxia and muscle spindle agenesis in mice lacking the transcription factor Egr3. **Nat Genet** 20: 87–91, 1998.

Tripodi M, Stepien AE, and Arber S. Motor Antagonism Exposed by Spatial Segregation and Timing of Neurogenesis. **Nature** 479 (7371): 61–66, 2011. https://doi.org/10.1038/nature10538.

Tseng S, Morton SM. Impaired Interlimb Coordination of Voluntary Leg Movements in Poststroke Hemiparesis. **J Neurophysiology** 104: 248–257, 2010.

Tuthill JC, Azim E. Proprioception. **Curr Biol** 28: R187–R207, 2018. doi:10.1016/j.cub.2018.01.064.

Valero-Cabré A, Forés J, Navarro X. Reorganization of Reflex Responses Mediated by Different Afferent Sensory Fibers After Spinal Cord Transection. **J Neurophysiol** 91: 2838–2848, 2004.

Vanderhorst VGJM, Holstege G. Organization of lumbosacral motoneuronal cell groups innervating hindlimb, pelvic floor, and axial muscles in the cat. **J Comp Neurol** 382: 46–76, 1997. doi:10.1002/(SICI)1096-9861(19970526)382:1

Wand P, Pompeiano O, Fayein NA. Impulse decoding process in extensor motoneurons of different size during the vibration reflex. **Arch Ital Biol** 118: 205–242, 1980.

Wang Z, Li N, Goulding M, Frank E. Early postnatal development of reciprocal Ia inhibition in the murine spinal cord. **J Neurophysiol** 100:185–196, 2008.

Wehr M, and Zador AM. Balanced Inhibition Underlies Tuning and Sharpens Spike Timing in Auditory Cortex. **Nature** 426 (6965): 442–46, 2003. https://doi.org/10.1038/nature02116.

Wetzel MC, Atwater AE, Wait J V., Stuart DG. Kinematics of locomotion by cats with a single hindlimb deafferented. **J Neurophysiol** 39: 667–678, 1976.

Wilent BW, and Contreras D. Dynamics of Excitation and Inhibition Underlying Stimulus Selectivity in Rat Somatosensory Cortex. **Nature Neuroscience** 8 (10): 1364–70, 2005. https://doi.org/10.1038/nn1545.

Wilson SI, Shafer B, Lee KJ, Dodd J. A Molecular Program for Contralateral Trajectory: Rig-1 Control by LIM Homeodomain Transcription Factors. **Neuron** 59:413–424, 2008.
Witschi R, Johansson T, Morscher G, Scheurer L, Deschamps J, Zeilhofer HU. Hoxb8-Cre mice: A tool for brain-sparing conditional gene deletion. **Genesis** 48: 596–602, 2010.

Wu H, Petitpré C, Fontanet P, Sharma A, Bellardita C, Quadros RM, Jannig PR, Wang Y, Heimel AJ, Cheung KKY, Wanderoy S, Xuan Y, Meletis K, Ruas J, Gurumurthy CB, Kiehn O, Hadjab S & Lallemend F. Distinct Subtypes of Proprioceptive Dorsal Root Ganglion Neurons Regulate Adaptive Proprioception in Mice. **Nature Communications** 12 (1): 1026, 2021. https://doi.org/10.1038/s41467-021-21173-9.

Yuengert R, Hori K, Kibodeaux EE, McClellan JX, Morales JE, Huang TWP, Neul JL, Lai HC. Origin of a Non-Clarke's Column Division of the Dorsal Spinocerebellar Tract and the Role of Caudal Proprioceptive Neurons in Motor Function. **Cell Rep** 13:1258–1271, 2015. http://dx.doi.org/10.1016/j.celrep.2015.09.064.

Zagoraiou L, Akay T, Martin JF, Brownstone RM, Jessell TM, Miles GB. A Cluster of Cholinergic Premotor Interneurons Modulates Mouse Locomotor Activity. **Neuron** 64: 645–662, 2009.

Zhang H, Shevtsova NA, Deska-Gauthier D, Mackay C, Dougherty KJ, Danner SM, Zhang Y, Rybak IA. The role of V3 neurons in speed-dependent interlimb coordination during locomotion in mice. **Elife** 11: 1–34, 2022.

Zhang J, Lanuza GM, Britz O, Wang Z, Siembab VC, Zhang Y, Velasquez T, Alvarez FJ, Frank E, Goulding M. V1 and V2b Interneurons Secure the Alternating Flexor-Extensor Motor Activity Mice Require for Limbed Locomotion. **Neuron** 82: 138–150, 2014.

Zhang Y, Narayan S, Geiman E, Lanuza GM, Velasquez T, Shanks B, Akay T, Dyck J, Pearson K, Gosgnach S, Fan CM, Goulding M. V3 Spinal Neurons Establish a Robust and Balanced Locomotor Rhythm during Walking. **Neuron** 60: 84–96, 2008.

Zheng Y, Liu P, Bai L, Trimmer JS, Bean BP, and Ginty DD. Deep Sequencing of Somatosensory Neurons Reveals Molecular Determinants of Intrinsic Physiological Properties. **Neuron** 103 (4): 598-616.e7, 2019.

Zhong G, Shevtsova NA, Rybak IA, Harris-Warrick RM. Neuronal activity in the isolated mouse spinal cord during spontaneous deletions in fictive locomotion: insights into locomotor central pattern generator organization. **J Physiol** 590: 4735–4759, 2012.

Zimmermann K, Hein A, Hager U, Kaczmarek JS, Turnquist BP, Clapham DE, Reeh PW. Phenotyping sensory nerve endings in vitro in the mouse. **Nat Protoc** 4: 174–196, 2009. doi:10.1038/nprot.2008.223.

Appendix

Copyright and Permissions

THE AMERICAN PHYSIOLOGICAL SOCIETY LICENSE
TERMS AND CONDITIONS
Jul 01, 2022

This Agreement between Dalhousie University -- Olivier Laflamme ("You") and The American Physiological Society ("The American Physiological Society") consists of your license details and the terms and conditions provided by The American Physiological Society and Copyright Clearance Center.

License Number	5340240014104
License date	Jul 01, 2022
Licensed Content Publisher	The American Physiological Society
Licensed Content Publication	Journal of Neurophysiology
Licensed Content Title	Excitatory and inhibitory crossed reflex pathways in mice
Licensed Content Author	Olivier D. Laflamme, Turgay Akay
Licensed Content Date	Dec 1, 2018
Licensed Content Volume	120
Licensed Content Issue	6
Type of Use	Thesis/Dissertation
Requestor type	author of original work
Format	electronic
Portion	full article
Will you be translating?	no
World Rights	no
Title	Crossed reflex responses to flexor nerve stimulation in mice
Institution name	Dalhousie University
Expected presentation date	Aug 2022
Requestor Location	Dalhousie University 5959 Spring Garden Road #206 Halifax, NS B3H 1Y5 Canada Attn: Dalhousie University
Billing Type	Invoice

Billing Address	Dalhousie University 5959 Spring Garden Road #206 Halifax, NS B3H 1Y5 Canada Attn: Dalhousie University
Total	0.00 CAD

Terms and Conditions

Terms and Conditions:

works that are commercially supported or sponsored including reuse in a work produced by a commercial publisher without seeking permission.

Video and photographs: Some material published in APS publications may belong to other copyright holders and cannot be republished without their permission. The copyright holder of photographs must be ascertained from the original source by the permission requestor. Videos and podcasts may not be rebroadcast without proper attribution and permission as requested here. For further inquiries on reuse of these types of materials, please contact cvillemez@the-aps.org

Figures/Tables/Images are available to the requestor from the APS journals website at http://www.the-aps.org/publications/journals/. The obtaining of content is a separate transaction and does not involve Rightslink or CCC, and is the responsibility of the permission seeker. Higher resolution images are available at additional charge from APS; please contact cvillemez@the-aps.org

Original Authors of Published Works: To see a full list of original authors rights concerning their own published work http://www.the-aps.org/publications/authorinfo/copyright.htm

Content reuse rights awarded by the APS may be exercised immediately upon issuance of this license, provided full disclosure and complete and accurate details of the proposed reuse have been made; no license is finally granted unless and until full payment is received either by the publisher or by CCC as provided in CCC's Billing and Payment Terms and Conditions. If full payment is not received on a timely basis, then any license preliminarily granted shall be deemed automatically revoked and shall be void as if never granted. Further, in the event that you breach any of these Terms and Conditions or any of CCC's Billing and Payment Terms and Conditions, the license is automatically revoked and shall be void as if never granted. Use of materials as described in a revoked license, as well as any use of the materials beyond the scope of the license, may constitute copyright infringement and the Publisher reserves the right to take action to protect its copyright of its materials.

The APS makes no representations or warranties with respect to the licensed material. You hereby indemnify and agree to hold harmless the publisher and CCC, and their respective officers, directors, employees and agents, from and against any and all claims arising out of your use of the licensed material other than as specifically authorized pursuant to this license.

This license is personal to you /your organization and may not be sublicensed, assigned, or transferred by you /your organization to another person /organization without the publisher's permission.This license may not be amended except in writing signed by both parties, or in the case of the publisher, by CCC on the publisher's behalf.

The APS reserves all rights not specifically granted in the combination of (i) the license details provided by you and accepted in the course of this licensing transaction, (ii) these Terms and Conditions and (iii) CCC's Billing and Payment Terms and Conditions.

THE AMERICAN PHYSIOLOGICAL SOCIETY ORDER DETAILS

Jul 01, 2022

This Agreement between Olivier D Laflamme ("You") and The American Physiological Society ("The American Physiological Society") consists of your order details and the terms and conditions provided by The American Physiological Society and Copyright Clearance Center.

Order Number	501742957
Order date	Jun 30, 2022
Licensed Content Publisher	The American Physiological Society
Licensed Content Publication	Journal of Neurophysiology
Licensed Content Title	Crossed reflex responses to flexor nerve stimulation in mice
Licensed Content Author	Olivier D. Laflamme, Marwan Ibrahim, Turgay Akay
Licensed Content Date	Feb 1, 2022
Licensed Content Volume	127
Licensed Content Issue	2
Type of Use	Thesis/Dissertation
Requestor type	author of original work
Format	electronic
Portion	full article
Will you be translating?	no
World Rights	no
Title	Excitatory and inhibitory crossed reflex pathways in mice
Institution name	Dalhousie University
Expected presentation date	Aug 2022
Requestor Location	Dalhousie University 5959 Spring Garden Road #206 Halifax, NS B3H 1Y5 Canada Attn: Dalhousie University
Billing Type	Invoice
Billing Address	Dalhousie University 5959 Spring Garden Road #206 Halifax, NS B3H 1Y5

Canada
Attn: Dalhousie University

Total 0.00 CAD

Terms and Conditions

Terms and Conditions:

requested here. For further inquiries on reuse of these types of materials, please contact cvillemez@the-aps.org

Figures/Tables/Images are available to the requestor from the APS journals website at http://www.the-aps.org/publications/journals/. The obtaining of content is a separate transaction and does not involve Rightslink or CCC, and is the responsibility of the permission seeker. Higher resolution images are available at additional charge from APS; please contact cvillemez@the-aps.org

Original Authors of Published Works: To see a full list of original authors rights concerning their own published work http://www.the-aps.org/publications/authorinfo/copyright.htm

Content reuse rights awarded by the APS may be exercised immediately upon issuance of this license, provided full disclosure and complete and accurate details of the proposed reuse have been made; no license is finally granted unless and until full payment is received either by the publisher or by CCC as provided in CCC's Billing and Payment Terms and Conditions. If full payment is not received on a timely basis, then any license preliminarily granted shall be deemed automatically revoked and shall be void as if never granted. Further, in the event that you breach any of these Terms and Conditions or any of CCC's Billing and Payment Terms and Conditions, the license is automatically revoked and shall be void as if never granted. Use of materials as described in a revoked license, as well as any use of the materials beyond the scope of the license, may constitute copyright infringement and the Publisher reserves the right to take action to protect its copyright of its materials.

The APS makes no representations or warranties with respect to the licensed material. You hereby indemnify and agree to hold harmless the publisher and CCC, and their respective officers, directors, employees and agents, from and against any and all claims arising out of your use of the licensed material other than as specifically authorized pursuant to this license.

This license is personal to you /your organization and may not be sublicensed, assigned, or transferred by you /your organization to another person /organization without the publisher's permission.This license may not be amended except in writing signed by both parties, or in the case of the publisher, by CCC on the publisher's behalf.

The APS reserves all rights not specifically granted in the combination of (i) the license details provided by you and accepted in the course of this licensing transaction, (ii) these Terms and Conditions and (iii) CCC's Billing and Payment Terms and Conditions.

v1.0